



Norwegian University of
Science and Technology

Syntheses and Studies on New Dual Functionalized Zwitterions and Ionic Liquids

Imidazolium and 1,2,3-Triazolium based
structures

Ingrid Grøssereid

Chemical Engineering and Biotechnology

Submission date: June 2018

Supervisor: Anne Fiksdahl, IKJ

Co-supervisor: Kallidanthyil Chellappan Lethesh, IKJ

Norwegian University of Science and Technology
Department of Chemistry

Declaration

I hereby declare that I wrote this report independently and that I have used only the sources of information given in the list of references. The study was conducted in accordance with the rules and regulations at the Department of Chemistry at the Norwegian University of Science and Technology (NTNU). The work was performed as a member of the Fiksdahl group and was conducted from January 2018 to June 2018.

Trondheim, 10.06.2018

Ingrid Grøssereid
Ingrid Grøssereid

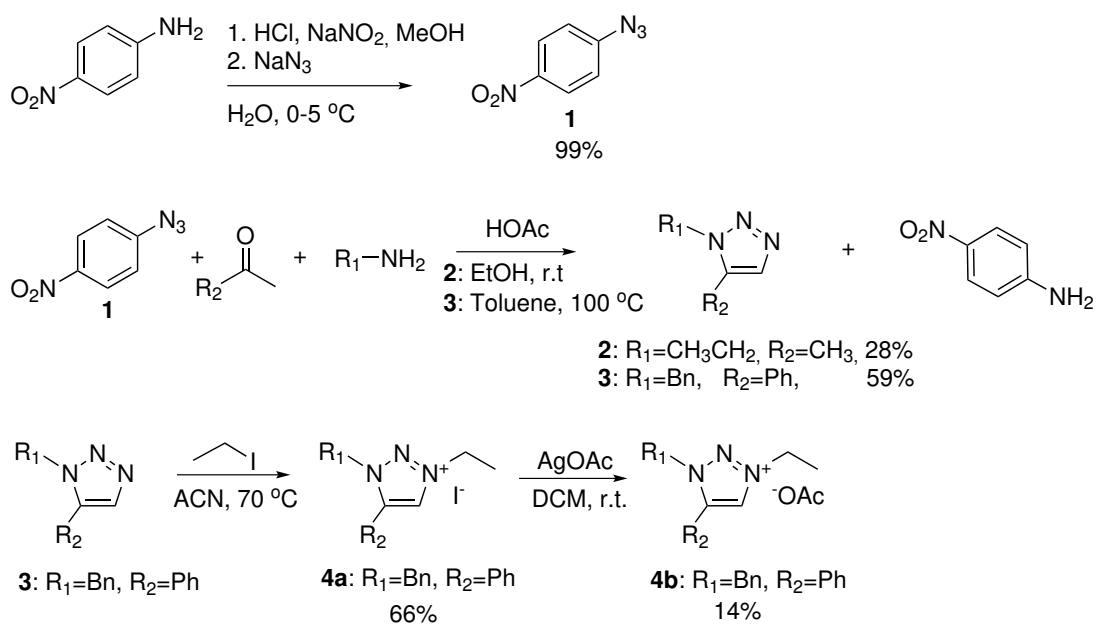
Acknowledgements

I am grateful to thank my supervisor, Professor Anne Fiksdahl, for accepting me as part of her research group and giving me excellent guiding. The encouragement and guidance along the way have truly been appreciated. I would also like to thank my co-supervisor postdoc Lethesh Kallidanthiyil Chellappan for all the help and guidance through this project.

Abstract

The purpose of this master's project was to synthesize new dual functionalized non-toxic imidazolium based zwitterions (ZIs), and ionic liquids (ILs) with high cellulose dissolution potential. As well as new 1,5-disubstituted 1,2,3-triazoles and 1,3,5-trisubstituted 1,2,3-triazolium ILs.

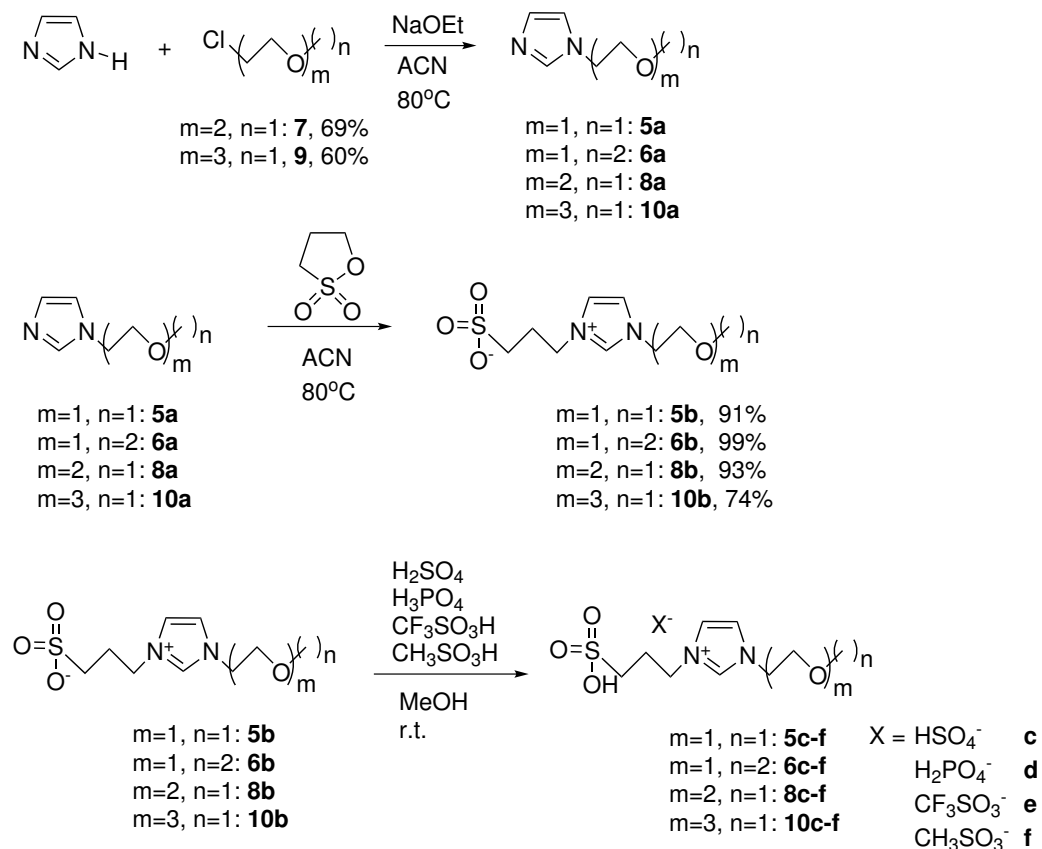
Metal-free approaches towards regioselective preparation of 1,5-disubstituted 1,2,3-triazoles are scarce, but recently a new synthetic route using readily available substrates has been presented. 1,5-Disubstituted 1,2,3-triazoles **2** and **3** were respectively prepared in 28 % and 59 % yield, by a metal-free synthesis using 4-nitrophenyl azide (**1**) as azide transfer reagent. 1-Benzyl-3-ethyl-5-phenyl-1,2,3-triazolium iodide (**4a**) was prepared in 66 % yield by quaternization of triazole **3**. IL 1-benzyl-3-ethyl-5-phenyl-1,2,3-triazolium acetate (**4b**) was prepared in 14 % yield by anion exchange through Finkelstein reaction from IL **4a** using silver acetate. Synthetic routes to triazoles **2** and **3**, as well as ILs **4a** and **4b** are presented:



The toxicity of ILs for cellulose dissolution is a general problem when synthesized for industrial use. A new synthetic method of IL preparation through less toxic dual functionalized ZIs was used. The ZI intermediates **5a**, **6a**, **8a** and **10a** were synthesized by addition of ether substituents to imidazole through S_N2 reactions. The ZIs **5b**, **6b**, **8b** and **10b** were synthesized from intermediates by addition of alkyl sulfate through nucleophilic attack

and ring opening of 1,3-propanesultone in 91 %, 99 %, 93 % and 74 % yield, respectively. By protonation with sulfuric acid, phosphoric acid, trimethanesulfonic acid and methanesulfonic acid the ILs **5c-f**, **6c-f**, **8c-f** and **10c-f** were prepared in high yields. The ILs were tested for cellulose dissolution in a mixture with dimethylformamide (DMF) at 100 °C and showed moderate cellulose dissolution abilities. X-ray diffraction (XRD) analysis showed that IL **5c** with the shortest ether chain substituent and $[\text{HSO}_4^-]$ anion was most efficient for cellulose dissolution, with dissolution of 7.57 wt% microcrystalline cellulose (MCC) at 100 °C in 72 hours. Thermal stability of ILs were tested by thermogravimetric analysis (TGA), which showed that ILs **5c-f** had the most thermally stable cation, and that $[\text{H}_2\text{PO}_4^-]$ was the most thermally stable anion.

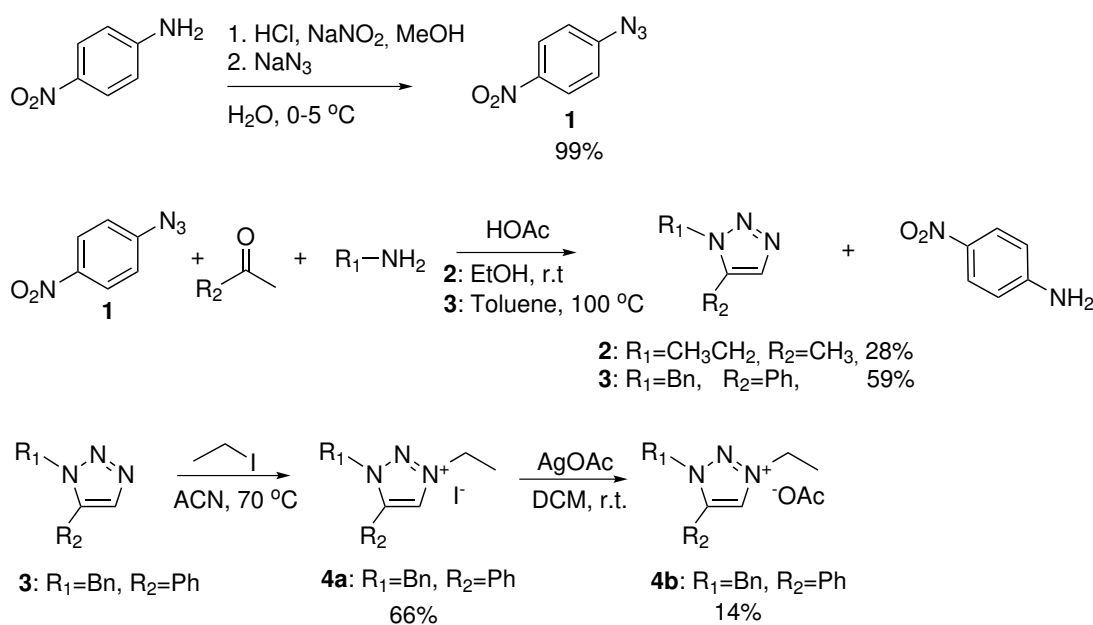
Synthetic routes to intermediates **5a**, **6a**, **8a** and **10a**, ZIs **5b**, **6b**, **8b** and **10b** and ILs **5c-f**, **6c-f**, **8c-f** and **10c-f** are presented:



Sammendrag

Målet med dette masterprosjektet var å syntetisere nye dobbelfunksjonaliserte ikke-toksiske imidazolium-baserte zwitterioner, og imidazolium-baserte ioniske væsker med gode celluloseoppløsningsegenskaper, i tillegg til nye 1,5-disubstituerte 1,2,3-triazoler og 1,3,5-trisubstituerte 1,2,3-triazolium ioniske væsker.

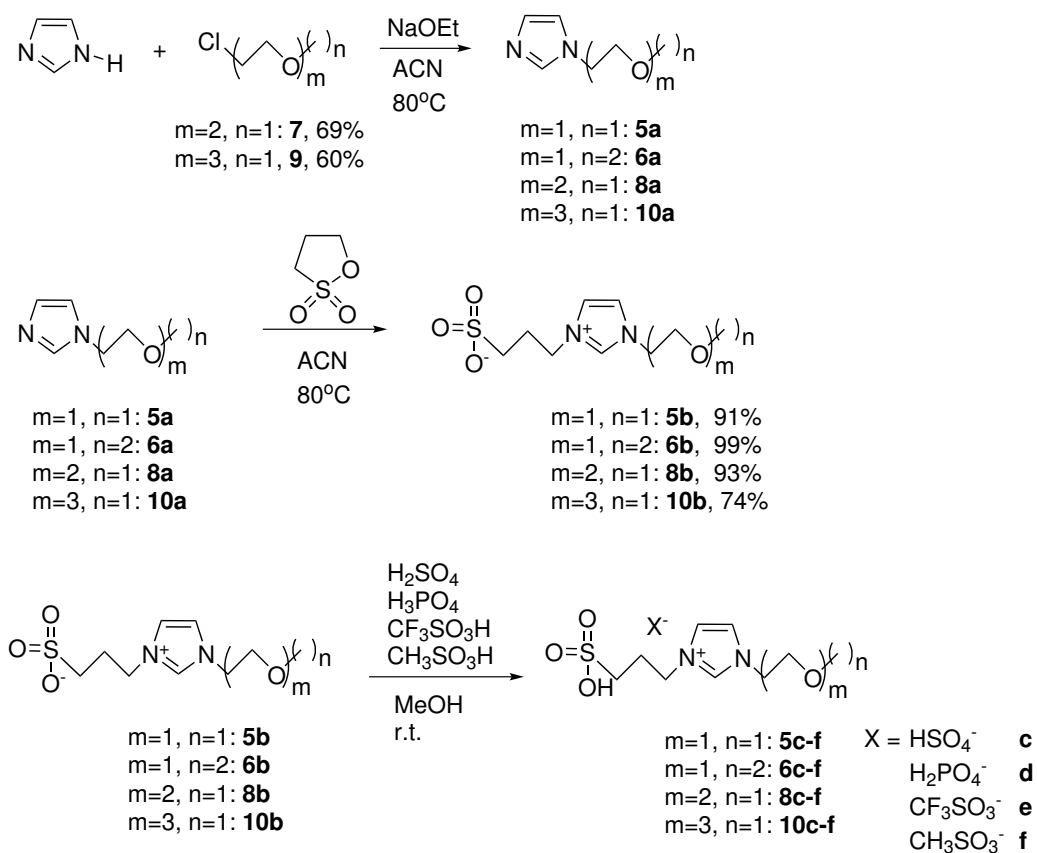
Metallfrie tilnæringer til regioselektiv syntese av 1,5-disubstituerte 1,2,3-triazoler er mangelfulle, men det har nylig blitt publisert en synteserute som bruker lett tilgjengelige substrater. 1,5-Disubstituerte 1,2,3-triazoler **2** og **3** ble respektivt syntetisert med 28 % og 59 % utbytte ved bruk av metallfri syntese hvor 4-nitrofenyl azid (**1**) ble brukt som azid-overføringsreagens. 1-Bensyl-3-etyl-5-fenyl-1,2,3-triazolium jodid (**4a**) ble dannet med 66 % utbytte ved kvaternisering av triazol **3**. Ved anion bytte via Finkelsteinreaksjon fra IL **4a** ved bruk av sòlvacetat ble IL 1-bensyl-3-etyl-5-fenyl-1,2,3-triazolium acetat (**4b**) dannet med 14 % utbytte. Synteseruter til triazol **2** og **3**, samt IL **4a** og **4b** er presentert:



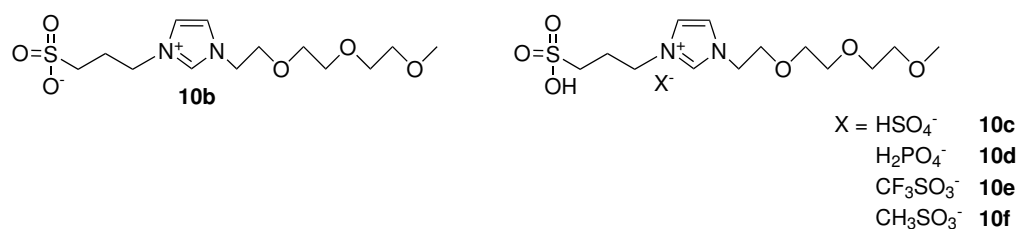
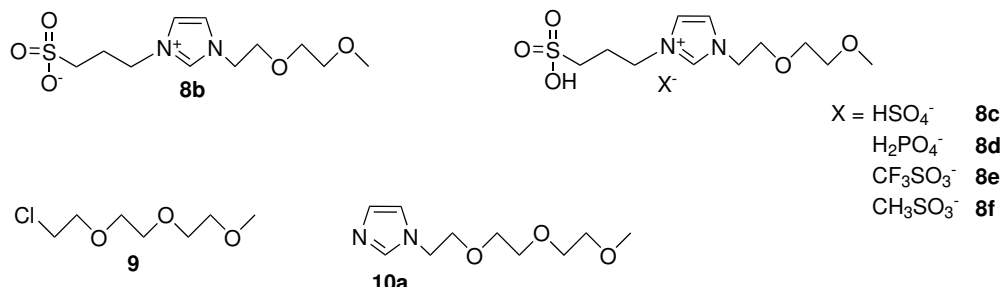
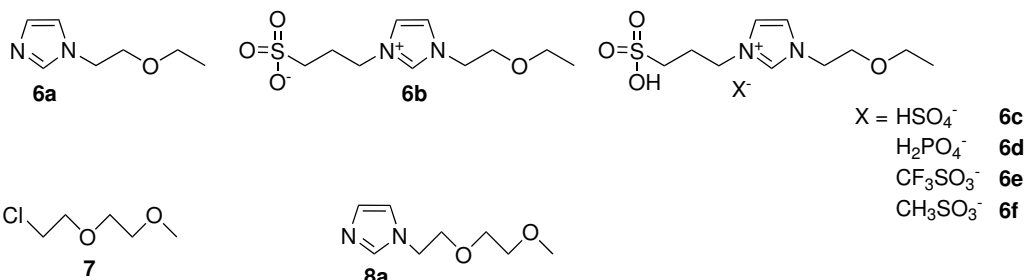
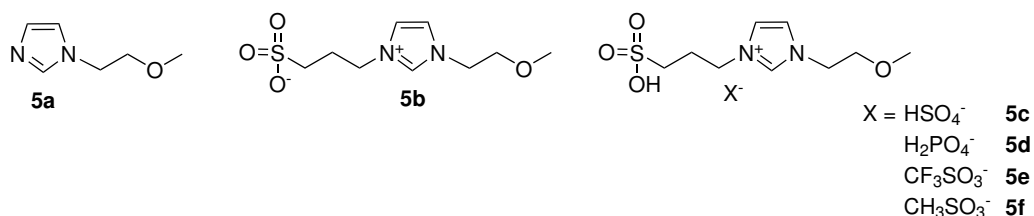
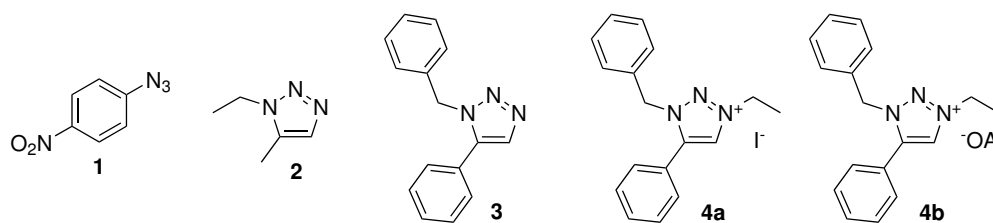
Høy toksisitet for ioniske væsker som brukes til celluloseoppløsing er et problem når de syntetiseres for bruk i industrien. En ny syntesemetode for dannelsen av ioniske væsker via mindre giftige dobbelfunksjonaliserte zwitterioner ble gjennomført. ZI intermediatene **5a**, **6a**, **8a** og **10a** ble syntetisert ved addisjon av etersubstituenter til imidazol via S_N2 reaksjoner. Zwitterionene **5b**, **6b**, **8b** og **10b** ble syntetisert fra intermediatene ved addisjon av alkylsulfat via nukleofilt angrep og ringåpning av 1,3-propansulton med 91 %, 99 %,

93 % og 74 % utbytter. Via protonering med svovelsyre, fosforsyre, trimetansulfonsyre og metansulfonsyre ble de ioniske væskene **5c-f**, **6c-f**, **8c-f** og **10c-f** syntetisert med høye utbytter. De ioniske væskene ble testet for oppløsning av mikrokristallinsk cellulose (MCC) i blanding med dimetylformamid (DMF) ved 100 °C, og viste moderate celluloseoppløsningsegenskaper. Røntgendiffraksjons analyse (XRD) viste at ionisk væske **5c** med kortest eterkjedesubstituent og $[\text{HSO}_4^-]$ anion var mest effektiv for celluloseoppløsning, og løste opp 7.57 wt% MCC ved 100 °C på 72 timer. Den termiske stabiliteten av de ioniske væskene ble testet ved hjelp av termogravimetrisk analyse (TGA), som viste at de ioniske væskene **5c-f** hadde det mest stabile kationet, mens $[\text{H}_2\text{PO}_4^-]$ var det mest stabile anionet.

Synteseruter til intermediatene **5a**, **6a**, **8a** og **10a**, zwitterionene **5b**, **6b**, **8b** og **10b** samt ioniske væsker **5c-f**, **6c-f**, **8c-f** og **10c-f** er presentert:



List of compounds



Symbols and Abbreviations

δ	Chemical shift
θ	Incident angle
λ	Wavelength
APIL	Aprotic ionic liquid
Ar	Aromatic
b	Broad
bp	Boiling point
CDCl ₃	Deuterated chloroform
CI	Crystallinity index
CuAAC	Copper-catalyzed azide-alkyne cycloaddition
d	Doublet
d	Lattice spacing
DFT	Density functional theory
eq	Equivalent
FTIR	Fourier transform infrared spectroscopy
HMBC	Heteronuclear multiple-bond correlation spectroscopy
HRMS	High resolution mass spectrometry
HSQC	Heteronuclear single-quantum correlation spectroscopy
Hz	Hertz
IL	Ionic liquid
IR	Infrared spectroscopy
J	Coupling constant
m	Multiplet
M+	Molecular ion
MCC	Microcrystalline cellulose
MeOD	Deuterated methanol
MTT	3-(4,5-Dimethylthiazol-2-yl)-2,5-diphenyltetrazolium bromide
n	Order of diffraction
NMMO	<i>N</i> -methylmorpholine- <i>N</i> -oxide monohydrate
NMR	Nuclear magnetic resonance
PIL	Polyionic liquid\Protic ionic liquid
ppm	Parts per million

q	Quartet
RTIL	Room temperature ionic liquid
RuAAC	Ruthenium-catalyzed azide-alkyne cycloaddition
s	Singlet
SILM	Supported ionic liquid membrane
t	Triplet
TGA	Thermogravimetric analysis
TG-MS	Thermogravimetric analysis-mass spectroscopy
TLC	Thin-layer chromatography
TMS	Tetramethylsilane
TSIL	Task specific ionic liquid
wt	Weight
XPS	X-ray photoelectron spectroscopy
XRD	X-ray diffraction
ZI	Zwitterion
ZIL	Zwitterionic liquid

Contents

1	Introduction	1
1.1	Aim of project	2
2	Theory	5
2.1	Ionic liquids (ILs)	5
2.1.1	Background	5
2.1.2	Properties	6
2.1.3	Synthesis of ILs	8
2.1.4	Applications	10
2.1.5	ILs for use in batteries	10
2.1.6	ILs for use in membranes for CO ₂ capture	11
2.1.7	Cellulose dissolution with ILs	12
2.1.8	Dissolution of cellulose with ILs/organic solvent solution	14
2.2	Zwitterions (ZIs)	15
2.2.1	ILs derived from ZIs and IL toxicity	15
2.3	Characterization methods for ILs and cellulose	16
2.3.1	Thermogravimetric analysis and thermal stability of ILs	16
2.3.2	X-ray diffraction	17
2.4	Triazoles	18
2.4.1	Azides	20
2.5	Preliminary studies	21
3	Results and discussion	23
3.1	Preparation of 1,5-disubstituted 1,2,3-triazoles	23
3.1.1	Synthesis of 4-nitrophenyl azide (1)	23
3.1.2	Synthesis of 1-ethyl-5-methyl-1,2,3-triazole (2)	24
3.1.3	Synthesis of 1-benzyl-5-phenyl-1,2,3-triazole (3)	25
3.1.4	Mechanism for formation of 1,5-disubstituted 1,2,3-triazoles	26
3.1.5	Optimization of triazole reactions	27
3.2	Preparation of triazolium based ILs	30
3.2.1	Synthesis of 1-benzyl-3-ethyl-5-phenyl-1,2,3-triazolium iodide (4a) .	30
3.2.2	Optimization of triazole alkylation	30

3.2.3	Synthesis of 1-benzyl-3-ethyl-5-phenyl-1,2,3-triazolium acetate (4b) through anion exchange	32
3.3	Preparation of imidazolium based ZIs	33
3.3.1	Synthesis of ZIs 5b and 6b	33
3.3.2	Synthesis of precursor 7 and ZI 8b	34
3.3.3	Synthesis of precursor 9 and ZI 10b	35
3.3.4	Comparing ZIs	36
3.4	Preparation of imidazolium based ILs	37
3.4.1	Synthesis of ILs from ZI 5b , 6b , 8b and 10b	37
3.4.2	Thermal stability of ILs	38
3.4.3	Thermal decomposition mechanism	42
3.5	Cellulose dissolution with imidazolium ILs	45
3.5.1	Results from cellulose dissolution testing	49
4	Conclusion	55
5	Further work	57
6	Experimental and methods	59
6.1	General methods	59
6.2	Synthesis of 4-nitrophenyl azide (1)	60
6.3	Synthesis of 1-ethyl-5-methyl-1,2,3-triazole (2)	60
6.4	Synthesis of 1-benzyl-5-phenyl-1,2,3-triazole (3)	61
6.5	Synthesis of IL 1-benzyl-3-ethyl-5-phenyl-1,2,3-triazolium iodide (4a)	62
6.6	Synthesis of IL 1-benzyl-3-ethyl-5-phenyl-1,2,3-triazolium acetate (4b)	63
6.7	General Procedure A for preparation of imidazolium based ZIs	63
6.8	General Procedure B for preparation of imidazolium based ILs	64
6.9	Synthesis of 3-(1-(2-methoxyethyl)-1H-imidazol-3-ium-3-yl)propane-1-sulfonate (5b)	64
6.10	Synthesis of ILs based on ZI 5b	65
6.10.1	Synthesis of IL 1-(2-methoxyethyl)-3-(3-sulfopropyl)-1H-imidazol-3-ium hydrogen sulfate (5c)	65
6.10.2	Synthesis of IL 1-(2-methoxyethyl)-3-(3-sulfopropyl)-1H-imidazol-3-ium dihydrogen phosphate (5d)	66
6.10.3	Synthesis of IL 1-(2-methoxyethyl)-3-(3-sulfopropyl)-1H-imidazol-3-ium trifluoromethanesulfonate (5e)	67

6.10.4 Synthesis of IL 1-(2-methoxyethyl)-3-(3-sulfopropyl)-1H-imidazol-3-ium methanesulfonate (5f)	67
6.11 Synthesis of 3-(1-(2-ethoxyethyl)-1H-imidazol-3-ium-3-yl)propane-1-sulfonate (6b)	68
6.12 Synthesis of ILs based on ZI 6b	69
6.12.1 Synthesis of IL 1-(2-ethoxyethyl)-3-(3-sulfopropyl)-1H-imidazol-3-ium hydrogen sulfate (6c)	69
6.12.2 Synthesis of IL 1-(2-ethoxyethyl)-3-(3-sulfopropyl)-1H-imidazol-3-ium dihydrogen phosphate (6d)	70
6.12.3 Synthesis of IL 1-(2-ethoxyethyl)-3-(3-sulfopropyl)-1H-imidazol-3-ium trifluoromethanesulfonate (6e)	71
6.12.4 Synthesis of IL 1-(2-ethoxyethyl)-3-(3-sulfopropyl)-1H-imidazol-3-ium methanesulfonate (6f)	71
6.13 Synthesis of 1-chloro-2-(2-methoxyethoxy)ethane (7)	72
6.14 Synthesis of 3-(1-(2-(2-methoxyethoxy)ethyl)-1H-imidazol-3-ium-3-yl)propane-1-sulfonate (8b)	72
6.15 Synthesis of ILs based on ZI 8b	74
6.15.1 Synthesis of IL 1-(2-(2-methoxyethoxy)ethyl)-3-(3-sulfopropyl)-1H-imidazol-3-ium hydrogen sulfate (8c)	74
6.15.2 Synthesis of IL 1-(2-(2-methoxyethoxy)ethyl)-3-(3-sulfopropyl)-1H-imidazol-3-ium dihydrogen phosphate (8d)	75
6.15.3 Synthesis of IL 1-(2-(2-methoxyethoxy)ethyl)-3-(3-sulfopropyl)-1H-imidazol-3-ium trifluoromethanesulfonate (8e)	75
6.15.4 Synthesis of IL 1-(2-(2-methoxyethoxy)ethyl)-3-(3-sulfopropyl)-1H-imidazol-3-ium methanesulfonate (8f)	76
6.16 Synthesis of 1-chloro-2-(2-(2-methoxyethoxy)ethoxy)ethane (9)	76
6.17 Synthesis of 3-(1-(2-(2-(2-methoxyethoxy)ethoxy)ethyl)-1H-imidazol-3-ium-3-yl)propane-1-sulfonate (10b)	77
6.18 Synthesis of ILs based on ZI 10b	78
6.18.1 Synthesis of IL 1-(2-(2-(2-methoxyethoxy)ethoxy)ethyl)-3-(3-sulfopropyl)-1H-imidazol-3-ium hydrogen sulfate (10c)	79
6.18.2 Synthesis of IL 1-(2-(2-(2-methoxyethoxy)ethoxy)ethyl)-3-(3-sulfopropyl)-1H-imidazol-3-ium dihydrogen phosphate (10d)	79
6.18.3 Synthesis of IL 1-(2-(2-(2-methoxyethoxy)ethoxy)ethyl)-3-(3-sulfopropyl)-1H-imidazol-3-ium trifluoromethanesulfonate (10e)	80

6.18.4 Synthesis of IL 1-(2-(2-methoxyethoxy)ethoxy)-3-(3-sulfopropyl)-1H-imidazol-3-ium methanesulfonate (10f)	81
6.19 Cellulose dissolution	81
Bibliography	86
A Poster from Organic Chemical Winter meeting 2018	I
B Spectrum of azide 1	II
C Spectra of triazole 2	III
D Spectra of triazole 3	X
E Spectra of IL 4a	XVII
F Spectra of IL 4b	XXI
G Spectrum of intermediate 5a	XXVII
H Spectra of ZI 5b	XXVIII
I Spectra of IL 5c	XXXV
J Spectra of IL 5d	XL
K Spectra of IL 5e	XLV
L Spectra of IL 5f	LI
M Spectrum of intermediate 6a	LVI
N Spectra of ZI 6b	LVII
O Spectra of IL 6c	LXIV
P Spectra of IL 6d	LXIX
Q Spectra of IL 6e	LXXIV
R Spectra of IL 6f	LXXX

S Spectrum of precursor 7	LXXXV
T Spectrum of intermediate 8a	LXXXVI
U Spectra of ZI 8b	LXXXVII
V Spectra of IL 8c	XCIV
W Spectra of IL 8d	XCIX
X Spectra of IL 8e	CIV
Y Spectra of IL 8f	CX
Z Spectrum of precursor 9	CXV
AA Spectrum of intermediate 10a	CXVI
AB Spectra of ZI 10b	CXVII
AC Spectra of IL 10c	CXXIV
AD Spectra of IL 10d	CXXIX
AE Spectra of IL 10e	CXXXIV
AF Spectra of IL 10f	CXL

1 Introduction

The search for renewable technologies replacing fossil sources of carbon is important in the quest of a sustainable future. The research focus has moved from coal, gas and oil to more renewable products like biofuels. Doing this by using abundantly available resources that neither compete with food production, nor increase the greenhouse gas emissions, would be the best option. Today biofuels are made from biomass consisting of edible components of food crops like starch, sucrose and vegetable oils. The vegetable oils are converted to biodiesel, while sugars are converted to bioethanol by microbial fermentation. They can both be mixed with gasoline in different ratios and thereby being used as fuels.^[1] It is a concern that using edible biomass for production of biofuels and chemicals competes with food production, consequently reducing the CO₂ emission savings at the expense of larger land use.^[2] Therefore, the search for a new and efficient way of using renewable and abundantly available resources is of great importance.^[3]

Biomass is the only renewable organic carbon resource in nature,^[4] and is the fourth largest energy source in the world for generation of heat and power, after oil, coal and natural gas.^[3] In addition, it also has the potential of being used for production of fuels. Lignocellulosic biomass is the most abundant plant material on earth, and would therefore be a much better option for fuel production than starch and sucrose based biomass, given that it can not be used for food production. Lignocellulose makes up the cell walls of woody plants, and is built up by lignin, hemicellulose and cellulose. The cellulose strands consists of polyglucose units connected through hydrogen bonds and is insoluble in water and most common organic solvents. Therefore, still it is challenging to find ways to break down the cellulose efficiently in an environmentally-friendly way. Doing this in an industrial scale, is particularly more challenging. However, it has been shown that ionic liquids (ILs) are promising for cellulose dissolution, some more efficiently than others.^[5]

ILs for cellulose dissolution was first reported in 2002,^[5] and has since then been further studied for various applications. ILs based on imidazolium cations are the most common, and a variety of them are commercially available. In the present thesis the synthesis of imidazolium based zwitterions (ZIs) and ILs derived from these ZIs, will be presented. The ILs are synthesized for cellulose dissolution purposes. Since the viscosity of ILs can be a problem when performing cellulose dissolution, researchers have presented a solution. That is, to dissolve the ILs in a polar solvent that does not it self dissolve cellulose, but significantly decreases the viscosity, thereby allowing vigorous stirring and faster dissolution

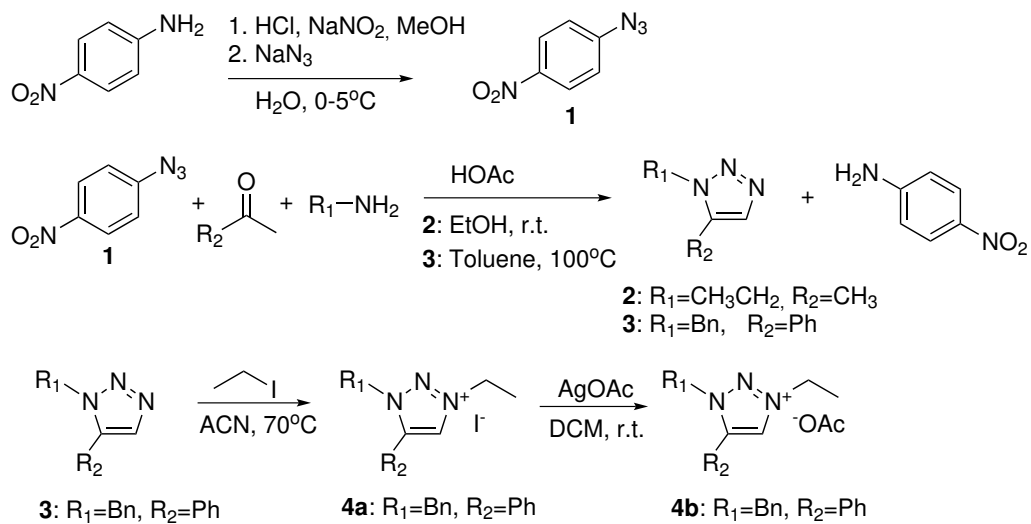
1.1 Aim of project

by enhanced mass transport.^[6] In this thesis the new ILs' ability to dissolve cellulose in a solution with a polar solvent will be presented and discussed.

Interesting results concerning the regioselective preparation of 1,5-disubstituted 1,2,3-triazoles from amines, ketones and 4-nitrophenyl azide have been presented by Thomas et al. in 2016.^[7] The first part of the project presented in this thesis is based on the idea from this communication, and builds on work performed in preliminary studies leading up to this master's project.^[8] In the previous project it was found that 1:1:2 equivalents of 4-nitrophenyl azide, acetone and butylamine, with addition of 0.3 equivalents acetic acid gave the best yield for synthesis of 1-butyl-5-methyl-1,2,3-triazole. It was also found that the reaction could be performed without acid and still give satisfying yield.^[8] In this thesis the optimization studies on the synthesis of new 1,5-disubstituted 1,2,3-triazoles and 1,3,5-trisubstituted 1,2,3-triazolium ILs will be discussed.

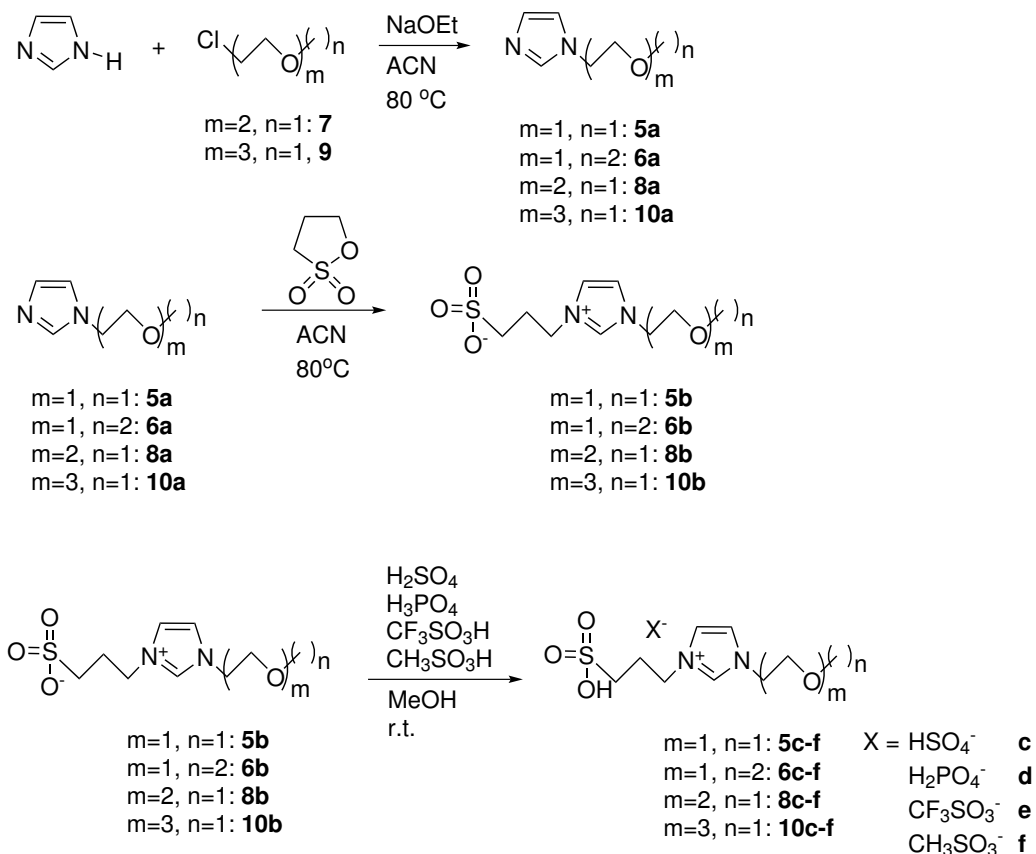
1.1 Aim of project

The overall aim of this master's project is to synthesize new ILs for cellulose dissolution. The focus of the first part of the project is to synthesize new regioselective 1,5-disubstituted 1,2,3-triazoles and 1,3,5-trisubstituted 1,2,3-triazolium ILs. Aromatic substituents on 1,2,3-triazole is particularly interesting and will be investigated. Synthesis steps used in the first part of the project is shown in Scheme 1.1.



Scheme 1.1: Overview of synthesis steps conducted for the regioselective synthesis of 1,5-disubstituted 1,2,3-triazoles and 1,3,5-trisubstituted 1,2,3-triazolium ILs.

In the second and main part of the project, the interest will be on preparation of new dual functionalized non-toxic imidazolium based ZIs and cellulose dissolving ILs derived from these ZIs. Ether substituents of different length will be in focus. An overview of synthesis steps used in the second part of the project is presented in Scheme 1.2. The synthesis is based on S_N2 reactions for formation of intermediates and alkylation through nucleophilic attack and ring opening of 1,3-propanesultone to form the ZIs. Protonation of ZIs with coordination of anion creates the final ILs.



Scheme 1.2: Overview of synthesis steps conducted for the synthesis of ZI and ILs.

2 Theory

This chapter will cover theoretical concepts of relevance to this master's thesis. It will start with an introduction to the field of ionic liquids (ILs), its background, properties, synthesis and applications, with elaboration of three specific areas of use. Zwitterions (ZI) and ILs derived from ZIs will be discussed along with some analytical techniques commonly used for the characterization of ILs. Finally, a description of properties, preparation methods and mechanisms of triazoles and azides will be introduced, along with information about preliminary triazole studies. ILs are a new field of research within energy-related organic chemistry at the Department of Chemistry at NTNU, and is preformed by the Fiksdahl group. Because it is a new research field at the department, applications going beyond the scope of this project will be presented.

2.1 Ionic liquids (ILs)

2.1.1 Background

An IL is a liquid that consists only of ions. In the broad sense, ILs include all the molten salts, also those only existing as liquids at high temperatures. Today, however, the term IL only include organic salts that have a melting point below 100 °C.^[9]

The field of ILs' physical chemistry were pioneered by Humphrey Davy and his work on the electrolytic decomposition of simple molten salts under the influence of an applied electric field in the early 1800. Davy's studies were collected in his major work,^[10] and lead the focus on to ILs, making this the topic of investigation at the beginning of organized chemical science. Davy's main focus was the high temperature melting simple salts.^[11]

The first person to use medium temperature ILs for scientific purposes was the Nobel Prize-winning physicist, Sir William Ramsay, who is reported by Laus and co-workers^[9] to have described highly viscous ILs for the first time in 1876.^[11]

The history of ILs as they are defined today, started when the physical properties of ethylammonium nitrate ($[(\text{C}_2\text{H}_5)\text{NH}_3^+][\text{NO}_3^-]$) were first reported by Paul Walden in 1914. At the time, he did not realize the potential of the new compounds and therefore, the systematic utilization of room-temperature ILs (RTILs) were not reported until 1951 by Wier and Hurley.^[12] They studied the electrodeposition of metals from fused mixtures of

2.1 Ionic liquids (ILs)

ethylpyridinium bromide and metal chlorides.

During the past two decades ILs as innovative fluids have received wide attention. The number of scientific papers published on ILs increased from 11 in 1974 to more than 8000 in 2017 (Figure 2.1). This indicates that the interest in ILs has increased, and researchers have published many new interesting findings.

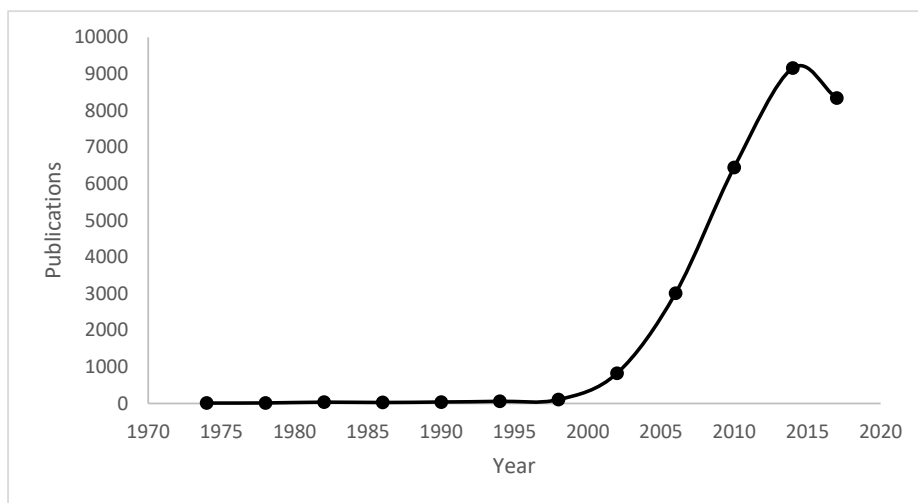


Figure 2.1: Publications on ILs as a function of years. Data collected from SciFinder.

Generally ILs can be divided into two broad categories: protic ILs (PILs) and aprotic ILs (APIls).^[13] However, due to the recent developments in the field of ILs, they can now be separated into several types, including room-temperature ILs (RTILs),^[14] task-specific ILs (TSILs),^[15] polyionic liquids (PILs),^[16] and supported IL membranes (SILMs).^[17] Because of their interesting properties and applications, ILs are of interest within various fields, including chemistry, electrochemistry, materials science, chemical engineering and environmental science.^[18]

2.1.2 Properties

ILs are built up from a variety of combinations of cations and anions. The cation is a positively charged "skeleton" and is usually organic, while the anion can be both organic and inorganic.^[19] These cations and anions are designed so that the resulting salt cannot pack compactly, and as a consequence, they do not easily crystallize and therefore remain liquid through a range of temperatures.^[9]

ILs have many unique physical properties that makes them useful in multiple fields. They can be non-volatile, have a near-zero vapor pressure, rate acceleration effects, a wide electrochemical window and high thermal stability. They can also be nonflammable and have solvating properties for diverse kinds of materials, as well as being stable in water and organic solvent.^[9] However, due to the increased research on ILs in the last decades, it has been found that they also can be volatile, flammable and unstable in other solvents.^[18]

The structure of ILs are generally easy to vary. This is useful when preparing ILs for different purposes. Length and number of side chains on the cation, as well as functionalization of the alkyl chains and choice of anions, can be tuned to meet the required properties of the IL and their compatibility with water and organic solvents.^[9] In other words the properties of ILs when it comes to hydrophobicity, polarity and solvent power can be tuned by appropriately combining or modifying the cations and anions.^[3] ILs can also be modified to function as acids, bases or ligands.^[9]

ILs are sometimes categorized into four different types based on the most common types of cations. There are tetraalkylammonium-, tetraalkylphosphonium-, dialkylimidazolium- and *N*-alkylpyridinium-based ILs, see Figure 2.2.^[13]

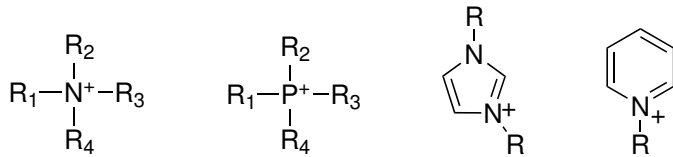


Figure 2.2: Tetraalkylammonium, tetraalkylphosphonium, dialkylimidazolium and *N*-alkylpyridinium cations.

The most popular class of ILs are based on imidazolium cations. The imidazolium rings are often chosen as cations because of their stability within reductive and oxidative conditions,^[20] asymmetry, low viscosity and easy synthetic routes.^[21] They are also popular because of their many applications as catalysts for improvement of reaction time, yield and chemoselectivity.^[13,22] A series of imidazolium ILs are commercially available. This often limits the field of research on ILs, because researchers outside the field of organic chemistry only use the ILs that are readily accessible. Background and expertise within the field of organic chemistry allows for synthesis and design of new ILs.

The properties of ILs strongly depends on the length of the alkyl chain on the cation, and particularly on the type of anion. ILs with acetate anions, for example 1-ethyl-3-methylimidazolium acetate, have shown to be good solvents for cellulose,^[5] while ILs with

2.1 Ionic liquids (ILs)

sulfonate anions, for example 1,3-dialkylimidazolium with trifluoromethanesulfonate (triflate, $[OTf]^-$) as anion, have very good lignin solubility.^[1] Other examples of common cations and anions are illustrated in Figure 2.3.

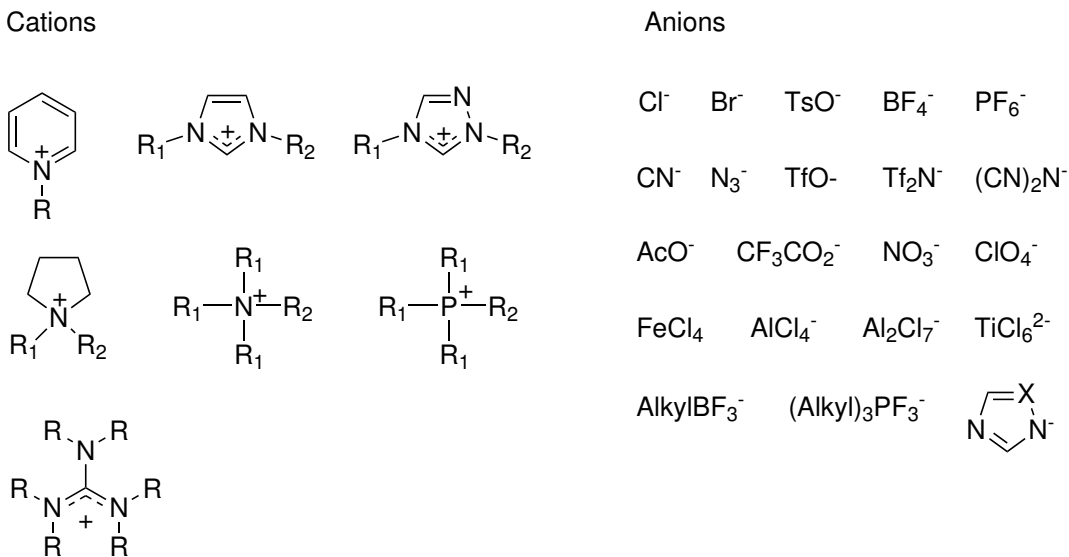


Figure 2.3: Examples of different cations and anions used in ILs.^[9]

2.1.3 Synthesis of ILs

ILs can be synthesized in various ways, but they all follow the same concept. It starts with preparation of the halide salt of cation through quaternization reactions, followed by anion exchange reactions to introduce the desired anion (metathesis). The metathesis can be done in various ways, either by addition of metal salts to precipitate the undesired anion through a Finkelstein reaction^[23] (Figure 2.4 a)), or by addition of a strong Brønsted acid, so the unwanted anion is released as the volatile corresponding acid (Figure 2.4 b)). It can also be done with the use of ionexchange resins or polymer through ion-exchange chromatography (Figure 2.4 c)), or by treatment with Lewis acid to form complex anions (Figure 2.4 d)). Traces of remaining halide ions or acids in the product can alter the melting point, or it can lead to unwanted chemical reactivity.^[9,24]

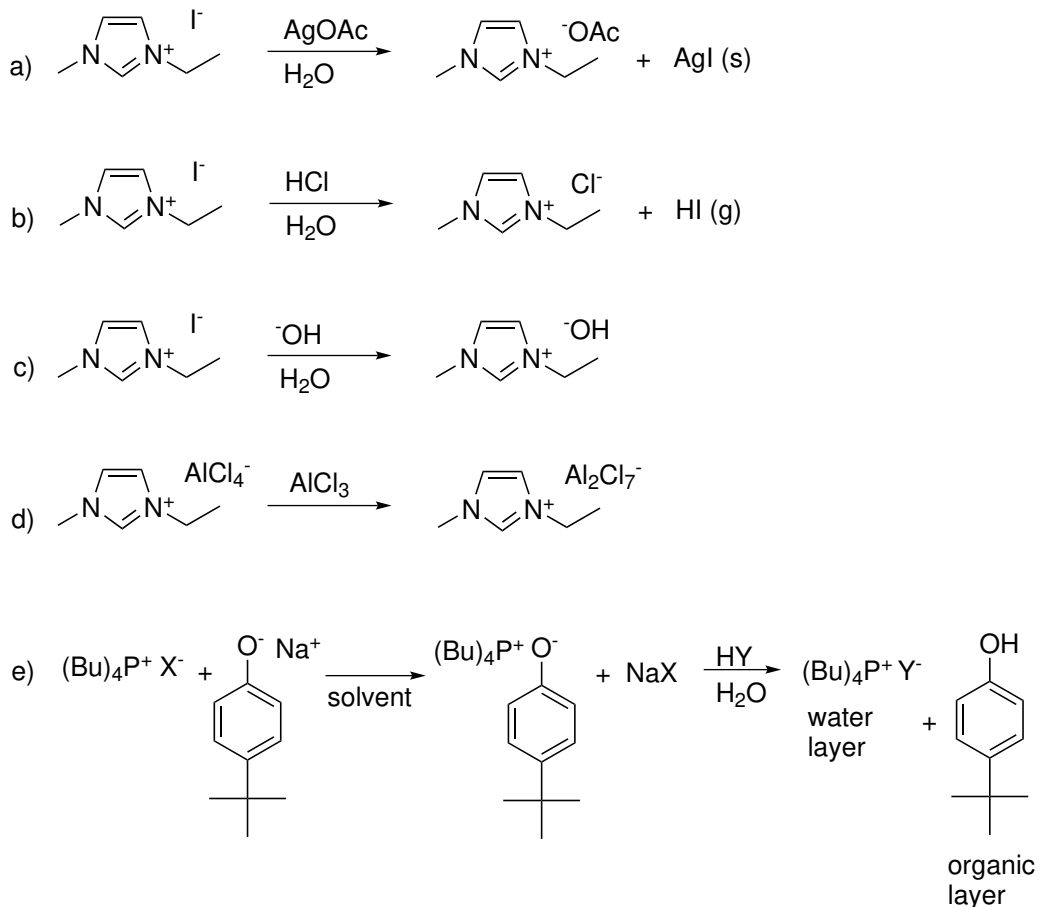


Figure 2.4: Examples of methods for anion exchange. a) Exchange by Finkelstein reaction. b) Exchange by addition of strong Brønsted acid. c) Exchange by the use of exchange resins. d) Exchange by treatment with Lewis acid. e) Exchange by the method called *the phenolate platform*.

A new anion exchange method called the "phenolate platform", involving the use of phenolate anions, was presented by Lethesh K. C. et al. in 2012.^[25] The method takes advantage of the strong basicity of phenolate anions, and an example is presented in Figure 2.4 e). First the 4-*tert*-butylphenolate salt of the desired cation is prepared, then the 4-*tert*-butylphenolate salt is reacted with a Brønsted acid in a two phase system formed by water and a water-insoluble organic solvent. The method was showed to be successful for the synthesis of ILs with 1-butyl-3-methylimidazolium, tetrabutylammonium, tetrabutylphosphonium and 1-butyl-1-methylpyrrolidinium cations and a range of anions. The method can be used for synthesis of ILs that are highly soluble in water, consequently it is not suitable for the synthesis of hydrophobic ILs.

2.1 Ionic liquids (ILs)

2.1.4 Applications

ILs have various applications in chemical reaction processes, and have been suggested as both green solvents, catalysts and reagents.^[18] They can be used for batteries^[19] and in fuel cells,^[26] as well as for nuclear fuel processing.^[27] Also, they can work in nanomaterials,^[28] enzymatic reactions,^[29] pharmaceuticals,^[30] waste recycling^[31] and in solar energy conversion;^[32] not to mention for CO₂ capture,^[33] gas handling^[34] and coal processing.^[35] Furthermore, they can be used for cellulose dissolution,^[5] which is one of the aimed applications of the ILs made by the Fiksdahl group.

As previously mentioned, ILs can be functionalized to work as acids or bases. The group called PILs (protic ILs) are used as Brønsted acid or base in traditional acid-base-catalyzed reactions such as Knovenagel condensation,^[36] Diels-Alder reaction,^[37] Aldol condensation,^[38] Fischer esterification^[39] and pinacol condensation.^[13,40] ILs can also be used for catalytic conversion of lignocellulosic biomass into chemicals and fuel products.^[3] The aim of biomass dissolution is environmentally-friendly production of value added chemicals and fuels.^[3,41]

The main goal of using ILs instead of other solvents or reagents is often to reduce the environmental impact from the industrial process. With this in mind, an important question is whether the ILs will be environmentally-friendly when widely used in industry. Here the toxicity of the ILs will be of importance. Studies of the aquatic toxicity of ILs have shown that they are as toxic or more, as many currently used solvents. Finding the balance between minimal emissions of volatile organic compounds, as well as avoiding spills into waterways is of high priority. Therefore, the focus has been on designing ILs with desired physical properties with low toxicity.^[9]

2.1.5 ILs for use in batteries

The use of ILs in lithium and lithium-ion batteries have been widely studied because of their low vapor pressure. The ILs function as an electrolyte in the batteries, transferring electrons between the electrodes. In theory, the ILs can be used as a one-component electrolyte, instead of the normal three-component system consisting of solvent, supporting electrolyte and electroactive species. However, this is not the case for lithium batteries, as there are no known practical IL with Li cations.^[19] When the vapor pressure of the electrolyte is low, it will increase the battery life because it takes longer time to dry out.

Another positive thing with the IL based battery electrolyte is that they are non-flammable, since they do not contain anything volatile.^[42]

The Fiksdahl research group is studying the use of different ILs as electrolytes in magnesium-ion rechargeable batteries, and the focus is on functionalized ILs containing nitrile and hydroxide groups on the cation. Functional groups on ILs are used to improve the dissolution of magnesium salts in ILs. The ILs in this study are based on imidazolium, pyridinium, pyrrolinium, morpholinium and piperidinium as cations, and bis(trifluoromethylsilyl)amide (Tf_2N^-) as anion. $[\text{Tf}_2\text{N}]^-$ is chosen as anion because $[\text{Tf}_2\text{N}]^-$ -anion based ILs are hydrophobic, which is important because even a small amount of water can affect the performance of ILs as electrolytes. Electrical conductivity and electrochemical stability are the other properties most relevant for the use of ILs as electrolytes in batteries.

2.1.6 ILs for use in membranes for CO_2 capture

ILs have been under investigation for the use as solvents in separation of carbon dioxide from gas streams since the end of the 1990s. Today the most common way of removing CO_2 from gas stream involves passing the CO_2 rich gas through an aqueous amine solution. CO_2 reacts with amine and therefore stays in the solution, while the other components sieve through, still remaining in gas phase. The process has some disadvantages, like the high amine loss due to ILs high volatility, as well as degradation of product due to reaction with oxygen, not to mention the potentially toxic by-products and the high energy requirements.^[33]

Solvents based on ILs maintain consistent capacity of CO_2 absorption because of their characteristic properties. This will not only reduce the CO_2 emissions but also the cost of the process. Till now, most of the studies have focused on RTILs with imidazolium-based cations. Although these ILs have favorable properties, they do lack some important characteristics, such as capacity, gas selectivity, viscosity, stability, solvent cost and overall process cost, compared to the amine solvents.^[43] Because of this, the research focus was moved on to functionalized ILs, where desired characteristic of the ILs are improved by introducing functional moieties, such as amines on ILs.^[33]

The application of ILs as solvents in supported liquids membranes show more potential than the use of IL as solvents alone. The system consists of a supporting porous membrane with IL as solvent, where the IL is incorporated into the pores of the membrane. This method overcomes some of the previous problems concerning viscosity, but not those regarding

2.1 Ionic liquids (ILs)

toxicity and volatility. This field of research is also one of the areas of focus for the Fiksdahl group. Specifically, the focus is on the synthesis of imidazolium and pyridinium based ILs for incorporation into polymer based membranes.

2.1.7 Cellulose dissolution with ILs

Finding a green way for efficiently breaking down cellulose in lignocellulosic biomass is currently under investigation by many research groups. ILs were first reported to be used for the dissolution of cellulose in 2002.^[5] Since then, various ILs have been shown to have the same effect.^[44] However, the challenge is to find an IL that efficiently break down a large wt% cellulose within a reasonable time period. ILs prepared for the purpose of cellulose dissolution need to exhibit specific properties, such as low viscosity, H-bond basicity and low water content.^[44] The ILs also need to exhibit high thermal stability and low toxicity, as well as being easy to recycle and have moderate melting temperature.^[45] ILs designed for cellulose dissolution should possess anions with strong H-bond acceptability and cations containing strong acidic protons. The cations should be without bulky groups that can create steric hindrance, and without highly electronegative atoms such as oxygen. It is stated that the electronegative atoms will decrease the acidity of the protons thereby decreasing the solvation effect.^[46] However, research has shown that poly(ethylene glycol)-functionalized ILs are capable of dissolving 8-12 wt% cellulose.^[47]

Lignocellulosic biomass represents the most abundant form of plant material and comes from woody and herbaceous plants. Lignocellulose makes up the cell walls of woody plants, and consists of 30-50 wt% cellulose, 20-35 wt% hemicellulose and 15-30 wt% lignin.^[3] A schematic illustration of lignocellulose is shown in Figure 2.5.

Cellulose is a polysaccharide consisting of D-glucose units linked together by β -1,4-glycosidic bonds, see Figure 2.5. The stable glucosidic bonds are positioned at the C₁ and C₄ carbon of the glucose molecules, and are reinforced by intramolecular hydrogen bonds, see Figure 2.6. The poly-glucose chains are connected by intermolecular hydrogen bonds, forming stacked layers. The high chemical and mechanical stability of cellulose are formed by the large degree of hydrogen bonds, and makes it difficult to separate cellulose into individual poly-glucose chains. Individual chains on the other hand, can easily be broken down by fermentation or enzymatic treatment.^[1] The inter- and intramolecular hydrogen bonds also make cellulose insoluble in water and common organic solvents.^[44] Efficient and green dissolution of cellulose releases great potential, since various chemicals and high-quality

fuels can be generated from it.^[3]

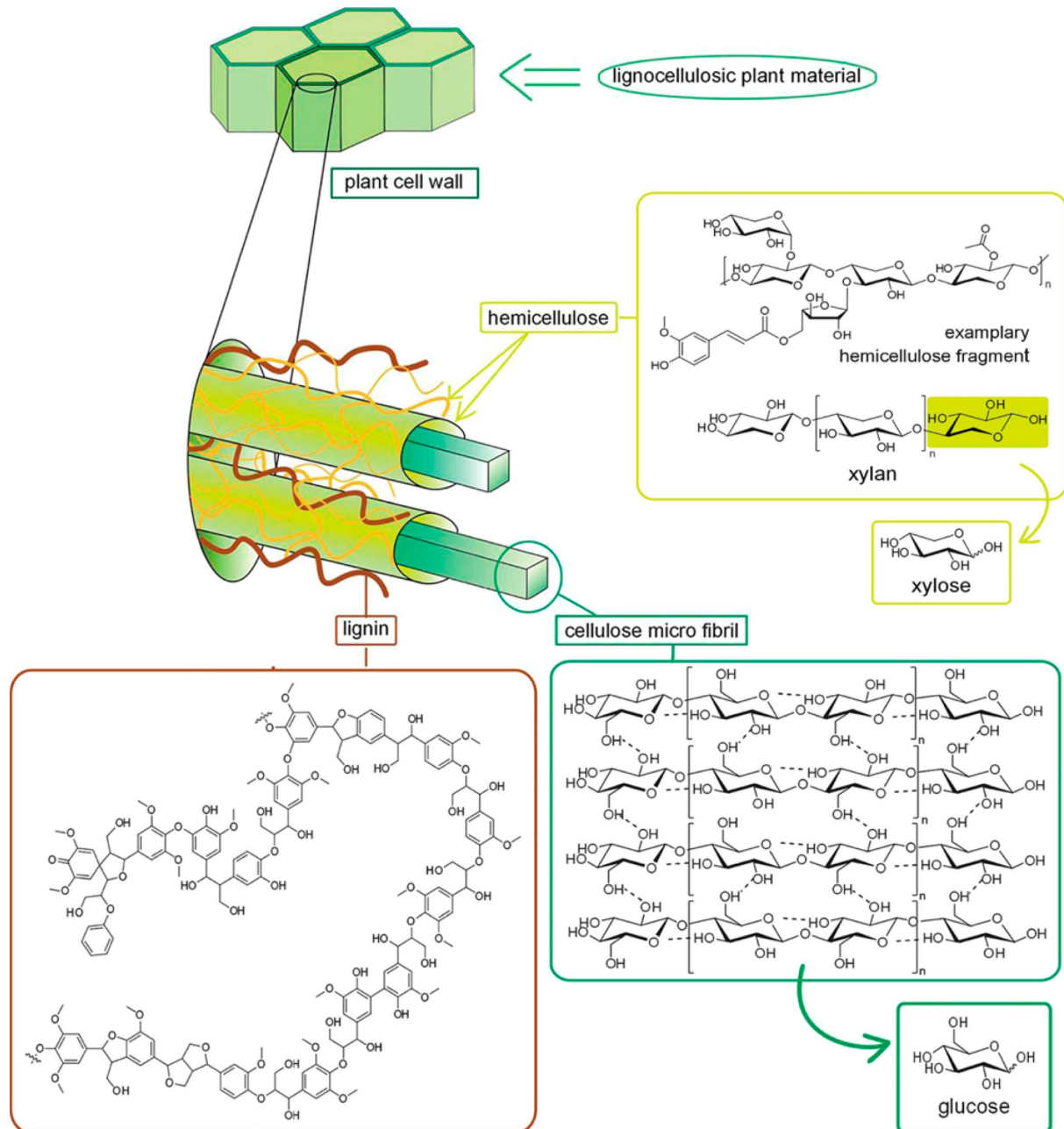


Figure 2.5: Schematic illustration of lignocellulose, from "Catalytic transformation of lignocellulose into chemicals and fuel products in ionic liquids" by Zhan, Song, Han.^[3] Copyright 2013 Royal Society of Chemistry.

2.1 Ionic liquids (ILs)

Due to the interesting properties and potential of ILs, they are still under investigation for use as solvents for cellulose dissolution. The present project in the Fiksdahl group is focusing on the development of new imidazolium based ILs derived from ZIs for cellulose dissolution.

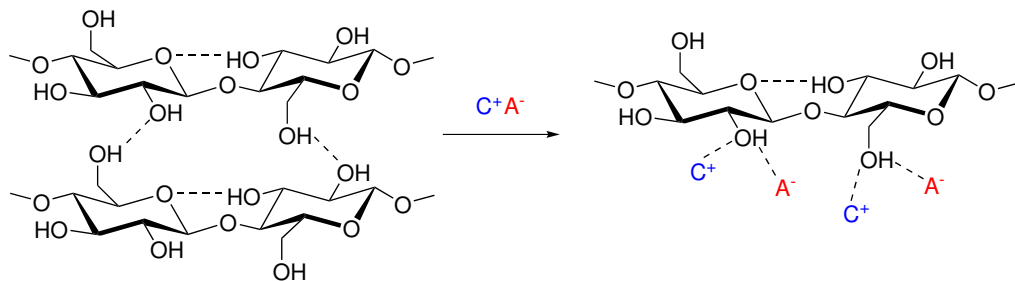


Figure 2.6: Dissolution of glucose chain by IL $[C^+][A^-]$, with C^+ representing cation and A^- representing anion.

The dissolution of cellulose takes place when the hydrogen and oxygen atoms of the cellulose forms electron donor-electron acceptor complexes with the cation and anion of the IL.^[44] A postulated mechanism for cellulose dissolution by ILs is shown in Figure 2.6. ILs with cations based on methylimidazolium and methylpyridinium with allyl-, ethyl-, or butyl-side chains, and chloride, acetate and formate as anions, have shown to be the best options for this purpose so far.^[44]

Research has shown that cellulose can be dissolved in a number of ILs in various degree,^[44] mostly between 5-20 wt%,^[1] and that the cellulose can be regenerated by addition of water, mixtures of water and organic solvents or protic organic solvents.^[1] This can potentially give simple systems for breaking cellulose into more usable materials. An example is the deconstruction of lignocellulosic biomass using ILs, where the IL breaks down the cellulose into single poly-glucose chains as presented in Figure 2.6. The poly-glucose chains can again be depolymerized to glucose using enzymes, or by fermentation with microorganism, making the units usable in the production of bioethanol.

2.1.8 Dissolution of cellulose with ILs/organic solvent solution

Even though dissolution of cellulose using ILs is efficient, it also have some downsides, such as high viscosity of the obtained IL-cellulose solution,^[48] slow dissolution rate^[44] and high costs of ILs.^[6] Research has shown that problems due to the high viscosity can be avoided by the use of polar solvents in the dissolution process.^[6,49] Polar solvents such as DMSO

and DMF have shown to be particularly efficient.^[6] Research by Rinaldi also shows that the hydrogen-bond basicity of the solvent system is essential for the dissolution of cellulose, which means that cellulose acts like a hydrogen-bond donor in the solution.^[6] The cellulose is not soluble in pure solvent, but dissolves in the low viscosity solution of IL and solvent.^[6]

2.2 Zwitterions (ZIs)

Zwitterions (ZIs) are molecules that contains both positive and a negative charge on the same molecule, making the molecule electrically neutral. Amino acids are examples of natural zwitterions.^[50] Zwitterions that are liquid at room temperature are called zwitterionic liquids (ZILs).^[51] Research has shown that the use of repeating units of ethylene oxide can reduce the melting points of ZI making them ZILs at room temperature.^[52]

2.2.1 ILs derived from ZIs and IL toxicity

A new method for preparation of ILs that was not mentioned in Section 2.1.3 is the synthesis of ILs via ZIs. ILs can be derived from ZIs by addition of acid. Hydrogen from the acid will protonate the ZI and the corresponding conjugated of the acid will act as the anion forming an IL (Figure 2.7).

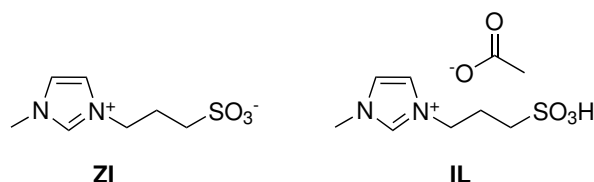


Figure 2.7: Example of ZI and IL derived from ZI.

Toxicity is an important property to consider when designing new ILs, especially if they are going to replace common organic solvents or be used for cellulose dissolution. As previously mentioned, research has shown that the toxicity of ILs can be similar to, or worse than that of common organic solvents.^[53] Research has also shown that one of the most commonly used cations, the imidazolium cation, is relatively toxic, and that ILs toxicity is mostly a function of the alkyl chain length of the cation.^[54] Fortunately, toxicity of ILs is one of the properties that can be altered by design. Research by Tang et al. has shown that the toxicity of imidazolium based ILs can be lowered by introducing hydroxyl and ether

2.3 Characterization methods for ILs and cellulose

functionalities to the side chains of the imidazolium.^[55] Also, research by Kuroda et al. shows that the toxicity problem of ILs can be solved by introduction of polar anions at the end of the alkyl chain on cation, thereby making ZIs.^[54] From the ZI, less-toxic ILs can be made by protonation with addition of a strong acid.

2.3 Characterization methods for ILs and cellulose

Identification and characterization of ILs and their properties involve analytical techniques not commonly used in organic chemistry. Thermogravimetric analysis (TGA) is used to determine the thermal stability of ILs and cellulose, and X-ray diffraction (XRD) is used to measure the crystallinity of cellulose. Details of these techniques will be presented in this section.

2.3.1 Thermogravimetric analysis and thermal stability of ILs

TGA is a technique used to measure the mass of a substance as a function of temperature or time while the sample is subjected to a temperature program in a controlled atmosphere.^[56] TGA measurements provides a weight loss curve as the temperature changes. The measured curve give information on changes in sample composition, the samples thermal stability, and kinetic parameters for chemical reactions.^[57] Both the short-term and long-term thermal stability can be measured using TGA. The short-term thermal stability of ILs are usually presented as the temperature at which the mass has decreased by 10 wt%.

Thermal stability of ILs depends on the molecular structure, i.e. the type of cation and anion as well as modifications on cation like chain length or the nature of the substituents. Anion type has most impact on thermal stability of ILs, then comes the type of cation and cation modifications which has the least impact. The thermal stability of an IL increases with shorter chain length and for ILs with hydroxyl-functionalization the thermal stability depends on type of anion.^[58]

For investigation of the thermal decomposition mechanism of ILs, thermogravimetric analysis-mass spectroscopy (TG-MS), nuclear magnetic resonance (NMR), Fourier transform infrared spectroscopy (FTIR), density functional theory (DFT) and X-ray photoelectron spectroscopy (XPS) are commonly used.^[59] Degradation mechanisms for imidazolium ILs will be discussed in Section 3.4.2.

2.3.2 X-ray diffraction

XRD is a non-destructive analytical technique used for phase identification and studies of crystal structure of crystalline materials. X-rays are electromagnetic radiation with wavelengths between 0.1 Å and 100 Å. Since this is similar to the interatomic distance in a crystal, it allows crystal structure to diffract X-rays.^[60]

Interactions like absorption and scattering effects takes place when X-ray photons reach matter. When the matter is a crystalline material, the X-rays will be scattered in constructive and destructive radiation which leads to characteristic diffraction phenomena. These diffraction patterns can be studied to investigate the crystal structure of the material.^[60]

A crystal structure is built up by planes. X-rays with a wavelength similar to these planes can be reflected such that the angle of the reflection is equal to the angle of the incidence. This is called diffraction, and is described by Bragg's law:

$$2dsin\theta = n\lambda \quad (2.1)$$

Here d is the lattice spacing between the diffraction planes in nm, θ is the incident angle in degree, n is the order of diffraction, and λ is the wavelength of the beam in nm. The geometrical conditions for diffraction is illustrated in Figure 2.8.^[60]

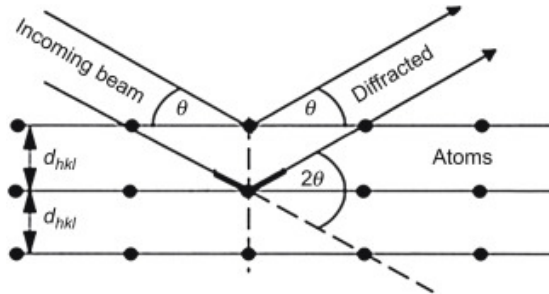


Figure 2.8: Geometrical condition for diffraction from lattice planes.^[61]

The pattern created from electron diffraction of crystals can reveal the nature of the crystallographic symmetry, which means the periodicity of the structure, the distribution of atoms in the unit cell and the shape of the crystal. Using peak position, the lattice parameter, chemical composition and space group can be investigated. The peak intensity can give information about the crystal structure and texture. The shape of the peak gives information about sample broadening contribution, meaning microstains and crystallite size.^[60]

2.4 Triazoles

After cellulose has been dissolved in ILs, it can be regenerated by use of an appropriate solvent. XRD can then be used to study changes in the crystal structure of the regenerated cellulose.

2.4 Triazoles

Triazoles are five member heteroaromatic rings that contain three nitrogens and two carbons. Depending on the position of the nitrogens, two different isomers are possible, as depicted in Figure 2.9

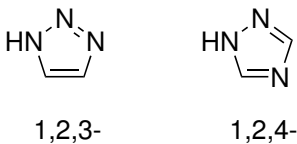
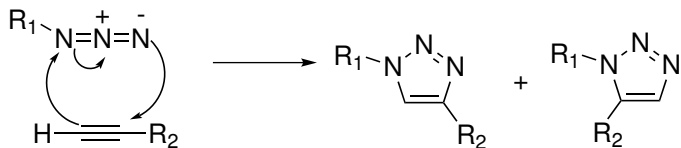


Figure 2.9: 1,2,3-triazole and 1,2,4-triazole.

1,2,4-Triazoles can be prepared by various methods, for example by reacting hydrazines and formamide under microwave irradiation, thereby ending up with substituted 1,2,4-triazoles.^[62] They can also be prepared by a multicomponent process reacting anilines, amino pyridine and pyrimidines, ending up with 1-aryl-1,2,4-triazoles.^[63]

1,2,3-Triazoles can also be prepared in different ways, that all goes under the common name, Click reactions. The most common is by the Huisgen azide-alkyne 1,3-dipolar cycloaddition,^[64] depicted in Scheme 2.1. Other commonly known preparation methods are copper-catalyzed azide-alkyne cycloaddition (CuAAC)^[65,66] or ruthenium-catalyzed azide-alkyne cycloaddition (RuAAC).^[67,68]

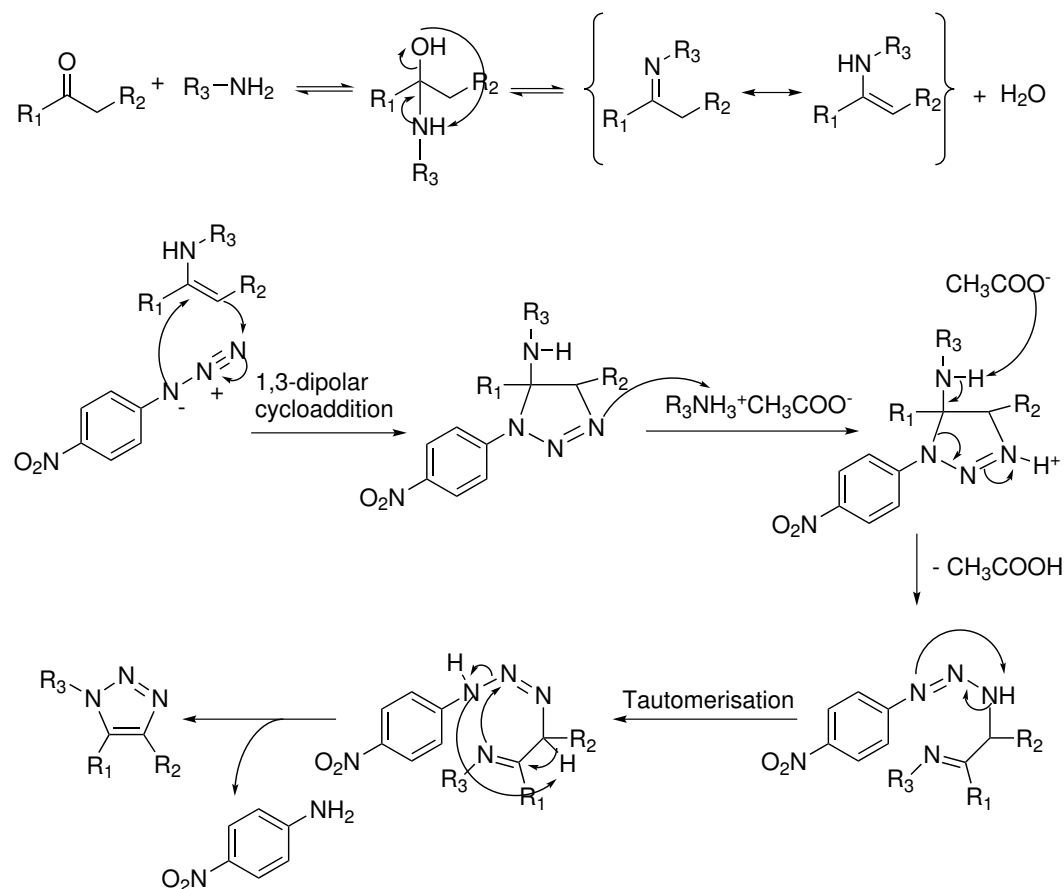


Scheme 2.1: Mechanism for Huisgen azide-alkyne 1,3-dipolar cycloaddition.

The 1,2,3-triazoles can have substituents in various positions. The 1,4- and 1,5-disubstituted products are most commonly accessed by CuAAC or RuAAC reactions, respectively. A problem with the CuAAC and RuAAC are the presence of trace metal contamination following the production of triazoles.^[69] Exploration of CuAAC and RuAAC reactions have

come to a halt, because of the limited access of terminal alkynes, as well as the toxicity of heavy metal catalysts.^[7] Organocatalytic methods for preparation of functionalized 1,2,3-triazoles have been studied, but are limited to aromatic groups at the N1 position of the triazole, and they are mostly based on hazardous, non-commercial azides.^[70–72] Metal-free methods for the synthesis of 1,4-disubstituted 1,2,3-triazoles have been developed,^[73] but options for regioselective preparation of 1,5-disubstituted 1,2,3-triazoles are limited.^[69,74] Therefore, a general metal-free procedure for regioselective synthesis of 1,5-disubstituted 1,2,3-triazoles under mild conditions and with the use of readily available substrates are of great interest.

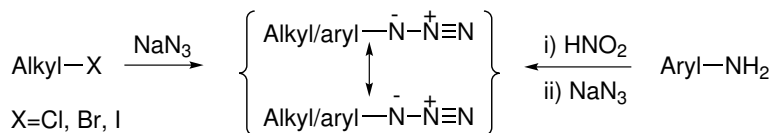
In 2016 Thomas et al. presented a new method for regioselective preparation of 1,5-disubstituted 1,2,3-triazoles from readily available primary amine, azides and ketones.^[7] The method starts with condensation of ketone and amine, forming imine and water. The equilibrium can be shifted towards imine by the removal of water, or in this case by further reaction of the imine with azide. The method for triazole formation is not based on the conventional Click chemistry, but is a rather new reaction. The reaction makes it possible to access regioselective 1,5-disubstituted products that otherwise would be difficult to prepare. Proposed mechanism for the reaction is presented in Scheme 2.2.



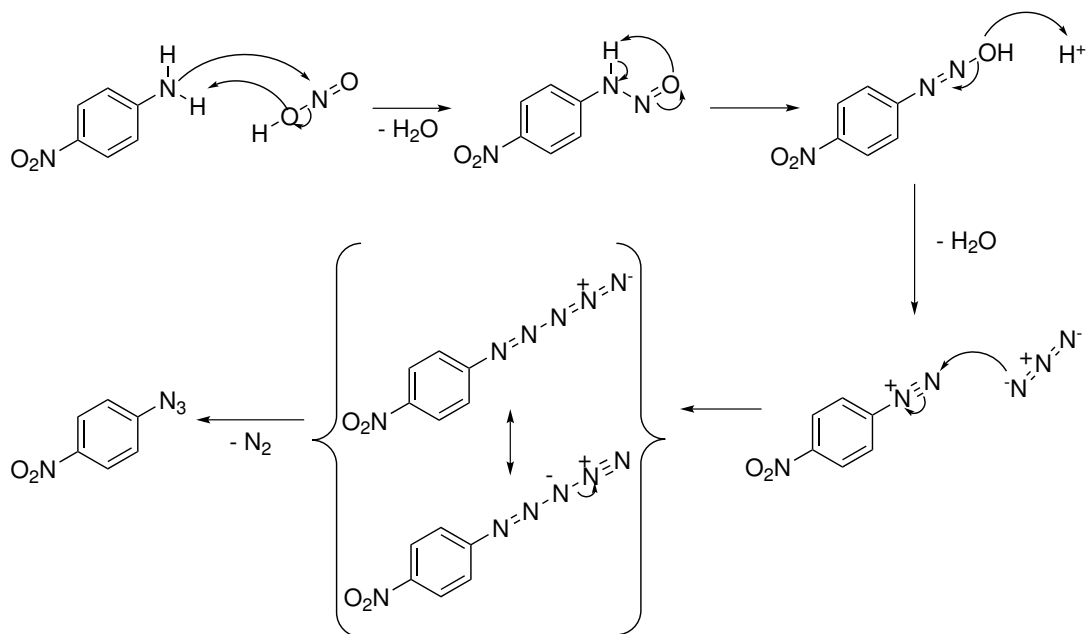
Scheme 2.2: Mechanism for the regioselective formation of 1,5-disubstituted 1,2,3-triazole from ketone, amine, 4-nitrophenyl azide and acetic acid, suggested by Thomas et al. in 2016.^[7]

2.4.1 Azides

Azides are known to be explosive, especially inorganic azides and low molecular weight covalent organic azides.^[75] They often function as intermediates for synthesis of various nitrogen-containing compounds, and are prepared by nucleophilic substitution, specifically $\text{S}_{\text{N}}2$ of alkyl halide with an inorganic azide. Aryl azides are prepared by diazotization of the appropriate diazonium salt with sodium azide.^[76] The preparation of organic azides are illustrated in Scheme 2.3, and mechanism for the formation of 4-nitrophenyl azide is depicted in Scheme 2.4.



Scheme 2.3: Formation of alkyl/aryl azide from alkyl halide and aryl amine. Azide shown with resonance structures. Reproduced from^[77] with permission.



Scheme 2.4: Mechanism for formation of 4-nitrophenyl azide from 4-nitroaniline and nitrous acid.

Azides are useful in many reactions, like the Curtius rearrangement^[78] or the Schmidt reaction,^[79] but the most famous is the previously mentioned Huisgen azide-alkyne 1,3-dipolar cycloaddition giving substituted 1,2,3-triazole.^[80]

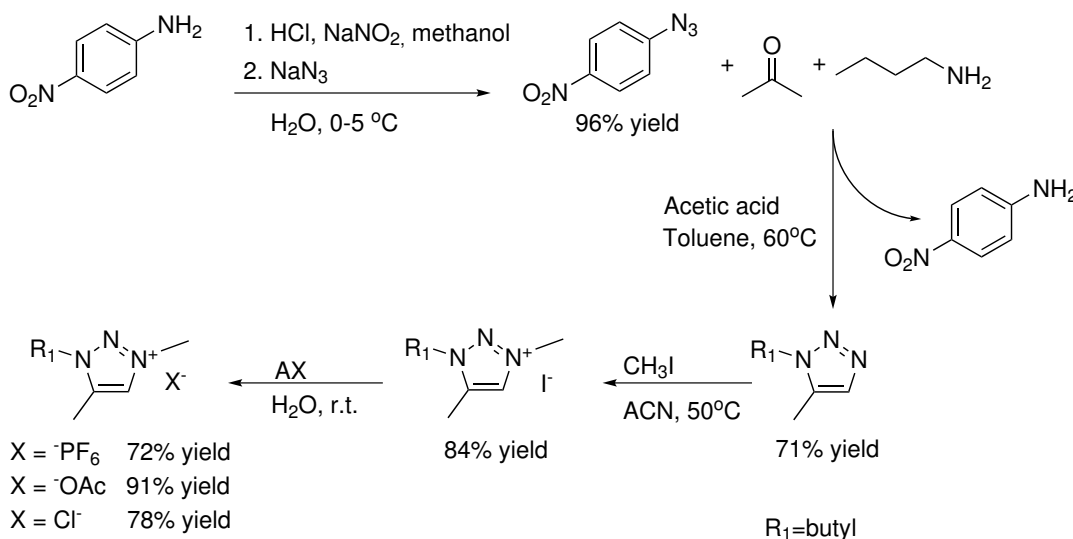
2.5 Preliminary studies

Studies and optimization of the regioselective synthesis of 1,5-disubstituted 1,2,3-triazoles, previously mentioned in Section 2.4, was performed by the Fiksdahl group in the fall of 2017.^[8] From the novel 1,5-disubstituted 1,2,3-triazole, new 1,3,5-trisubstituted 1,2,3-triazolium ILs were prepared for cellulose dissolution purposes. A poster from the Organic Chemical Winter meeting in 2018, showing some of the results from the study, is presented

2.5 Preliminary studies

in Appendix A.^[81]

From the optimization studies I found that 1:1:2 equivalents of 4-nitrophenyl azide, acetone and butylamine, with addition of 0.3 equivalent acetic acid gave the best yield, with 71 % of 1-butyl-5-methyl-1,2,3-triazole. The total synthesis performed in the preliminary project is presented in Scheme 2.5. 4-Nitrophenyl azide was needed for the optimization studies and was synthesized in 96 % yield. From 1-butyl-5-methyl-1,2,3-triazole, IL 1-butyl-3,5-dimethyl-1,2,3-triazolium iodide was obtain in 84 % yield, by quaternization using methyl iodide. From the iodide IL, three new ILs with the same triazolium scaffold were prepared by anion exchange. The exchanges were done using the inorganic salt KPF₆, through a Finkelstein reaction with AgOAc and by ion-exchange chromatography using Amberlite in hydroxide form followed by an acid-base reaction using addition of HCl, respectively. The reactions respectively yielded the ILs in 72 %, 91 % and 78 %.



Scheme 2.5: Synthesis and yields of compounds produced in preliminary project.

It was also found that the reaction could be performed without addition of acetic acid, still obtaining satisfying yield.^[8] Based on this finding, a new reaction mechanism was proposed, and is presented in Scheme 3.4 in Section 3.1.4.

3 Results and discussion

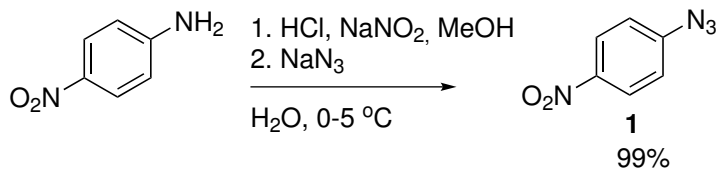
This section covers the synthesis of triazoles and triazolium ILs, as well as the synthesis of imidazolium based ZIs and their corresponding ILs. Thermal stability of the synthesized ZI derived ILs are discussed along with their thermal degradation mechanism, as well as a thorough discussion on the ILs cellulose dissolution abilities.

All new compounds are fully characterized by NMR, FTIR and HRMS. ILs are characterized by both positive and negative mode HRMS. The chemical shift values of the new compounds are presented in this section. Thermal stability of ILs are measured by TGA and the crystallinity of untreated cellulose and regenerated cellulose from ILs are measured with XRD.

3.1 Preparation of 1,5-disubstituted 1,2,3-triazoles

1,5-Disubstituted triazoles (**2**, **3**) were synthesized using the synthetic approach of Thomas et al.^[7] Optimization of the triazole reaction using various aromatic substituents was performed.

3.1.1 Synthesis of 4-nitrophenyl azide (**1**)



Scheme 3.1: Synthesis of azide **1**.

4-Nitrophenyl azide (**1**) was required for preparation of 1,5-disubstituted 1,2,3-triazoles. Preparation of azide **1** was done through diazotization of 4-nitroaniline by reaction with hydrochloric acid, sodium nitrite and sodium azide as presented in Scheme 3.1. The reaction goes by azide substitution of the diazonium ion, with release of water and nitrogen gas. The reaction mechanism is described in Scheme 2.4 in Section 2.4.1. After work up by extraction using ethyl acetate and washing with saturated NaHCO_3 , azide **1** was obtained in 99 % yield as a yellow solid. The ^1H NMR shifts of azide **1** were assigned (Figure 3.1) and corresponded to literature values.^[82] Spectrum for azide **1** is presented in Appendix B.

3.1 Preparation of 1,5-disubstituted 1,2,3-triazoles

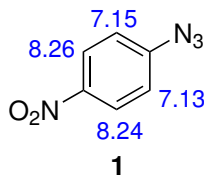
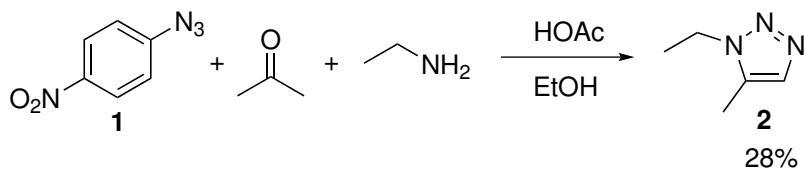


Figure 3.1: ^1H NMR shifts of azide **1**.

3.1.2 Synthesis of 1-ethyl-5-methyl-1,2,3-triazole (**2**)

The method used to synthesize triazoles **2** and **3** was first presented by Thomas et al. in 2016.^[7] This synthesis makes it possible to prepare regioselective 1,5-disubstituted 1,2,3-triazoles without the use of metal- or organo-catalyst. Consequently, the method makes it possible to synthesize triazoles that can not be prepared by conventional methods. The standard Cu- or Ru-catalyzed azide-alkyne [2+3] cycloadditions (CuAAC, RuAAC) have limitations concerning regioselective preparation of 1,5-disubstituted 1,2,3-triazoles. CuAAC regioselectively makes 1,4-disubstituted triazoles, while RuAAC makes 1,5-disubstituted triazoles, but only from terminal alkynes, which strongly limits the scope of the reaction. Therefore, neither CuAAC nor RuAAC are optimal for regioselective preparation of 1,5-disubstituted 1,2,3-triazole compounds. Studies have been done on the preparation of 1,2,3-triazoles via organo-catalysis instead of metal-catalysis, but the reactions have limitations.^[70–72] The reactions are limited to substituents at the triazoles N1 position. Also, most of the reported transformations use non-commercial and potentially hazardous organic azides.^[7]



Scheme 3.2: Synthesis of triazole **2**.

Triazole **2** was prepared from azide **1** by reaction with acetone, ethylamine and acetic acid, as presented in Scheme 3.2. The reaction starts with formation of Schiff base from acetone and ethylamine. The Schiff base further reacts with azide **1**, forming triazole **2** through a mechanism involving tautomerisation of enamine followed by 3+2 cycloaddition and aromatization with formation of 4-nitroaniline (Scheme 2.2, Section 2.4). Isolation of the product by flash column chromatography produced triazole **2** as a dark brown liquid

3.1 Preparation of 1,5-disubstituted 1,2,3-triazoles

in 28 % yield. ^1H and ^{13}C NMR shifts of triazole **2** were assigned, and are presented in Figure 3.2. Spectra for triazole **2** are presented in Appendix C.

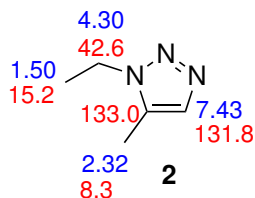


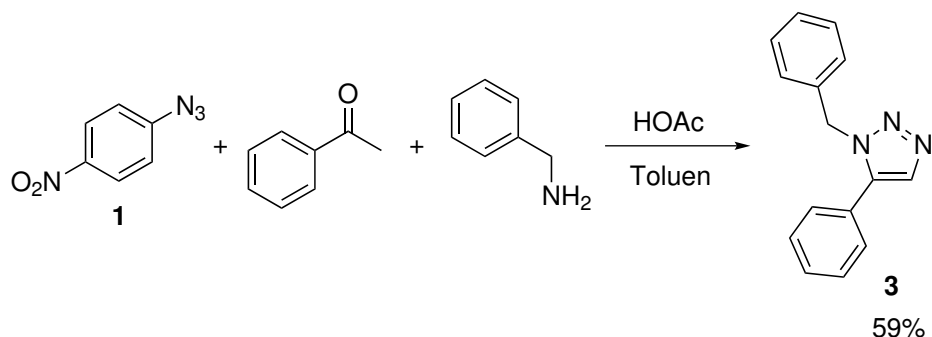
Figure 3.2: ^1H and ^{13}C NMR shifts of triazole **2**.

The yield of the reaction was low, and it is believed to be due to the low boiling point of ethylamine (bp = 16.6 °C). Even with large excess (8.0 eq) ethylamine, substantial parts of the amine will evaporate at room temperature before the reaction has started. The ethylamine used in the reaction was a solution of 70 % ethylamine in H₂O. Water from this solution along with the water produced during the reaction shift the carbonyl + amine ⇌ imine + H₂O equilibrium, thereby decreasing the formation of Schiff base and resulted in a lowering of the final yield. Addition of molecular sieves favors imine formation by shifting the equilibrium to the left, and could therefore improve the final yield. Because of the low yields further alkylation and preparation of IL was not attempted.

3.1.3 Synthesis of 1-benzyl-5-phenyl-1,2,3-triazole (**3**)

1-Benzyl-5-phenyl-1,2,3-triazole (**3**) was prepared from azide **1**, acetophenone, benzylamine and acetic acid, following the same mechanism as described for triazole **2** in Section 3.1.2. The reaction is presented in Scheme 3.3. Isolation of the product using flash column chromatography gave triazole **3** in 59 % yield as a dark brown semi liquid/solid.

3.1 Preparation of 1,5-disubstituted 1,2,3-triazoles



Scheme 3.3: Synthesis of triazole **3**.

^1H and ^{13}C NMR shifts of triazole **3** were assigned and are presented in Figure 3.3. Due to overlapping of peaks in the aromatic region in both ^1H NMR, ^{13}C NMR and HSQC, specific shifts were not assigned to aromatic atoms, but are listed next to the molecule. Spectra for triazole **3** can be seen in Appendix D.

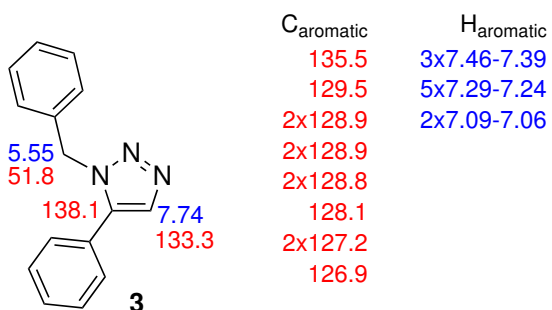
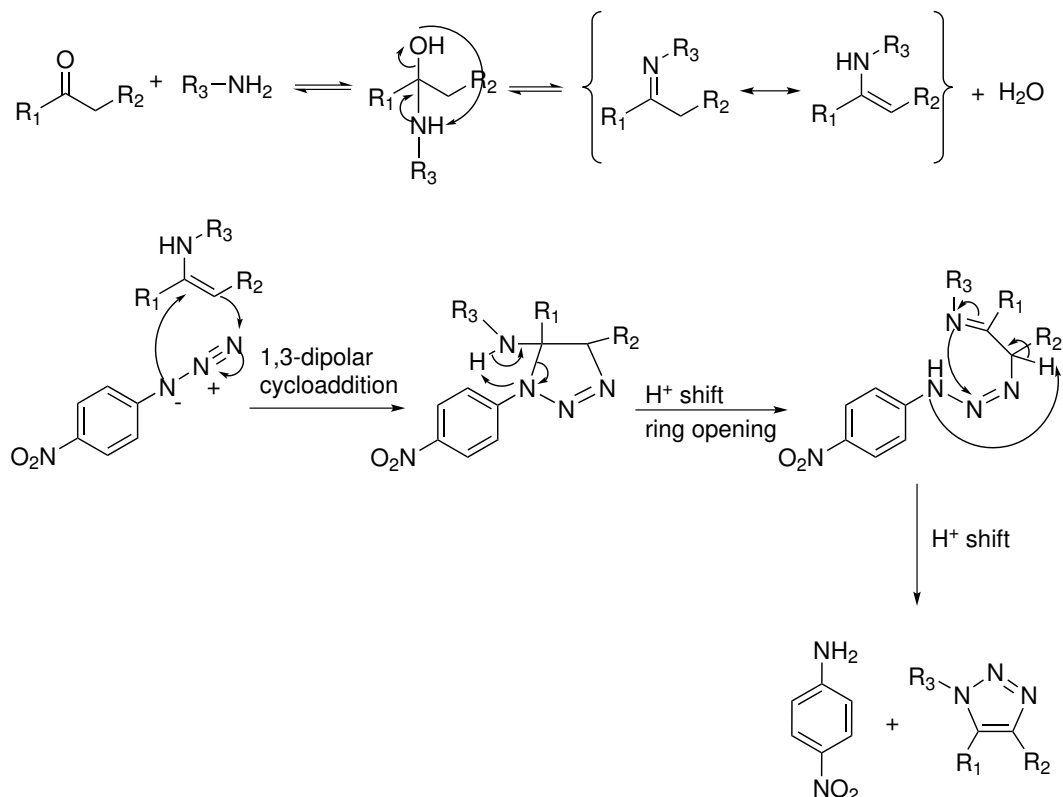


Figure 3.3: ^1H and ^{13}C NMR shifts of triazole **3**.

3.1.4 Mechanism for formation of 1,5-disubstituted 1,2,3-triazoles

In the preliminary studies leading up to this master's project, a new possible mechanism for the regioselective formation of 1,5-disubstituted 1,2,3-triazoles was postulated based on experimental results.^[8] The mechanism is presented in Scheme 3.4, and is a simplified version of the mechanistic proposal of Thomas et al. presented in Scheme 2.2 in Section 2.4. Both mechanism starts with a Schiff base formation, followed by a 1,3-dipolar cycloaddition. The mechanism proposed by Thomas et al.^[7] goes through two acid catalyzed steps followed by tautomerisation and then an aromatization reaction to give the final product. The new mechanism only goes through a proton shift with ring opening followed by aromatization forming the final product. The preliminary project showed that the reaction

gives good yield even without the addition of acid, therefore, the new proposed mechanism does not include any acid catalyzed steps.^[8] In contrast to regular Click chemistry (Huisgen cycloaddition, CuAAC and RuAAC) where the azide is the source of all three nitrogens, the azide in this reaction is only the source of two nitrogens. This makes the reaction an indirect type of Click reaction.



Scheme 3.4: Mechanism for the regioselective formation of a 1,5-disubstituted 1,2,3-triazole from ketone, amine and 4-nitrophenyl azide.^[8]

3.1.5 Optimization of triazole reactions

Several new 1,5-disubstituted 1,2,3-triazoles were synthesized using the synthetic method of Thomas et al.^[7] described in Section 3.1.2. Syntheses and results are described in Table 3.1.

As aforementioned, triazole **2** was successfully synthesized, but in low yields (27-28 %) (entries 1, 2 and 3). The reaction was first performed at 60 °C with toluene as solvent, assuming that ethylamine would reflux and participate in the synthesis. Unfortunately that was not the case and the synthesis did not give any product. Lowering the reaction

3.1 Preparation of 1,5-disubstituted 1,2,3-triazoles

temperature to room temperature, changing solvent to EtOH and increasing the amount of amine from 2.0 to 3.0 equivalents gave triazole **2** in 27 % yield. Increasing the amount of amine from 3.0 to 8.0 equivalents on the other hand, only increased the yield by 1 % (28 %).

Addition of an oxygen containing aromatic group on the triazole was attempted based on a previous reported reaction with 4-methoxyaniline and acetophenone.^[7] The synthesis was attempted by the use of 3-aminophenol and acetone (entry 4), but the reaction was unsuccessful and did not give any of the desired product. Since the reaction did not give any product, a new reaction was performed using aniline instead of 3-aminophenol (entry 5-7), assuming that the oxygen in meta position lowered the reactivity. The solvent was changed back to toluene and the first reaction (entry 5) was performed with the same conditions as the previous one (entry 4). Still the reaction did not give any product, so the temperature was increased from 60 °C to 120 °C (entry 6). Since this did not give any positive results either, a new attempt was made, this time using 5.0 equivalent acetone instead of 1.0 equivalent (entry 7). Again, the reaction was unsuccessful.

The reaction was attempted yet again, this times using acetophenone as reactive ketone along with aniline as amine (entry 8). Unfortunately, this was not a success, neither at 60 °C (entry 8) nor 100 °C (entry 9). Realizing that the problem might be due to the choice of aryl amine. The low reactivity of amine is because of delocalization of the nitrogens electrons to the aromatic ring. A final reaction was performed (entry 10) by use of an amine with a benzyl substituent instead of a phenyl substituent, and it gave triazole **3** in 59 % yield. The carbon between the nitrogen and the benzyl group prevents the delocalization of nitrogen electrons and therefore increase the reactivity of the amine.

3.1 Preparation of 1,5-disubstituted 1,2,3-triazoles

Table 3.1: Optimization of the synthesis of 1,5-disubstituted 1,2,3-triazoles.

Entry	Azide (eq)	Ketone (eq)	Amine (eq)	Acid (eq)	Solvent	Temp.	Yield
					Toluene		
1	1	1	2	0.3	toluene	60 °C	0 %
2	1	1	3	0.3	EtOH	r.t.	27 %
3	1	1	8	0.3	EtOH	r.t.	28 %
					X EtOH		
4	1	1	2	0.3	EtOH	60 °C	0 %
					X Toluene		
5	1	1	2	0.3	toluene	60 °C	0 %
6	1	1	2	0.3	toluene	120 °C	0 %
7	1	5	2	0.3	toluene	120 °C	0 %
					X Toluene		
8	1	1	2	0.3	toluene	60 °C	0 %
9	1	1	2	0.3	toluene	100 °C	0 %
					Toluene		
10	1	1	2	0.3	toluene	100 °C	59 %

3.2 Preparation of triazolium based ILs

3.2 Preparation of triazolium based ILs

Beside investigation of the triazole reaction itself, the intention of synthesizing new 1,5-disubstituted 1,2,3-triazoles were preparation of 1,3,5-trisubstituted 1,2,3-triazolium ILs. The IL was prepared by *N*-alkylation of the triazole followed by anion exchange. Because of the low yields obtained for triazole **2**, preparation of IL was only pursued for triazole **3**.

3.2.1 Synthesis of 1-benzyl-3-ethyl-5-phenyl-1,2,3-triazolium iodide (**4a**)

IL **4a** was prepared by quaternization of triazole **3** with an excess of iodoethane, and was obtained in 66 % yield as a brown viscous liquid. The reaction scheme is depicted in Table 3.2. The quaternization was a slow process and the reaction time was 46 hours.

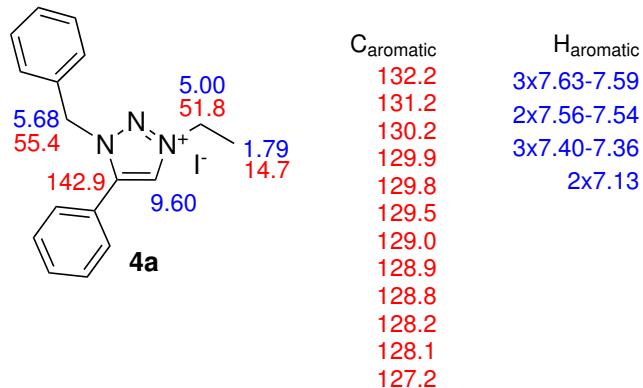


Figure 3.4: ¹H and ¹³C NMR shifts of triazole **4**.

¹H and ¹³C NMR shifts of triazole **4a** were assigned and are presented in Figure 3.4. Because of overlapping chemical shift values in the aromatic region on both ¹H and ¹³C NMR, the aromatic shifts were not assigned to specific atoms, but are listed next to the molecule. Spectra for IL **4a** are presented in Appendix E. IR was not taken due to small amount of sample and the need for use of triazole **4a** in further synthesis.

3.2.2 Optimization of triazole alkylation

The synthesis of triazolium IL was performed by *N*-alkylation of triazole **3** through a quaternization reaction. Triazole **3** was alkylated using different alkyl halides (iodide and bromide). Bromide is preferred as counter ion over iodide, because it makes anion exchange

in a further step easier and less expensive. When using alkyl bromide as quaternization reagent, the subsequent anion exchange to acetate can be done using NaOAc or KOAc, because NaBr and KBr can easily be precipitated in common solvents like dichloromethane. NaI on the other hand, is soluble in most common solvents, including water, methanol, acetone, acetonitrile, dimethylformamide and dichloromethane. This makes removal of iodide after anion exchange using NaOAc very challenging. If alkyl iodide is used in the quaternization reaction, AgOAc should be used when performing the final anion exchange. For laboratory scale this will not cause any problems, as AgI is easy to precipitate and gives clean, halide free ILs, but from an industrial point of view, AgOAc is too expensive. Complete removal of halides after anion exchange is essential, because halide impurities can influence the chemical and physical properties of ILs, such as viscosity, density and thermal stability.^[83]

Table 3.2: Triazole alkylation

Entry	Alkyl (eq)	n	Temp	Rx. time	Yield
1	Bromoethane	1	40 °C	66h	0 %
2	Bromobutane	3	80 °C	48h	0 %
3	Iodoethane	1	70 °C	46h	66 %

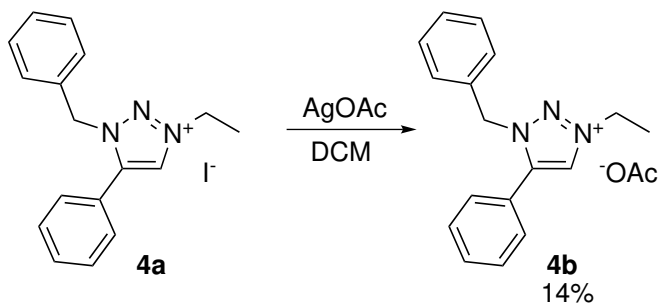
The first alkylation was attempted using bromoethane (entry 1, Table 3.2). Because of the low boiling point of bromoethane ($\text{bp} = 38\text{ }^\circ\text{C}$) the reaction temperature had to be kept low and a cooler was used to make the reaction mixture reflux. After a reaction time of 66 hours no alkylation had taken place on the triazole. The next reaction was performed using bromobutane, which has a higher boiling point ($\text{bp} = 102\text{ }^\circ\text{C}$), allowing harsher reaction conditions (entry 2). After 48 hours at $80\text{ }^\circ\text{C}$ there had not been formed any alkylation product. Since neither bromoethane nor bromobutane gave any alkylated product, iodoethane was used as alkylating reagent. After 46 hours at $70\text{ }^\circ\text{C}$ this yielded 66 % alkylated product (IL **4a**) as a dark brown viscous liquid.

3.2 Preparation of triazolium based ILs

Upscaling of the alkylation reaction was attempted, but the viscosity of the IL made the purification by washing with organic solvent difficult. The upscaled reaction mixture still contained unreacted triazole after washing ethyl acetate, diethyl ether and water. Due to time limitations, new attempts of upscaling were not performed.

3.2.3 Synthesis of 1-benzyl-3-ethyl-5-phenyl-1,2,3-triazolium acetate (**4b**) through anion exchange

Anion exchange from iodide (IL **4a**) to acetate (IL **4b**) was performed using silver acetate through a Finkelstein reaction (Scheme 3.5). After workup by removal of precipitated AgI by filtration, the reaction obtained IL **4b** in 14 % yield as a dark brown liquid. The low yield is a result of repeated washing and filtration, normally the yield after anion exchange would be between 60 % and 70 %. Because of the low yield testing of cellulose dissolution could not be performed.



Scheme 3.5: Synthesis of IL **4b**.

Negative mode HRMS of IL **4b** shows acetate but no iodide anion in the product, and the positive mode HRMS shows alkylated triazole, but no unalkylated triazole. The NMR results on the other hand, are a bit unclear. NMRs were taken within one day after the anion exchange was performed, and shows a small amount of unalkylated triazole. A new NMR was taken after 8 weeks, and both the ¹H and ¹³C NMR now show that the product had decomposed. This is especially clear on the ¹³C NMR where there are twice the number of peaks. ¹H and ¹³C NMR after 1 day and 8 weeks can be seen in Appendix F. From these results we can conclude that the product is not stable at room temperature.

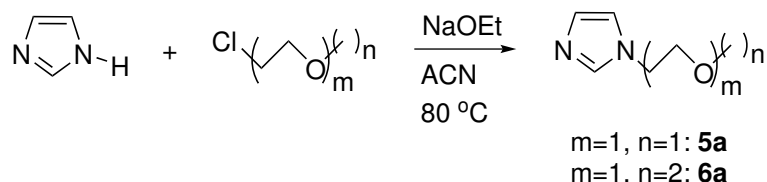
3.3 Preparation of imidazolium based ZIs

This section will cover the synthesis of new ILs prepared from imidazolium based ZIs. Unlike common preparation of ILs, this method does not require anion exchange, which also eliminates problems with halide impurities in the final IL.

A variety of less toxic dual functionalized imidazolium ZIs (**5b**, **6b**, **8b**, **10b**) have been synthesized with the purpose of giving ILs with good cellulose dissolution abilities. The ZIs were all synthesized through a two step *N*-alkylation procedure. The first step was preparation of ether alkylated imidazolium intermediates (**5a**, **6a**, **8a** and **10a**), followed by a final alkylation using 1,3-propanesultone.

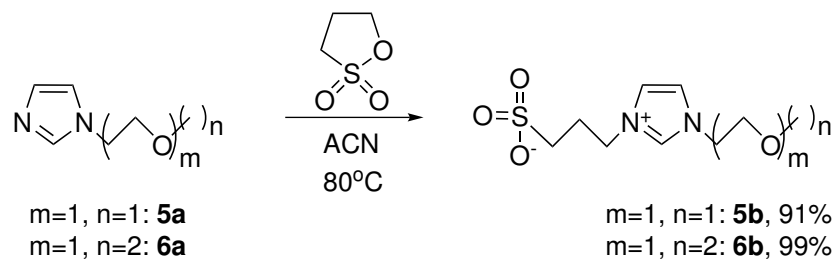
3.3.1 Synthesis of ZIs **5b** and **6b**

All ZIs were synthesized via mono substituted imidazole ethers. Intermediates **5a** and **6a** were synthesized through S_N2 reactions from imidazole and commercially available 2-chloroethyl methyl ether and 2-chloroethyl ethyl ether, respectively. Synthesis of intermediates **5a** and **6a** are presented in Scheme 3.6. The intermediates were *N*-alkylated via nucleophilic attack and ring opening of 1,3-propanesultone (Scheme 3.7) to afford ZIs **5b** and **6b**. ZI **5b** was obtained as a light yellow solid in 91 % yield and ZI **6b** was obtained as a light brown gel in 99 % yield. This shows that an increase in carbons on the ether chain will decrease the melting point of the product.



Scheme 3.6: Synthesis of ZI intermediates **5a** and **6a**.

3.3 Preparation of imidazolium based ZIs



Scheme 3.7: Synthesis of ZIs **5b** and **6b**.

^1H and ^{13}C NMR shifts of ZIs **5b** and **6b** were assigned and are presented in Figure 3.5 and Figure 3.6, respectively. Spectra for intermediate **5a** and ZI **5b** are presented in Appendix G and H, while spectra for intermediate **6a** and ZI **6b** are presented in Appendix M and N.

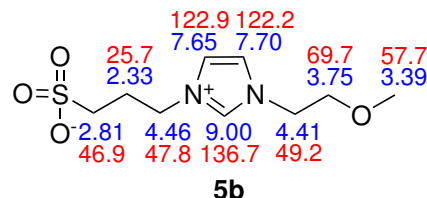


Figure 3.5: ^1H and ^{13}C NMR shifts of ZI **5b**.

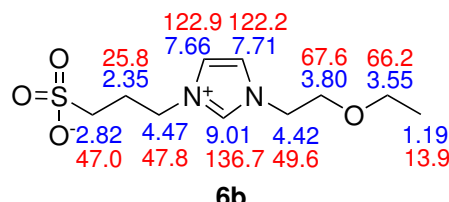
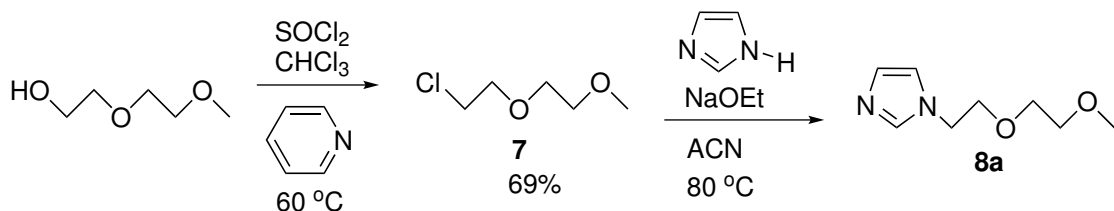


Figure 3.6: ^1H and ^{13}C NMR shifts of ZI **6b**.

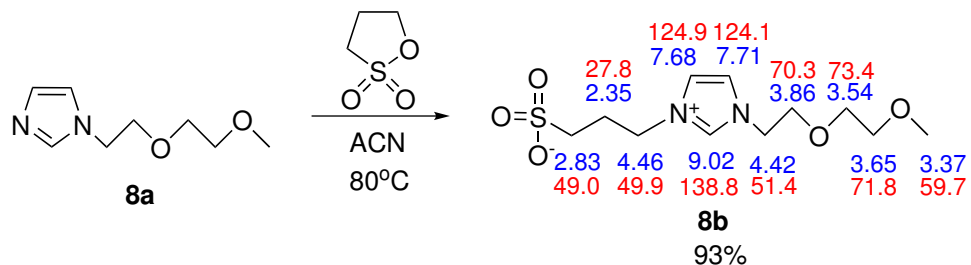
3.3.2 Synthesis of precursor **7** and ZI **8b**

For synthesis of ZI **8b**, 1-chloro-2-(2-methoxyethoxy)ethane (**7**) had to be synthesized as a precursor. Precursor **7** was synthesized through a chlorination reaction of 2-(2-methoxyethoxy)ethanol with SOCl_2 followed by aqueous workup, and was obtained in 69 % yield as a dark yellow liquid (Scheme 3.8).



Scheme 3.8: Synthesis of precursor **7** and intermediate **8a**.

The precursor was used in further synthesis of intermediate **8a** via a $\text{S}_{\text{N}}2$ reaction (Scheme 3.8). ZI **8b** was prepared by *N*-alkylation of intermediate **8a** via nucleophilic attack and ring opening of 1,3-propanesultone (Scheme 3.9), and was obtained in 93 % yield as a brown viscous liquid. ^1H and ^{13}C NMR shifts of ZI **8b** were assigned and are presented in Scheme 3.9. Spectra for precursor **7**, intermediate **8a** and ZI **8b** are respectively presented in Appendix S, T and U.

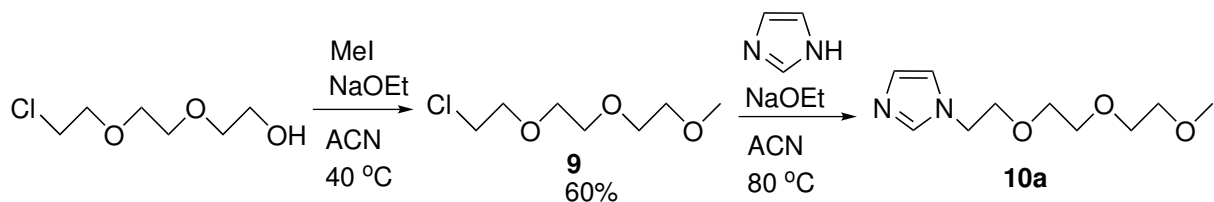


Scheme 3.9: Synthesis and ^1H and ^{13}C NMR shifts of ZI **8b**.

3.3.3 Synthesis of precursor **9** and ZI **10b**

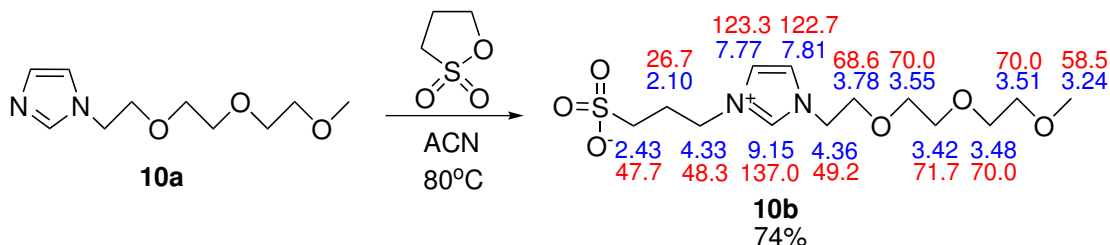
1-Chloro-2-(2-(2-methoxyethoxy)ethoxy)ethane (**9**) needed to be synthesized for use as precursor for preparation of ZI **10b**. Precursor **9** was synthesized by methylation of 2-(2-chloroethoxy)ethanol using iodomethane and gave after work up and filtration through silica plug, a bright yellow liquid in 60 % yield, as presented in Scheme 3.10.

3.3 Preparation of imidazolium based ZIs



Scheme 3.10: Synthesis of precursor **9** and intermediate **10a**.

The precursor was used in further synthesis of intermediate **10a** through a $\text{S}_{\text{N}}2$ reaction (Scheme 3.10). ZI **10b** was prepared by *N*-alkylation of intermediate **10a** via nucleophilic attack and ring opening av 1,3-propanesultone (Scheme 3.11). ZI **10b** was obtained in 74 % yield as a brown viscous liquid. As previously mentioned, the solid nature of ZIs decrease as the number of oxygen and length of ether chain increase. This is also visible for ZIs **8b** and **10b**, as ZI **8b** is a liquid with higher viscosity than **10b**. ^1H and ^{13}C NMR shifts of ZI **10b** were assigned and are presented in Scheme 3.11. Spectra of precursor **9**, intermediate **10a** and ZI **10b** are respectively presented in Appendix Z, AA and AB.



Scheme 3.11: Synthesis and ^1H and ^{13}C NMR shifts of ZI **10b**.

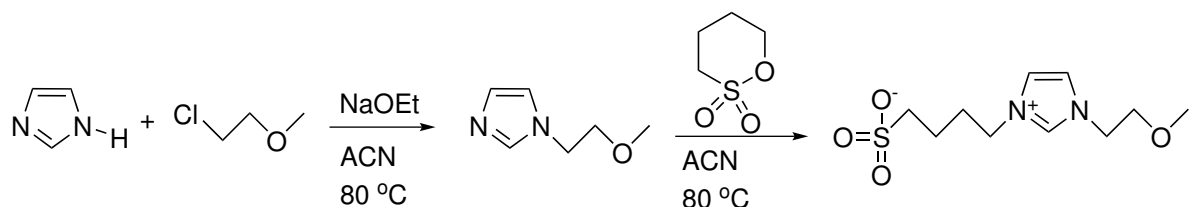
3.3.4 Comparing ZIs

All ZIs were synthesized for the purpose of being non-toxic and produce corresponding ILs that are able to dissolve cellulose. As mentioned in Section 2.2.1, imidazolium ILs with simple alkyl groups are known to be toxic. Toxicity of the imidazolium based ZIs were reduced by ether substituents of various length.^[55] To reduce the toxicity of the alkyl chain on the imidazolium, it was tethered with a negatively charged $[\text{SO}_3]^-$ group by use of 1,3-propanesultone.^[54] The introduction of ether functionalities also induces a lower melting point and lower viscosity.^[55] The lowering of viscosity was clearly seen for the ZIs as the viscosity decreases when the length of the ether chain increased. The ether chain also increases the polarity, hydrophilicity and hydrogen bonding capability of the IL,

but lowers the thermal stability.^[55] An increase in hydrogen bonding capacity is especially favorable for cellulose dissolution, as it more easily can coordinate to the hydrogen atoms in the glucose molecules.

From an industrial point of view non-toxic ILs for cellulose dissolution is a necessity. If the ILs used for cellulose dissolution are toxic, their disposal will be an issue because the release of toxic hydrophilic ILs will contaminate the waste water system. Toxicity of ZIs and ILs can amongst other be tested by MTT (3-(4,5-dimethylthiazol-2-yl)-2,5-diphenyltetrazolium bromide) assay, which is a colorimetric analysis for assessing cell metabolic activity. This was not done for these samples due to time constrains.

Attempts were done on synthesis of a ZI with a longer alkyne chain. ZI 4-(1-(2-methoxyethyl)-1H-imidazol-3-ium-3-yl)butane-1-sulfonate was synthesized using 1,4-butane sultone instead of 1,3-propanesultone (Scheme 3.12). Even after a reaction time of 114 hours, the reaction mixture contained both product and starting materials. Since the yield of the synthesis would be very low, it was not pursued further.



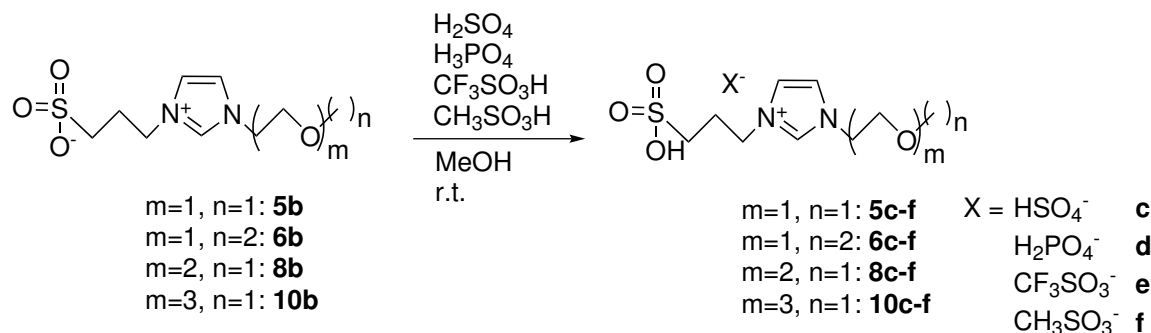
Scheme 3.12: Synthesis of ZI 4-(1-(2-methoxyethyl)-1H-imidazol-3-ium-3-yl)butane-1-sulfonate.

3.4 Preparation of imidazolium based ILs

3.4.1 Synthesis of ILs from ZI 5b, 6b, 8b and 10b

ILs **5c-f**, **6c-f**, **8c-f** and **10c-f** with counter ions $[\text{HSO}_4]^-$, $[\text{H}_2\text{PO}_4]^-$, $[\text{CF}_3\text{SO}_3]^-$ and $[\text{CH}_3\text{SO}_3]^-$, respectively, were synthesized by protonation of ZIs **5b**, **6b**, **8b** and **10b** with sulfuric, phosphoric, trifluoromethanesulfonic and methanesulfonic acid. The mixtures were dissolved in MeOH and stirred for 6-24 hours, before they were dried on rotary evaporator and by freeze drying. A general scheme for synthesis of the ILs is shown in Scheme 3.13. Preparation of IL using a less strong acid like CH_3COOH ($\text{pK}_a = 4.8$) was attempted, but did not form an IL with ZI **5b**.

3.4 Preparation of imidazolium based ILs



Scheme 3.13: General synthetic scheme for preparation of ILs.

Table 3.3: Water content of ILs in ppm.

IL	ppm	IL	ppm	IL	ppm	IL	ppm
5c	255	6c	1752	8c	2446	10c	viscous
5d	814	6d	viscous	8d	viscous	10d	viscous
5e	13921	6e	19820	8e	9332	10e	viscous
5f	3133	6f	826	8f	802	10f	viscous

The ILs are all hydrophilic because of their good hydrogen bond ability due to the large number of oxygen atoms. This made complete water removal from the very viscous liquids a challenge. The water content of all the possible ILs were measured before any further investigation of properties and abilities were conducted, and are presented in Table 3.3. IL **5c** with the shortest ether chain has the lowest water content (255 ppm), and is followed by ILs **8f** (802 ppm), **5d** (814 ppm) and **6f** (826 ppm). The IL with the highest water content is **6e** (19820 ppm), and it is followed by ILs **5e** (13921 ppm) and **8e** (9332 ppm). The presence of water alters the properties of ILs, in particular the heat transfer properties and it will reduce the thermal stability.^[84] Large amounts of water in the IL will be visible in the TGA graph.

3.4.2 Thermal stability of ILs

Thermal stability is a substance's resistance to permanent changes to its chemical or physical structure caused solely by heat. Thermal decomposition temperature is commonly used to assess the thermal stability of a substance. Information about the thermal stability and the thermal decomposition temperature of ILs are found by TGA. ILs have a large liquid range, and because of their non-boiling character, the upper temperature limit is given by

their thermal degradation point.^[84] For the ILs reported in this thesis, the thermal degradation point is given as the temperature at which the amount of IL has decreased by 10 wt%.

The thermal stability of ILs are dependent on the structure, i.e. cation, anion and modifications on cation, such as chain length, number of substituents and functionalization.^[58] It is worth noting that there are no strict guidelines for the measurement conditions for determining thermal stability of ILs. Therefore, thermal stability data from different literature are not necessarily comparable.^[58] For investigation of short-term thermal stability of ILs synthesized in this project, TGA was performed with a heating rate of 10 °C per minute from 30 °C to 600 °C, under nitrogen gas. For investigation of long-term thermal stability the temperature program of the TGA would have to include an isothermal step that is held for a relatively long time.^[59] The temperature profiles collected from TGA data are dependent on factors like viscosity and heat transfer, heating rate, exo- and endothermic decomposition reactions, instrumentation, sample geometry and mass.^[84] Temperature profiles for ILs **5c-f**, **6c-f**, **8c-f** and **10c-f** are depicted in Figure 3.7 and Figure 3.8, where the wt% is plotted along the y-axis and temperature in °C along the x-axis. Figures 3.7a, 3.7b, 3.7c and 3.7d show temperature profile of ILs with the same cation, while Figures 3.8a, 3.8b, 3.8c and 3.8d show temperature profile of ILs with the same anion.

As mentioned in Section 2.3.1 it has been reported that type of anion impacts the thermal stability of ILs more than type of cation.^[58] This can clearly be seen from Figure 3.7 and Figure 3.8, where the temperature profiles of ILs with the same anion (Figure 3.8) coincide more than the temperature profile of ILs with the same cation (Figure 3.7). We can also see that the ILs with anion $[\text{CF}_3\text{SO}_3]^-$ and $[\text{CH}_3\text{SO}_3]^-$ (Figure 3.8c and Figure 3.8d) coincide more than the ILs with $[\text{HSO}_4]^-$ and $[\text{H}_2\text{PO}_4]^-$ as anion (Figure 3.8a and Figure 3.8b). This means that anions $[\text{CF}_3\text{SO}_3]^-$ and $[\text{CH}_3\text{SO}_3]^-$ make the ILs follow a more similar thermal decomposition mechanism. The thermal decomposition mechanism of ILs will be further discussed in Section 3.4.3.

3.4 Preparation of imidazolium based ILs

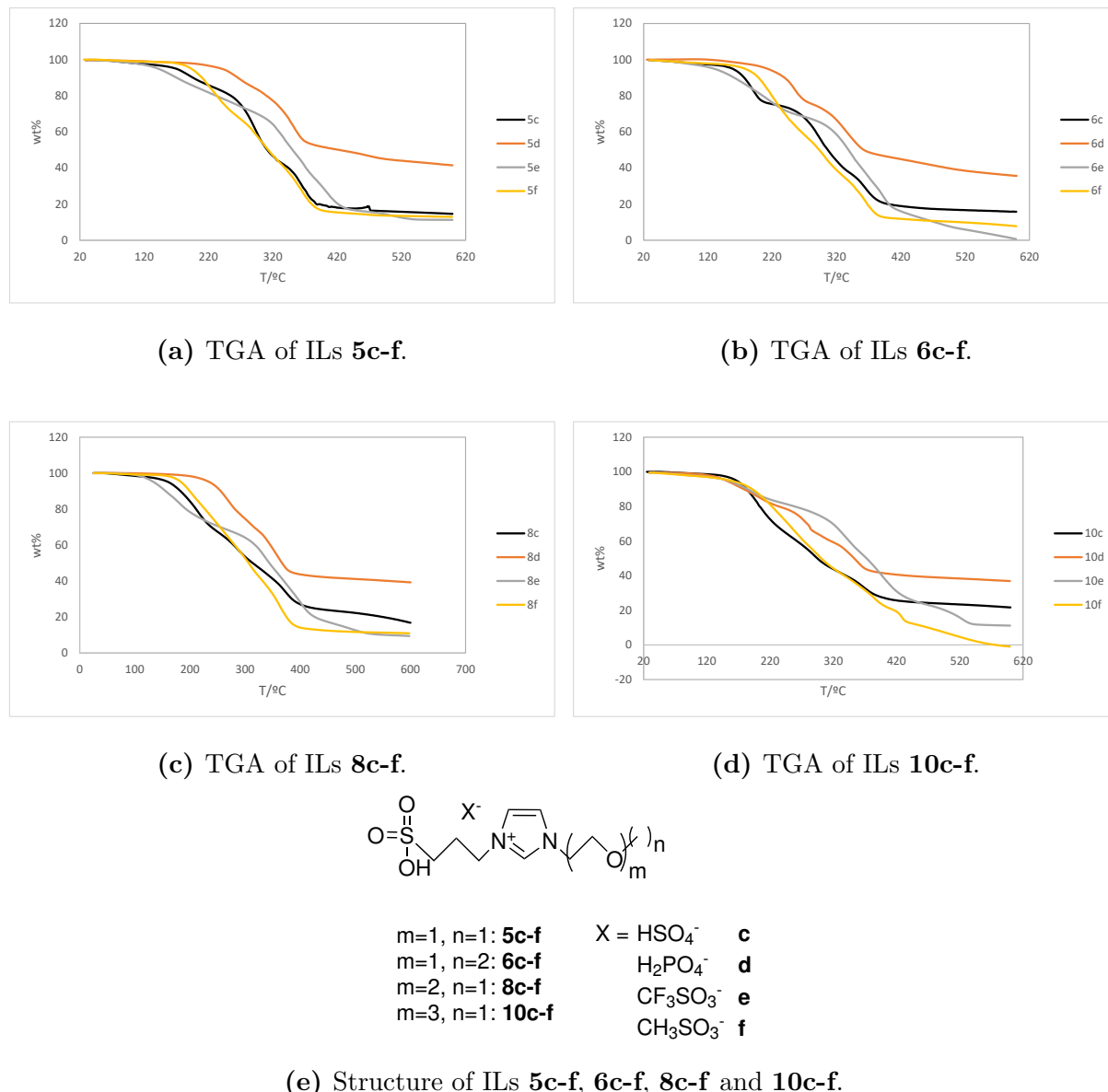


Figure 3.7: TGA results of ILs with mass in wt% along y-axis and temperature in °C along x-axis. (a) ILs 5c-f. (b) ILs 6c-f. (c) ILs 8c-f. (d) ILs 10c-f. (e) Structure of ILs 5c-f, 6c-f, 8c-f and 10c-f.

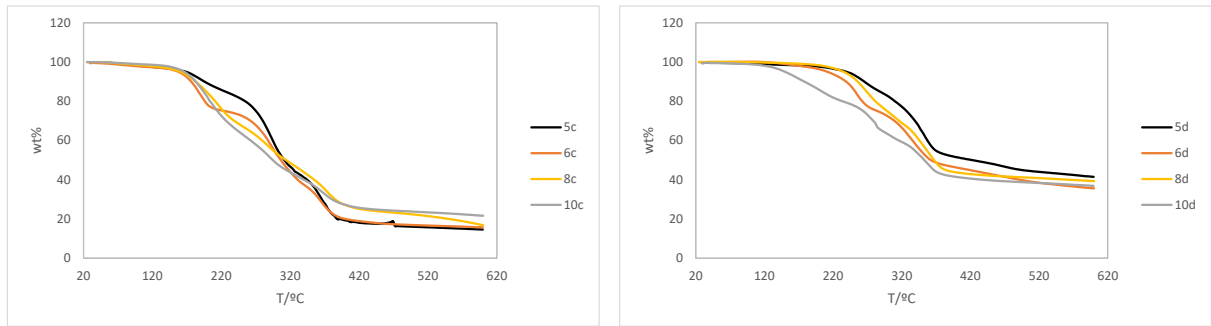
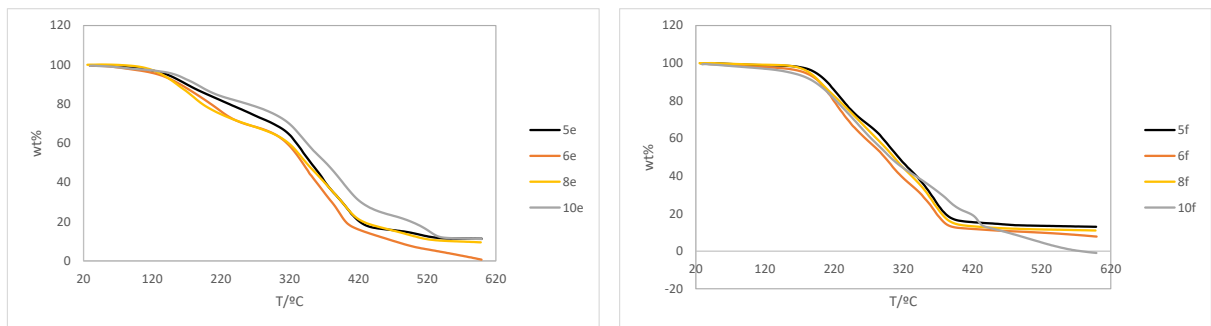
(a) TGA of ILs **5c**, **6c**, **8c**, **10c** with anion $[\text{HSO}_4]^-$.(b) TGA of ILs **5d**, **6d**, **8d**, **10d** with anion $[\text{H}_2\text{PO}_4]^-$.(c) TGA of ILs **5e**, **6e**, **8e**, **10e** with anion $[\text{CF}_3\text{SO}_3]^-$.(d) TGA of ILs **5f**, **6f**, **8f**, **10f** with anion $[\text{CH}_3\text{SO}_3]^-$.

Figure 3.8: TGA results of ILs with mass in wt% along y-axis and temperature in °C along x-axis. (a) ILs **5c**, **6c**, **8c**, **10c** with anion $[\text{HSO}_4]^-$. (b) ILs **5d**, **6d**, **8d**, **10d** with anion $[\text{H}_2\text{PO}_4]^-$. (c) ILs **5e**, **6e**, **8e**, **10e** with anion $[\text{CF}_3\text{SO}_3]^-$. (d) ILs **5f**, **6f**, **8f**, **10f** with anion $[\text{CH}_3\text{SO}_3]^-$.

Thermal degradation temperature (T_d) of the ILs are presented in Table 3.4. For ILs **5c-f**, **6c-f** and **8c-f** the T_d values increase in the same order regarding anion. Starting from the lowest T_d value it increases from $[\text{CF}_3\text{SO}_3]^-$ to $[\text{HSO}_4]^-$, $[\text{CH}_3\text{SO}_3]^-$ and $[\text{H}_2\text{PO}_4]^-$. This means that ILs with $[\text{H}_2\text{PO}_4]^-$ as anion (**5d**, **6d** and **8d**) have the highest T_d values at 268 °C, 239 °C and 256 °C, and are the most thermally stable. While the ILs with $[\text{CF}_3\text{SO}_3]^-$ as anion (**5e**, **6e** and **8e**) have the lowest T_d values at 173 °C, 164 °C and 156 °C and are the least thermally stable. From the T_d values we can also see that the ILs with the shortest ether chain length (**5c,d,f**) are most thermally stable. Compared to ILs **5c-f** ($T_d = 197$ °C, 268 °C, 173 °C, 210 °C, respectively) addition of methoxymethane to the ether substituent (**8c,d,f**) decreases the stability ($T_d = 183$ °C, 256 °C, 200 °C, respectively), while increasing

3.4 Preparation of imidazolium based ILs

the ether substituent by going from a methoxyethyl substituent to ethoxyethyl substituent (**6c,d,f**) decreases the stability even further ($T_d = 178\text{ }^\circ\text{C}$, $239\text{ }^\circ\text{C}$, $200\text{ }^\circ\text{C}$, respectively). For ILs with $[\text{CF}_3\text{SO}_3]^-$ as anion addition of ether (IL **8e** $T_d = 156\text{ }^\circ\text{C}$) decreases the T_d value more than addition of only carbon (IL **6e** $T_d = 164\text{ }^\circ\text{C}$).

Table 3.4: Thermal degradation temperature (T_d) for ILs given in $^\circ\text{C}$.

Anion	IL	$T_d(10\text{wt}\%)$	IL	$T_d(10\text{wt}\%)$	IL	$T_d(10\text{wt}\%)$	IL	$T_d(10\text{wt}\%)$
$[\text{HSO}_4]^-$	5c	197	6c	178	8c	183	10c	183
$[\text{H}_2\text{PO}_4]^-$	5d	268	6d	239	8d	256	10d	182
$[\text{CF}_3\text{SO}_3]^-$	5e	173	6e	164	8e	156	10e	187
$[\text{CH}_3\text{SO}_3]^-$	5f	210	6f	200	8f	200	10f	194

The ILs with the longest ether chain (**10c-f**), containing three oxygen atoms, does not follow the same trend as the other ILs. From lowest to highest T_d value it goes **10d** ($182\text{ }^\circ\text{C}$), **10c** ($183\text{ }^\circ\text{C}$), **10e** ($187\text{ }^\circ\text{C}$) and **10f** ($194\text{ }^\circ\text{C}$), meaning that anion $[\text{H}_2\text{PO}_4]^-$ is least thermally stable and $[\text{CH}_3\text{SO}_3]^-$ is the most stable. It can also be seen that when the length of the ether chain increase, the difference in T_d value for the different anions decreases.

3.4.3 Thermal decomposition mechanism

The thermal decomposition mechanism of the ILs were not investigated by any of the methods mentioned in Section 2.3.1, but it can be seen from the graphs in Figure 3.7 that the degradation of the ILs occur stepwise. This means that the ILs decomposes at different steps as the temperature increase or that some amount of the ILs evaporate before decomposition.^[85] Stepwise degradation has previously been reported in literature.^[85,86] The stepwise degradation may be due to the decomposition of the anions followed by decomposition of the ether groups. An accurate mechanism for the decomposition can not be given only based on the TGA data, but a postulated mechanism will be given further on.

Most of the degradation of ILs follow a substitution mechanism, but they can also follow an elimination or rearrangement mechanism when the anions are non-coordinating.^[59,87] Previous studies^[87] report that the degradation of ILs can be attributed to the nucleophilic attack of an anion to alkyl groups on cation, causing dealkylation of the IL. In

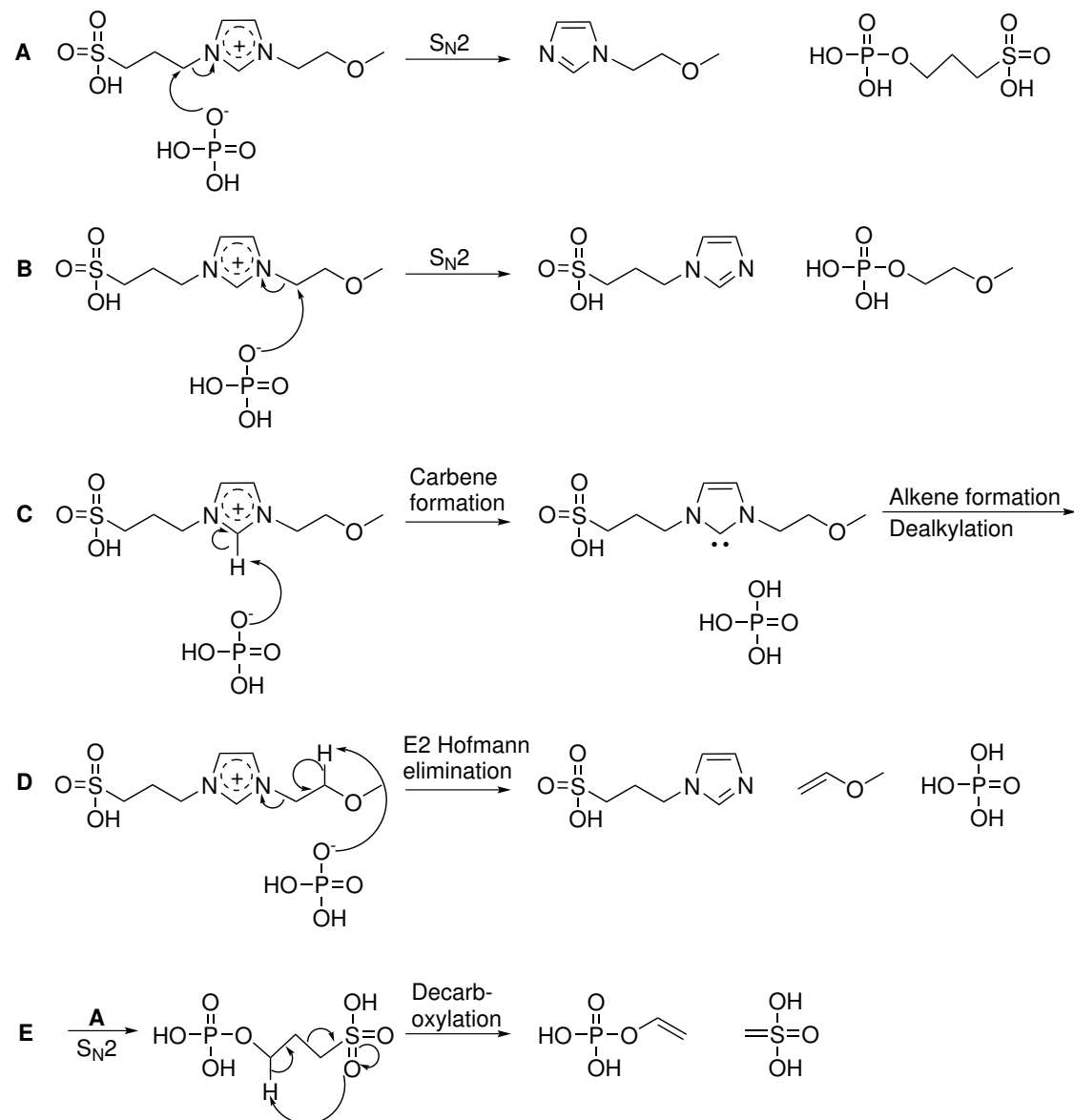
3.4 Preparation of imidazolium based ILs

fact, the main breakdown mechanism in the temperature range of thermogravimetric experiments will include loss of an alkyl chain.^[84] It was also shown that a S_N2 mechanism generally seems to be more favorable than a S_N1, which means that the thermal stability of ILs correlates well with the anion nucleophilicity. ILs with poorly nucleophile anions such as bis(trifluoromethylsulfonyl)imide have high thermal stability. ILs with strongly nucleophilic anions like Cl⁻ are thermally less stable.^[87]

The acids used for the synthesis of ILs have various acidic strength, trifluoromethane-sulfonic acid being the strongest ($pK_a = -14.0$) followed by sulfuric acid ($pK_a = -3.0$), methanesulfonic acid ($pK_a = -2.6$) and phosphoric acid as the weakest ($pK_a = 2.1$). Most of the experimental TGA results is consistent with previously reported theory.^[87] The weakest acid (H₃PO₄) giving the strongest conjugated base, which is also a poor nucleophile, have the highest thermal stability. Furthermore, the ILs with the strongest acid (CF₃SO₃H) as anion have low thermal stability due to the high nucleophilicity of the anion.

The IL with highest thermal stability was, as previously mentioned, IL **5d** with cation containing the shortest ether chain and the weakest nucleophilic anion. Proposed decomposition mechanisms for IL **5d** are shown in Scheme 3.14.^[88] The scheme shows various decomposition mechanisms, amongst them is the most likely S_N2 nucleophilic substitution seen in Scheme 3.14 **A** and **B**. The anion attacks one of the α carbon atoms of the imidazolium cation, followed by dealkylation of the imidazolium and creation of molecules that can be further decomposed. One of the intermediates formed in Scheme 3.14 **A** can further decompose via decarboxylation as shown in Scheme 3.14 **E**. As seen in Scheme 3.14 **C**, the IL can also decompose through carbene formation by deprotonation of the C₂-hydrogen of the imidazolium cation by base. The N-heterocyclic carbene can further decompose by double bond formation and dealkylation. The last mechanism to mention is E2 Hofmann elimination as seen in Scheme 3.14 **D**, where the base initiate elimination by deprotonation of the β hydrogen atom. The intermediates can further decompose also by mechanism not mentioned in the Scheme, explaining the steps in the TGA graphs seen in Figure 3.7 and Figure 3.8.^[88]

3.4 Preparation of imidazolium based ILs



Scheme 3.14: Postulated decomposition mechanism of IL 5d. **A, B:** S_N2 nucleophilic substitution, **C:** N-heterocyclic carbene formation, **D:** E2 Hofmann elimination and **E:** decarboxylation of decomposition intermediate.^[88]

3.5 Cellulose dissolution with imidazolium ILs

Cellulose is the most abundant organic compound on earth and have many attractive properties, such as thermal and chemical stability and biodegradability.^[89] Cellulose can be extracted from biomass by use of an appropriate solvent, and can be utilized in the development of environmentally friendly products and fuels. One of the currently used and the oldest method to process cellulose into cellulose fibers is the viscose process. This process involves treating cellulose with sodium hydroxide, followed by derivatizing cellulose with carbon disulfide, giving a highly viscous sodium xanthogenate solution.^[90] From this solution cellulose is reformed by treatment with acidic solution.^[89] The process requires a large amount of waste water and exhaust air treatment and therefore has problems meeting the though environmental requirements.^[90] A newer method used for cellulose treatment is the *N*-methylmorpholine-*N*-oxide monohydrate (NMMO) process, where NMMO is used as solvent for production of Lyocell fibers in a homogeneous polymer solution.^[91] Even though the NMMO process possess many advantages, it has not replaced the viscose process, mainly due to cost and the difference in nature of the fibers produces in the two processes.^[89]

In 2002 the research group of Swatloski et al. reported the first dissolution of cellulose using ILs, such as 1-butyl-3-methylimidazolium chloride.^[5] This lead to a new class of cellulose solvent systems. Since then many ILs have been reported to have cellulose dissolving abilities.^[89] In Table 3.5 various ILs with high cellulose dissolution abilities are presented. The table shows that both the anion and cation of ILs influence the dissolution of cellulose. ILs with the same cation are presented in Entry 1-3^[92] and ILs with the same anion are presented in Entry 4-7.^[93,94] Anions that are good hydrogen bond acceptors ($[\text{OAc}]^-$, etc.) and have high dipolarity are effective in dissolution of cellulose.^[89] Xu et al. have presented a study where cellulose dissolution using ILs with cation $[\text{C}_2\text{mim}]^+$ and various anions were investigated. They reported that anions hydrogen bond accepting ability was closely linked to the ILs ability to dissolve cellulose, and that $[\text{OAc}]^-$ was most efficient for this purpose.^[93] ILs with imidazolium based cations are known to show good cellulose solubility.^[89] From Table 3.5 we see that different imidazolium based ILs with acetate anions (entry 4-7) show good solubility of cellulose (Avicel or MCC) varying from 12-15.5 wt% at 110 °C. Although literature suggest oxygen containing cations to have poor dissolution power,^[46] the literature results presented in Table 3.5 shows otherwise. Though it does show that $[\text{C}_2\text{mim}][\text{OAc}]$ (entry 4), having a cation without any oxygen atoms, does present better solubility with 15.5 wt% MCC at 70 °C, than the ether containing cations (entry 6-7) which both dissolves 12 wt% at 110 °C.

3.5 Cellulose dissolution with imidazolium ILs

Table 3.5: Cellulose dissolution capacity of different imidazolium based ILs.^[89,92,94]

Entry	ILs ^a	Structure of ILs	Cellulose type ^b	Conditions	Solubility (wt%)	Ref.
1	[A ₂ im][CH ₃ OCH ₂ COO]		MCC	Heat (50 °C)	25.7	[92]
2	[A ₂ im][CH ₂ CHCOO]		MCC	Heat (50 °C)	23	[92]
3	[A ₂ im][CH ₃ COO]		MCC	Heat (50 °C)	19.5	[92]
4	[C ₄ mim][OAc]		MCC	Heat (70 °C)	15.5	[93]
5	[C ₂ mim][OAc]		Avicel	Heat (110 °C)	15	[94]
6	[Me(OEt) ₂ -Et-Im][OAc]		Avicel	Heat (110 °C)	12	[94]
7	[Me(OEt) ₃ -Et-Im][OAc]		Avicel	Heat (110 °C)	12	[94]

^a A₂im: 1,3-diallylimidazolium; C₄mim: 1-butyl-3-methylimidazolium; OAc: acetate; C₂mim: 1-ethyl-3-methylimidazolium; Me(OEt)₂-Et-Im: 1-(3,6-dioxaheptyl)-3-ethylimidazolium; Me(OEt)₃-Et-Im: 1-(3,6,9-trioxadecyl)-3-ethylimidazolium; Me(OEt)3-Et3N: N,N,Ntriethyl-3,6,9-trioxadecylammonium.

^b Avicel: a microcrystalline cellulose powder; MCC: microcrystalline cellulose.

Research published by Xu and coworkers in May 2018 show remarkable results for cellulose dissolution using imidazolium based ILs (entry 1-3).^[92] The ILs have the same 1,3-diallylimidazolium cation [A₂mim]⁺ but various anions. With [CH₃COO]⁻ as anion (entry 3) the IL was able to dissolve 19.5 wt% MCC at 50 °C, while the IL with [CH₂CHCOO]⁻ as anion (entry 2) dissolved 23 wt%. The best results for dissolution of MCC was obtained with [CH₃OCH₂COO]⁻ as anion (entry 1), which dissolved the remarkable amount of 25.7 wt% at 50 °C. The good solvation abilities of these ILs are mainly due to the increased capacity of hydrogen bonding from the anions to OH protons in cellulose, because of the electron-donating effect of the CH₃-, CH₂= and CH₃OCH₂- groups.^[92] By comparing various cations, Xu et al. report that more allyl substituents on the imidazolium cation also contribute to higher cellulose solubility.^[92]

How IL cations work in cellulose dissolution is still under debate amongst scientist, but most studies suggest strong van der Waals forces and weak hydrogen bonds between the cations and cellulose.^[1] Brandt et al. suggest ILs with small, non-coordinating cations and small hydrogen-bonding anions as most suitable for cellulose dissolution because of their bi-functionality. They postulate that cations interact with the top and bottom surface of the cellulose strands through dispersion forces, while the anions coordinate to the equatorial hydroxyl groups, thereby separating the strands from each other.^[1] It has also been suggested by researchers that both the cation and anion form electron donor-electron acceptor complexes with cellulose.^[44] A postulated mechanism for cellulose dissolution is presented in Figure 3.9.^[44]

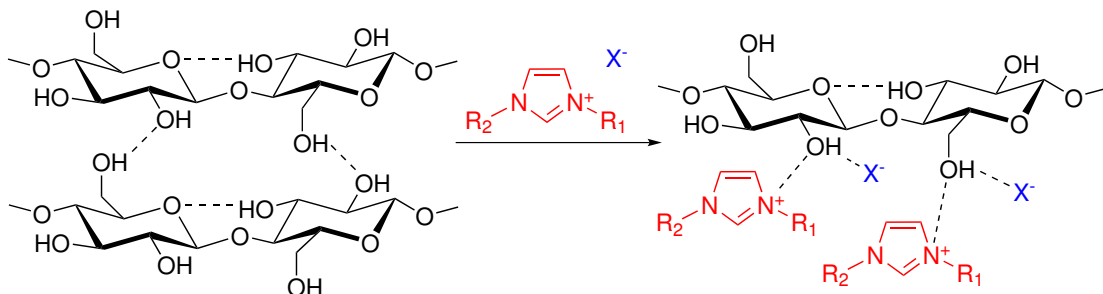


Figure 3.9: Postulated cellulose dissolution mechanism using imidazolium IL.^[44]

One of the reasons for synthesizing new imidazolium ILs in this master's project, was their high ability to dissolve cellulose. As previously mentioned, the ether substituents were added to decrease the toxicity of imidazolium while sulfur trioxide was used to reduce the toxicity of the alkyl chain. The high cellulose dissolution abilities of imidazolium can be related to its aromatic nature, which gives it ability to shield the dissolved anion/cellulose polymer complexes.^[89] The aromatic ring in the imidazole allows charge delocalization and reduction of electrostatic strength between cation and anion. When the interaction between cation and anion is weakened, it makes it easier for the anion to form hydrogen bonds with cellulose. In addition, it is proposed that the C₂-hydrogen on the imidazolium ring can interact with cellulose due to its acidic nature.^[89]

Cellulose dissolution with the use of a polar solvent was performed based on a communication by Rinaldi, which reports that a mixture of 1-butyl-3-methylimidazolium chloride (5 g) and 1,3-dimethyl-2-imidazolidinone (DMI, 5 g) dissolves 10 wt% cellulose (Avicel) in few minutes.^[6] The cellulose dissolution in this master's project was performed using 0.5 g IL and 0.5 g dry dimethylformamide (DMF). The polar solvent reduces the viscosity and allows for vigorous stirring, without participating in the dissolution process. When

3.5 Cellulose dissolution with imidazolium ILs

testing solubility of cellulose in the ILs, the first step was addition of 1 wt% microcrystalline cellulose (MCC) to the IL/DMF mixture at 100 °C. Subsequently, additional 1 wt% was added to the mixtures when the previously added cellulose was completely dissolved. The addition of MCC was continued until the ILs were no longer capable of dissolving more cellulose. The results of cellulose dissolution testing are presented in Table 3.6 in the following section.

Many of the new ILs had a dark brown color even before drying, but none of the ¹H or ¹³C NMR spectra showed any impurities. This means that the color should not affect the performance of the ILs for cellulose dissolution. During cellulose dissolution at 100 °C, the ILs became darker in color. Even though the color change should not affect the ILs ability to dissolve cellulose, it makes the visualization of the cellulose dissolution process more challenging. Because of this it was desirable to perform the testing at a lower temperature. Cellulose dissolution was therefore also attempted at 40 °C, but that resulted in precipitation of IL in the mixture. From the upcoming results, we can see that dissolution at 40 °C would most likely not give any satisfactory results.

The aforementioned method for testing cellulose dissolution with ILs have some disadvantages. Repeated opening of the vial to add more cellulose allows the hydrophilic ILs to absorb water from the surroundings. This will alter the properties of the ILs and their cellulose dissolution potential. An exact reason for the high sensitivity of the IL/cellulose mixture to water is still unknown, but it is suggested that water strongly bonds to the IL anion through hydrogen-bonds, or that water hydrogen-bonds to cellulose, both preventing cellulose and anion to coordinate to each other.^[1] Another disadvantage of the cellulose dissolution method is that it is time consuming. That means that the ILs are exposed to high temperature for several days, which can affect their thermal stability. For many of the ILs tested here, the color darkened within one or two days at 100 °C, and this made the testing more challenging. When the color of the ILs is dark, it is difficult to see if cellulose has fully dissolved or not.

The method for cellulose dissolution can be improved by different measures. To prevent the IL from absorbing water, the vial can be flushed with nitrogen gas during the addition of cellulose. To perform cellulose dissolution with a dark IL, a microscope can be used. A drop of the IL/DMF/MCC mixture can be taken out and checked under microscope to see if there is any large MCC particles left. Though this method does not work for very viscous mixture where the cellulose often gather as lumps when the IL is fully saturated, meaning that you might take out the wrong part of the mixture for testing under microscope. The

dissolution can also be improved by ultrasonic treatment, which has been reported to enhance cellulose dissolution.^[95]

3.5.1 Results from cellulose dissolution testing

When dissolving cellulose in ILs, the inter- and intramolecular hydrogen bonds between the poly-glucose layers breaks and the crystallinity of the cellulose decrease. Being a master's thesis in organic chemistry, we are not going in to the details of solid state theory and changes in lattice space. However, it is important to mention that when cellulose is dissolved in IL the crystallinity decreases and it transforms from cellulose I to cellulose II. This can be seen from XRD graphs as the intensity peaks decrease when cellulose transforms from cellulose I to cellulose II (Figure 3.10 and Figure 3.11).

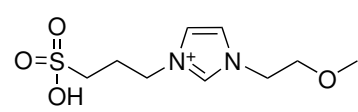
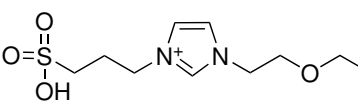
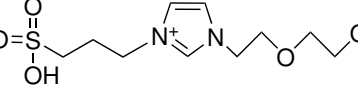
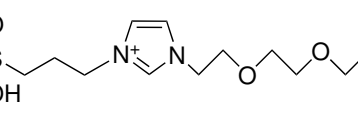
The stability of ILs during cellulose dissolution was investigated by NMR. ¹H NMR of IL **5c** was taken before and after cellulose dissolution, and did not show any changes in the IL structure. This means that the ILs can perform cellulose dissolution at 100 °C without decomposition.

As seen from Table 3.6, ILs **5c-f** (entry 1-4) and **6c-f** (entry 5-8) show the best cellulose dissolution abilities and dissolved between 7.57-8.20 wt% and 9.23-9.92 wt%, respectively. The dissolution was performed with addition of MCC over 72 hours. These are the ILs with the shortest ether chain, confirming the theory that fewer electronegative atoms on the cation gives highest cellulose dissolution. It is also easier for small ILs to move between the poly-glucose layers and coordinate to glucose, thereby breaking the hydrogen bonds.

When the ether chain on the imidazolium cation increase, the dissolution abilities of the ILs decrease, as seen from ILs **8c-f** (entry 9-12) and **10c-f** (entry 13-16) in Table 3.6. For ILs **8c**, **8d**, **10e** and **10f** MCC was added over 48 hours and they dissolved 5.47 wt%, 4.87 wt%, 6.87 wt% and 6.70 wt%, respectively. ILs **8e** and **8f** dissolved 7.24 wt% and 6.97 wt% over 96 hours, and ILs **10c** and **10d** dissolved 4.52 wt% and 4.10 wt% over 24 hours. The dissolution testing was stopped after 24 hours because the ILs were saturated and would not dissolve more cellulose.

3.5 Cellulose dissolution with imidazolium ILs

Table 3.6: Cellulose dissolution with ILs in dry DMF at 100 °C showing wt% dissolved MCC.

Entry	ILs	IL cation	IL anion	Solubility (wt%)	Time (h)
1	5c		[HSO ₄] ⁻	7.57	72
2	5d		[H ₂ PO ₄] ⁻	8.03	72
3	5e		[CF ₃ SO ₃] ⁻	8.20	72
4	5f		[CH ₃ SO ₃] ⁻	7.71	72
5	6c		[HSO ₄] ⁻	9.92	72
6	6d		[H ₂ PO ₄] ⁻	9.79	72
7	6e		[CF ₃ SO ₃] ⁻	9.37	72
8	6f		[CH ₃ SO ₃] ⁻	9.23	72
9	8c		[HSO ₄] ⁻	5.47	48
10	8d		[H ₂ PO ₄] ⁻	4.87	48
11	8e		[CF ₃ SO ₃] ⁻	7.24	96
12	8f		[CH ₃ SO ₃] ⁻	6.97	96
13	10c		[HSO ₄] ⁻	4.52	24
14	10d		[H ₂ PO ₄] ⁻	4.10	24
15	10e		[CF ₃ SO ₃] ⁻	6.37	48
16	10f		[CH ₃ SO ₃] ⁻	6.70	48

After cellulose dissolution with the ILs, MCC was regenerated by addition of water. Regenerated MCC from ILs **6c-f** were analyzed by XRD, while regenerated MCC from ILs **5c-f** were analyzed by both XRD and TGA. As aforementioned, the crystallinity of a sample can be studied by XRD, and from Figure 3.10 we can see that the crystallinity of MCC regenerated from IL **5c** has decreased the most, compared to ILs **5d-f**. The same can be seen in Figure 3.11, where the crystallinity of MCC regenerated from IL **6c** has decreased the most, compared to **6d-f**. This means that anion [HSO₄]⁻ is the most efficient for cellulose dissolution. By comparing the graphs with literature,^[95] it can be seen that the regenerated MCC has not been completely transformed from cellulose I to cellulose II. In an XRD graph of cellulose II the diffraction curve will have one broad crystalline peak at around 20° replacing the crystalline peaks at 15° and 22°.^[95]

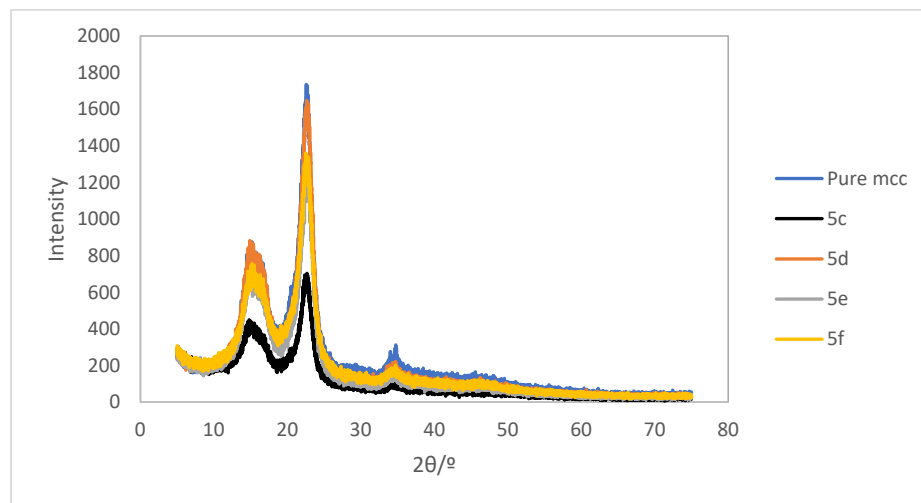


Figure 3.10: XRD of ILs 5c, 5d, 5e, 5f and pure MCC with intensity along y-axis and 2θ in degrees along x-axis.

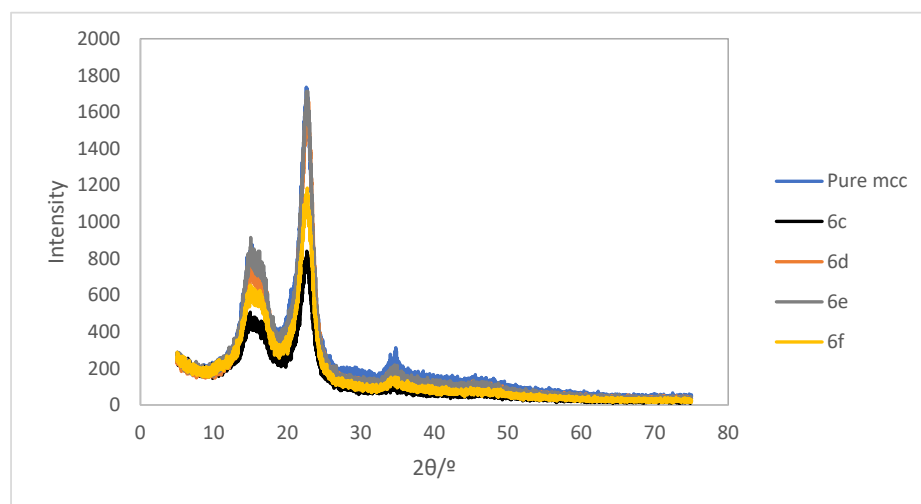


Figure 3.11: XRD of ILs 6c, 6d, 6e, 6f and pure MCC with intensity along y-axis and 2θ in degrees along x-axis.

3.5 Cellulose dissolution with imidazolium ILs

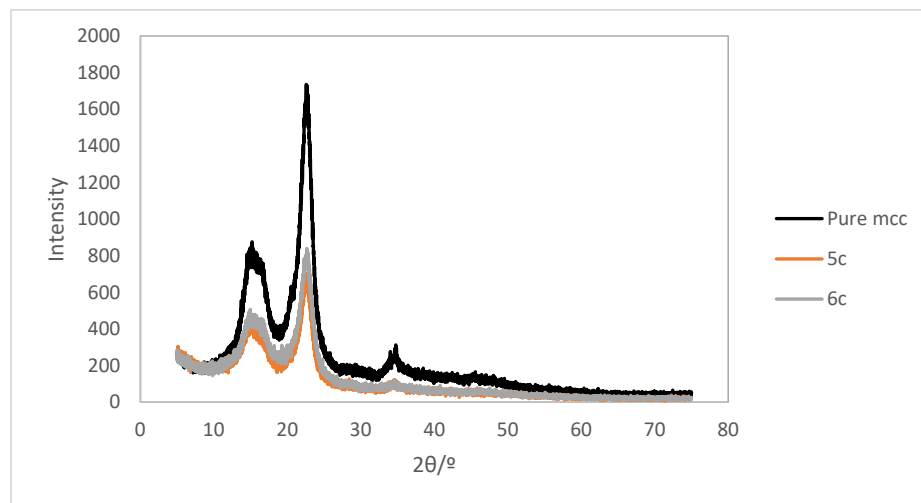


Figure 3.12: XRD of ILs **5c**, **6c** and pure MCC with intensity along y-axis and 2θ in degrees along x-axis.

In Figure 3.12 the XRD results of pure MCC are compared with MCC regenerated from IL **5c** and IL **6c**. From this graph we can see that IL **5c** dissolves cellulose slightly better than IL **6c**, but given the fact that approximately 2 wt% more MCC was added to IL **6c**, comparison of the two are difficult.

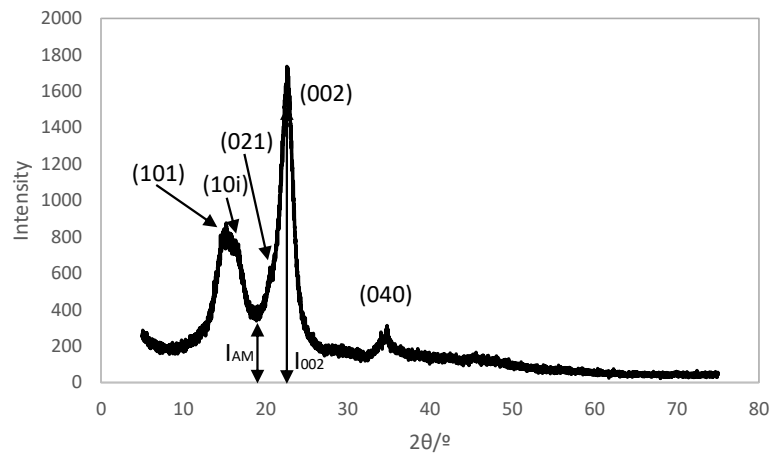


Figure 3.13: XRD spectra showing calculation of CI using the Segal method.^[96]

$$CI = \frac{I_{002} - I_{AM}}{I_{002}} \cdot 100\% \quad (3.1)$$

A parameter called the crystallinity index (CI) is used to describe the relative amount of crystalline material in cellulose.^[96] The CI of pure untreated MCC, MCC regenerated from IL **5c** and MCC regenerated from IL **6c** have been calculated using the Segal method.^[97] Which is the most commonly used method for calculation of CI. The CI is calculated using the height between the intensity of the crystalline peaks ($I_{002} - I_{AM}$) and the total intensity (I_{002}) (Figure 3.13, Equation 3.1). The method is useful for comparison of relative difference between samples, but has some disadvantages. One important disadvantage is that the method neglects variations in peak width, and since the peaks vary considerably in width and the width can also be affected by the crystallite size, a comparison of height cannot give a reasonable estimate of cellulose crystallinity.^[96] The CI of untreated MCC was calculated to be 78 %, for MCC regenerated from IL **5c** it was 74 % and for MCC regenerated from IL **6c** it was 71 %. This confirms that the crystallinity of regenerated MCC has somewhat decreased.

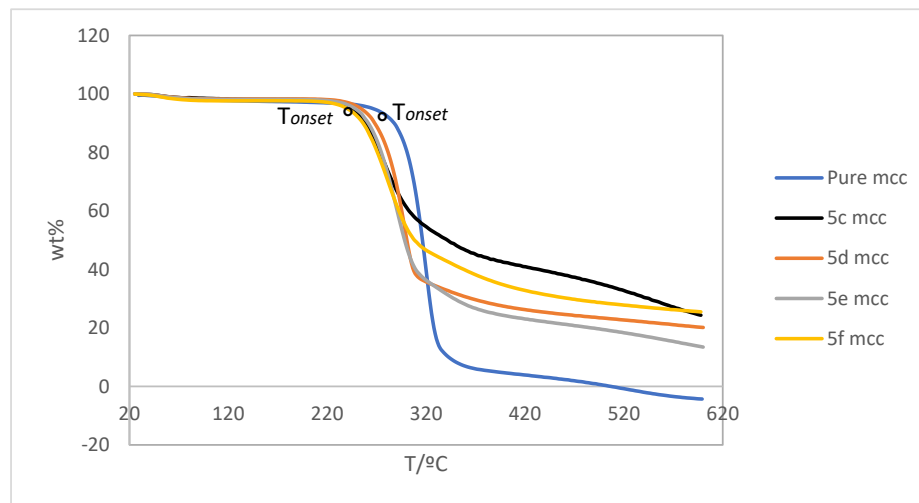


Figure 3.14: TGA of ILs **5c**, **5d**, **5e**, **5f** and pure MCC, with mass in wt% along y-axis and temperature in °C along x-axis.

Thermogravimetric analysis was performed on regenerated MCC from ILs **5c-f**, as well as pure MCC (see Figure 3.14). The analysis was performed to confirm that there have been changes in the thermal stability of cellulose during treatment with IL. The graphs show that regenerated MCC has a lower onset temperature (the temperature where cellulose

3.5 Cellulose dissolution with imidazolium ILs

starts to decompose) than pure untreated MCC. Literature also shows that cellulose regenerated after dissolution with IL has a lower onset temperature than untreated cellulose.^[95] Untreated MCC starts to decompose at around 280 °C, while MCC regenerated from ILs **5c-f** starts to decompose at around 240 °C. The decomposition curve of untreated MCC shows that it decomposes continuously, not stepwise as seen from the ILs in Figure 3.7 and Figure 3.8. The curves for MCC regenerated from ILs have the same continuous decrease without any significant steps, indicating that also they decompose continuously. The TGA results confirm the results from XRD, that there have been changes in the crystal structure of the cellulose.

4 Conclusion

This master's project was aiming at the preparation of new 1,5-disubstituted 1,2,3-triazoles and 1,3,5-trisubstituted 1,2,3-triazolium ILs, as well as new dual functionalized non-toxic imidazolium based ZIs and ZI derived ILs with high cellulose dissolution abilities.

1-Ethyl-5-methyl-1,2,3-triazole (**2**) was successfully synthesized through a regioselective metal-free approach in 28 % yield with the use of excess ethylamine. An optimization of the 1,5-disubstituted 1,2,3-triazole synthesis was performed using aromatic reagents, and it was found that acetophenone with benzylamine, 4-nitrophenyl azide and acetic acid (1:2:1:0.3 eq) gave 1-benzyl-5-phenyl-1,2,3-triazole (**3**) in 59 % yield. From triazole **3** new ILs were made. 1-Benzyl-3-ethyl-5-phenyl-1,2,3-triazolium iodide (**4a**) was successfully prepared in 66 % yield by quaternization, but required long reaction time. From IL **4a**, 1-benzyl-3-ethyl-5-phenyl-1,2,3-triazolium acetate was synthesized in 14 % yield by anion exchange through Finkelstein reaction using silver acetate.

Imidazolium based ZIs **5b**, **6b**, **8b** and **10b** were synthesized from intermediates **5a**, **6a**, **8a** and **10a**, respectively. Intermediates were prepared by addition of ether substituents to imidazole through S_N2 reactions. ZIs **5b**, **6b**, **8b** and **10b** were prepared in 91 %, 99 %, 93% and 74 % yield, respectively, by addition of alkyl sulfate through nucleophilic attack and ring opening of 1,3-propanesultone. From these ZIs, sixteen new ILs (**5c-f**, **6c-f**, **8c-f**, **10c-f**) were made with anions [HSO₃]⁻, [H₂PO₄]⁻, [CF₃SO₃]⁻ and [CH₃SO₃]⁻. All ILs were analyzed by TGA, which showed that ILs **5c-f** had the most thermally stable cation and that [H₂PO₄]⁻ was the most thermally stable anion. The ILs showed moderate dissolution of cellulose when tested for cellulose dissolution by mixing with DMF. XRD analysis showed that IL **5c** is the most efficient IL for dissolution of cellulose, and it dissolved 7.57 wt% MCC at 100 °C in 72 hours.

ILs offer tremendous possibilities as the basis for a revolutionary technological platform, for conversion of biomass into valuable chemicals and fuels, through new industrial chemical processes. In the present study a new concept for preparation of ILs through ZIs were presented, and novel ILs with moderate cellulose dissolution abilities were synthesized. By implementing new allyl functionalities on the imidazolium ZIs, novel ILs with potentially high cellulose dissolution abilities can be prepared.

5 Further work

From previous reports it is well known that a variety of aromatic 1,5-disubstituted 1,2,3-triazoles have been prepared, but the synthesis can be further studied and optimized. Because of the size of the aromatic groups, ILs made from these triazoles are likely to have poor cellulose dissolution abilities. 1,5-Disubstituted 1,2,3-triazoles with short alkyl or ether substituents may on the other hand have cellulose dissolution potential.

The ZIs and ILs in this master's project were synthesized for being non-toxic. Because of time constraints their toxicity was not tested. Further work will include toxicity-testing and altering the synthesis of target products if the toxicity is too high. Based on recent reports, allyl substituents on imidazole based ZIs will be investigated, and new ILs with this functionalization will be prepared and tested for cellulose dissolution.

Further work will include optimization of cellulose dissolution using ILs **5c-f**. Their previously reported maximum dissolved cellulose will be added in one go, and the time taken for complete dissolution will be reported. Cellulose dissolution will be tested with ultrasound and the use of microscope. The thermal degradation mechanism of the ILs can be studied by analyzing the gas evolved during heating cycle by using TGA-MS.

6 Experimental and methods

6.1 General methods

All commercially available chemicals were used without further purification. MCC was pretreated by drying at 105 °C. All reactions were monitored by NMR and/or thin-layer chromatography (TLC) using silica gel 60 F254 (0.25 mm thickness). The TLC plates were developed by UV-light and/or a solution of *p*-anisaldehyde stain (5 mL conc. H₂SO₄, 1.5 mL absolute acetic acid and 3.7 mL *p*-anisaldehyde in 137 mL absolute EtOH) with heating. Flash column chromatography was carried out using Merck silica gel 60 (0.040 - 0.063 mm) in glass columns.

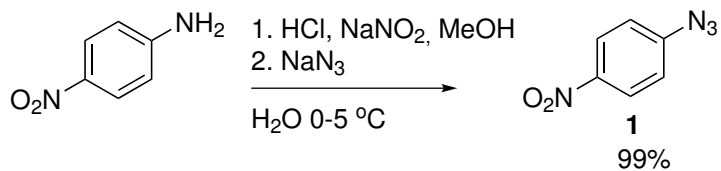
¹H and ¹³C NMR spectra were recorded either on an Bruker Avance DPX 400 MHz or a Bruker Avance III 600 MHz spectrometer under the conditions stated next to the NMR data. Chemical shifts (δ) are given in parts per million (ppm) and are referenced to tetramethylsilane (TMS). Coupling constants (J) are given in Hertz. The multiplicities of the signals are reported as singlet (s), doublet (d), triplet (t), quartet (q), multiplet (m), broad (b) or a combination of these. Solvents used for NMR were deuterated chloroform (CDCl₃) with shifts δ (ppm)=7.26 (s) for ¹H NMR and δ (ppm) = 77.36 for ¹³C NMR. Deuterated methanol (CD₃OD) with shifts δ (ppm) = 3.31 (s) for ¹H NMR and δ (ppm) = 49 for ¹³C NMR. Deuterated dimethyl sulfoxide ((CD₃)₂SO) with shifts δ (ppm) = 2.50 for ¹H NMR and δ (ppm) = 39.52 for ¹³C NMR.

IR spectra were recorded with a Nicolet 20SXC FT-IR spectrometer using EZ OMNIC software and a Bruker Alpha FTIR spectrometer using OPUS V7 software to analyse the spectra. Accurate mass determination by HRMS in positive and negative mode was performed on a "Synapt G2-S" Q-TOF instrument from Waters TM. Samples were ionized by the use of ASAP probe (APCI) or ESI probe. No chromatographic separation was used previous to the mass analysis. Calculated exact mass and spectra processing was done by Waters TM Software Masslynx V4.1 SCN871.

Thermogravimetric analyzes were performed using a TG 209 F1 Libra instrument from Netzsch, with ceramic crucibles under nitrogen atmosphere with a heating rate of 10 °C/min from 30 °C to 600 °C. The crystallinity of cellulose samples were determined by X-ray Diffraction using a Bruker D8 Advance DaVinci X-Ray Diffractometer, with a 30 min scan from 5-75 degrees with a 0.1 degree slit.

6.2 Synthesis of 4-nitrophenyl azide (**1**)

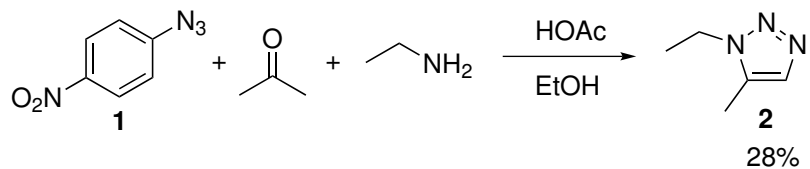
6.2 Synthesis of 4-nitrophenyl azide (**1**)



4-Nitroaniline (0.20 mol, 28.0 g, 1.0 eq) was dissolved in 2.4 N HCl solution (300 mL). Methanol (60 mL) was added to increase the solubility. The solution was cooled to 0 °C and 6.0 M NaNO₂ (0.24 mol, 16.6 g, 1.18 eq) in water (40 mL) was added dropwise. The mixture was stirred at 0 °C for 30 minutes, before 4.1 M solution of NaN₃ (0.24 mol, 16.0 g, 1.21 eq) in water (60 mL) was added dropwise over 15 minutes. The reaction mixture was stirred at room temperature for one hour. The reaction mixture was extracted with EtOAc and washed with saturated NaHCO₃ solution, organic phase was dried over MgSO₄ and concentrated under reduced pressure to afford the product as a yellow solid (33.0 g, 99 %).

¹H NMR (400 MHz, CDCl₃): δ(ppm) = 8.27 (d, *J* = 9.2 Hz, 2H, H_{Ar}), 7.16 (d, *J* = 9.2 Hz, 2H, H_{Ar}). ¹H NMR corresponds to previously reported data,^[82] and is presented in Appendix B.

6.3 Synthesis of 1-ethyl-5-methyl-1,2,3-triazole (**2**)



To ethylamine solution in water (70 % in H₂O)(48.74 mmol, 2.20 g, 8.0 eq), acetone (6.09 mmol, 0.35 g, 1.0 eq), acetic acid (1.83 mmol, 0.10 g, 0.3 eq) and 4-nitrophenyl azide (6.09 mmol, 1.00 g, 1.0 eq) were mixed in the respective order. The mixture was dissolved in absolute EtOH (30 mL) and stirred at room temperature for 71 hours. The crude reaction mixture was concentrated under reduced pressure, and purified by flash column chromatography using silica gel. Dichloromethane was used as the first eluent and EtOAc:pentane (1:1) as the second eluent. The product was concentrated under reduced pressure affording trizole **2** as a dark brown viscous liquid (0.19 g, 28 %).

6.4 Synthesis of 1-benzyl-5-phenyl-1,2,3-triazole (**3**)

¹H NMR (600 MHz, CDCl₃): δ (ppm) = 7.43 (s, 1H, CHN), 4.30 (q, J = 7.3 Hz, 2H, CH₂N), 2.32 (s, 3H, CH₃C), 1.50 (t, J = 7.4 Hz, 3H, CH₃CH₂).

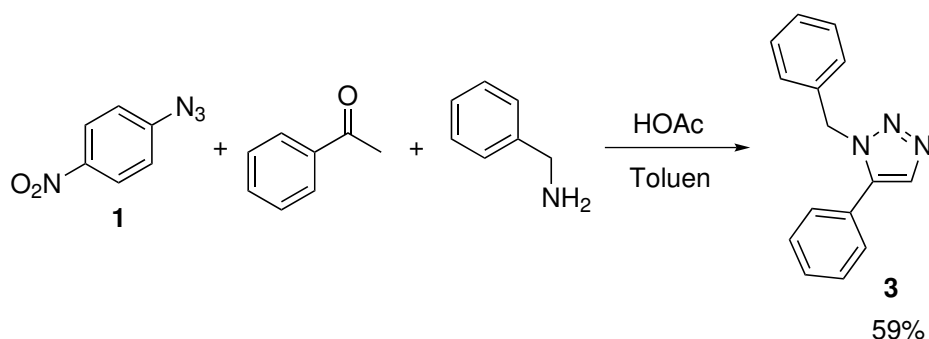
¹³C NMR (600 MHz, CDCl₃): δ (ppm) = 133.0 (CCH₃), 131.8 (CHN), 42.6 (CH₂N), 15.2 (CH₃CH₂), 8.3 (CH₃C).

IR (thin film, cm⁻¹): 2985, 2941, 1558, 1463, 1448, 1421, 1386, 1357, 1320, 1304, 1239, 1217, 1175, 1113, 1088, 1051, 967, 820, 699, 666, 634.

HRMS (ASAP+): calcd for C₅H₁₀N₃ [M+H] 112.0875, obsd 112.0874.

Spectra are presented in Appendix C.

6.4 Synthesis of 1-benzyl-5-phenyl-1,2,3-triazole (**3**)



Benzylamine (60.94 mmol, 6.53 g, 2.0 eq), acetophenone (30.47 mmol, 3.66 g, 1.0 eq), acetic acid (9.14 mmol, 0.55 g, 0.3 eq) and 4-nitrophenyl azide (30.47 mmol, 5.00 g, 1.0 eq) were mixed in the respective order. The mixture was dissolved in toluene and stirred at 100 °C for 19 hours. The crude reaction mixture was concentrated under reduced pressure and purified by flash column chromatography using silica gel. Dichloromethane was used as the first eluent and EtOAc:pentane (1:1) as the second eluent. The product was concentrated under reduced pressure affording triazole **3** as a dark brown semi liquid/semi solid in 59 % yield (4.20 g).

¹H NMR (600 MHz, CDCl₃): δ (ppm) = 7.74 (s, 1H, CHN), 7.46-7.39 (m, 3H, H_{Ar}), 7.29-7.24 (m, 5H, H_{Ar}), 7.09-7.06 (s, 2H, H_{Ar}), 5.55 (s, 2H, CH₂N).

¹³C NMR (600 MHz, CDCl₃): δ (ppm) = 138.1 (CN), 135.5 (C_{Ar}), 133.3 (CHN), 129.5 (C_{Ar}), 128.9 (2 x C_{Ar}), 128.9 (2 x C_{Ar}), 128.8 (2 x C_{Ar}), 128.1 (C_{Ar}), 127.2 (2 x C_{Ar}), 126.9 (C_{Ar}), 51.8 (CH₂N).

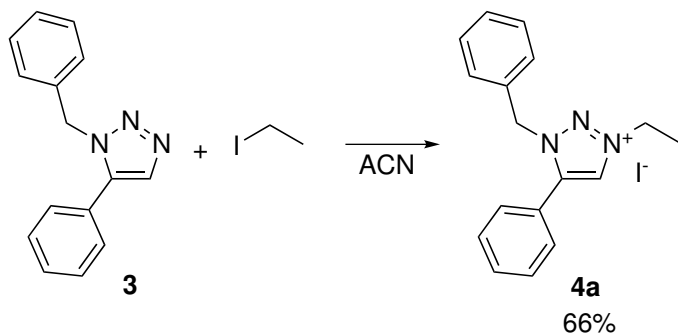
6.5 Synthesis of IL 1-benzyl-3-ethyl-5-phenyl-1,2,3-triazolium iodide (**4a**)

IR (thin film, cm^{-1}): 3340, 3062, 3031, 1733, 1661, 1600, 1496, 1483, 1453, 1372, 1359, 1311, 1240, 1210, 1179, 1157, 1132, 1110, 1075, 1043, 1028, 1015, 1001, 975, 946, 922, 847, 835, 782, 761, 726, 692.

HRMS (ASAP+): calcd for $\text{C}_{15}\text{H}_{14}\text{N}_3$ [$\text{M}+\text{H}$] 236.1188, obsd 236.1187.

^1H NMR shifts corresponds with previously reported data^[98] and spectra are presented in Appendix D.

6.5 Synthesis of IL 1-benzyl-3-ethyl-5-phenyl-1,2,3-triazolium iodide (**4a**)



1-Benzyl-5-phenyl-1,2,3-triazole (0.467 mmol, 0.11 g, 1.0 eq) was mixed with iodoethane (0.935 mmol, 0.15 g, 2.0 eq). The mixture was dissolved in acetonitrile (2 mL) and stirred at 70 °C for 46 hours. The mixture was washed with ethyl acetate and concentrated under reduced pressure affording triazolium IL **4a** as a brown viscous liquid in 66 % yield (0.12 g).

^1H NMR (600 MHz, CDCl_3): δ (ppm) = 9.60 (s, 1H, CHN^+), 7.63-7.59 (m, 3H, H_{Ar}), 7.56-7.54 (m, 2H, H_{Ar}), 7.40-7.36 (m, J = 7.4 Hz, 3H, H_{Ar}), 7.13 (d, J = 7.1 Hz, 2H, H_{Ar}), 5.68 (s, 2H, CH_2N), 5.00 (q, J = 7.4 Hz, 2H, N^+CH_2), 1.79 (t, J = 7.4 Hz, 3H, CH_3).

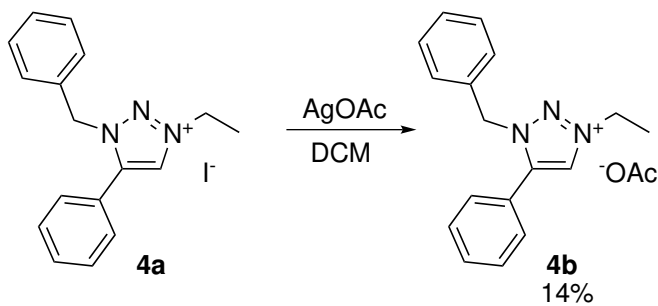
^{13}C NMR (600 MHz, CDCl_3): δ (ppm) = 142.9 (CN), 132.2 (C_{Ar}), 131.2 (C_{Ar}), 130.2 (C_{Ar}), 129.9 (C_{Ar}), 129.8 (C_{Ar}), 129.5 (C_{Ar}), 129.0 (C_{Ar}), 128.9 (C_{Ar}), 128.8 (C_{Ar}), 128.2 (C_{Ar}), 128.1 (C_{Ar}), 127.2 (C_{Ar}), 121.7 (CHN^+), 55.4 (CH_2N), 51.8 (N^+CH_2), 14.7 (CH_3).

HRMS (ES+): calcd for $\text{C}_{17}\text{H}_{18}\text{N}_3$ [M] 264.1501, obsd 264.1504.

HRMS (ES-): calcd for I [M] 126.9045, obsd 126.9047.

Spectra are presented in Appendix E.

6.6 Synthesis of IL 1-benzyl-3-ethyl-5-phenyl-1,2,3-triazolium acetate (**4b**)



1-Benzyl-5-phenyl-1,2,3-triazolium iodide (**4a**) (0.281 mmol, 0.11 g, 1.0 eq) was mixed with AgOAc (0.309 mmol, 0.052 g, 1.1 eq) and dissolved in dichloromethane (15 mL). The mixture was stirred for 24 hours at room temperature. Precipitated AgI was filtered off and solvent was removed under reduced pressure. Absolute EtOH was added to precipitate remaining AgI . The precipitate was filtered off and solvent was removed under reduced pressure affording IL **4b** as a dark brown viscous liquid in 14 % yield (0.013 g).

$^1\text{H NMR}$ (400 MHz, CDCl_3): 9.93 (s, 1H, CHN^+), 7.56-7.35 (m, 8H, H_{Ar}), 7.08-7.06 (m, 2H, H_{Ar}), 5.52 (s, 2H, CH_2N), 4.63 (q, $J = 7.3$ Hz, 2H, N^+CH_2), 1.71 (t, $J = 7.0$ Hz, 3H, CH_3).

$^{13}\text{C NMR}$ (400 MHz, CDCl_3): 133.1 (CN), 130.2 (C_{Ar}), 129.7 (C_{Ar}), 129.7 (C_{Ar}), 129.7 (C_{Ar}), 129.5 (C_{Ar}), 129.2 (C_{Ar}), 129.2 (C_{Ar}), 129.1 (C_{Ar}), 128.8 (C_{Ar}), 127.8 (C_{Ar}), 127.5 (C_{Ar}), 127.4 (C_{Ar}), 122.3 (CHN^+), 53.6 (CH_2N), 51.8 (N^+CH_2), 16.1 (CH_3).

HRMS (ES+): calcd for $\text{C}_{17}\text{H}_{18}\text{N}_3$ [M] 264.1501, obsd 264.1506.

HRMS (ES-): calcd for $\text{C}_2\text{H}_3\text{O}_2$ [M] 59.0133, obsd 59.0133.

Spectra are presented in Appendix F.

6.7 General Procedure A for preparation of imidazolium based ZIs

Sodium ethoxide (2.0 eq) was dissolved in acetonitrile and stirred for 10 minutes at room temperature. Imidazole (1.0 eq) was added to the reaction mixture and stirred for additional 15 minutes at room temperature. Etherchloride (1.0 eq) was added to the reaction

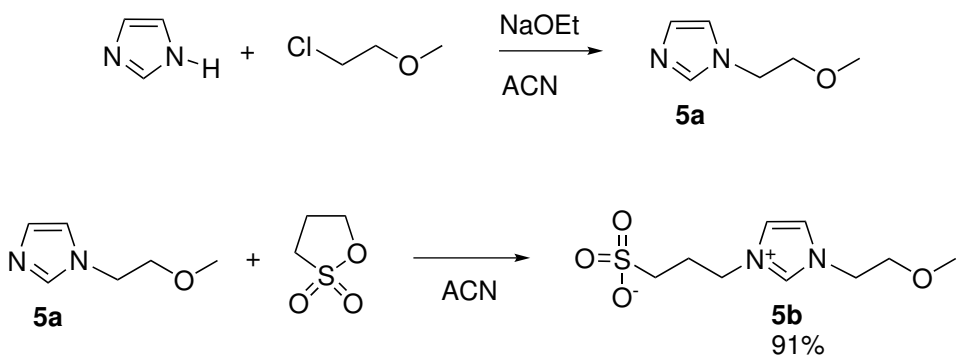
6.8 General Procedure B for preparation of imidazolium based ILs

mixture and the mixture was stirred for 24 hours at 80 °C. Excess sodium ethoxide was filtered off and sultone (1.0 eq) was added. The reaction mixture was heated and stirred at 80 °C for 24 hours. Solvent was removed by rotary evaporator and the zwitterion was further dried by Schlenk line for 24 hours with stirring at 50 °C.

6.8 General Procedure B for preparation of imidazolium based ILs

Zwitterion (1.0 eq) was dissolved in methanol (2.0 eq), and acid (2.0 eq) was added to the mixture. The mixture was stirred at room temperature for 6-24 hours. Solvent and excess acid was removed under reduced pressure and the ionic liquid was further dried on Schlenk line for minimum 24 hours with stirring at 50 °C and by freeze drying for 24 hours.

6.9 Synthesis of 3-(1-(2-methoxyethyl)-1H-imidazol-3-ium-3-yl)propane-1-sulfonate (5b)



Following general procedure A, sodium ethoxide (0.294 mol, 20.0 g, 2.0 eq) was mixed with imidazole (0.147 mol, 10.0 g, 1.0 eq) and 2-chloroethyl methyl ether (0.147 mol, 13.9 g, 1.0 eq), forming intermediate **5a**. The reaction mixture was filtered and 1,3-propanesultone (0.147 mol, 17.95 g, 1.0 eq) was added. The reaction yielded ZI **5b** as a light yellow solid in 91 % yield (33.23 g).

¹H NMR **5a** (400 MHz, CDCl₃): δ(ppm) = 7.53 (s, 1H, NCHN), 7.06 (t, *J* = 1.2 Hz, 1H, CHN), 6.99 (t, *J* = 1.3 Hz, 1H, NCH), 4.11 (t, *J* = 4.9 Hz, 2H, NCH₂CH₂), 3.64 (t, *J* = 5.5 Hz, 2H, CH₂CH₂O), 3.36 (s, 3H, OCH₃).

¹H NMR shifts corresponds with previously reported data^[52] and the spectrum is presented in Appendix G.

¹H NMR 5b (400 MHz, MeOD): δ (ppm) = 9.00 (s, 1H, N⁺CHN), 7.70 (t, J = 1.8 Hz, 1H, CHN), 7.65 (t, J = 1.8 Hz, 1H, N⁺CH), 4.46 (t, J = 7.1 Hz, 2H, CH₂CH₂N⁺), 4.41 (t, J = 4.7 Hz, 2H, NCH₂CH₂), 3.75 (t, J = 4.8 Hz, 2H, CH₂CH₂O), 3.39 (s, 3H, OCH₃), 2.81 (t, J = 7.3 Hz, 2H, SCH₂CH₂), 2.34-2.32 (m, J = 14.3, 7.3 Hz, 2H, CH₂CH₂CH₂).

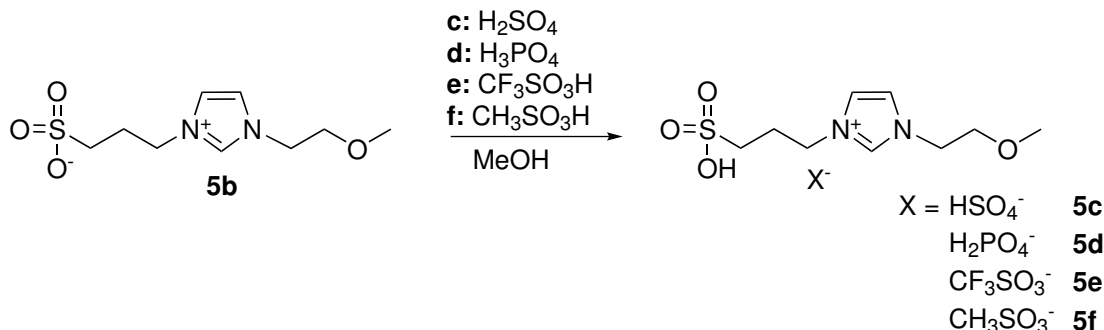
¹³C NMR 5b (600 MHz, MeOD): δ (ppm) = 136.7 (N⁺CHN), 122.9 (N⁺CH), 122.2 (CHN), 69.7 (CH₂CH₂O), 57.7 (OCH₃), 49.2 (NCH₂), 47.8 (CH₂N⁺), 46.9 (SCH₂CH₂), 25.7 (CH₂CH₂CH₂).

IR 5b (thin film, cm⁻¹): 3433, 3402, 3303, 3136, 3097, 2979, 2948, 2821, 2365, 2337, 1731, 1667, 1562, 1448, 1392, 1343, 1265, 1200, 1183, 1166, 1115, 1093, 1033, 1016, 924, 895, 840, 808, 756, 699, 658, 640, 611.

HRMS 5b (ASAP+): calcd for C₉H₁₇N₂SO₄ [M+H] 249.0909, obsd 249.0907.

¹H NMR shifts corresponds with previously reported data^[52] and spectra are presented in Appendix H.

6.10 Synthesis of ILs based on ZI 5b



6.10.1 Synthesis of IL 1-(2-methoxyethyl)-3-(3-sulfopropyl)-1H-imidazol-3-i um hydrogen sulfate (5c)

Following general procedure B, zwitterion **5b** was mixed with sulfuric acid producing IL **5c** as a dark brown viscous liquid in 99 % yield.

6.10 Synthesis of ILs based on ZI **5b**

¹H NMR (600 MHz, MeOD): δ (ppm) = 8.89 (s, 1H, N⁺CHN), 7.59 (t, J = 1.6 Hz, 1H, CHN), 7.55 (t, J = 1.9 Hz, 1H, N⁺CH), 4.35 (t, J = 7.0 Hz, 2H, CH₂CH₂N⁺), 4.32 (t, J = 4.7 Hz, 2H, NCH₂CH₂), 3.64 (t, J = 5.1 Hz, 2H, CH₂CH₂O), 3.27 (s, 3H, OCH₃), 2.74 (t, J = 7.2 Hz, 2H, SCH₂CH₂), 2.28-2.21 (m, J = 13.0, 7.2 Hz, 2H, CH₂CH₂CH₂).

¹³C NMR (600 MHz, MeOD): δ (ppm) = 136.7 (N⁺CHN), 123.0 (N⁺CH), 122.1 (CHN), 69.7 (CH₂CH₂O), 57.7 (OCH₃), 49.4 (NCH₂), 47.8 (CH₂N⁺), 47.0 (SCH₂CH₂), 25.7 (CH₂CH₂CH₂).

IR (thin film, cm⁻¹): 3153, 3096, 2841, 2420, 1694, 1565, 1454, 1352, 1271, 1147, 1039, 878, 814, 741, 657, 641.

HRMS (ES+): calcd for C₉H₁₇N₂SO₄ [M] 249.0909, obsd 249.0914.

HRMS (ES-): calcd for HSO₄ [M] 96.9596, obsd 96.9595.

T_d(10%): 197 °C.

Spectra of IL **5c** are presented in Appendix I.

6.10.2 Synthesis of IL 1-(2-methoxyethyl)-3-(3-sulfopropyl)-1H-imidazol-3-ium dihydrogen phosphate (**5d**)

Following general procedure B, zwitterion **5b** was mixed with phosphoric acid producing IL **5d** as a orange viscous liquid in 99 % yield.

¹H NMR (600 MHz, MeOD): δ (ppm) = 9.00 (s, 1H, N⁺CHN), 7.70 (t, J = 1.9 Hz, 1H, CHN), 7.64 (t, J = 1.6 Hz, 1H, N⁺CH), 4.46 (t, J = 7.2 Hz, 2H, CH₂CH₂N⁺), 4.41 (t, J = 4.7 Hz, 2H, NCH₂CH₂), 3.75 (t, J = 5.1 Hz, 2H, CH₂CH₂O), 3.39 (s, 3H, OCH₃), 2.81 (t, J = 6.8 Hz, 2H, SCH₂CH₂), 2.38-2.31 (m, J = 14.0, 7.0 Hz, 2H, CH₂CH₂CH₂).

¹³C NMR (600 MHz, MeOD): δ (ppm) = 136.7 (N⁺CHN), 122.9 (N⁺CH), 122.2 (CHN), 69.7 (CH₂CH₂O), 57.8 (OCH₃), 49.4 (NCH₂), under solvent peak (CH₂N⁺), 46.9 (SCH₂CH₂), 25.7 (CH₂CH₂CH₂).

IR (thin film, cm⁻¹): 2833, 2352, 2319, 1651, 1565, 1454, 1119, 963, 821, 738, 657, 640.

HRMS (ES+): calcd for C₉H₁₇N₂SO₄ [M] 249.0909, obsd 249.0906.

HRMS (ES-): calcd for H₂PO₄ [M] 96.9691, obsd 96.9691.

T_d(10%): 268 °C.

Spectra of IL **5d** are presented in Appendix J.

6.10.3 Synthesis of IL 1-(2-methoxyethyl)-3-(3-sulfopropyl)-1H-imidazol-3-i um trifluoromethanesulfonate (**5e**)

Following general procedure B, zwitterion **5b** was mixed with trifluoromethanesulfonic acid producing IL **5e** as a brown viscous liquid in 99 % yield.

¹H NMR (600 MHz, MeOD): δ (ppm) = 9.00 (s, 1H, N⁺CHN), 7.70 (t, J = 1.8 Hz, 1H, CHN), 7.65 (t, J = 1.8 Hz, 1H, N⁺CH), 4.46 (t, J = 7.1 Hz, 2H, CH₂CH₂N⁺), 4.41 (t, J = 4.6 Hz, 2H, NCH₂CH₂), 3.75 (t, J = 5.0 Hz, 2H, CH₂CH₂O), 3.39 (s, 3H, OCH₃), 2.83 (t, J = 7.0 Hz, 2H, SCH₂CH₂), 2.38-2.31 (m, J = 14.1, 7.2 Hz, 2H, CH₂CH₂CH₂).

¹³C NMR (600 MHz, MeOD): δ (ppm) = 136.7 (N⁺CHN), 122.9 (N⁺CH), 122.1 (CHN), 69.7 (CH₂CH₂O), 57.7 (OCH₃), 49.4 (NCH₂), under solvent peak (CH₂N⁺), 46.9 (SCH₂CH₂), 25.7 (CH₂CH₂CH₂).

¹⁹F NMR (600 MHz, MeOD, hexafluorobenzene): -80.2 (s, 3F, CF₃).

IR (thin film, cm⁻¹): 3153, 2942, 1698, 1565, 1451, 1354, 1292, 1160, 1016, 904, 827, 761, 745, 630.

HRMS (ES+): calcd for C₉H₁₇N₂SO₄ [M] 249.0909, obsd 249.0910.

HRMS (ES-): calcd for CF₃SO₃ [M] 148.9520, obsd 148.9521.

T_d(10%): 173 °C.

Spectra of IL **5e** are presented in Appendix K.

6.10.4 Synthesis of IL 1-(2-methoxyethyl)-3-(3-sulfopropyl)-1H-imidazol-3-i um methanesulfonate (**5f**)

Following general procedure B, zwitterion **5b** was mixed with methanesulfonic acid producing IL **5f** as a light brown viscous liquid in 99 % yield.

¹H NMR (600 MHz, MeOD): δ (ppm) = 9.01 (s, 1H, N⁺CHN), 7.70 (t, J = 1.8 Hz, 1H, CHN), 7.66 (t, J = 1.8 Hz, 1H, N⁺CH), 4.46 (t, J = 7.3 Hz, 2H, CH₂CH₂N⁺), 4.41 (t, J = 5.1 Hz, 2H, NCH₂CH₂), 3.75 (t, J = 5.0 Hz, 2H, CH₂CH₂O), 3.39 (s, 3H, OCH₃), 2.84 (t, J = 7.1 Hz, 2H, SCH₂CH₂), 2.38-2.31 (m, J = 14.0, 7.1 Hz, 2H, CH₂CH₂CH₂).

6.11 Synthesis of 3-(1-(2-ethoxyethyl)-1H-imidazol-3-ium-3-yl)propane-1-sulfonate (**6b**)

¹³C NMR (600 MHz, MeOD): δ (ppm) = 136.7 (N⁺CHN), 122.9 (N⁺CH), 122.2 (CHN), 69.7 (CH₂CH₂O), 57.7 (OCH₃), 49.4 (NCH₂), under solvent peak (CH₂N⁺), 47.0 (SCH₂CH₂), 25.7 (CH₂CH₂CH₂).

IR (thin film, cm⁻¹): 3150, 3114, 3024, 2940, 2388, 1694, 1565, 1451, 1420, 1335, 1291, 1237, 1160, 1113, 1082, 1032, 975, 888, 832, 760, 658, 642.

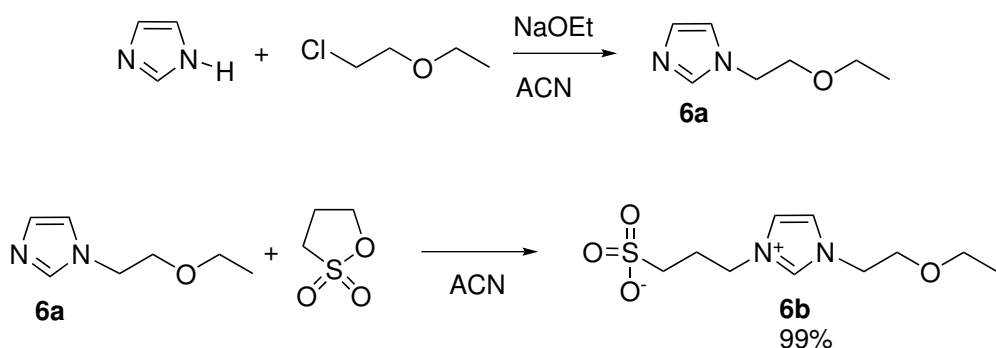
HRMS (ES+): calcd for C₉H₁₇N₂SO₄ [M] 249.0909, obsd 249.0907.

HRMS (ES-): calcd for CH₃SO₃ [M] 94.9803, obsd 94.9802.

T_d(10%): 210 °C.

Spectra of IL **5f** are presented in Appendix L.

6.11 Synthesis of 3-(1-(2-ethoxyethyl)-1H-imidazol-3-ium-3-yl)propane-1-sulfonate (**6b**)



Following general procedure A, sodium ethoxide (0.294 mol, 20.0 g, 2.0 eq) was mixed with imidazole (0.147 mol, 10.0 g, 1 eq) and 2-chloroethyl ethyl ether (0.147 mol, 16.0 g, 1.0 eq), forming intermediate **6a**. The reaction mixture was filtered and 1,3-propanesultone (0.147 mol, 17.95 g, 1.0 eq) was added. The reaction mixture yielded ZI **6b** as a light brown solid in 99 % yield (38.5 g).

¹H NMR **6a** (400 MHz, MeOD): δ (ppm) = 7.66 (s, 1H, NCHN), 7.16 (t, *J* = 1.3 Hz, 1H, CHN), 6.96 (t, *J* = 1.2 Hz, 1H, NCH), 4.19 (t, *J* = 5.0 Hz, 2H, NCH₂CH₂), 3.70 (t, *J* = 5.2 Hz, 2H, CH₂CH₂O), 3.52-3.47 (m, *J* = 7.0 Hz, 2H, OCH₂CH₃), 1.17 (t, *J* = 7.2 Hz, 3H, CH₂CH₃).

The spectrum is presented in Appendix M.

¹H NMR **6b** (600 MHz, MeOD): δ (ppm) = 9.01 (s, 1H, N⁺CHN), 7.71 (t, J = 1.9 Hz, 1H, CHN), 7.66 (t, J = 1.7 Hz, 1H, N⁺CH), 4.47 (t, J = 7.1 Hz, 2H, CH₂CH₂N⁺), 4.42 (t, J = 4.8 Hz, 2H, NCH₂CH₂), 3.80 (t, J = 5.0 Hz, 2H, CH₂CH₂O), 3.57-3.53 (m, J = 6.9 Hz, 2H, OCH₂CH₃), 2.82 (t, J = 7.0 Hz, 2H, SCH₂CH₂), 2.37-2.33 (m, J = 14.1, 7.1 Hz, 2H, CH₂CH₂CH₂), 1.19 (t, J = 6.9 Hz, 3H, CH₂CH₃).

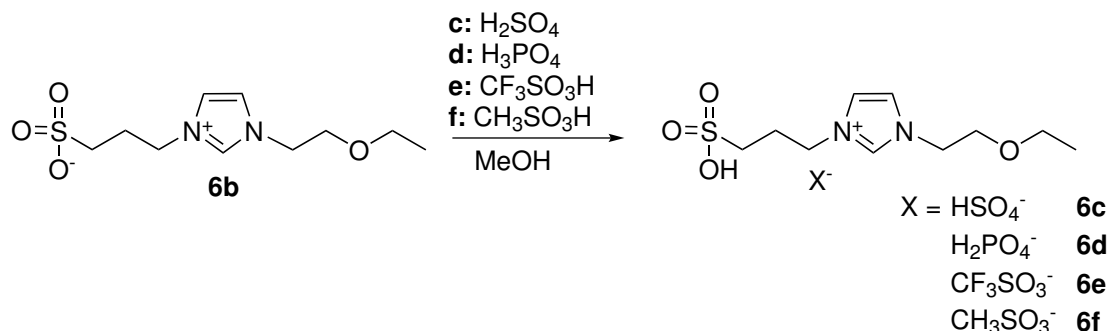
¹³C NMR **6b** (600 MHz, MeOD): δ (ppm) = 136.7 (N⁺CHN), 122.9 (N⁺CH), 122.2 (CHN), 67.6 (CH₂CH₂O), 66.2 (OCH₂CH₃), 49.6 (NCH₂), 47.8 (CH₂N⁺), 47.0 (SCH₂CH₂), 25.8 (CH₂CH₂CH₂), 13.9 (CH₂CH₃).

IR **6b** (thin film, cm⁻¹): 3517, 3468, 3445, 3413, 3359, 3335, 3313, 3209, 3175, 3138, 3096, 3075, 3058, 2974, 2876, 2744, 2636, 1668, 1563, 1449, 1384, 1339, 1267, 1160, 1032, 958, 922, 889, 860, 773, 752, 657, 645.

HRMS **6b** (ASAP+): calcd for C₁₀H₁₉N₂SO₄ [M+H] 263.1066, obsd 263.1061.

Spectra are presented in Appendix N.

6.12 Synthesis of ILs based on ZI **6b**



6.12.1 Synthesis of IL 1-(2-ethoxyethyl)-3-(3-sulfopropyl)-1H-imidazol-3-ium hydrogen sulfate (**6c**)

Following general procedure B, zwitterion **6b** was mixed with sulfuric acid producing IL **6c** as a dark brown viscous liquid in 99 % yield.

¹H NMR (600 MHz, MeOD): δ (ppm) = 9.00 (s, 1H, N⁺CHN), 7.70 (t, J = 1.8 Hz, 1H, CHN), 7.67 (t, J = 1.7 Hz, 1H, N⁺CH), 4.47 (t, J = 7.0 Hz, 2H, CH₂CH₂N⁺), 4.42 (t, J = 4.9 Hz, 2H, NCH₂CH₂), 3.80 (t, J = 4.8 Hz, 2H, CH₂CH₂O), 3.56-3.53 (m, J = 7.0 Hz,

6.12 Synthesis of ILs based on ZI **6b**

2H, OCH_2CH_3), 2.85 (t, $J = 7.2$ Hz, 2H, SCH_2CH_2), 2.38-2.33 (m, $J = 14.1, 7.2$ Hz, 2H, $\text{CH}_2\text{CH}_2\text{CH}_2$), 1.18 (t, $J = 6.8$ Hz, 3H, CH_2CH_3).

^{13}C NMR (600 MHz, MeOD): δ (ppm) = 136.7 (N^+CHN), 123.0 (N^+CH), 122.2 (CHN), 67.6 ($\text{CH}_2\text{CH}_2\text{O}$), 66.2 (OCH_2CH_3), 49.6 (NCH_2), 47.8 (CH_2N^+), 47.1 (SCH_2CH_2), 25.7 ($\text{CH}_2\text{CH}_2\text{CH}_2$), 14.0 (CH_2CH_3).

IR (thin film, cm^{-1}): 3151, 2881, 1697, 1565, 1448, 1109, 1017, 867, 741, 657, 642.

HRMS (ES+): calcd for $\text{C}_{10}\text{H}_{19}\text{N}_2\text{SO}_4$ [M] 263.1066, obsd 263.1071.

HRMS (ES-): calcd for HSO_4 [M] 96.9596, obsd 96.9598.

T_d(10%): 178 °C.

Spectra of IL **6c** are presented in Appendix O.

6.12.2 Synthesis of IL 1-(2-ethoxyethyl)-3-(3-sulfopropyl)-1*H*-imidazol-3-iun dihydrogen phosphate (6d)

Following general procedure B, zwitterion **6b** was mixed with phosphoric acid producing IL **6d** as a dark orange viscous liquid in 99 % yield.

^1H NMR (600 MHz, MeOD): δ (ppm) = 9.01 (s, 1H, N^+CHN), 7.70 (t, $J = 1.8$ Hz, 1H, CHN), 7.66 (t, $J = 1.5$ Hz, 1H, N^+CH), 4.47 (t, $J = 7.2$ Hz, 2H, $\text{CH}_2\text{CH}_2\text{N}^+$), 4.41 (t, $J = 4.8$ Hz, 2H, NCH_2CH_2), 3.80 (t, $J = 4.9$ Hz, 2H, $\text{CH}_2\text{CH}_2\text{O}$), 3.57-3.53 (m, $J = 7.1$ Hz, 2H, OCH_2CH_3), 2.83 (t, $J = 6.9$ Hz, 2H, SCH_2CH_2), 2.37-2.32 (m, $J = 14.0, 6.9$ Hz, 2H, $\text{CH}_2\text{CH}_2\text{CH}_2$), 1.19 (t, $J = 7.0$ Hz, 3H, CH_2CH_3).

^{13}C NMR (600 MHz, MeOD): δ (ppm) = 136.6 (N^+CHN), 122.9 (N^+CH), 122.2 (CHN), 67.6 ($\text{CH}_2\text{CH}_2\text{O}$), 66.2 (OCH_2CH_3), 49.6 (NCH_2), 47.8 (CH_2N^+), 46.9 (SCH_2CH_2), 25.7 ($\text{CH}_2\text{CH}_2\text{CH}_2$), 13.9 (CH_2CH_3).

IR (thin film, cm^{-1}): 2876, 2319, 1651, 1564, 1449, 1352, 1124, 967, 739, 657, 641.

HRMS (ES+): calcd for $\text{C}_{10}\text{H}_{19}\text{N}_2\text{SO}_4$ [M] 263.1066, obsd 263.1070.

HRMS (ES-): calcd for H_2PO_4 [M] 96.9691, obsd 96.9693.

T_d(10%): 239 °C.

Spectra of IL **6d** are presented in Appendix P.

6.12.3 Synthesis of IL **1-(2-ethoxyethyl)-3-(3-sulfopropyl)-1H-imidazol-3-ium trifluoromethanesulfonate (6e)**

Following general procedure B, zwitterion **6b** was mixed with trifluoromethanesulfonic acid producing IL **6e** as a dark brown viscous liquid in 99 % yield.

¹H NMR (600 MHz, MeOD): δ (ppm) = 9.00 (s, 1H, N⁺CHN), 7.71 (t, J = 1.7 Hz, 1H, CHN), 7.66 (t, J = 1.7 Hz, 1H, N⁺CH), 4.46 (t, J = 7.0 Hz, 2H, CH₂CH₂N⁺), 4.41 (t, J = 5.0 Hz, 2H, NCH₂CH₂), 3.80 (t, J = 5.0 Hz, 2H, CH₂CH₂O), 3.56-3.53 (m, J = 7.1 Hz, 2H, OCH₂CH₃), 2.85 (t, J = 7.0 Hz, 2H, SCH₂CH₂), 2.38-2.33 (m, J = 14.3, 7.1 Hz, 2H, CH₂CH₂CH₂), 1.18 (t, J = 7.4 Hz, 3H, CH₂CH₃).

¹³C NMR (600 MHz, MeOD): δ (ppm) = 136.6 (N⁺CHN), 123.0 (N⁺CH), 122.2 (CHN), 67.6 (CH₂CH₂O), 66.2 (OCH₂CH₃), 49.6 (NCH₂), under solvent peak (CH₂N⁺), 47.0 (SCH₂CH₂), 25.7 (CH₂CH₂CH₂), 13.9 (CH₂CH₃).

¹⁹F NMR (600 MHz, MeOD, hexafluorobenzene): -80.3 (s, 3F, CF₃).

IR (thin film, cm⁻¹): 3153, 2981, 1714, 1565, 1449, 1352, 1286, 1210, 1161, 1020, 910, 760, 745, 632.

HRMS (ES+): calcd for C₁₀H₁₉N₂SO₄ [M] 263.1066, obsd 263.1071.

HRMS (ES-): calcd for CF₃SO₃ [M] 148.9520, obsd 148.9523.

T_d(10%): 164 °C.

Spectra of IL **6e** are presented in Appendix Q.

6.12.4 Synthesis of IL **1-(2-ethoxyethyl)-3-(3-sulfopropyl)-1H-imidazol-3-ium methanesulfonate (6f)**

Following general procedure B, zwitterion **6b** was mixed with methanesulfonic acid producing IL **6f** as a dark brown viscous liquid in 99 % yield.

¹H NMR (600 MHz, MeOD): δ (ppm) = 9.02 (s, 1H, N⁺CHN), 7.71 (t, J = 1.8 Hz, 1H, CHN), 7.67 (t, J = 1.6 Hz, 1H, N⁺CH), 4.47 (t, J = 7.2 Hz, 2H, CH₂CH₂N⁺), 4.42 (t, J = 4.7 Hz, 2H, NCH₂CH₂), 3.80 (t, J = 4.9 Hz, 2H, CH₂CH₂O), 3.56-3.53 (m, J = 7.0 Hz, 2H, OCH₂CH₃), 2.86 (t, J = 7.3 Hz, 2H, SCH₂CH₂), 2.38-2.33 (m, J = 14.0, 7.1 Hz, 2H, CH₂CH₂CH₂), 1.18 (t, J = 7.1 Hz, 3H, CH₂CH₃).

6.13 Synthesis of 1-chloro-2-(2-methoxyethoxy)ethane (**7**)

¹³C NMR (600 MHz, MeOD): δ (ppm) = 136.7 (N⁺CHN), 123.0 (N⁺CH), 122.2 (CHN), 67.6 (CH₂CH₂O), 66.2 (OCH₂CH₃), 49.6 (NCH₂), 47.0 (CH₂N⁺), 38.0 (SCH₂CH₂), 25.7 (CH₂CH₂CH₂), 14.0 (CH₂CH₃).

IR (thin film, cm⁻¹): 3149, 3113, 3024, 2977, 2939, 2875, 2385, 1695, 1564, 1448, 1420, 1336, 1234, 1160, 1104, 1032, 975, 891, 761, 658, 643.

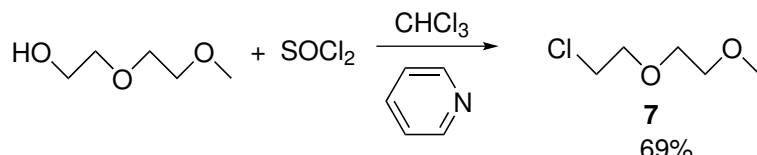
HRMS (ES+): calcd for C₁₀H₁₉N₂SO₄ [M] 263.1066, obsd 263.1070.

HRMS (ES-): calcd for CH₃SO₃ [M] 94.9803, obsd 94.9805.

T_d(10%): 200 °C.

Spectra of IL **6f** are presented in Appendix R.

6.13 Synthesis of 1-chloro-2-(2-methoxyethoxy)ethane (**7**)



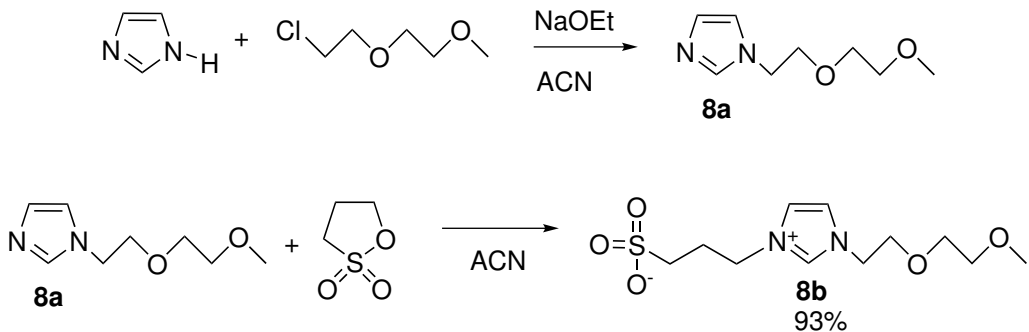
Diethylene glycol monomethylether (0.100 mol, 12.0 g, 1.0 eq) and pyridine (0.100 mol, 7.90 g, 1.0 eq) were mixed and dissolved in chloroform (40 mL). A solution of thionyl chloride (0.200 mol, 23.8 g, 2.0 eq) in chloroform (20 mL) was added dropwise to the mixture using a syringe. The mixture was refluxed at 60 °C for 16 h. The reaction mixture was washed with water (4 x 50 mL) and the organic phase was dried with MgSO₄ and concentrated under reduced pressure. Precursor **7** was obtained as a dark yellow liquid in 69 % yield (9.53 g).

¹H NMR (400 MHz, CDCl₃): 3.78 (t, *J* = 6.4 Hz, 2H, ClCH₂), 3.70-3.65 (m, 4H, CH₂O, CH₂O), 3.59-3.57 (m, 2H, OCH₂), 3.41 (s, 3H, OH₃).

¹H NMR corresponds to previously reported data^[99] and the spectrum is presented in Appendix S.

6.14 Synthesis of 3-(1-(2-(2-methoxyethoxy)ethyl)-1H-imidazol-3-ium-3-yl)propane-1-sulfonate (**8b**)

6.14 Synthesis of
3-(1-(2-methoxyethoxy)ethyl)-1H-imidazol-3-ium-3-ylpropane-1-sulfonate (**8b**)



Following general procedure A, sodium ethoxide (115.44 mmol, 7.86 g, 2.0 eq) was mixed with imidazole (57.72 mmol, 3.93 g, 1.0 eq) and precursor **7** (57.72 mmol, 8.0 g, 1.0 eq), forming intermediate **8a**. The sodium ethoxide was filtered off and 1,3-propanesultone (57.72 mmol, 7.05 g, 1.0 eq) was added. The reaction yielded 93 % (15.41 g) of ZI **8b** as a brown viscous liquid.

¹H NMR **8a** (400 MHz, MeOD): δ (ppm) = 7.69 (s, 1H, NCHN), 7.18 (t, J = 1.3 Hz, 1H, CHN), 6.96 (t, J = 1.2 Hz, 1H, NCH), 4.20 (t, J = 5.0 Hz, 2H, NCH₂CH₂), 3.76 (t, J = 5.0 Hz, 2H, CH₂CH₂O), 3.61-3.59 (m, 2H, CH₂CH₂O), 3.53-3.51 (m, 2H, OCH₂CH₂), 3.35 (s, 3H, OCH₃).

¹H NMR shifts corresponds with previously reported data^[52] and the spectrum is presented in Appendix T.

¹H NMR **8b** (600 MHz, MeOD): δ (ppm) = 9.02 (s, 1H, N⁺CHN), 7.71 (t, J = 1.8 Hz, 1H, CHN), 7.68 (t, J = 1.8 Hz, 1H, N⁺CH), 4.46 (t, J = 7.2 Hz, 2H, CH₂CH₂N⁺), 4.42 (t, J = 4.6 Hz, 2H, NCH₂CH₂), 3.86 (t, J = 5.1 Hz, 2H, CH₂CH₂O), 3.66-3.64 (m, 2H, CH₂CH₂O), 3.55-3.54 (m, 2H, OCH₂CH₂), 3.37 (s, 3H, OCH₃), 2.83 (t, J = 6.9 Hz, 2H, SCH₂CH₂), 2.38-2.33 (m, J = 14.4, 7.3 Hz, 2H, CH₂CH₂CH₂).

¹³C NMR **8b** (600 MHz, MeOD): δ (ppm) = 138.8 (N⁺CHN), 124.9 (N⁺CH), 124.1 (CHN), 73.4 (OCH₂CH₂), 71.8 (OCH₂CH₂), 70.3 (CH₂CH₂O), 59.7 (OCH₃), 51.4 (NCH₂), 49.9 (CH₂N⁺), 49.0 (SCH₂CH₂), 27.8 (CH₂CH₂CH₂).

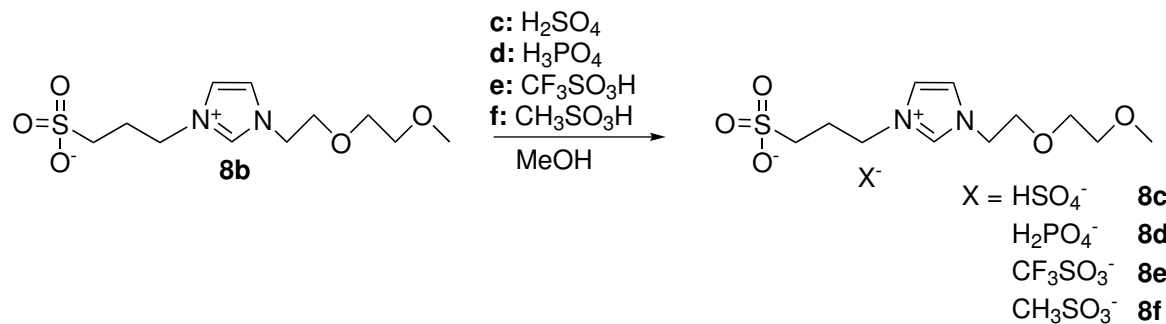
IR **8b** (thin film, cm⁻¹): 3139, 3093, 2926, 2878, 1673, 1564, 1452, 1351, 1290, 1184, 1137, 1098, 1032, 959, 923, 845, 757, 736, 659, 605.

HRMS **8b** (ES+): calcd for C₁₁H₂₁N₂O₅S [M+H] 293.1171, obsd 293.1177.

¹H NMR shifts corresponds with previously reported data^[52] and spectra are presented in Appendix U.

6.15 Synthesis of ILs based on ZI **8b**

6.15 Synthesis of ILs based on ZI **8b**



6.15.1 Synthesis of IL 1-(2-(2-methoxyethoxy)ethyl)-3-(3-sulfopropyl)-1H-imidazol-3-ium hydrogen sulfate (**8c**)

Following general procedure B, zwitterion **8b** was mixed with sulfuric acid producing IL **8c** as a dark brown viscous liquid in 99 % yield.

¹H NMR (600 MHz, MeOD): δ (ppm) = 9.01 (s, 1H, N^+CHN), 7.70 (t, J = 1.9 Hz, 1H, CHN), 7.68 (t, J = 1.6 Hz, 1H, N^+CH), 4.46 (t, J = 7.1 Hz, 2H, $\text{CH}_2\text{CH}_2\text{N}^+$), 4.42 (t, J = 5.0 Hz, 2H, NCH_2CH_2), 3.86 (t, J = 5.1 Hz, 2H, $\text{CH}_2\text{CH}_2\text{O}$), 3.66-3.64 (t, 2H, $\text{CH}_2\text{CH}_2\text{O}$), 3.55-3.53 (m, 2H, OCH_2CH_2), 3.37 (s, 3H, OCH_3), 2.87 (t, J = 6.9 Hz, 2H, SCH_2CH_2), 2.38-2.34 (m, J = 14.3, 7.2 Hz, 2H, $\text{CH}_2\text{CH}_2\text{CH}_2$).

¹³C NMR (600 MHz, MeOD): δ (ppm) = 136.8 (N^+CHN), 123.0 (N^+CH), 122.0 (CHN), 71.4 (OCH_2CH_2), 69.8 (OCH_2CH_2), 68.3 ($\text{CH}_2\text{CH}_2\text{O}$), 57.7 (OCH_3), 49.5 (NCH_2), 48.5 (CH_2N^+), 47.0 (SCH_2CH_2), 25.7 ($\text{CH}_2\text{CH}_2\text{CH}_2$).

IR (thin film, cm^{-1}): 3152, 3116, 2883, 2419, 1707, 1565, 1451, 1351, 1268, 1130 , 1053, 995, 885, 829, 773, 744, 658, 642.

HRMS (ES+): calcd for $\text{C}_{11}\text{H}_{21}\text{N}_2\text{SO}_5$ [M] 293.1171, obsd 293.1175.

HRMS (ES-): calcd for HSO_4 [M] 96.9596, obsd 96.9601.

T_d(10%): 183 °C.

Spectra of IL **8c** are presented in Appendix V.

6.15.2 Synthesis of IL 1-(2-(2-methoxyethoxy)ethyl)-3-(3-sulfopropyl)-1H-imidazol-3-ium dihydrogen phosphate (**8d**)

Following general procedure B, zwitterion **8b** was mixed with phosphoric acid producing IL **8d** as a dark brown viscous liquid in 99 % yield.

¹H NMR (600 MHz, MeOD): δ (ppm) = 9.01 (s, 1H, N⁺CHN), 7.70 (t, J = 1.7 Hz, 1H, CHN), 7.67 (t, J = 1.8 Hz, 1H, N⁺CH), 4.46 (t, J = 7.2 Hz, 2H, CH₂CH₂N⁺), 4.42 (t, J = 4.8 Hz, 2H, NCH₂CH₂), 3.86 (t, J = 4.9 Hz, 2H, CH₂CH₂O), 3.66-3.64 (m, 2H, CH₂CH₂O), 3.55-3.54 (m, 2H, OCH₂CH₂), 3.37 (s, 3H, OCH₃), 2.83 (t, J = 7.2 Hz, 2H, SCH₂CH₂), 2.38-2.33 (m, J = 14.2, 7.0 Hz, 2H, CH₂CH₂CH₂).

¹³C NMR (600 MHz, MeOD): δ (ppm) = 136.8 (N⁺CHN), 122.9 (N⁺CH), 122.1 (CHN), 71.5 (OCH₂CH₂), 69.8 (OCH₂CH₂), 68.3 (CH₂CH₂O), 57.8 (OCH₃), 49.5 (NCH₂), 47.9 (CH₂N⁺), 47.0 (SCH₂CH₂), 25.7 (CH₂CH₂CH₂).

IR (thin film, cm⁻¹): 2878, 2314, 1564, 1451, 1353, 1129, 964, 834, 738, 657, 641.

HRMS (ES+): calcd for C₁₁H₂₁N₂SO₅ [M] 293.1171, obsd 293.1170.

HRMS (ES-): calcd for H₂PO₄ [M] 96.9691, obsd 96.9689.

T_d(10%): 256 °C.

Spectra of IL **8d** are presented in Appendix W.

6.15.3 Synthesis of IL 1-(2-(2-methoxyethoxy)ethyl)-3-(3-sulfopropyl)-1H-imidazol-3-ium trifluoromethanesulfonate (**8e**)

Following general procedure B, zwitterion **8b** was mixed with trifluoromethanesulfonic acid producing IL **8e** as a dark brown viscous liquid in 99 % yield.

¹H NMR (600 MHz, MeOD): δ (ppm) = 9.00 (s, 1H, N⁺CHN), 7.69 (t, J = 1.9 Hz, 1H, CHN), 7.68 (t, J = 1.7 Hz, 1H, N⁺CH), 4.46 (t, J = 7.1 Hz, 2H, CH₂CH₂N⁺), 4.42 (t, J = 4.8 Hz, 2H, NCH₂CH₂), 3.86 (t, J = 4.8 Hz, 2H, CH₂CH₂O), 3.66-3.64 (m, 2H, CH₂CH₂O), 3.55-3.54 (m, 2H, OCH₂CH₂), 3.36 (s, 3H, OCH₃), 2.85 (t, J = 7.1 Hz, 2H, SCH₂CH₂), 2.38-2.33 (m, J = 14.5, 7.3 Hz, 2H, CH₂CH₂CH₂).

¹³C NMR (600 MHz, MeOD): δ (ppm) = 136.8 (N⁺CHN), 123.0 (N⁺CH), 122.1 (CHN), 71.4 (OCH₂CH₂), 69.8 (OCH₂CH₂), 68.2 (CH₂CH₂O), 57.7 (OCH₃), 49.5 (NCH₂), 47.8 (CH₂N⁺), 47.0 (SCH₂CH₂), 25.7 (CH₂CH₂CH₂).

6.16 Synthesis of 1-chloro-2-(2-(2-methoxyethoxy)ethoxy)ethane (**9**)

¹⁹F NMR (600 MHz, MeOD, hexafluorobenzene): -80.29 (CF_3SO_3^-).

IR (thin film, cm^{-1}): 3152, 3116, 2882, 1715, 1565, 1451, 1352, 1294, 1204, 1156, 1018, 905, 834, 759, 631.

HRMS (ES+): calcd for $\text{C}_{11}\text{H}_{21}\text{N}_2\text{SO}_5$ [M] 293.1171, obsd 293.1169.

HRMS (ES-): calcd for CF_3SO_3 [M] 148.9520, obsd 148.9520.

T_d(10%): 156 °C.

Spectra of IL **8e** are presented in Appendix X.

6.15.4 Synthesis of IL 1-(2-(2-methoxyethoxy)ethyl)-3-(3-sulfopropyl)-1H-imidazol-3-ium methanesulfonate (**8f**)

Following general procedure B, zwitterion **8b** was mixed with methanesulfonic acid producing IL **8f** as a dark brown viscous liquid in 99 % yield.

¹H NMR (600 MHz, MeOD): δ (ppm) = 9.01 (s, 1H, N^+CHN), 7.70 (t, J = 1.7 Hz, 1H, CHN), 7.68 (t, J = 1.8 Hz, 1H, N^+CH), 4.46 (t, J = 7.2 Hz, 2H, $\text{CH}_2\text{CH}_2\text{N}^+$), 4.42 (t, J = 4.7 Hz, 2H, NCH_2CH_2), 3.86 (t, J = 4.9 Hz, 2H, $\text{CH}_2\text{CH}_2\text{O}$), 3.66-3.64 (m, 2H, $\text{CH}_2\text{CH}_2\text{O}$), 3.55-3.53 (m, 2H, OCH_2CH_2), 3.36 (s, 3H, OCH_3), 2.85 (t, J = 7.1 Hz, 2H, SCH_2CH_2), 2.38-2.33 (m, J = 14.2, 7.1 Hz, 2H, $\text{CH}_2\text{CH}_2\text{CH}_2$).

¹³C NMR (600 MHz, MeOD): δ (ppm) = 136.8 (N^+CHN), 123.0 (N^+CH), 122.1 (CHN), 71.4 (OCH_2CH_2), 69.8 (OCH_2CH_2), 68.3 ($\text{CH}_2\text{CH}_2\text{O}$), 57.7 (OCH_3), 49.5 (NCH_2), 47.8 (CH_2N^+), 47.0 (SCH_2CH_2), 38.1 (CH_3SO_3^-), 25.7 ($\text{CH}_2\text{CH}_2\text{CH}_2$).

IR (thin film, cm^{-1}): 3149, 3113, 3023, 2938, 2881, 2382, 1692, 1564, 1452, 1420, 1335, 1290, 1240, 1162, 1092, 1026, 975, 890, 836, 760, 658, 642.

HRMS (ES+): calcd for $\text{C}_{11}\text{H}_{21}\text{N}_2\text{SO}_5$ [M] 293.1171, obsd 293.1174.

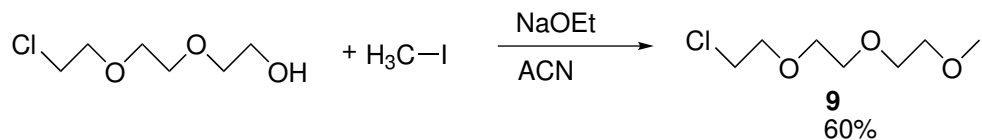
HRMS (ES-): calcd for CH_3SO_3 [M] 94.9803, obsd 94.9803.

T_d(10%): 200 °C.

Spectra of IL **8f** are presented in Appendix Y.

6.16 Synthesis of 1-chloro-2-(2-(2-methoxyethoxy)ethoxy)ethane (**9**)

6.17 Synthesis of
3-(1-(2-(2-methoxyethoxy)ethoxy)ethyl)-1H-imidazol-3-iium-3-yl)propane-1-sulfonate
(10b)

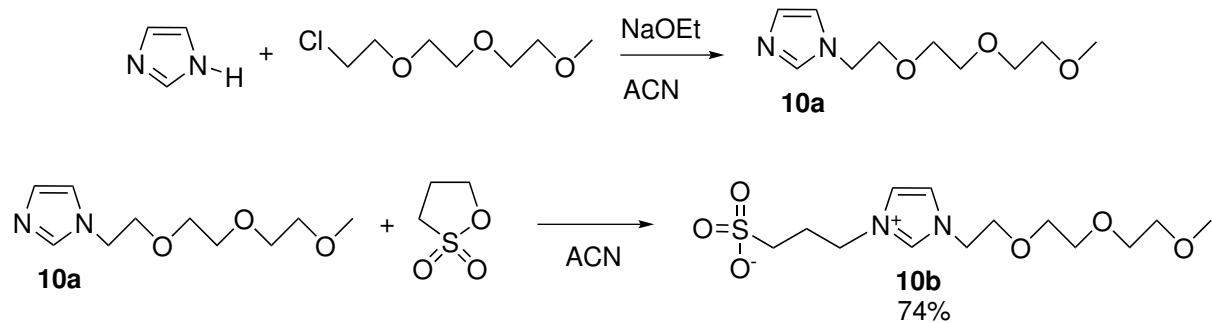


Sodium ethoxide (0.114 mol, 7.76 g, 2.0 eq) was dissolved in acetonitrile (100 mL) and stirred at room temperature for 10 minutes. 2-(2-Chloroethoxy)ethanol (0.057 mol, 9.61 g, 1.0 eq) was added to the reaction mixture and it was stirred for 10 minutes at room temperature. Iodomethane (0.114 mol, 16.24 g, 2.0 eq) was added and the reaction mixture was stirred at 40 °C for 13 hours. Excess sodium ethoxide was filtered off and the reaction mixture was dried on the rotary evaporator. Leftover sodium ethoxide was removed by filtration through silica plug, with DCM as first eluent and EtOAc as the second eluent. The reaction mixture was concentrated under reduced pressure and precursor **9** was obtained as a bright yellow liquid in 60 % yield (6.0 g).

¹H NMR (400 MHz, MeOD): δ (ppm) = 3.76 (dt, 2H, CH₂Cl), 3.69-3.64 (m, 8H, 4 x CH₂O), 3.57-3.55 (m, 2H, CH₂O), 3.38 (s, 3H, CH₃O).

¹H NMR shift corresponded with previously reported data^[100] and spectra are presented in Appendix Z.

6.17 Synthesis of 3-(1-(2-(2-methoxyethoxy)ethoxy)ethyl)-1H-imidazol-3-iium-3-yl)propane-1-sulfonate (**10b**)



Following general procedure A, sodium ethoxide (0.0602 mol, 4.09 g, 2.0 eq) was mixed with imidazole (0.0301 mol, 2.05 g, 1.0 eq) and precursor **9** (0.0301 mol, 5.50 g, 1.0 eq), forming intermediate **10a**. The sodium ethoxide was filtered off and 1,3-propanesultone (0.0301 mol, 3.68 g, 1.0 eq) was added. The reaction yielded ZI **10b** in 74 % (7.51 g) as a brown viscous liquid.

6.18 Synthesis of ILs based on ZI **10b**

¹H NMR 10a (400 MHz, MeOD): δ (ppm) = 7.69 (s, 1H, NCHN), 7.20 (t, J = 1.2 Hz, 1H, CHN), 6.96 (t, J = 1.0 Hz, 1H, NCH), 4.21 (t, J = 5.0 Hz, 2H, NCH₂CH₂), 3.78 (t, J = 5.4 Hz, 2H, NCH₂CH₂), 3.67-3.58 (m, 6H, OCH₂CH₂OCH₂CH₂), 3.55-3.52 (m, 2H, OCH₂CH₂), 3.37 (s, 3H, OCH₃).

The spectrum is presented in Appendix AA.

¹H NMR 10b (600 MHz, MeOD): δ (ppm) = 9.15 (s, 1H, N⁺CHN), 7.81 (t, J = 1.7 Hz, 1H, CHN), 7.77 (t, J = 1.7 Hz, 1H, N⁺CH), 4.36 (t, J = 4.7 Hz, 2H, NCH₂CH₂), 4.33 (t, J = 6.8 Hz, 2H, CH₂CH₂N⁺), 3.78 (t, J = 4.7 Hz, 2H, NCH₂CH₂), 3.56-3.54 (m, 2H, OCH₂CH₂), 3.51-3.48 (m, 4H, OCH₂CH₂), 3.43-3.41 (m, 2H, CH₂CH₂O), 3.24 (s, 3H, OCH₃), 2.43 (t, J = 7.1 Hz, 2H, SCH₂CH₂), 2.13-2.08 (m, J = 14.0, 7.5 Hz, 2H, CH₂CH₂CH₂).

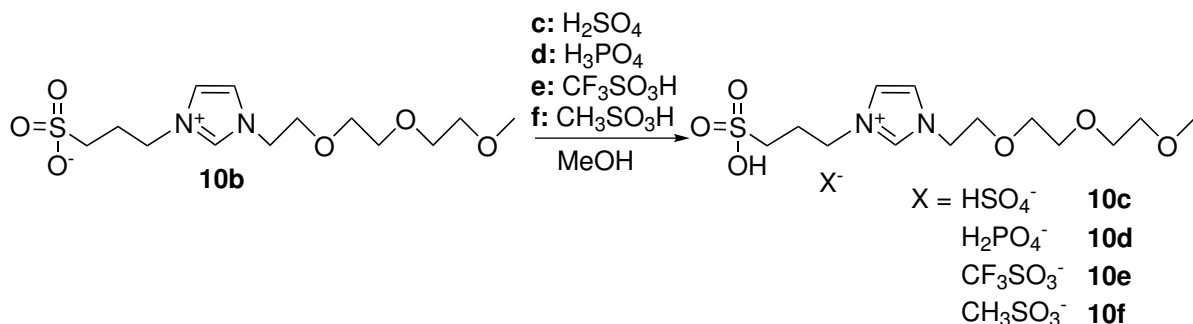
¹³C NMR 10b (600 MHz, MeOD): δ (ppm) = 137.0 (N⁺CHN), 123.3 (N⁺CH), 122.7 (CHN), 71.7 (CH₂CH₂O), 70.0 (OCH₂CH₂), 70.0 (OCH₂CH₂), 70.0 (OCH₂CH₂), 68.6 (CH₂CH₂O), 58.5 (OCH₃), 49.2 (NCH₂), 48.3 (CH₂N⁺), 47.7 (SCH₂CH₂), 26.7 (CH₂CH₂CH₂).

IR 10b (thin film, cm⁻¹): 3384, 3141, 3098, 2877, 1669, 1563, 1450, 1386, 1351, 1293, 1186, 1139, 1102, 1033, 933, 849, 802, 740, 608.

HRMS 10b (ES+): calcd for C₁₃H₂₅N₂O₆S [M+H] 337.1433, obsd 337.1432.

Spectra are presented in Appendix AB.

6.18 Synthesis of ILs based on ZI **10b**



6.18.1 Synthesis of IL **1-(2-(2-methoxyethoxy)ethoxyethyl)-3-(3-sulfopropyl)-1H-imidazol-3-ium hydrogen sulfate (10c)**

Following general procedure B, zwitterion **10b** was mixed with sulfuric acid producing IL **10c** as a dark brown viscous liquid in 99 % yield.

¹H NMR (600 MHz, MeOD): δ (ppm) = 9.01 (s, 1H, N⁺CHN), 7.71 (t, J = 1.8 Hz, 1H, CHN), 7.70 (t, J = 1.8 Hz, 1H, N⁺CH), 4.46 (t, J = 7.2 Hz, 2H, NCH₂CH₂), 4.43 (t, J = 4.7 Hz, 2H, CH₂CH₂N⁺), 3.87 (t, J = 5.0 Hz, 2H, CH₂CH₂O), 3.68-3.66 (m, 2H, OCH₂CH₂), 3.64-3.63 (m, 4H, OCH₂CH₂, OCH₂CH₂), 3.56-3.55 (m, 2H, CH₂CH₂O), 3.37 (s, 3H, OCH₃), 2.86 (t, J = 7.1 Hz, 2H, SCH₂CH₂), 2.37-2.34 (m, J = 14.3, 7.2 Hz, 2H, CH₂CH₂CH₂).

¹³C NMR (600 MHz, MeOD): δ (ppm) = 136.8 (N⁺CHN), 123.1 (N⁺CH), 122.1 (CHN), 71.5 (CH₂CH₂O), 70.0 (OCH₂CH₂), 69.9 (OCH₂CH₂), 68.3 (OCH₂CH₂), 57.7 (CH₂CH₂O), 49.5 (OCH₃), 48.5 (NCH₂), 47.8 (CH₂N⁺), 47.0 (SCH₂CH₂), 25.7 (CH₂CH₂CH₂).

IR (thin film, cm⁻¹): 3151, 3115, 2882, 2426, 1700, 1565, 1499, 1453, 1351, 1254, 1121, 1038, 994, 884, 764, 661, 643, 613.

HRMS (ES+): calcd for C₁₃H₂₅N₂SO₆ [M] 337.1433, obsd 337.1429.

HRMS (ES-): calcd for HSO₄ [M] 96.9596, obsd 96.9597.

T_d(10%): 183 °C.

Spectra of IL **10c** are presented in Appendix AC.

6.18.2 Synthesis of IL **1-(2-(2-methoxyethoxy)ethoxyethyl)-3-(3-sulfopropyl)-1H-imidazol-3-ium dihydrogen phosphate (10d)**

Following general procedure B, zwitterion **10b** was mixed with phosphoric acid producing IL **10d** as a dark orange viscous liquid in 99 % yield.

¹H NMR (600 MHz, MeOD): δ (ppm) = 9.01 (s, 1H, N⁺CHN), 7.70 (s, 2H, CHN, N⁺CH), 4.46 (t, J = 7.3 Hz, 2H, NCH₂CH₂), 4.43 (t, J = 4.8 Hz, 2H, CH₂CH₂N⁺), 3.87 (t, J = 4.9 Hz, 2H, CH₂CH₂O), 3.68-3.67 (m, 2H, OCH₂CH₂), 3.64-3.62 (m, 4H, OCH₂CH₂, OCH₂CH₂), 3.57-3.55 (m, 2H, CH₂CH₂O), 3.38 (s, 3H, OCH₃), 2.83 (t, J = 7.1 Hz, 2H, SCH₂CH₂), 2.37-2.33 (m, J = 14.0, 7.1 Hz, 2H, CH₂CH₂CH₂).

6.18 Synthesis of ILs based on ZI **10b**

^{13}C NMR (600 MHz, MeOD): δ (ppm) = 136.7 (N^+CHN), 123.1 (N^+CH), 122.1 (CHN), 71.6 ($\text{CH}_2\text{CH}_2\text{O}$), 70.0 (OCH_2CH_2), 70.0 (OCH_2CH_2), 70.0 (OCH_2CH_2), 68.3 ($\text{CH}_2\text{CH}_2\text{O}$), 57.7 (OCH_3), 49.2 (NCH_2), 49.5 (CH_2N^+), 47.8 (SCH_2CH_2), 25.7 ($\text{CH}_2\text{CH}_2\text{CH}_2$).

IR (thin film, cm^{-1}): 2877, 2325, 1650, 1563, 1452, 1352, 1130, 963, 880, 834, 740, 658, 640.

HRMS (ES+): calcd for $\text{C}_{13}\text{H}_{25}\text{N}_2\text{SO}_6$ [M] 337.1433, obsd 337.1439.

HRMS (ES-): calcd for H_2PO_4 [M] 96.9691, obsd 96.9689.

T_d(10%): 181 °C.

Spectra of IL **10d** are presented in Appendix AD.

6.18.3 Synthesis of IL 1-(2-(2-(2-methoxyethoxy)ethoxy)ethyl)-3-(3-sulfopropyl)-1*H*-imidazol-3-ium trifluoromethanesulfonate (**10e**)

Following general procedure B, zwitterion **10b** was mixed with trifluoromethanesulfonic acid producing IL **10e** as a dark brown viscous liquid in 99 % yield.

^1H NMR (600 MHz, MeOD): δ (ppm) = 9.01 (s, 1H, N^+CHN), 7.70-7.69 (m, J = 1.8 Hz, 2H, CHN, N^+CH), 4.46 (t, J = 7.3 Hz, 2H, NCH_2CH_2), 4.42 (t, J = 4.5 Hz, 2H, $\text{CH}_2\text{CH}_2\text{N}^+$), 3.88-3.86 (m, J = 4.5 Hz, 2H, $\text{CH}_2\text{CH}_2\text{O}$), 3.70-3.66 (m, 2H, OCH_2CH_2), 3.64-3.62 (m, 4H, OCH_2CH_2 , OCH_2CH_2), 3.58-3.55 (m, 2H, $\text{CH}_2\text{CH}_2\text{O}$), 3.38 (s, 3H, OCH_3), 2.84 (t, J = 7.3 Hz, 2H, SCH_2CH_2), 2.38-2.34 (m, J = 13.9, 6.8 Hz, 2H, $\text{CH}_2\text{CH}_2\text{CH}_2$).

^{13}C NMR (600 MHz, MeOD): δ (ppm) = 136.8 (N^+CHN), 123.1 (N^+CH), 122.0 (CHN), 72.2 ($\text{CH}_2\text{CH}_2\text{O}$), 71.5 (OCH_2CH_2), 69.9 (OCH_2CH_2), 68.3 (OCH_2CH_2), 60.8 ($\text{CH}_2\text{CH}_2\text{O}$), 57.7 (OCH_3), 49.5 (NCH_2), 47.8 (CH_2N^+), 47.0 (SCH_2CH_2), 25.7 ($\text{CH}_2\text{CH}_2\text{CH}_2$).

^{19}F NMR (600 MHz, MeOD, hexafluorobenzene): -80.31 (CF_3SO_3^-).

IR (thin film, cm^{-1}): 3151, 2883, 1716, 1566, 1454, 1351, 1278, 1224, 1158, 1025, 911, 847, 759, 632.

HRMS (ES+): calcd for $\text{C}_{13}\text{H}_{25}\text{N}_2\text{SO}_6$ [M] 337.1433, obsd 337.1436.

HRMS (ES-): calcd for CF_3SO_3 [M] 148.9520, obsd 148.9523.

T_d(10%): 187 °C.

Spectra of IL **10e** are presented in Appendix AE.

6.18.4 Synthesis of IL 1-(2-(2-methoxyethoxy)ethoxyethyl)-3-(3-sulfopropyl)-1H-imidazol-3-ium methanesulfonate (**10f**)

Following general procedure B, zwitterion **10b** was mixed with methanesulfonic acid producing IL **10f** as a dark brown viscous liquid in 99 % yield.

¹H NMR (600 MHz, MeOD): δ (ppm) = 9.02 (s, 1H, N⁺CHN), 7.71-7.70 (m, J = 1.8 Hz, 1H, CHN, N⁺CH), 4.46 (t, J = 7.1 Hz, 2H, NCH₂CH₂), 4.43 (t, J = 4.4 Hz, 2H, CH₂CH₂N⁺), 3.89-3.87 (m, J = 5.0, 4.4 Hz, 2H, CH₂CH₂O), 3.70-3.66 (m, 2H, OCH₂CH₂), 3.64-3.62 (m, 4H, OCH₂CH₂, OCH₂CH₂), 3.58-3.55 (m, 2H, CH₂CH₂O), 3.38 (s, 3H, OCH₃), 2.88-2.84 (m, J = 7.0 Hz, 2H, SCH₂CH₂), 2.38-2.34 (m, J = 14.0, 7.1 Hz, 2H, CH₂CH₂CH₂).

¹³C NMR (600 MHz, MeOD): δ (ppm) = 136.8 (N⁺CHN), 123.1 (N⁺CH), 122.1 (CHN), 72.2 (CH₂CH₂O), 71.6 (OCH₂CH₂), 70.0 (OCH₂CH₂), 68.3 (OCH₂CH₂), 60.8 (CH₂CH₂O), 57.7 (OCH₃), 49.5 (NCH₂), 47.8 (CH₂N⁺), 47.0 (SCH₂CH₂), 38.1 (CH₃SO₃), 25.7 (CH₂CH₂CH₂).

IR (thin film, cm⁻¹): 3145, 3108, 3019, 2877, 1696, 1564, 1453, 1335, 1219, 1203, 1168, 1101, 1072, 1027, 975, 894, 846, 790, 761, 659, 641.

HRMS (ES+): calcd for C₁₃H₂₅N₂SO₆ [M] 337.1433, obsd 337.1436.

HRMS (ES-): calcd for CH₃SO₃ [M] 94.9803, obsd 94.9802.

T_d(10%): 194 °C.

Spectra of IL **10f** are presented in Appendix AF.

6.19 Cellulose dissolution

Cellulose dissolution was performed with all synthesized ILs (**5c-f**, **6c-f**, **8c-f**, **10-f**). IL (0.5 g, 1.0 eq) were mixed with dry DMF (0.5 g, ~4.6-6.6 eq) and microcrystalline cellulose (MCC) were added 1 wt% at a time. When the MCC was dissolved an additional wt% were added until the IL/DMF mixture no longer dissolved the MCC. When dissolution of MCC was finalized the MCC was regenerated by addition of distilled water to the mixture. The mixture stirred for 12-24 hours and the MCC was filtered off, dried and collected for further studies.

List of Figures

2.1	Publications on ILs as a function of years. Data collected from SciFinder.	6
2.2	Tetraalkylammonium, tetraalkylphosphonium, dialkylimidazolium and <i>N</i> -alkylpyridinium cations.	7
2.3	Examples of different cations and anions used in ILs. ^[9]	8
2.4	Examples of methods for anion exchange. a) Exchange by Finkelstein reaction. b) Exchange by addition of strong Brønsted acid. c) Exchange by the use of exchange resins. d) Exchange by treatment with Lewis acid. e) Exchange by the method called <i>the phenolate platform</i> .	9
2.5	Schematic illustration of lignocellulose, from "Catalytic transformation of lignocellulose into chemicals and fuel products in ionic liquids" by Zhan, Song, Han. ^[3] Copyright 2013 Royal Society of Chemistry.	13
2.6	Dissolution of glucose chain by IL $[C^+][A^-]$, with C^+ representing cation and A^- representing anion.	14
2.7	Example of ZI and IL derived from ZI.	15
2.8	Geometrical condition for diffraction from lattice planes. ^[61]	17
2.9	1,2,3-triazole and 1,2,4-triazole.	18
3.1	^1H NMR shifts of azide 1 .	24
3.2	^1H and ^{13}C NMR shifts of triazole 2 .	25
3.3	^1H and ^{13}C NMR shifts of triazole 3 .	26
3.4	^1H and ^{13}C NMR shifts of triazole 4 .	30
3.5	^1H and ^{13}C NMR shifts of ZI 5b .	34
3.6	^1H and ^{13}C NMR shifts of ZI 6b .	34
3.7	TGA results of ILs with mass in wt% along y-axis and temperature in °C along x-axis. (a) ILs 5c-f . (b) ILs 6c-f . (c) ILs 8c-f . (d) ILs 10c-f . (e) Structure of ILs 5c-f , 6c-f , 8c-f and 10c-f .	40
3.8	TGA results of ILs with mass in wt% along y-axis and temperature in °C along x-axis. (a) ILs 5c , 6c , 8c , 10c with anion $[\text{HSO}_4]^-$. (b) ILs 5d , 6d , 8d , 10d with anion $[\text{H}_2\text{PO}_4]^-$. (c) ILs 5e , 6e , 8e , 10e with anion $[\text{CF}_3\text{SO}_3]^-$. (d) ILs 5f , 6f , 8f , 10f with anion $[\text{CH}_3\text{SO}_3]^-$.	41
3.9	Postulated cellulose dissolution mechanism using imidazolium IL. ^[44]	47
3.10	XRD of ILs 5c , 5d , 5e , 5f and pure MCC with intensity along y-axis and 2θ in degrees along x-axis.	51

LIST OF FIGURES

3.11 XRD of ILs 6c , 6d , 6e , 6f and pure MCC with intensity along y-axis and 2 θ in degrees along x-axis.	51
3.12 XRD of ILs 5c , 6c and pure MCC with intensity along y-axis and 2 θ in degrees along x-axis.	52
3.13 XRD spectra showing calculation of CI using the Segal method. ^[96]	52
3.14 TGA of ILs 5c , 5d , 5e , 5f and pure MCC, with mass in wt% along y-axis and temperature in °C along x-axis.	53

List of Schemes

1.1	Overview of synthesis steps conducted for the regioselective synthesis of 1,5-disubstituted 1,2,3-triazoles and 1,3,5-trisubstituted 1,2,3-triazolium ILs.	2
1.2	Overview of synthesis steps conducted for the synthesis of ZI and ILs.	3
2.1	Mechanism for Huisgen azide-alkyne 1,3-dipolar cycloaddition.	18
2.2	Mechanism for the regioselective formation of 1,5-disubstituted 1,2,3-triazole from ketone, amine, 4-nitrophenyl azide and acetic acid, suggested by Thomas et al. in 2016. ^[7]	20
2.3	Formation of alkyl/aryl azide from alkyl halide and aryl amine. Azide shown with resonance structures. Reproduced from ^[77] with permission.	21
2.4	Mechanism for formation of 4-nitrophenyl azide from 4-nitroaniline and nitrous acid.	21
2.5	Synthesis and yields of compounds produced in preliminary project.	22
3.1	Synthesis of azide 1	23
3.2	Synthesis of triazole 2	24
3.3	Synthesis of triazole 3	26
3.4	Mechanism for the regioselective formation of a 1,5-disubstituted 1,2,3-triazole from ketone, amine and 4-nitrophenyl azide. ^[8]	27
3.5	Synthesis of IL 4b	32
3.6	Synthesis of ZI intermediates 5a and 6a	33
3.7	Synthesis of ZIs 5b and 6b	34
3.8	Synthesis of precursor 7 and intermediate 8a	35
3.9	Synthesis and ¹ H and ¹³ C NMR shifts of ZI 8b	35
3.10	Synthesis of precursor 9 and intermediate 10a	36
3.11	Synthesis and ¹ H and ¹³ C NMR shifts of ZI 10b	36
3.12	Synthesis of ZI 4-(1-(2-methoxyethyl)-1H-imidazol-3-ium-3-yl)butane-1-sulfonate.	37
3.13	General synthetic scheme for preparation of ILs.	38
3.14	Postulated decomposition mechanism of IL 5d . A , B : S _N 2 nucleophilic substitution, C : N-heterocyclic carbene formation, D : E2 Hofmann elimination and E : decarboxylation of decomposition intermediate. ^[88]	44

List of Tables

3.1	Optimization of the synthesis of 1,5-disubstituted 1,2,3-triazoles.	29
3.2	Triazole alkylation	31
3.3	Water content of ILs in ppm.	38
3.4	Thermal degradation temperature (T_d) for ILs given in °C.	42
3.5	Cellulose dissolution capacity of different imidazolium based ILs. ^[89,92,94] . .	46
3.6	Cellulose dissolution with ILs in dry DMF at 100 °C showing wt% dissolved MCC.	50

Bibliography

- [1] Brandt, A., Gräsvik, J., Hallett, J. P., Welton, T., *Green Chem.* **2013**, *15*, 550–583.
- [2] Searchinger, T., Heimlich, R., Houghton, R., Dong, F., Elobeid, A., Fabiosa, J., Tokgoz, S., Hayes, D., Yu, T.-H., *Science* **2008**, *319*, 1238–1240.
- [3] Zhang, Z., Song, J., Han, B., *Chem. Rev.* **2017**, *117*, 6834–6880.
- [4] Klass, D. L., Biomass for renewable energy, fuels, and chemicals, San Diego, **1998**.
- [5] Swatloski, R. P., Spear, S. K., Holbrey, J. D., Rogers, R. D., *J. Am. Chem. Soc.* **2002**, *124*, 4974–4975.
- [6] Rinaldi, R., *Chem. Commun.* **2010**, *47*, 511–513.
- [7] Thomas, J., Jana, S., John, J., Liekens, S., Dehaen, W., *Chem. Commun.* **2016**, *52*, 2885–2888.
- [8] Grøssereid, I., *TKJ4520 Organic Chemistry Specialization Project: Synthesis and Optimization of 1,3,5-Trisubstituted 1,2,3-Triazolium Ionic Liquids for Cellulose Dissolution*, NTNU Trondheim, **2017**.
- [9] Laus, G., Bentivoglio, G., Schottenberger, H., *Lenzinger Ber.* **2005**, *84*, 71–85.
- [10] Davy, H., *Researches, chemical and philosophical*, printed for J. Johnson, St. Paul's Church-Yard. By Biggs and Cottle, Bristol, London, **1800**.
- [11] Angell, C., Ansari, Y., Zhao, Z., *Faraday Discuss.* **2011**, *154*, 9–27.
- [12] Hurley, F. H., Wier, T. P., *J. Electrochem. Soc.* **1951**, *98*, 203–206.
- [13] Ghandi, K., *Green Sus. Chem.* **2014**, *4*, 44–53.
- [14] Bara, J., Carlisle, T., Gabriel, C., Camper, D., Finotello, A., Gin, D., Noble, R., *Ind. Eng. Chem. Res.* **2009**, *48*, 2739–2751.
- [15] Ruckart, K. N., O'Brien, R. A., Woodard, S. M., West, K. N., Glover, T. G., *J. Phys. Chem.* **2015**, *119*, 20681–20697.
- [16] Qian, W., Texter, J., Yan, F., *Chem. Soc. Rev.* **2017**, *46*, 1124–1159.
- [17] Wickramanayake, S., Hopkinson, D., Myers, C., Hong, L., Feng, J., Seol, Y., Plasynski, D., Zeh, M., Luebke, D., *J. Membr. Sci.* **2014**, *470*, 52–59.
- [18] Lei, Z., Chen, B., Koo, Y., Macfarlane, D., *Chem. Rev.* **2017**, *117*, 6633–6635.
- [19] Eftekhari, A., Liu, Y., Chen, P., *J. Power Sources* **2016**, *334*, 221–239.
- [20] Weingarth, D., Czekaj, I., Fei, Z., Foelske-Schmitz, A., Dyson, P., Wokaun, A., Kotz, R., *J. Electrochem. Soc.* **2012**, *159*, 611–615.
- [21] Dai, S., Wang, C., Luo, H., Luo, X., Li, Q., Li, H., *Green Chem.* **2010**, *12*, 2019–2023.

- [22] Sarkar, A., Roy, S. R., Parikh, N., Chakraborti, A. K., *J. Org. Chem.* **2011**, *76*, 7132–7140.
- [23] Finkelstein, H., *Ber. Dtsch. Chem. Ges.* **1910**, *43*, 1528–1532.
- [24] Wasserscheid, P., Keim, W., *Angew. Chem. Int. Ed.* **2000**, *39*, 3772–3789.
- [25] Lethesh, K. C., Parmentier, D., Dehaen, W., Binnemans, K., *RSC Advances* **2012**, *2*, 11936–11943.
- [26] Díaz, M., Ortiz, A., Ortiz, I., *J. Membr. Sci.* **2014**, *469*, 379–396.
- [27] Sun, X., Luo, H., Dai, S., *Chem. Rev.* **2012**, *112*, 2100–2128.
- [28] Abo-Hamad, A., Alsaadi, M. A., Hayyan, M., Juneidi, I., Hashim, M. A., *Electrochim. Acta* **2016**, *193*, 321–343.
- [29] Gatard, S., Plantier-Ryon, R., Rémond, C., Muzard, M., Kowandy, C., Bouquillon, S., *Carbohydr. Res.* **2017**, *451*, 72–80.
- [30] Stoimenovski, J., MacFarlane, D., Bica, K., Rogers, R., *Pharm. Res.* **2010**, *27*, 521–526.
- [31] Bakkar, A., *J. Hazard. Mater.* **2014**, *280*, 191–199.
- [32] Wang, P., Wenger, B., Humphry-Baker, R., Moser, J.-E., Teuscher, J., Kantlehner, W., Mezger, J., Stoyanov, E., Zakeeruddin, S., Grätzel, M., *J. Am. Chem. Soc.* **2005**, *127*, 6850–6856.
- [33] Mumford, K. A., Mirza, N. R., Stevens, G. W., *Energy Procedia* **2017**, *114*, 2671–2674.
- [34] Lei, Z., Dai, C., Chen, B., *Chem. Rev.* **2014**, *114*, 1289–1326.
- [35] Wang, J., Yao, H., Nie, Y., Bai, L., Zhang, X., Li, J., *Ind. Eng. Chem. Res.* **2012**, *51*, 3776–3782.
- [36] Darvatkar, N. B., Deorukhkar, A. R., Bhilare, S. V., Salunkhe, M. M., *Synth. Commun.* **2006**, *36*, 3043–3051.
- [37] Janus, E., Goc-Maciejewska, I., Łożyński, M., Pernak, J., *Tetrahedron Lett.* **2006**, *47*, 4079–4083.
- [38] Zhu, A., Jiang, T., Wang, D., Han, B., Liu, L., Huang, J., Zhang, J., Sun, D., *Green Chem.* **2005**, *7*, 514–517.
- [39] Zhou, H., Yang, J., Ye, L., Lin, H., Yuan, Y., *Green Chem.* **2010**, *12*, 661–665.
- [40] Henderson, L. C., Byrne, N., *Green Chem.* **2011**, *13*, 813–816.
- [41] Zakzeski, J., Bruijnincx, P., Jongerius, A., Weckhuysen, B., *Chem. Rev.* **2010**, *110*, 3552–3599.
- [42] Lewandowski, A., Świderska-Mocek, A., *J. Power Sources* **2009**, *194*, 601–609.
- [43] Ramdin, M., Loos, T. W. de, Vlugt, T. J., *Ind. Eng. Chem. Res.* **2012**, *51*, 8149–8177.

BIBLIOGRAPHY

- [44] Pinkert, A., Marsh, K. N., Pang, S., Staiger, M. P., *Chem. Rev.* **2009**, *109*, 6712–6728.
- [45] Mohd, N., Draman, S. F. S., Salleh, M. S. N., Yusof, N. B., *Am. Inst. Phys.* **2017**, *1809*, 020035.
- [46] Isik, M., Sardon, H., Mecerreyes, D., *Int. J. Mol. Sci.* **2014**, *15*, 11922–11940.
- [47] Tang, S., Baker, G. A., Ravula, S., Jones, J. E., Zhao, H., *Green Chem.* **2012**, *14*, 2922–2932.
- [48] Kosan, B., Michels, C., Meister, F., *Cellulose* **2008**, *15*, 59–66.
- [49] Gericke, M., Liebert, T., Seoud, O. A. E., Heinze, T., *Macromol. Mater. Eng.* **2011**, *296*, 483–493.
- [50] Harris, L. J., Birch, T. W., *Biochem. J.* **1930**, *24*, 1080–1097.
- [51] Wu, B., Kuroda, K., Takahashi, K., Castner, E. W., *J. Chem. Phys.* **2018**, *148*, 193807.
- [52] Yoshizawa-Fujita, M., Tamura, T., Takeoka, Y., Rikukawa, M., *Chem. Commun.* **2011**, *47*, 2345–2347.
- [53] Zhao, D., Liao, Y., Zhang, Z., *Clean-Soil Air Water* **2007**, *35*, 42–48.
- [54] Kuroda, K., Satria, H., Miyamura, K., Tsuge, Y., Ninomiya, K., Takahashi, K., *J. Am. Chem. Soc.* **2017**, *139*, 16052–16055.
- [55] Tang, S., Baker, G., Zhao, H., *Chem. Soc. Rev.* **2012**, *41*, 4030–4066.
- [56] Earnest, C. M., *Compositional analysis by thermogravimetry*, ASTM, Philadelphia, PA, **1988**.
- [57] Mukasyan, A. S., *DTA/TGA-Based Methods*, **2017**, pp. 93–95.
- [58] Cao, Y., Mu, T., *Ind. Eng. Chem. Res.* **2014**, *53*, 8651–8664.
- [59] Xue, Z., Qin, L., Jiang, J., Mu, T., Gao, G., *Phys. Chem. Chem. Phys.* **2018**, *20*, 8382–8402.
- [60] Epp, J., *X-Ray Diffraction (XRD) Techniques for Materials Characterization*, Elsevier Inc., **2016**, pp. 81–124.
- [61] Spieß, L., Teichert, G., Schwarzer, R., Behnken, H., Genzel, C., *Moderne Röntgenbeugung: Röntgendiffraktometrie für Materialwissenschaftler, Physiker und Chemiker*, Vieweg+Teubner, Wiesbaden, **2009**.
- [62] Shelke, G., Rao, V., Jha, M., Cameron, T., Kumar, A., *Synlett* **2015**, *26*, 404–407.
- [63] Tam, A., Armstrong, I. S., La Cruz, T. E., *Org. Lett.* **2013**, *15*, 3586–3589.
- [64] Grashey, R., Huisgen, R., Leitermann, H., *Tetrahedron Lett.* **1960**, *1*, 9–13.
- [65] Tornøe, C. W., Christensen, C., Meldal, M., *J. Org. Chem.* **2002**, *67*, 3057–3064.
- [66] Rostovtsev, V. V., Green, L. G., Fokin, V. V., Sharpless, K. B., *Angew. Chem. Int. Ed.* **2002**, *41*, 2596–2599.

- [67] Zhang, L., Chen, X., Xue, P., Sun, H. H. Y., Williams, I. D., Sharpless, K. B., Fokin, V. V., Jia, G., *J. Am. Chem. Soc.* **2005**, *127*, 15998–15999.
- [68] Boren, B. C., Narayan, S., Rasmussen, L. K., Zhang, L., Zhao, H., Lin, Z., Jia, G., Fokin, V. V., *J. Am. Chem. Soc.* **2008**, *130*, 8923–8930.
- [69] Wan, J.-P., Cao, S., Liu, Y., *J. Org. Chem.* **2015**, *80*, 9028–9033.
- [70] Ramasastry, S. S. V., *Angew. Chem. Int. Ed.* **2014**, *53*, 14310–14312.
- [71] Ramachary, D. B., Ramakumar, K., Narayana, V. V., *Chem. Eur. J.* **2008**, *14*, 9143–9147.
- [72] Lima, C. G. S., Ali, A., Berkel, S. S. van, Westermann, B., Paixão, M. W., *Chem. Commun.* **2015**, *51*, 10784–10796.
- [73] Chen, Z., Yan, Q., Liu, Z., Zhang, Y., *Chem. Eur. J.* **2014**, *20*, 17635–17639.
- [74] Cheng, G., Zeng, X., Shen, J., Wang, X., Cui, X., *Angew. Chem. Int. Ed.* **2013**, *52*, 13265–13268.
- [75] Clayden, J., Greeves, N., Warren, S. G., *Org. Chem.* 2nd ed., Oxford University Press, **2012**.
- [76] Carey, F. A., *Advanced Organic Chemistry: Part B: Reactions and Synthesis 5th ed.* 5., Springer Science, **2007**.
- [77] Evjen, S., *Masters thesis*, Norwegian University of Science and Technology, **2015**.
- [78] Curtis, T., *Ber. Dtsch. Chem. Ges.* **1890**, *23*, 3023.
- [79] Schmidt, K. F. Z., *Angew. Chem.* **1923**, *36*, 511.
- [80] Kolb, H. C., Finn, M. G., Sharpless, K. B., *Angew. Chem. Int. Ed.* **2001**, *40*, 2004–2021.
- [81] Grøssereid, I., Evjen, S., Cheppellan, L. K., Fiksdahl, A., *Poster: Energy-related Organic Chemistry; Ionic Liquids for Cellulose Dissolution*, NTNU Trondheim, **2018**.
- [82] Sundhoro, M., Jeon, S., Park, J., Ramström, O., Yan, M., *Angw. Chem. Int. Ed.* **2017**, *56*, 12117–12121.
- [83] Hoogerstraete, T. V., Jamar, S., Wellens, S., Binnemans, K., *Anal. Chem.* **2014**, *86*, 3931–3938.
- [84] Maton, C., De Vos, N., Stevens, C. V., *Chem. Soc. Rev.* **2013**, *42*, 5963–5977.
- [85] Sun, J., Howlett, P. C., Macfarlane, D. R., Lin, J., Forsyth, M., *Electrochim. Acta* **2008**, *54*, 254–260.
- [86] Dong, Y., Shah, S. N., Pranesh, M., Prokkola, H., Kärkkäinen, J., Leveque, J.-M., Lassi, U., Lethesh, K. C., *J. Mol. Liq.* **2018**, *264*, 24–31.
- [87] Chen, Y., Cao, Y., Shi, Y., Xue, Z., Mu, T., *Ind. Eng. Chem. Res.* **2012**, *51*, 7418–7427.

BIBLIOGRAPHY

- [88] Clough, M. T., Geyer, K., Hunt, P. A., Mertes, J., Welton, T., *Phys. Chem. Chem. Phys.* **2013**, *15*, 20480–20495.
- [89] Wang, H., Gurau, G., Rogers, R., *Chem. Soc. Rev.* **2012**, *41*, 1519–1537.
- [90] Hermanutz, F., Gähr, F., Uerdingen, E., Meister, F., Kosan, B., *Macromol. Symp.* **2008**, *262*, 23–27.
- [91] Rosenau, T., Potthast, A., Sixta, H., Kosma, P., *Prog. Polym. Sci.* **2001**, *26*, 1763–1837.
- [92] Xu, A., Chen, L., Wang, J., *Macromol.* **2018**, *Ahead of print*, doi: 10.1021/acs.-macromol.8b00724.
- [93] Xu, A., Wang, J., Wang, H., *Green Chem.* **2010**, *12*, 268–275.
- [94] Zhao, H., Baker, G. A., Song, Z., Olubajo, O., Crittle, T., Peters, D., *Green Chem.* **2008**, *10*, 696–705.
- [95] Lan, W., Liu, C.-F., Yue, F.-X., Sun, R.-C., Kennedy, J. F., *Carbohydr. Polym.* **2011**, *86*, 672–677.
- [96] Sunkyu, P., Baker, J. O., Himmel, M. E., Parilla, P. A., Johnson, D. K., *Biotechnol. Biofuels.* **2010**, *3*, 1–10.
- [97] Segal, L., Creely, J., A.E. Martin, J., Conrad, C., *Tex. Res. J.* **1959**, *29*, 786–794.
- [98] Hemmaragala, N., Abrahamse, H., George, B., Gannimani, R., Govender, P., *Catal. Lett.* **2016**, *146*, 464–473.
- [99] Ferrero Vallana, F. M., Girling, R. P., Nimal Gunaratne, H. Q., Holland, L. A. M., Mcnamee, P. M., Seddon, K. R., Stonehouse, J. R., Todini, O., *New J. Chem.* **2016**, *40*, 9958–9967.
- [100] Depuydt, D., Liu, L., Glorieux, C., Dehaen, W., Binnemans, K., *Chem. Commun.* **2015**, *51*, 14183–14186.

Appendix

A Poster from Organic Chemical Winter meeting 2018

Energy-related Organic Chemistry; Ionic Liquids for Cellulose Dissolution

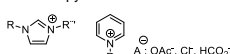
Ingrid Grøssereid¹, Sigvart Evjen, Lethesh K. Cheppelan, Anne Fiksdahl

Department of Chemistry, Norwegian University of Science and Technology, Trondheim, N-7491, Norway

ingrgrros@stud.ntnu.no

Background

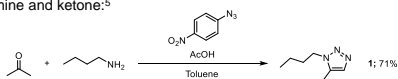
- Conversion of biomass, such as cellulose, to bio-fuels is an important approach to develop novel renewable technologies to replace fossil fuels.
- Unfortunately, current techniques require high temperature, have high cost, volatility, toxicity and give inefficient cellulose solvation.^{1,2}
- Ionic liquids (ILs) are promising for cellulose dissolution.
- ILs may dissolve cellulose without any chemical reaction,³ to allow recycling of the IL.⁴
- Commonly used ILs are based on imidazolium or pyridinium cations and OAc⁻, Cl⁻ and HCO₃⁻ anions:



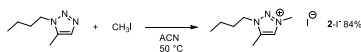
➤ We wanted to develop novel improved ILs for cellulose dissolution.

Triazolium-based ILs

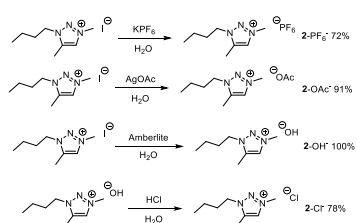
1,5-Alkyltriazole **1** was synthesized by a new selective metal-free approach from alkylamine and ketone:⁵



The triazolium IL **2**-⁻ was prepared by *N*-quaternization:

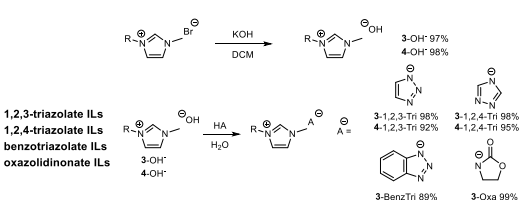
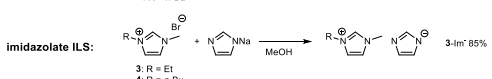
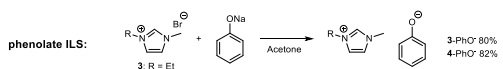


• Several novel ILs were prepared by anion exchange:



Unconventional organic anions

- Imidazolium-based ILs with unconventional organic anions; prepared by different counter-ion exchange methods:



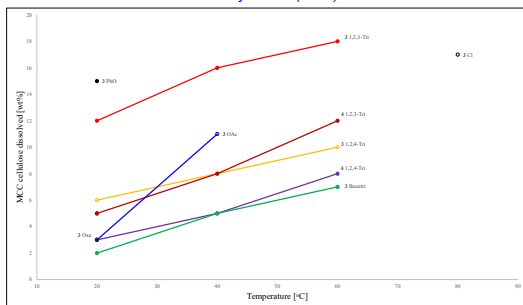
All reactions are readily scalable.

Cellulose dissolution

Cellulose dissolution experiments: cellulose samples were stirred in ILs.

Commercial ILs, 3-OAc⁻ and 3-Cl⁻, were used as references ('state of the art' ILs for cellulose dissolution).

Dissolution of microcrystalline (MCC) cellulose in ILs:

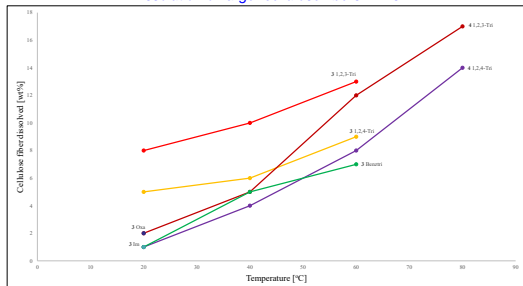


- Excellent dissolution results (12-15 wt%) were obtained with our novel ILs at r.t. compared to reference ILs (3 wt%);

Efficiency of MCC cellulose dissolution:

- novel IL: 3-PhO⁻: 15 wt% in < 5 h at r.t.
reference IL: 3-OAc⁻: 11 wt% in 4 days at 40 °C.

Dissolution of larger cellulose fibers in ILs:



- High cellulose dissolution was also observed for larger cellulose fibers.
- Cellulose regeneration: 95-100%; shows high MCC cellulose dissolution efficiency.
- Regenerated cellulose characterized by XRD, FTIR, TGA, SEM.

Conclusion

- New 1,2,3-triazolium-based ILs were prepared to be tested for cellulose diss.
- ILs with unconventional organic anions were studied for cellulose dissolution.
- The novel ILs showed exceptional cellulose dissolution ability.
- PhO⁻ based ILs are particularly promising, also at r.t.

Acknowledgements

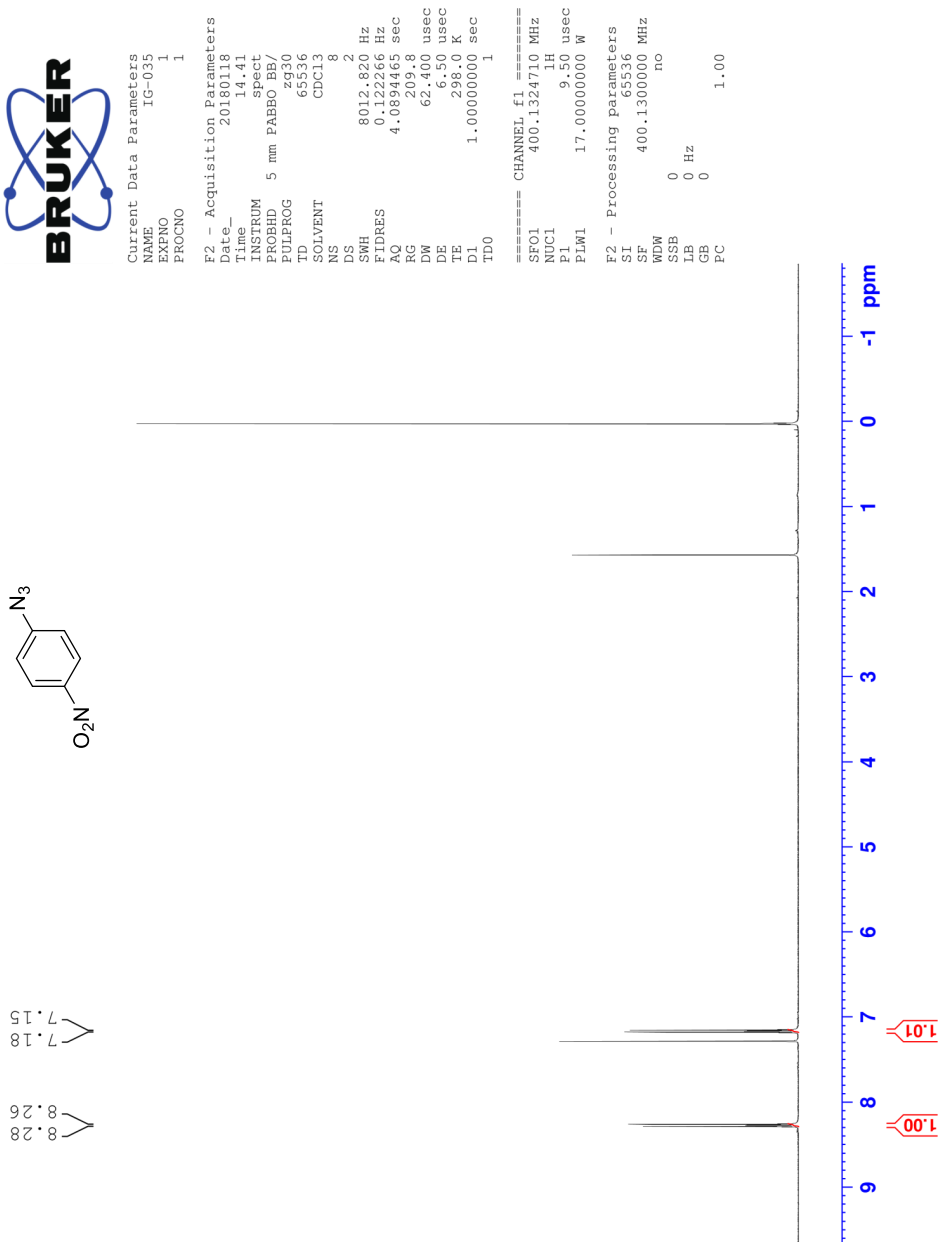
We would like to thank Norsk Kjemisk Selskap (NKS) for the travel grant.

References

- Rosenau, T.; Pothast, A.; Sixta, H.; Kosma, P. *Prog. Polym. Sci.* **2001**, *26*, 1763.
- Wang, H.; Gurau, G.; Rogers, R. D. *Chem. Soc. Rev.* **2012**, *41*, 1519.
- Sun, N.; Rahman, M.; Qin, Y.; Maxim, M. L.; Rodriguez, H.; Rogers, R. *Green Chem.* **2009**, *11*, 646.
- Swatoski, R. P.; Spear, S. K.; Holbrey, J. D.; Rogers, R. D. *J. Am. Chem. Soc.* **2002**, *124*, 4974.
- Thomas, J.; Jana, S.; John, J.; Liekens, S.; Dehaen, W. *Chem. Commun.* **2016**, *52*, 2885.

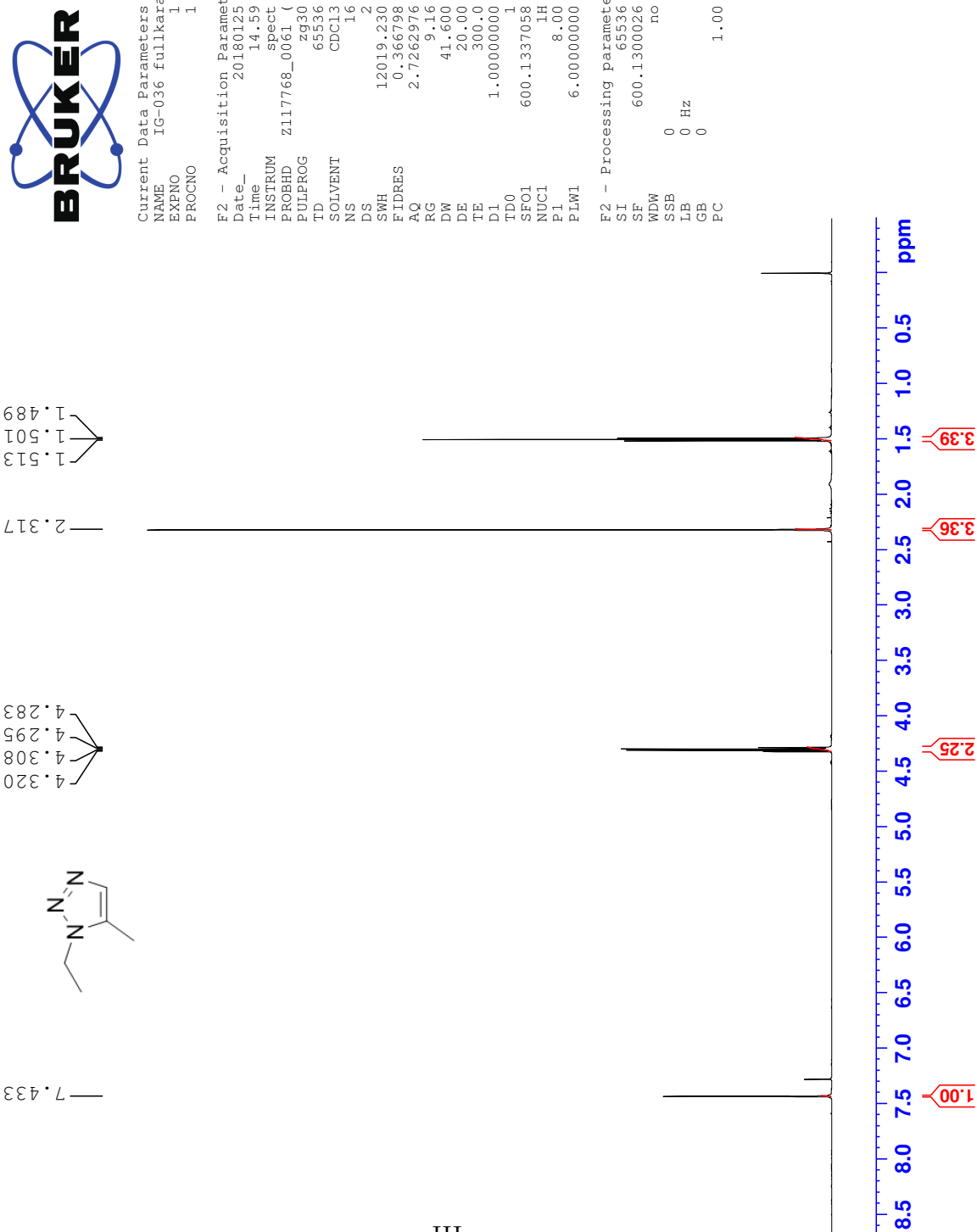
B Spectrum of 4-nitrophenyl azide (1)

¹H NMR Spectrum of 1

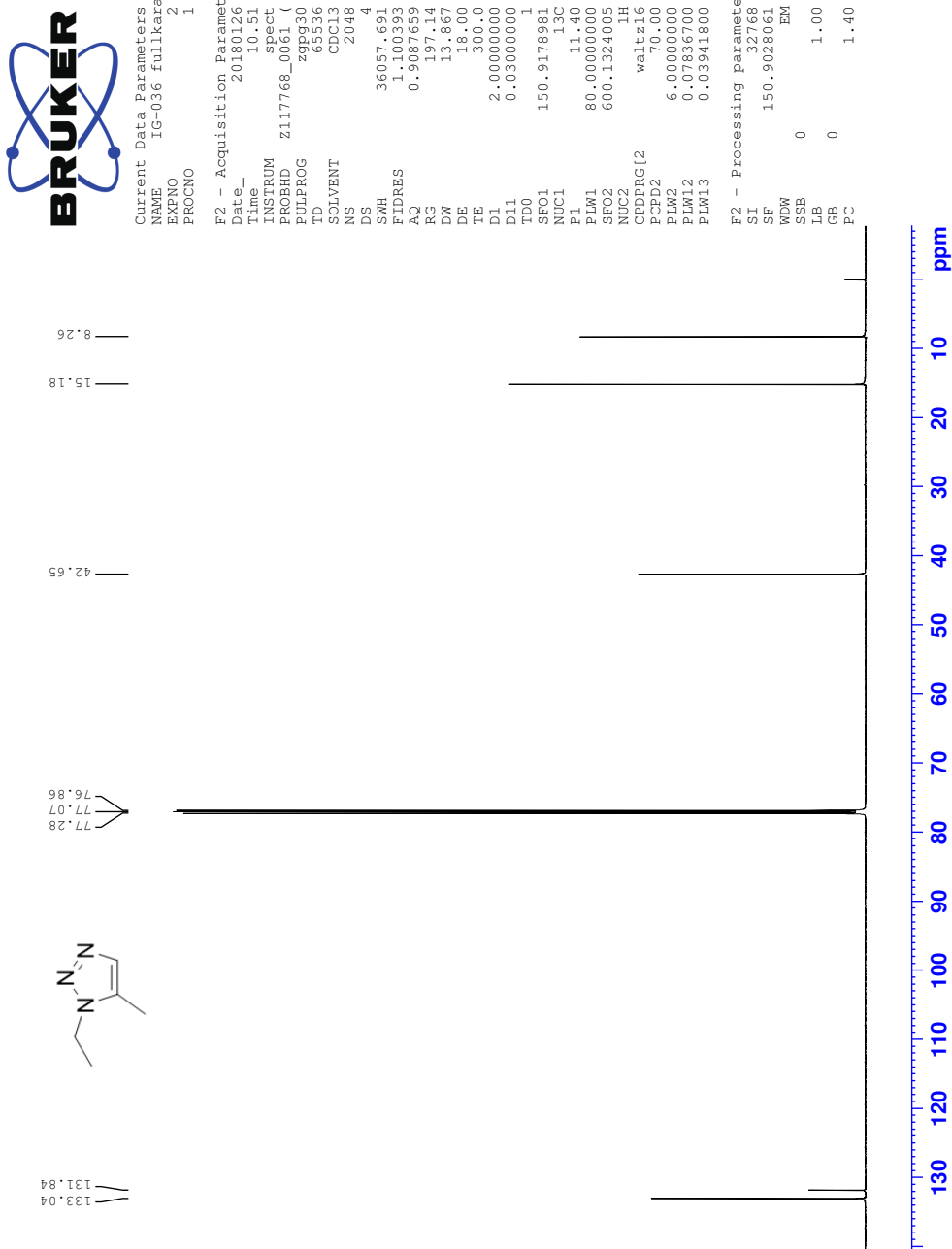


C Spectra of 1-ethyl-5-methyl-1,2,3-triazole (2)

¹H NMR Spectrum of 2

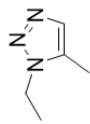
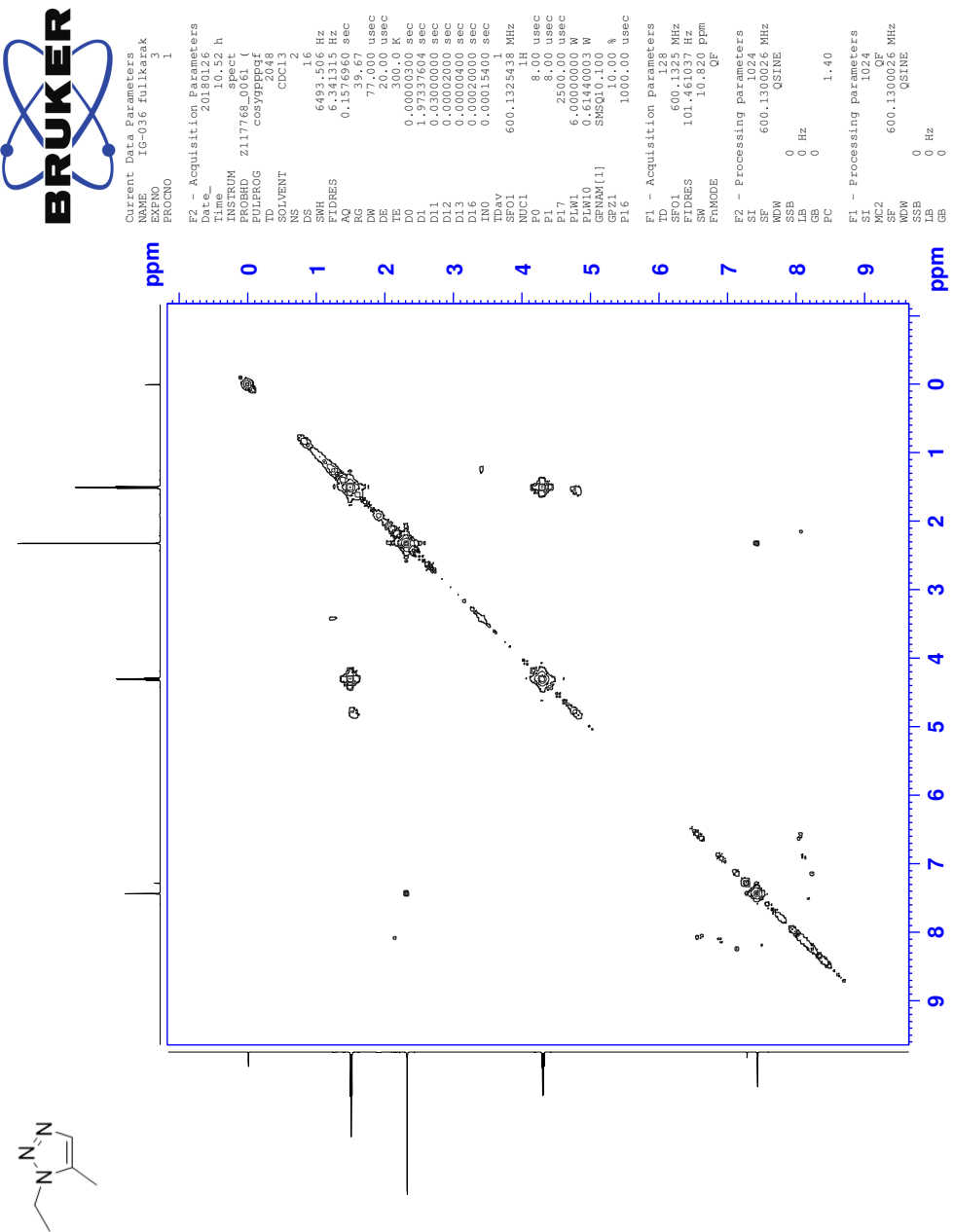


¹³C NMR Spectrum of 2



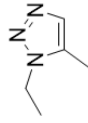
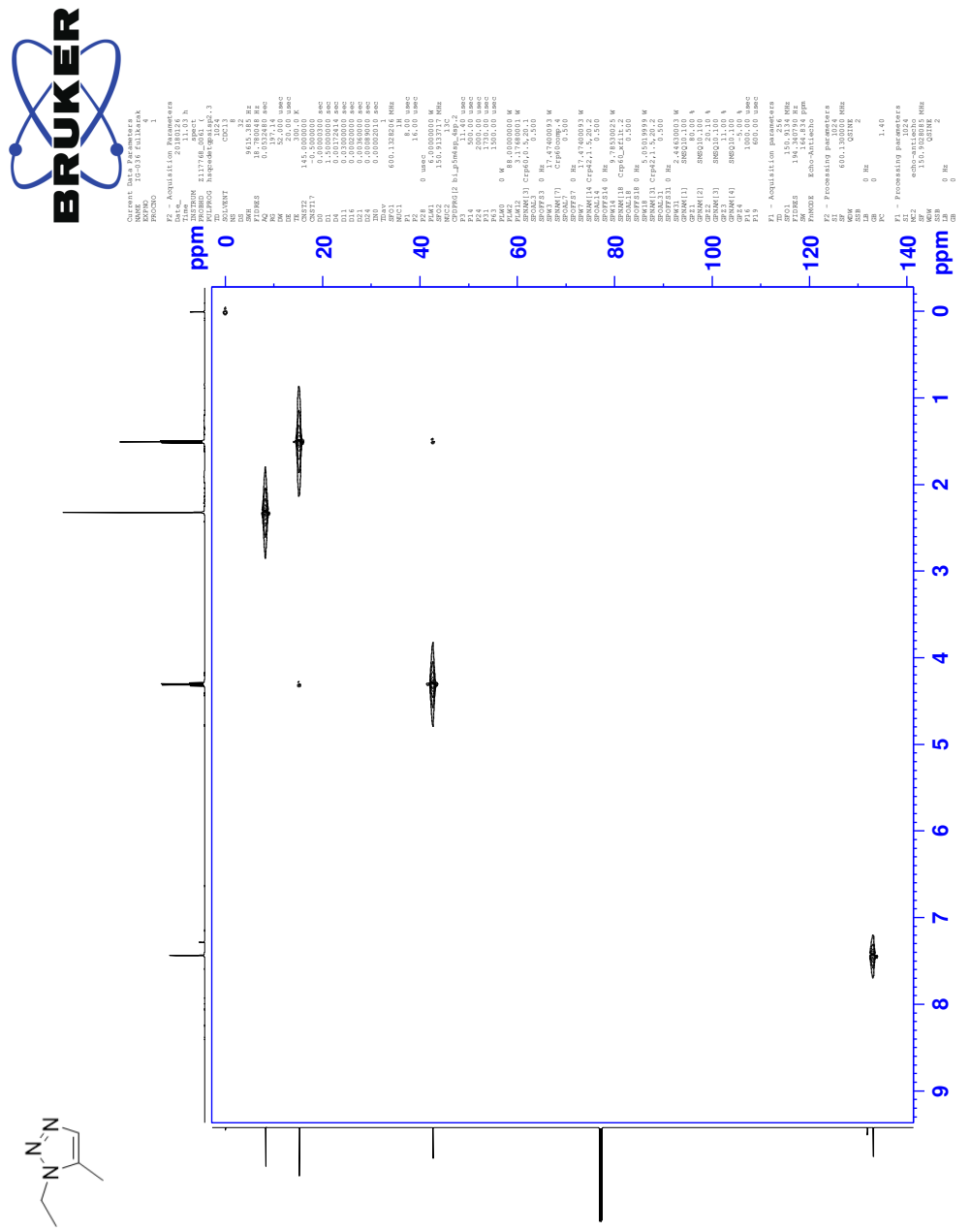
IV

COSY NMR Spectrum of 2

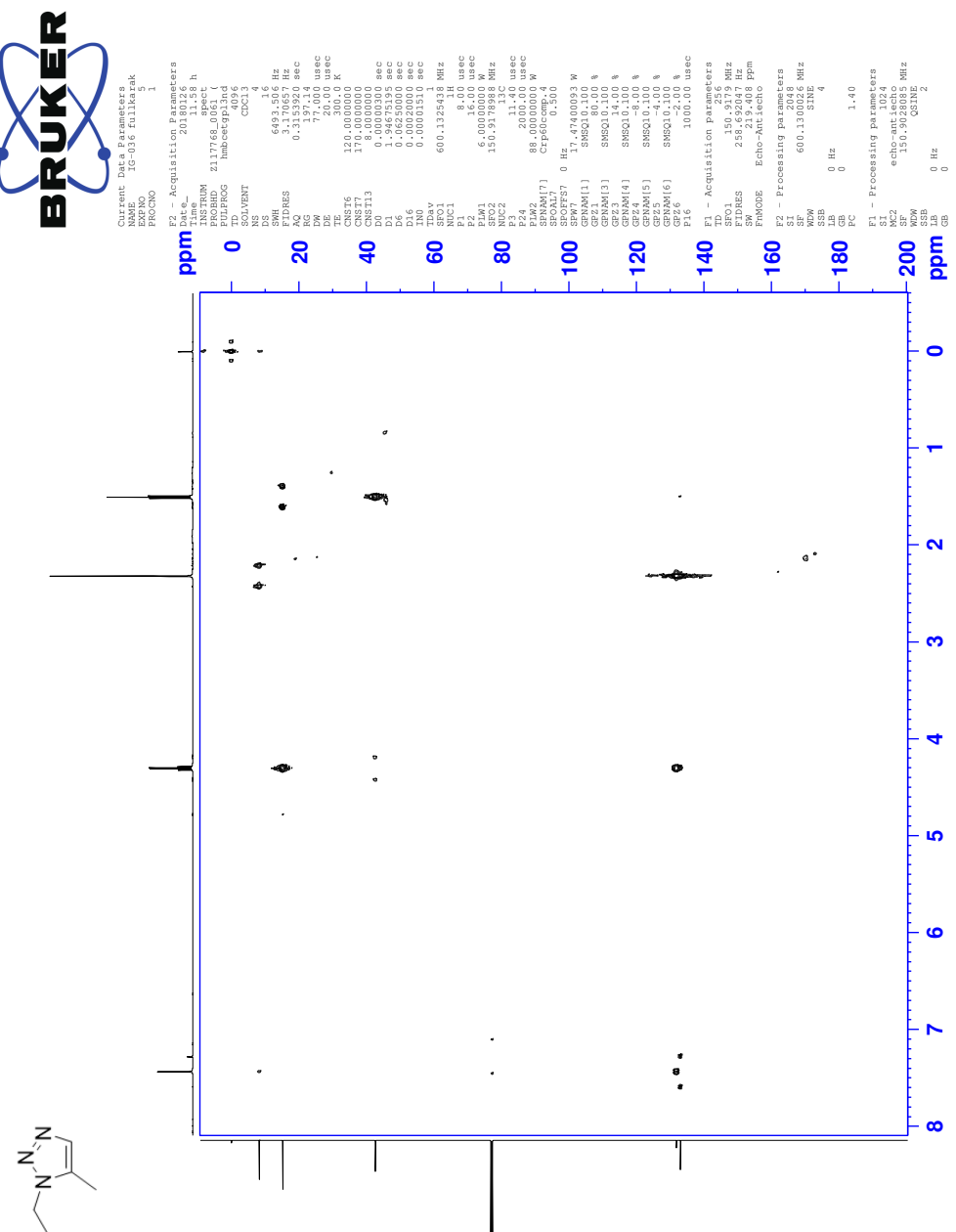


V

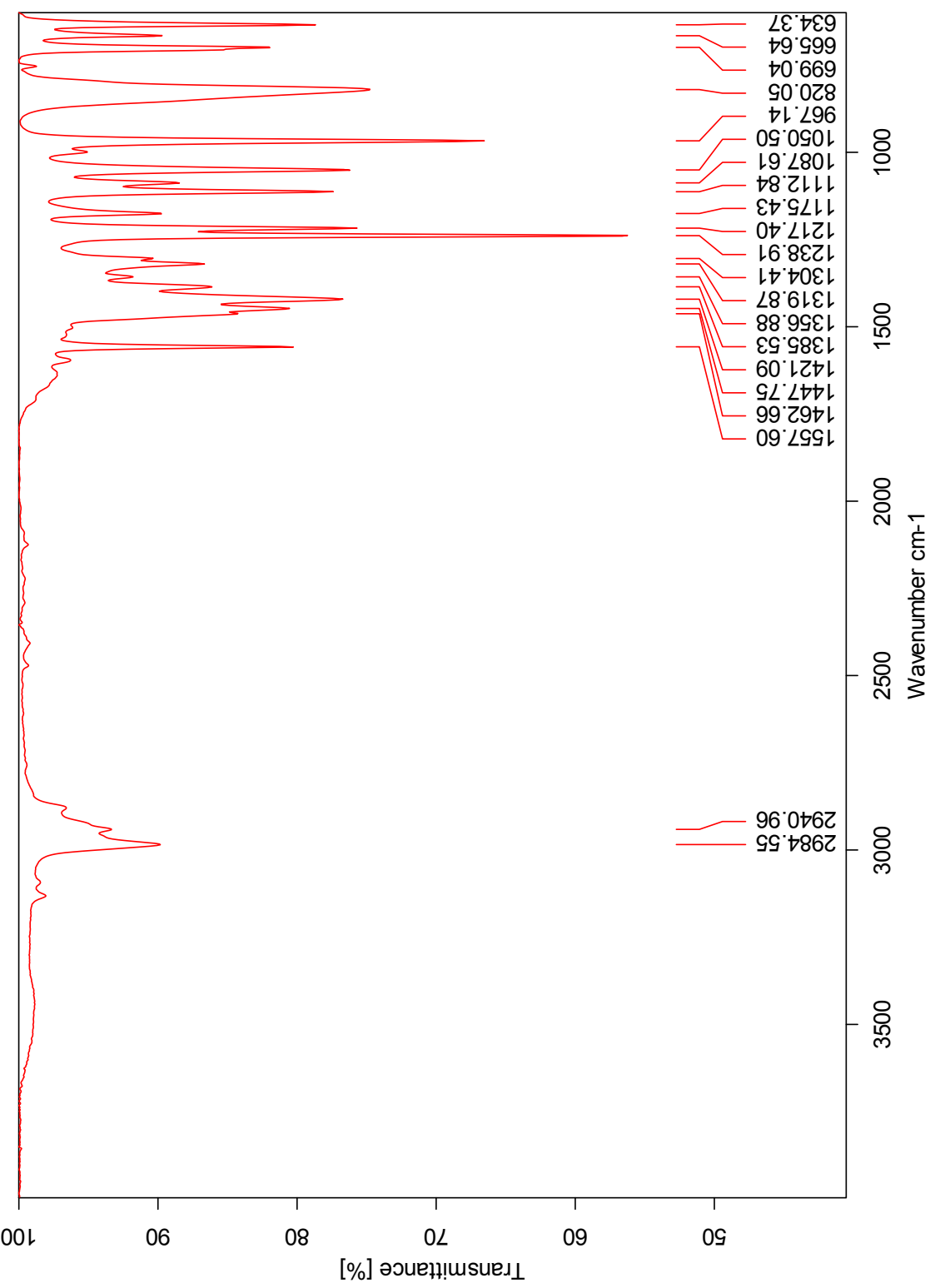
HSQC NMR Spectrum of 2



HMBC NMR Spectrum of 2



IR Spectrum of 2



VIII

HRMS Spectrum of 2

Elemental Composition Report

Page 1

Single Mass Analysis

Tolerance = 3.0 PPM / DBE: min = -1.5, max = 50.0

Element prediction: Off

Number of isotope peaks used for i-FIT = 3

Monoisotopic Mass, Even Electron Ions

127 formula(e) evaluated with 1 results within limits (all results (up to 1000) for each mass)

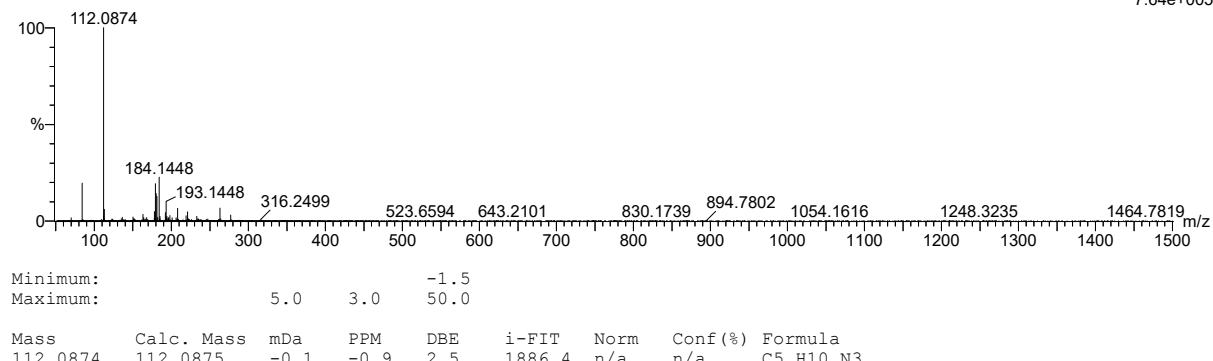
Elements Used:

C: 0-500 H: 0-1000 N: 0-100 O: 0-100 Si: 0-3

2018-19 12 (0.259) AM2 (Ar,35000.0,0.00,0.00); Cm (10:12)

1: TOF MS ASAP+

7.64e+005

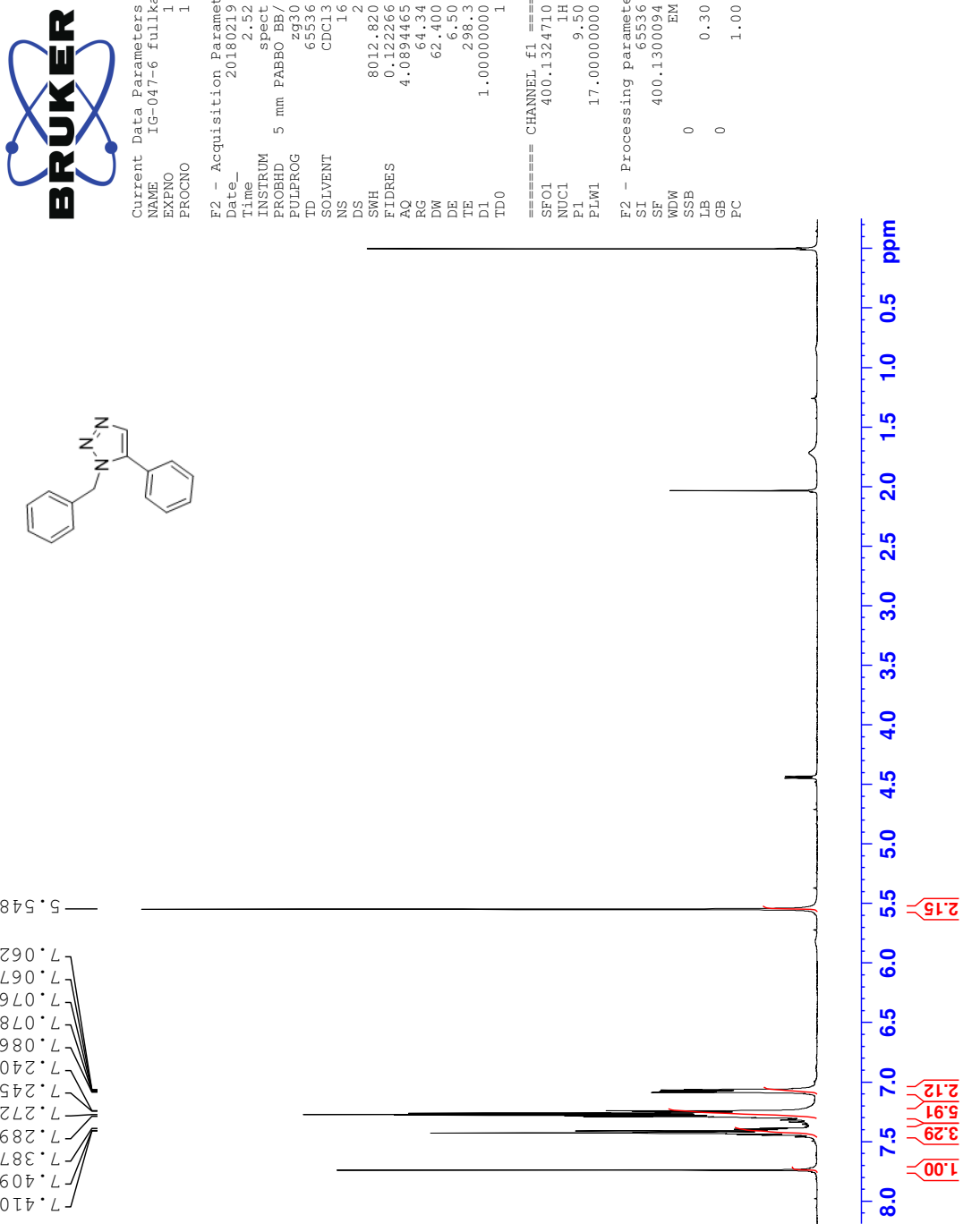


Minimum: -1.5
Maximum: 5.0 3.0 50.0

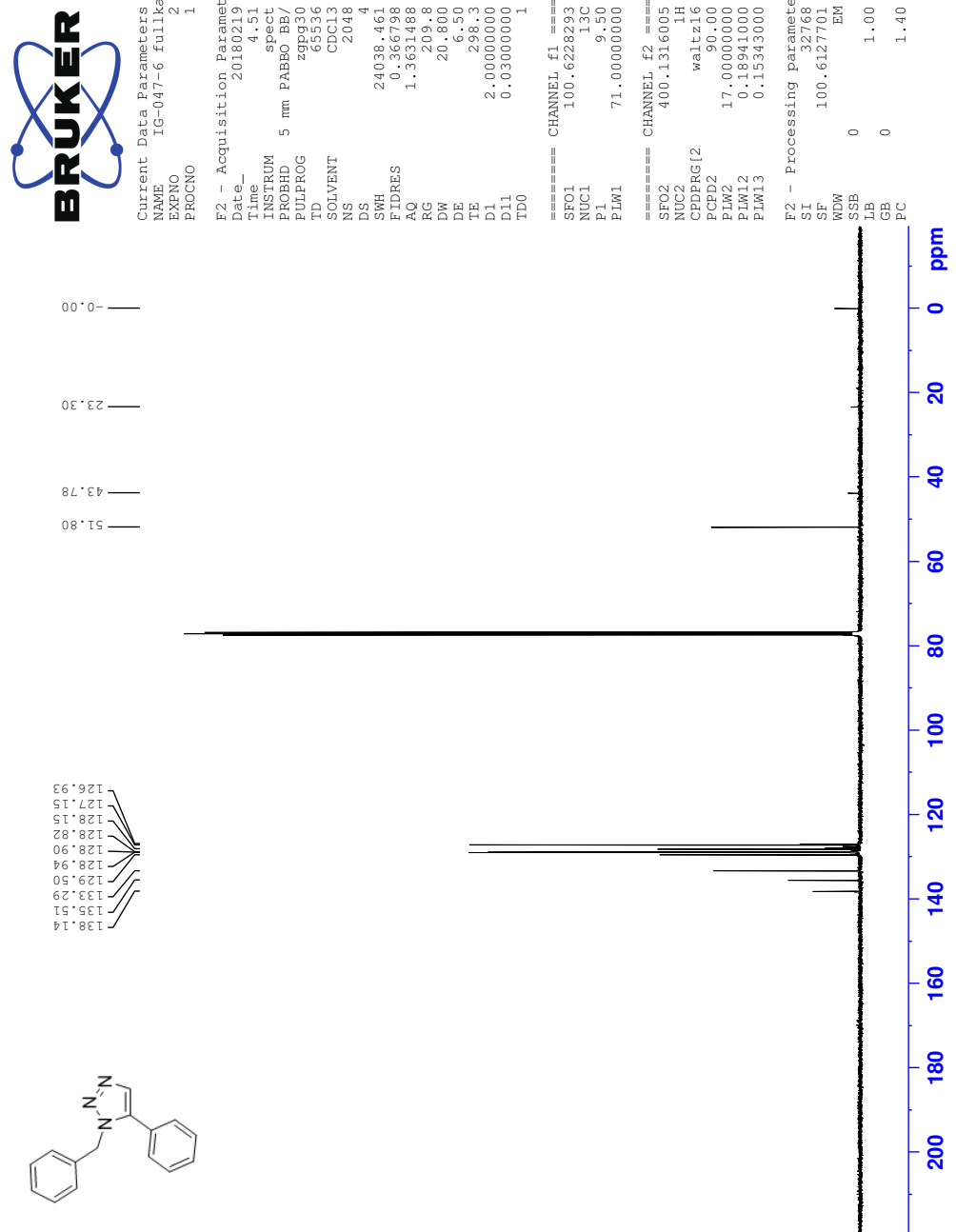
Mass	Calc. Mass	mDa	PPM	DBE	i-FIT	Norm	Conf (%)	Formula
112.0874	112.0875	-0.1	-0.9	2.5	1886.4	n/a	n/a	C5 H10 N3

D Spectra of 1-benzyl-5-phenyl-1,2,3-triazole (3)

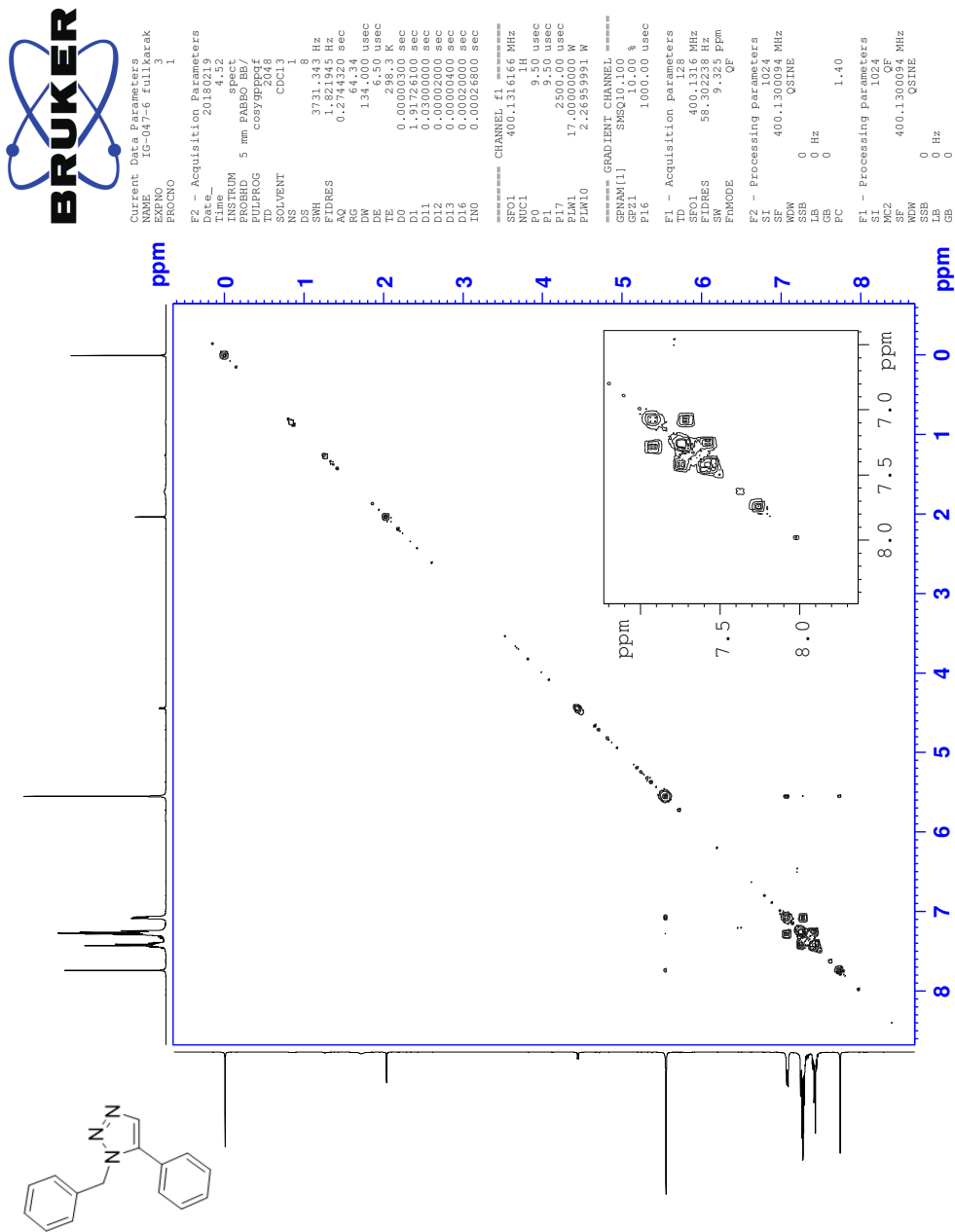
¹H NMR Spectrum of 3



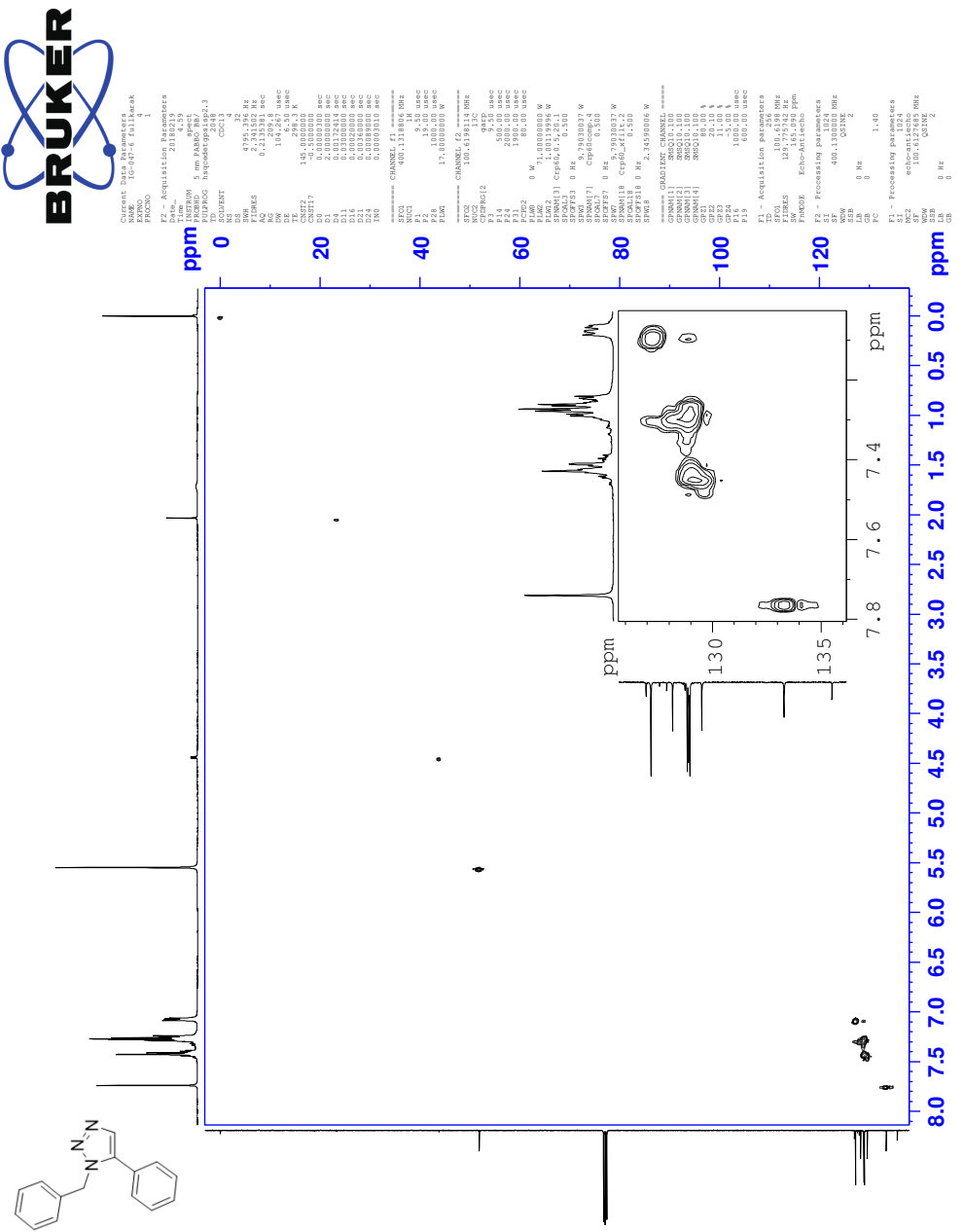
¹³C NMR Spectrum of 3



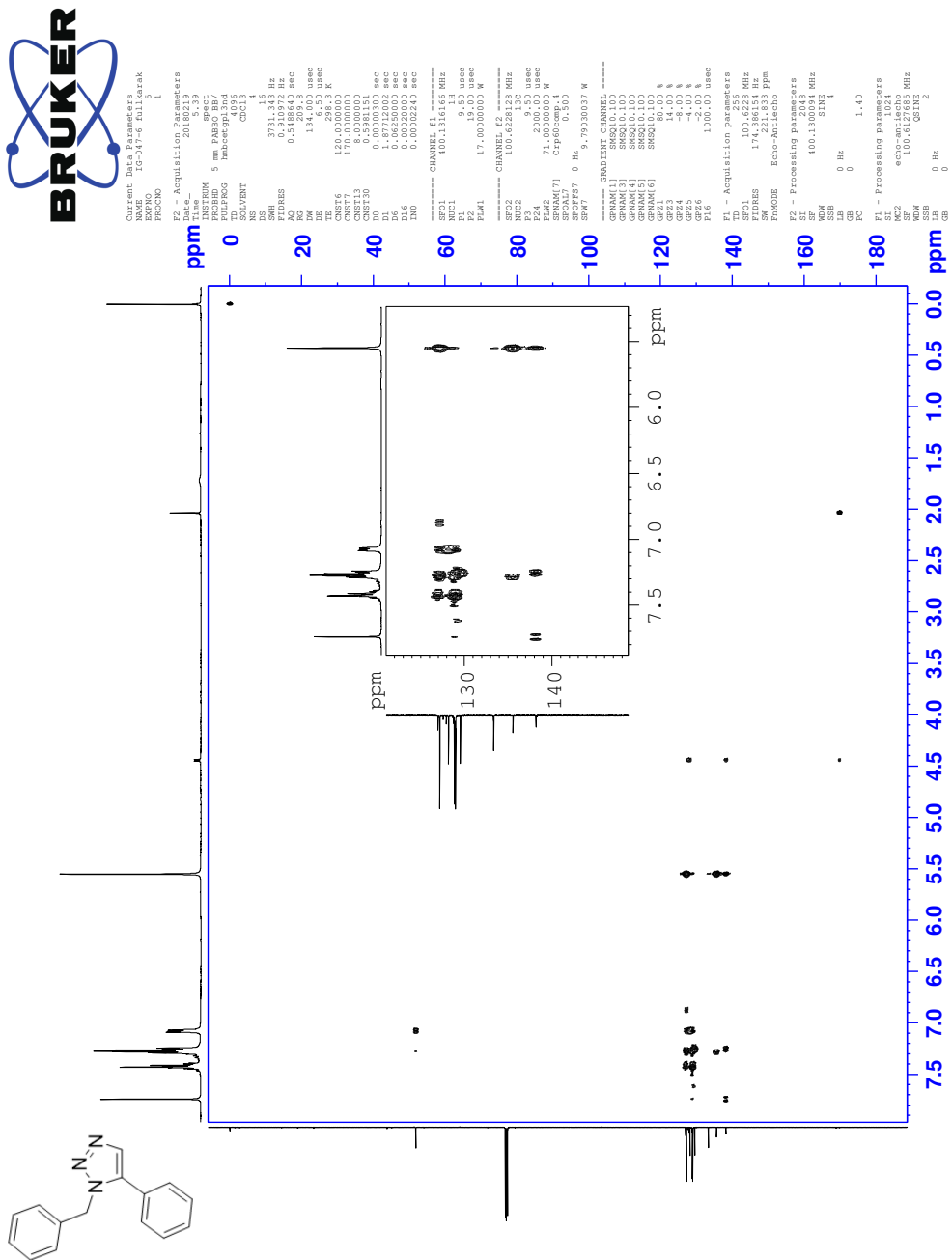
COSY NMR Spectrum of 3



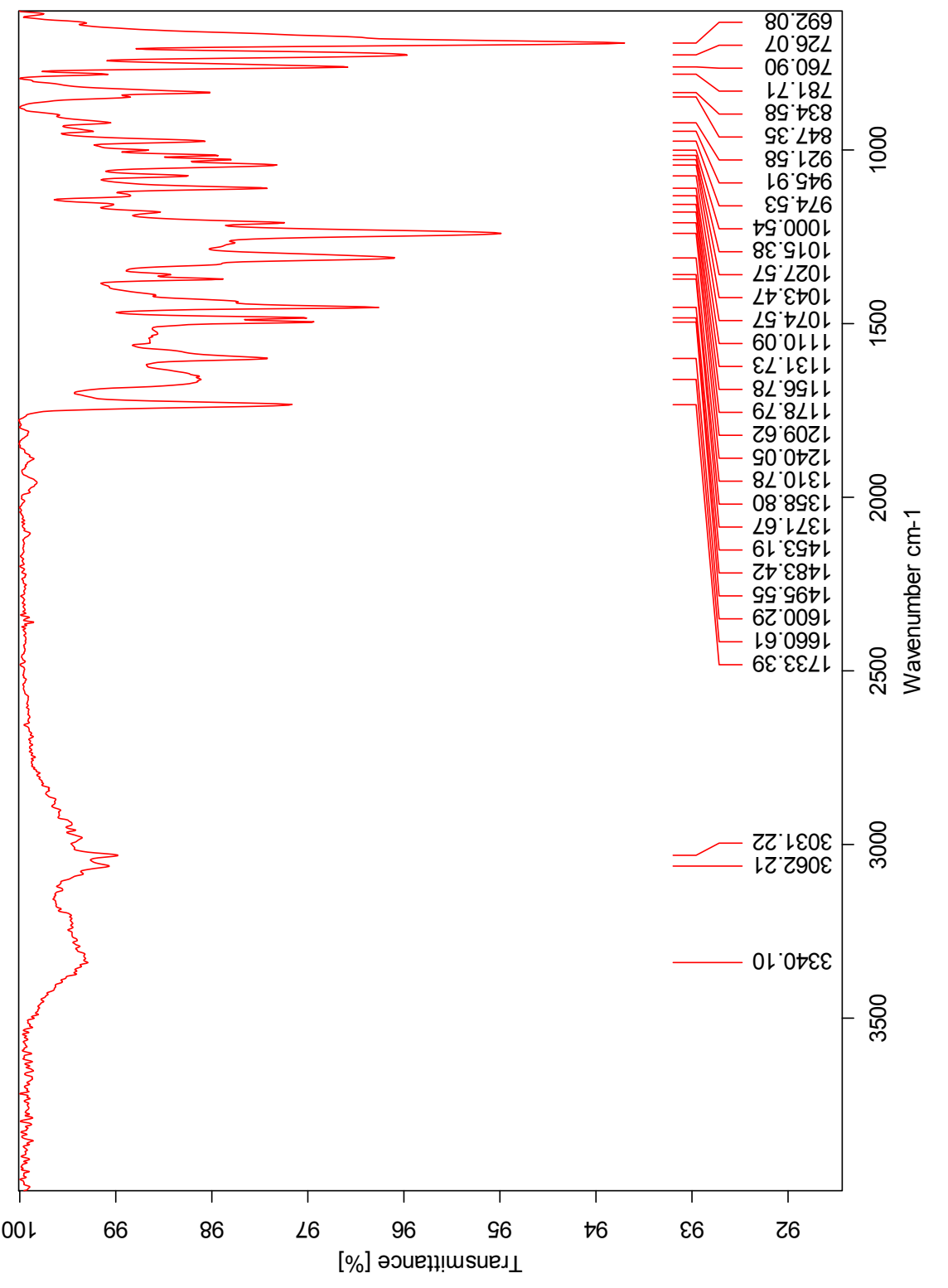
HSQC NMR Spectrum of 3



HMBC NMR Spectrum of 3



IR Spectrum of 3



HRMS Spectrum of 3

Elemental Composition Report

Page 1

Single Mass Analysis

Tolerance = 2.0 PPM / DBE: min = -1.5, max = 50.0

Element prediction: Off

Number of isotope peaks used for i-FIT = 3

Monoisotopic Mass, Even Electron Ions

577 formula(e) evaluated with 1 results within limits (all results (up to 1000) for each mass)

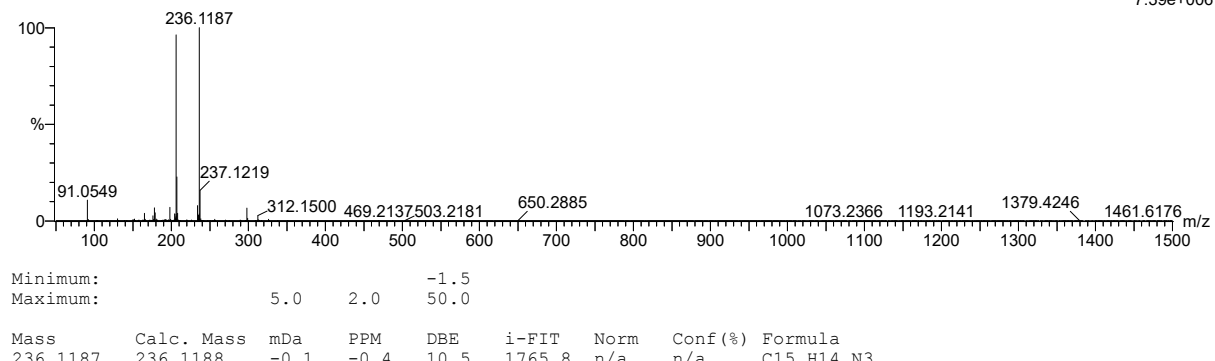
Elements Used:

C: 0-500 H: 0-1000 N: 0-50 O: 0-50 Na: 0-1

2018-78 52 (1.034) AM2 (Ar,35000.0,0.00,0.00); Cm (51:53)

1: TOF MS ASAP+

7.39e+006

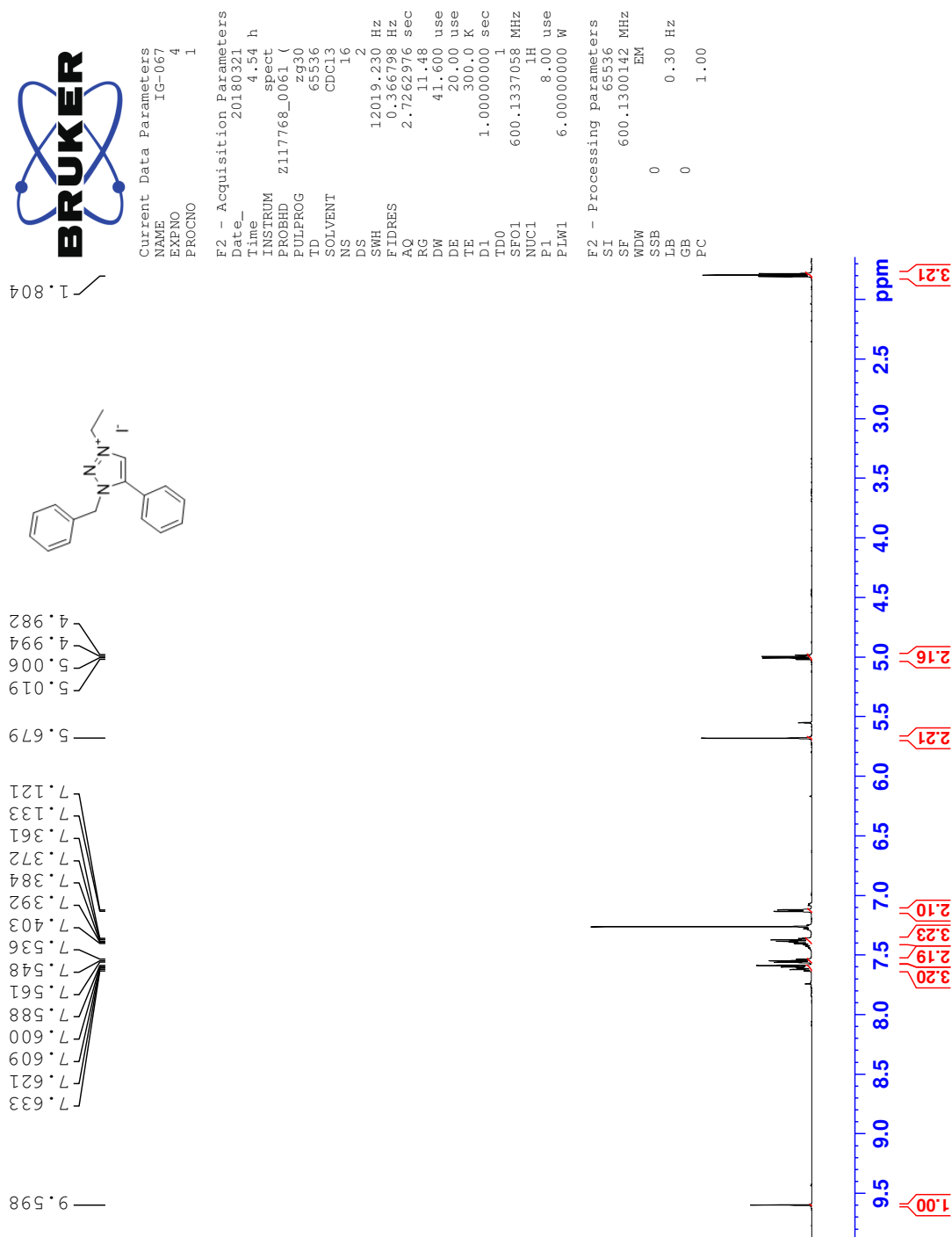


Minimum: -1.5
Maximum: 5.0 2.0 50.0

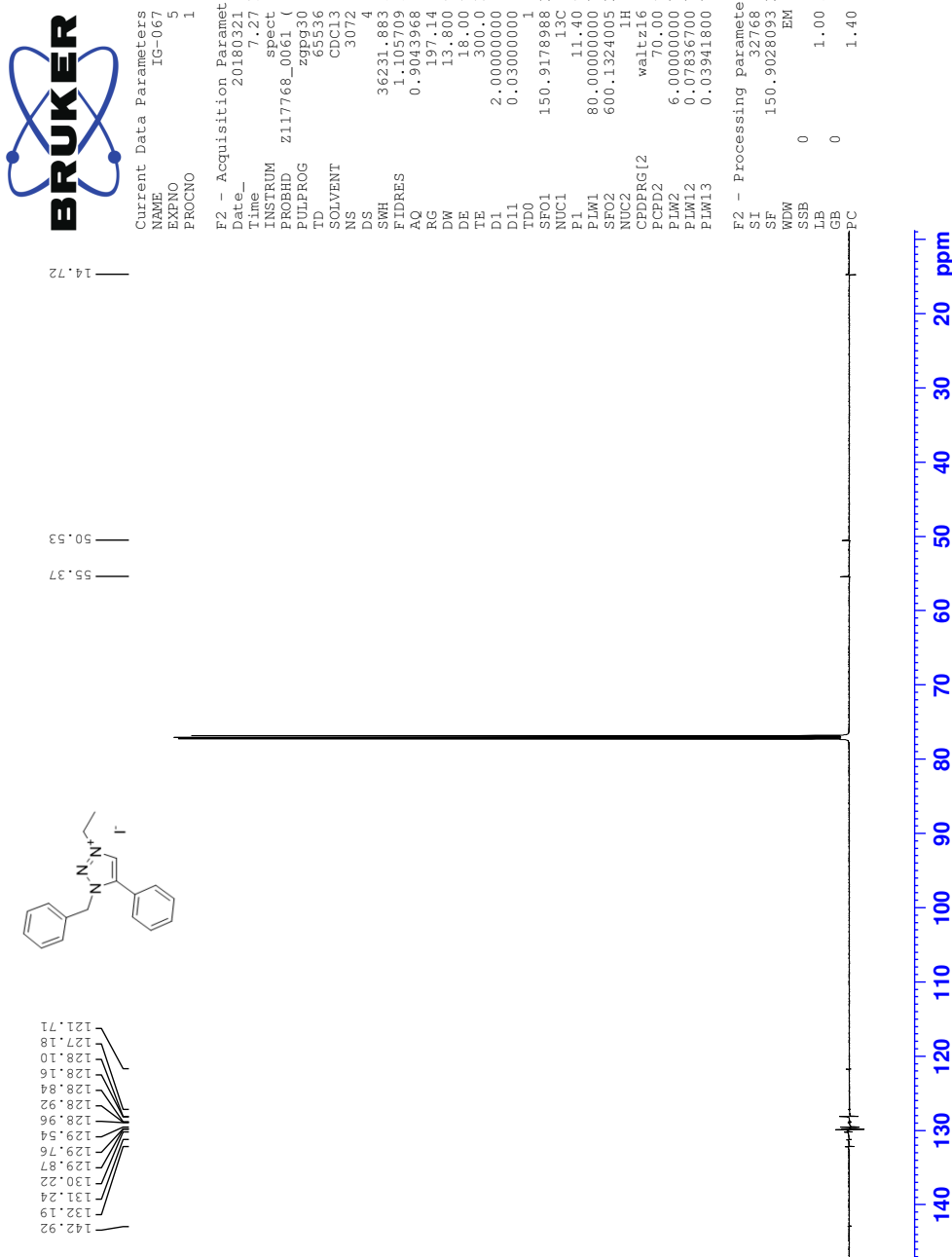
Mass	Calc. Mass	mDa	PPM	DBE	i-FIT	Norm	Conf (%)	Formula
236.1187	236.1188	-0.1	-0.4	10.5	1765.8	n/a	n/a	C15 H14 N3

E Spectra of 1-benzyl-3-ethyl-5-phenyl-1,2,3-triazolium iodide (4a)

¹H NMR Spectrum of 4a



¹³C NMR Spectrum of 4a



HRMS Positive mode spectrum of 4a

Elemental Composition Report

Page 1

Single Mass Analysis

Tolerance = 2.0 PPM / DBE: min = -1.5, max = 50.0

Element prediction: Off

Number of isotope peaks used for i-FIT = 3

Monoisotopic Mass, Even Electron Ions

1862 formula(e) evaluated with 2 results within limits (all results (up to 1000) for each mass)

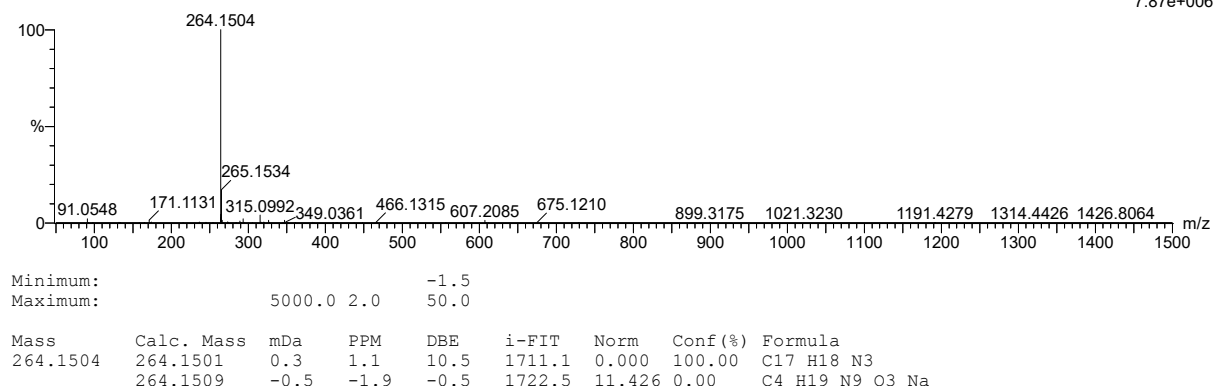
Elements Used:

C: 0-500 H: 0-1000 N: 0-10 O: 0-10 Na: 0-1 S: 0-5

2018-123post.22 (0.228) AM2 (Ar,35000.0,0.00,0.00); Cm (22:25)

1: TOF MS ES+

7.87e+006



HRMS Negative mode spectrum of 4a

Elemental Composition Report

Page 1

Single Mass Analysis

Tolerance = 5.0 PPM / DBE: min = -1.5, max = 50.0

Element prediction: Off

Number of isotope peaks used for i-FIT = 3

Monoisotopic Mass, Even Electron Ions

226 formula(e) evaluated with 1 results within limits (all results (up to 1000) for each mass)

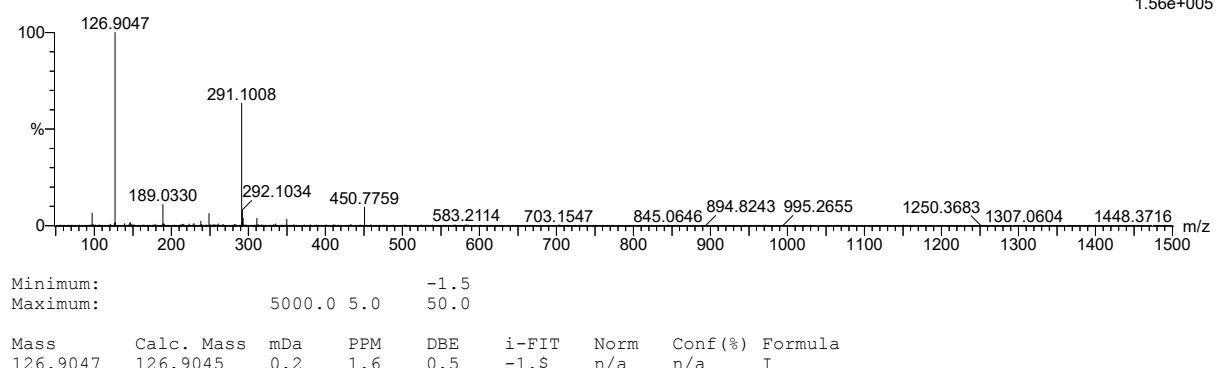
Elements Used:

C: 0-500 H: 0-1000 N: 0-10 O: 0-10 Na: 0-1 S: 0-5 I: 0-1

2018-123negb 8 (0.172) AM2 (Ar,35000.0,0.00,0.00); Cm (7:8)

1: TOF MS ES-

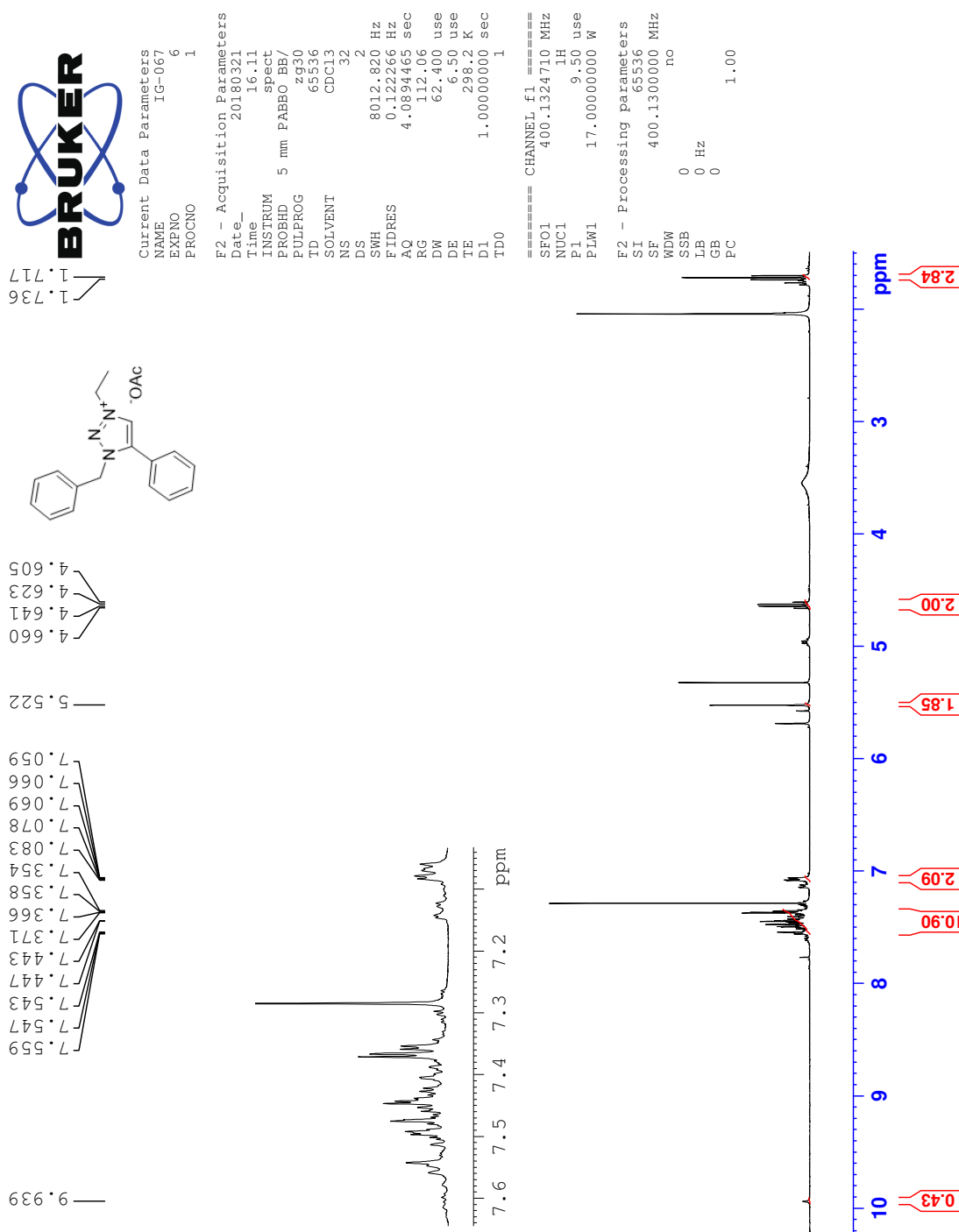
1.56e+005



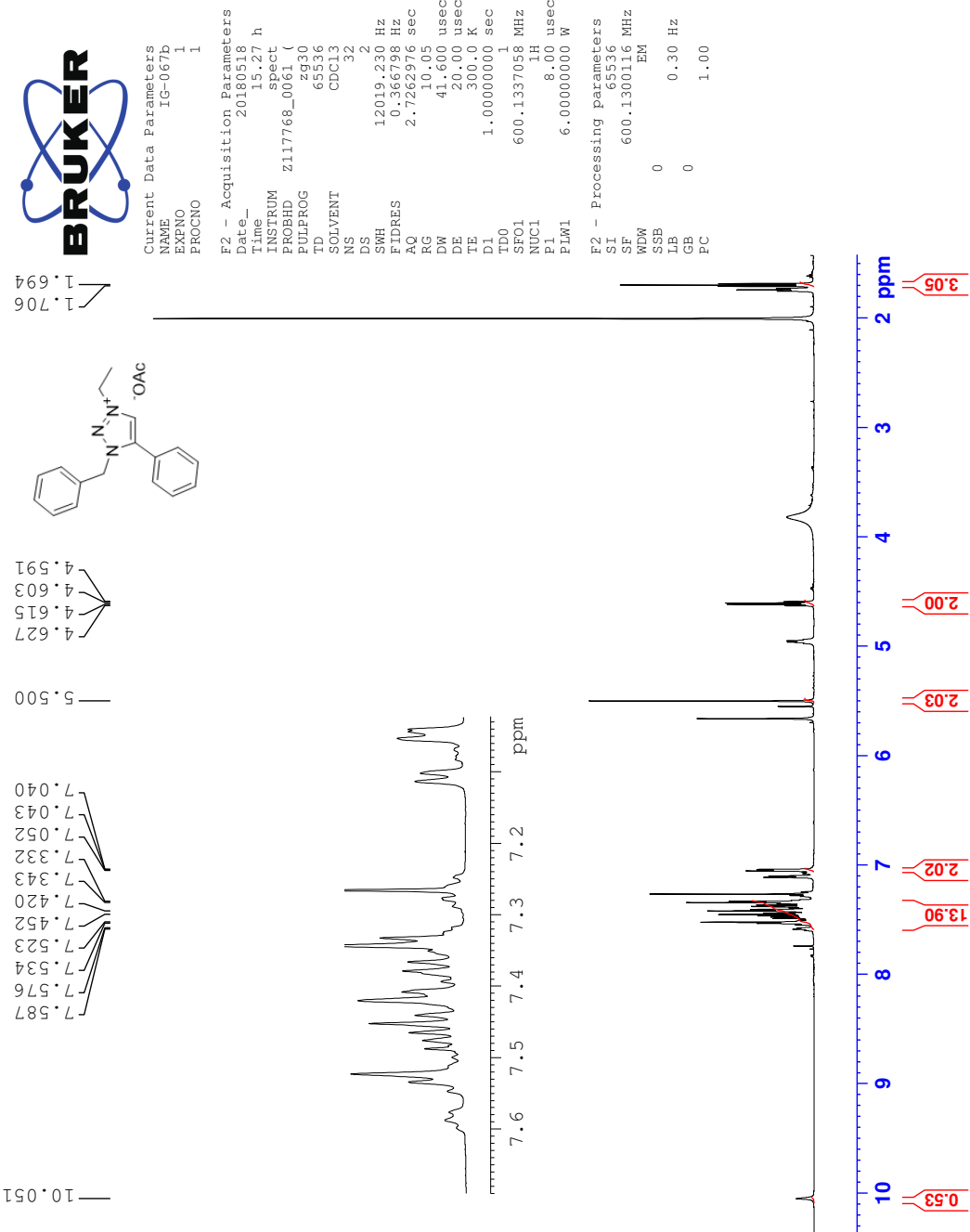
XX

F Spectra of 1-benzyl-3-ethyl-5-phenyl-1,2,3-triazolium acetate (4b)

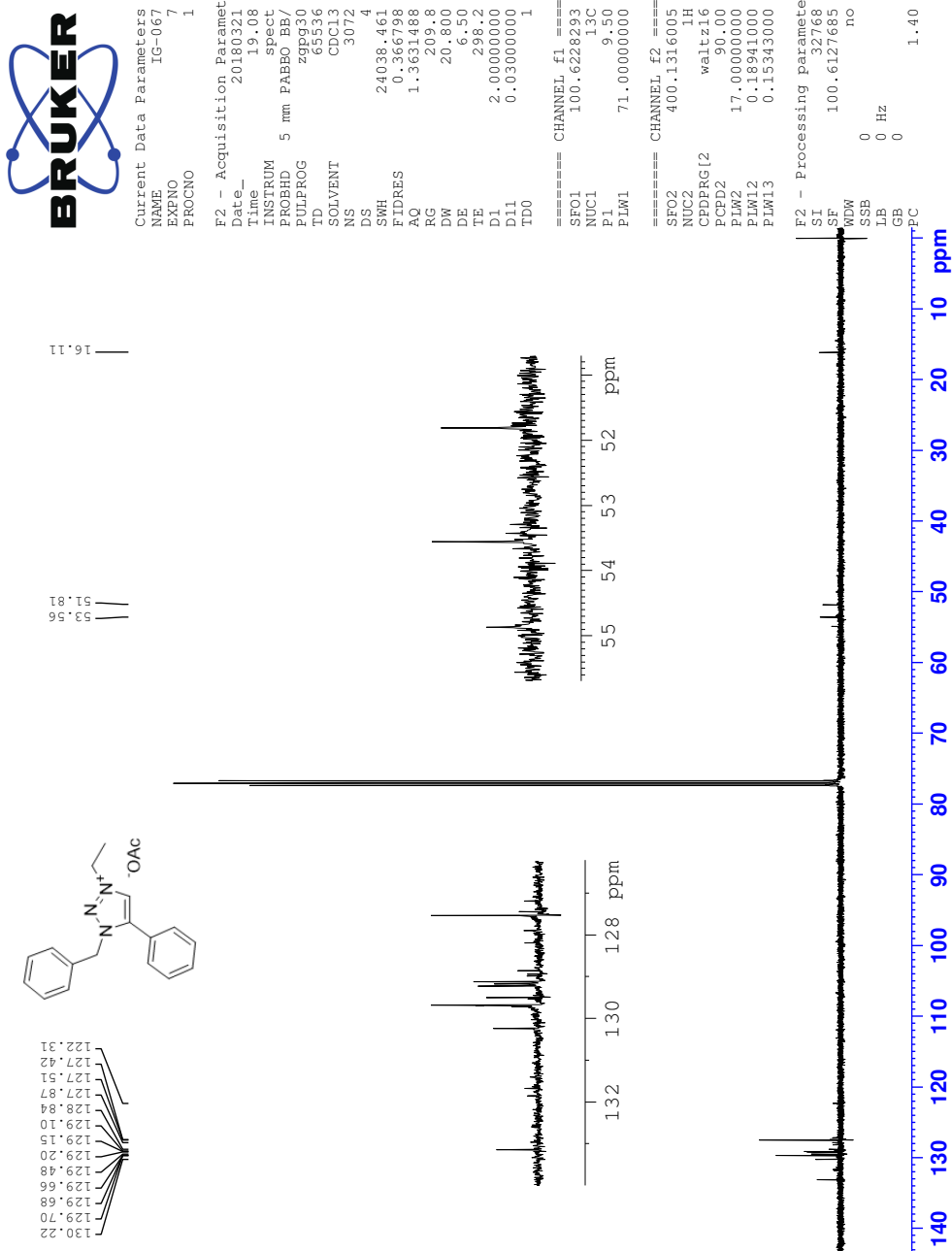
¹H NMR Spectrum of 4b



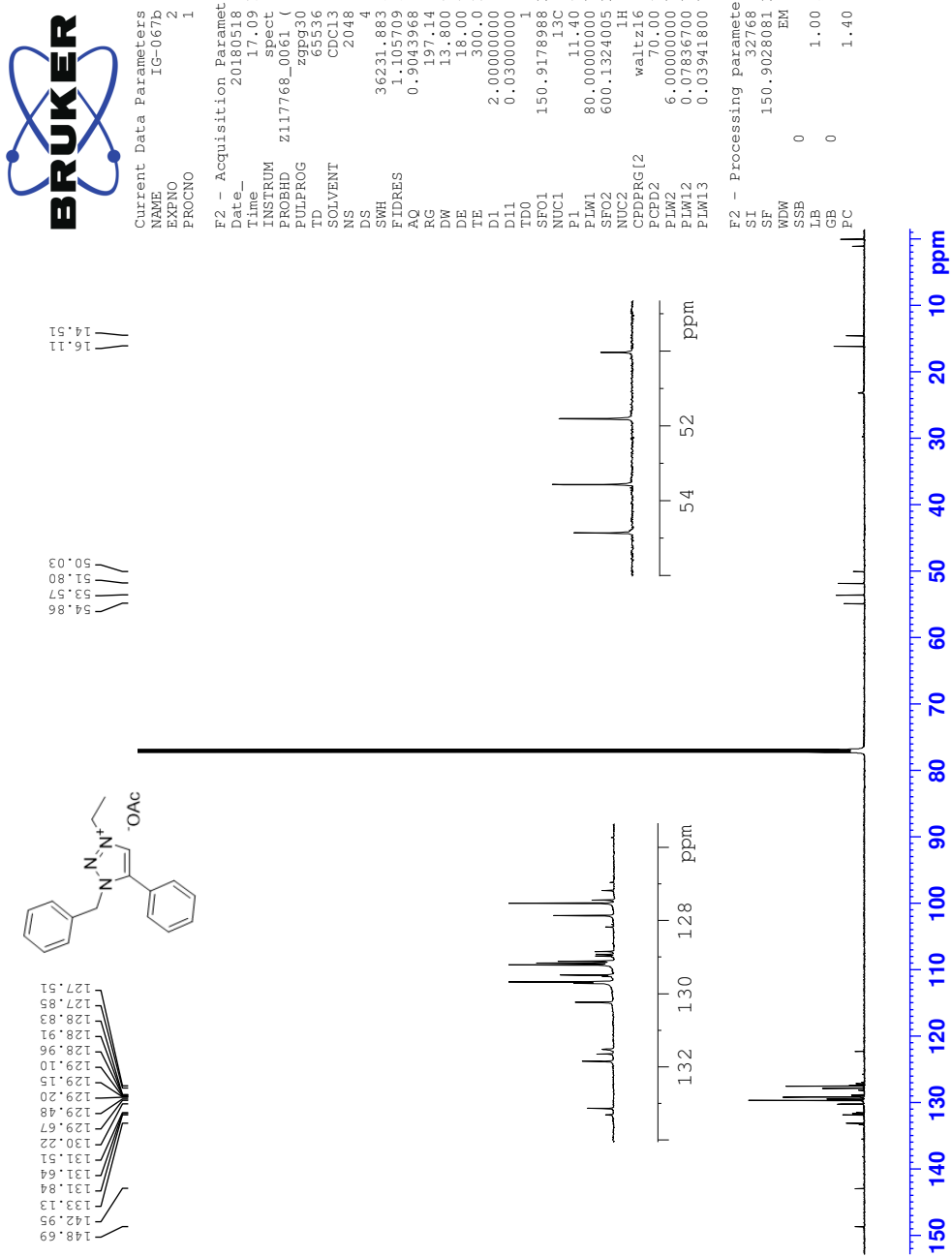
¹H NMR Spectrum of 4b after 8 weeks



¹³C NMR Spectrum of 4b



¹³C NMR Spectrum of 4b after 8 weeks



HRMS Positive mode spectrum of 4b

Elemental Composition Report

Page 1

Single Mass Analysis

Tolerance = 10.0 PPM / DBE: min = -100.0, max = 100.0

Element prediction: Off

Number of isotope peaks used for i-FIT = 2

Monoisotopic Mass, Even Electron Ions

174 formula(e) evaluated with 1 results within limits (all results (up to 1000) for each mass)

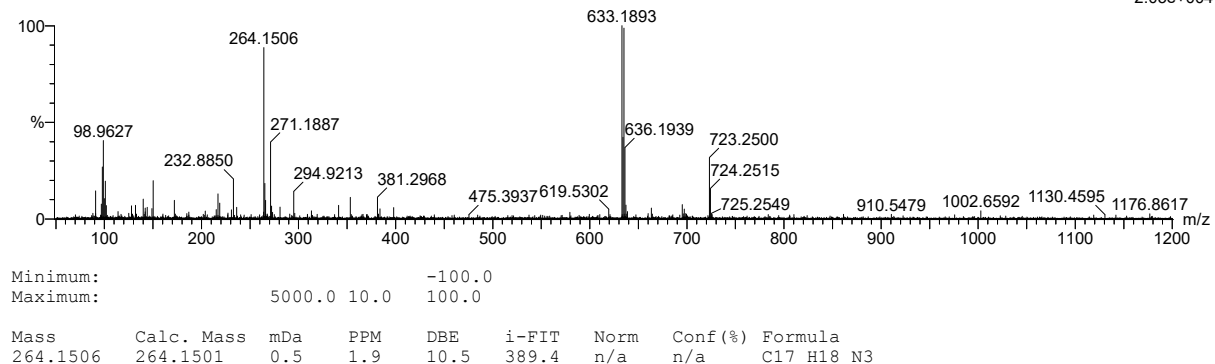
Elements Used:

C: 0-500 H: 0-1000 N: 0-10

2018-143 23 (0.437) AM2 (Ar,35000.0,0.00,0.00)

1: TOF MS ES+

2.05e+004



Minimum: -100.0
Maximum: 5000.0 10.0 100.0

Mass	Calc. Mass	mDa	PPM	DBE	i-FIT	Norm	Conf (%)	Formula
264.1506	264.1501	0.5	1.9	10.5	389.4	n/a	n/a	C17 H18 N3

HRMS Negative mode spectrum of 4b

Elemental Composition Report

Page 1

Single Mass Analysis

Tolerance = 10.0 PPM / DBE: min = -100.0, max = 100.0

Element prediction: Off

Number of isotope peaks used for i-FIT = 2

Monoisotopic Mass, Even Electron Ions

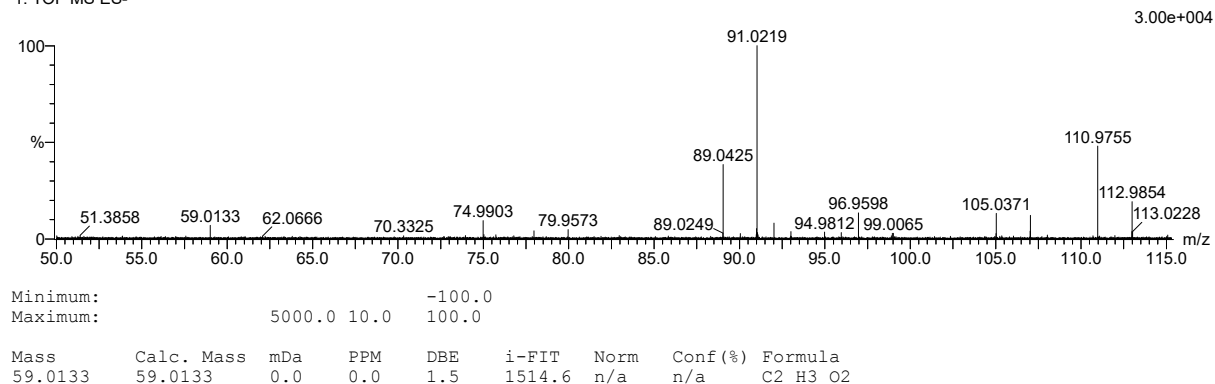
33 formula(e) evaluated with 1 results within limits (all results (up to 1000) for each mass)

Elements Used:

C: 0-500 H: 0-1000 N: 0-10 O: 0-20

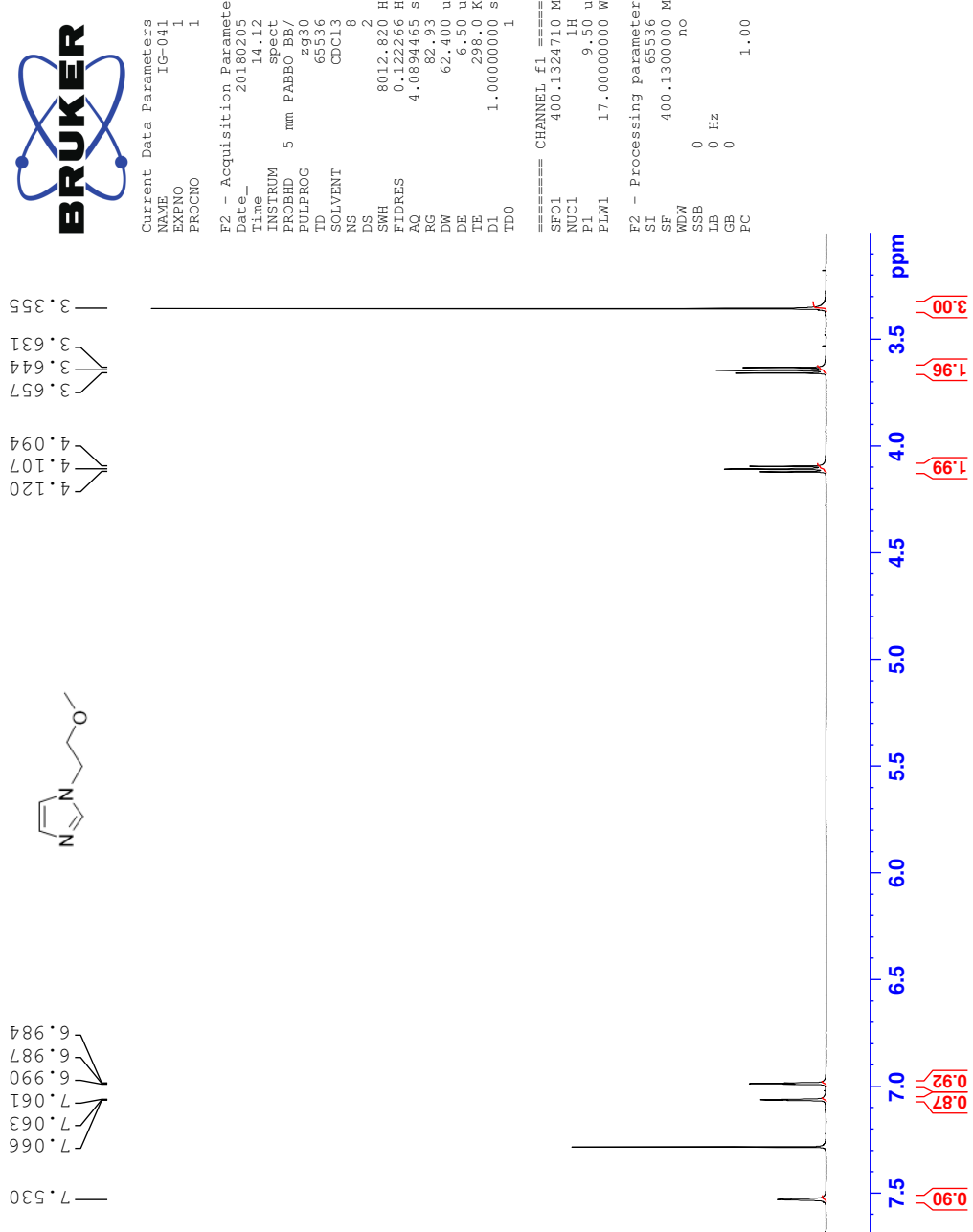
2018-143negZ2 73 (1.449) AM2 (Ar,35000.0,0.00,0.00); Cm (72:75)

1: TOF MS ES-



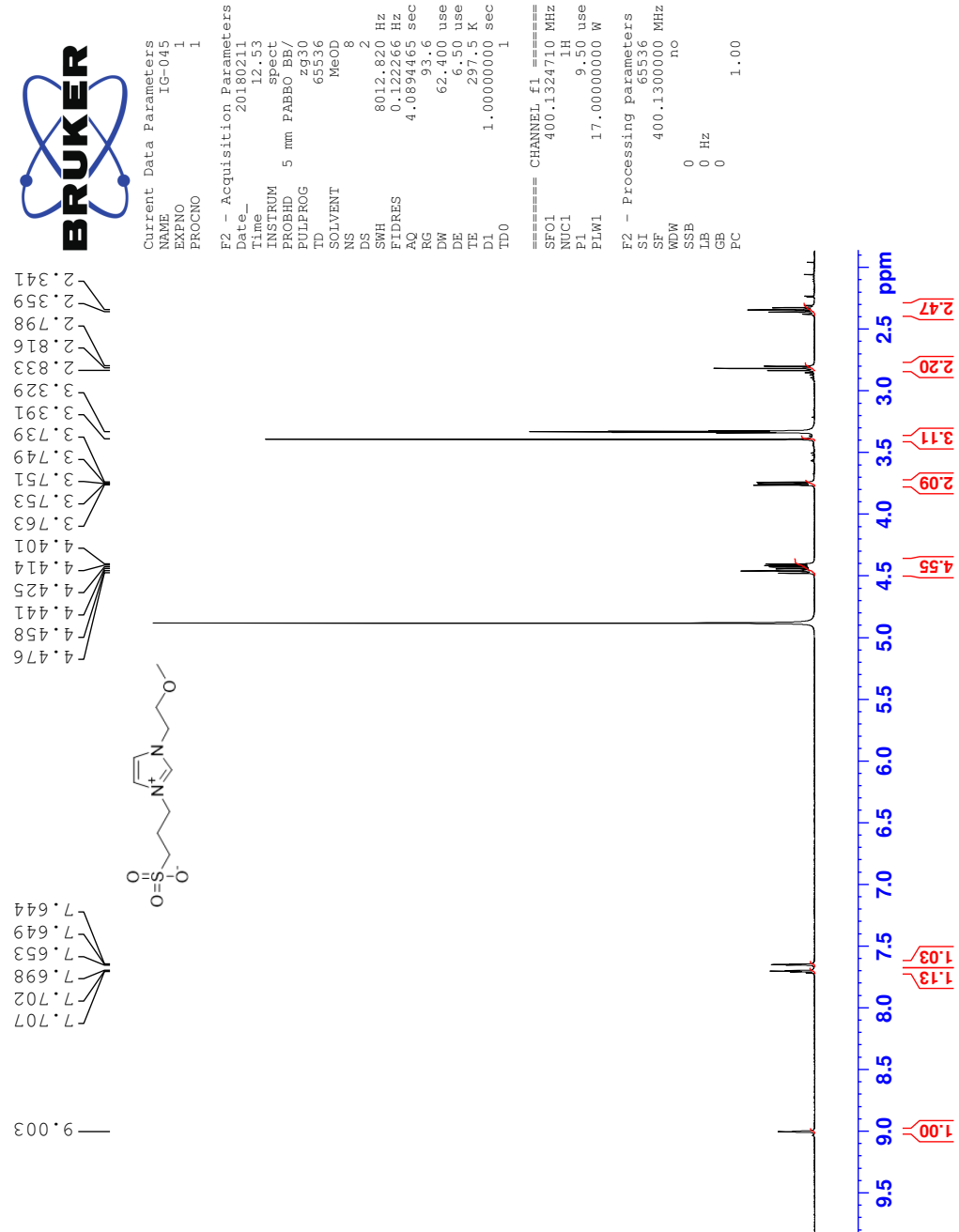
G Spectrum of 1-(2-methoxyethyl)-imidazole (5a)

¹H NMR Spectrum of 5a

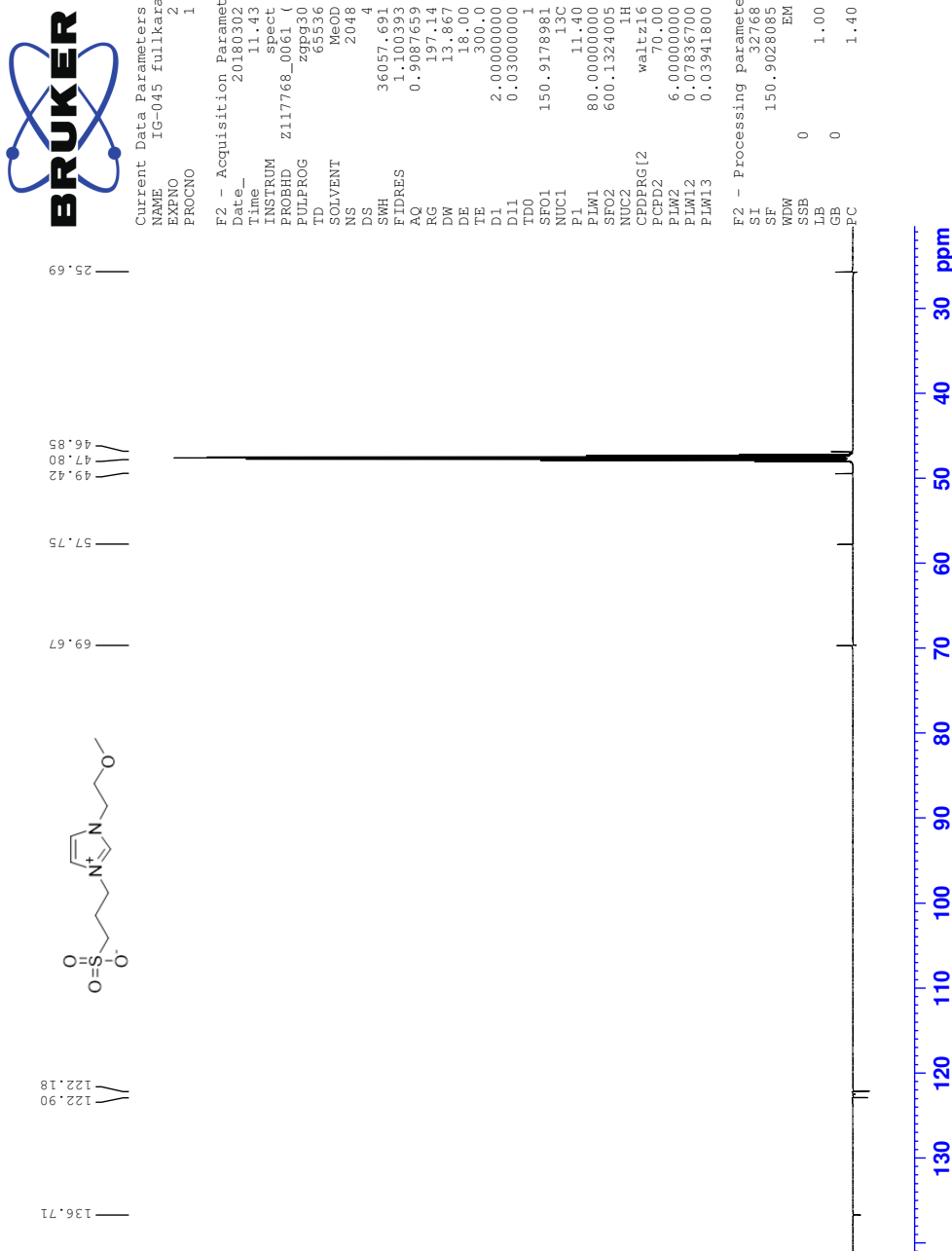


H Spectra of 3-(1-(2-methoxyethyl)-imidazol-3-ium-3-yl)-propane-1-sulfonate (5b)

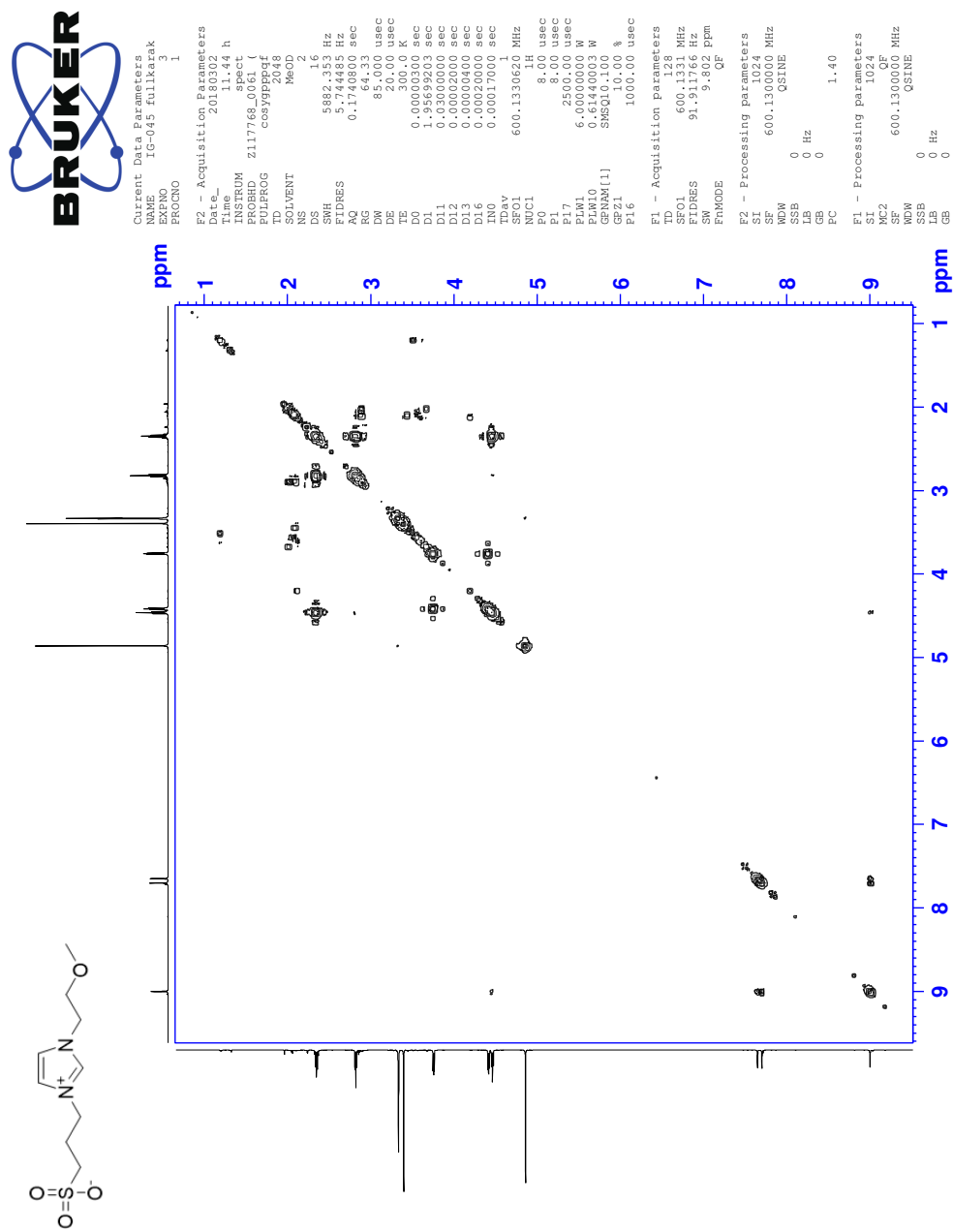
¹H NMR Spectrum of 5b



¹³C NMR Spectrum of 5b

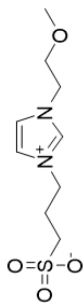
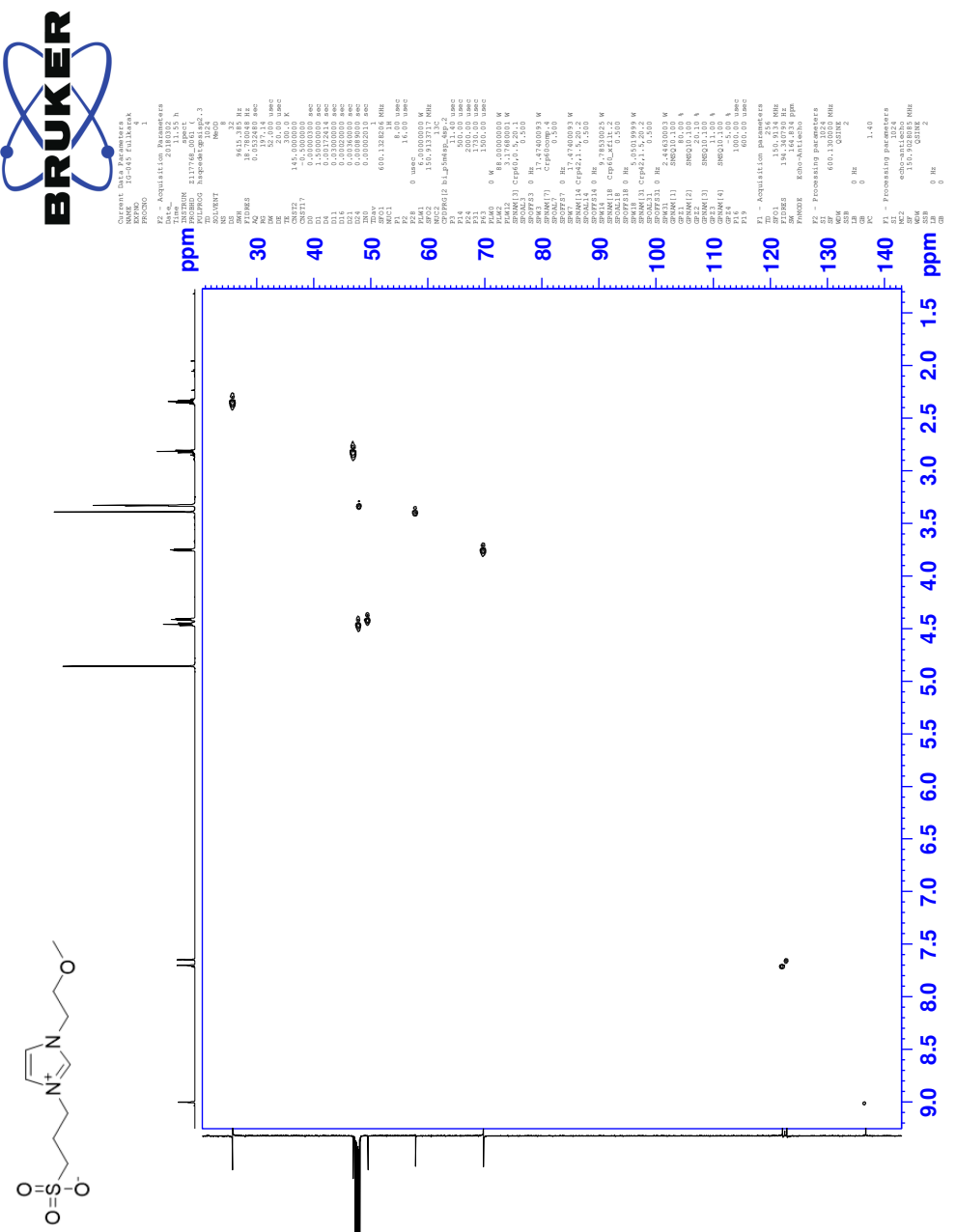


COSY NMR Spectrum of 5b

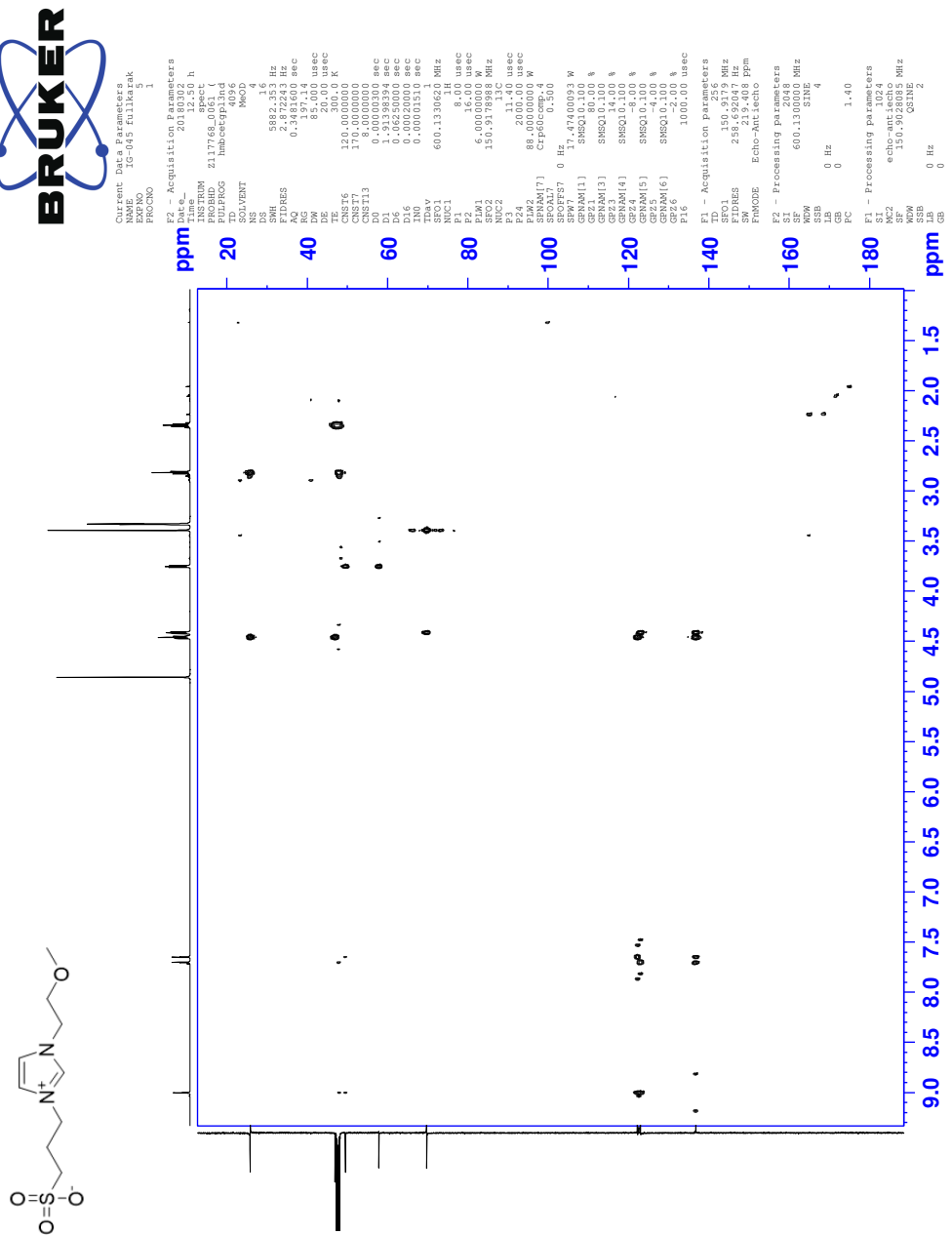


XXX

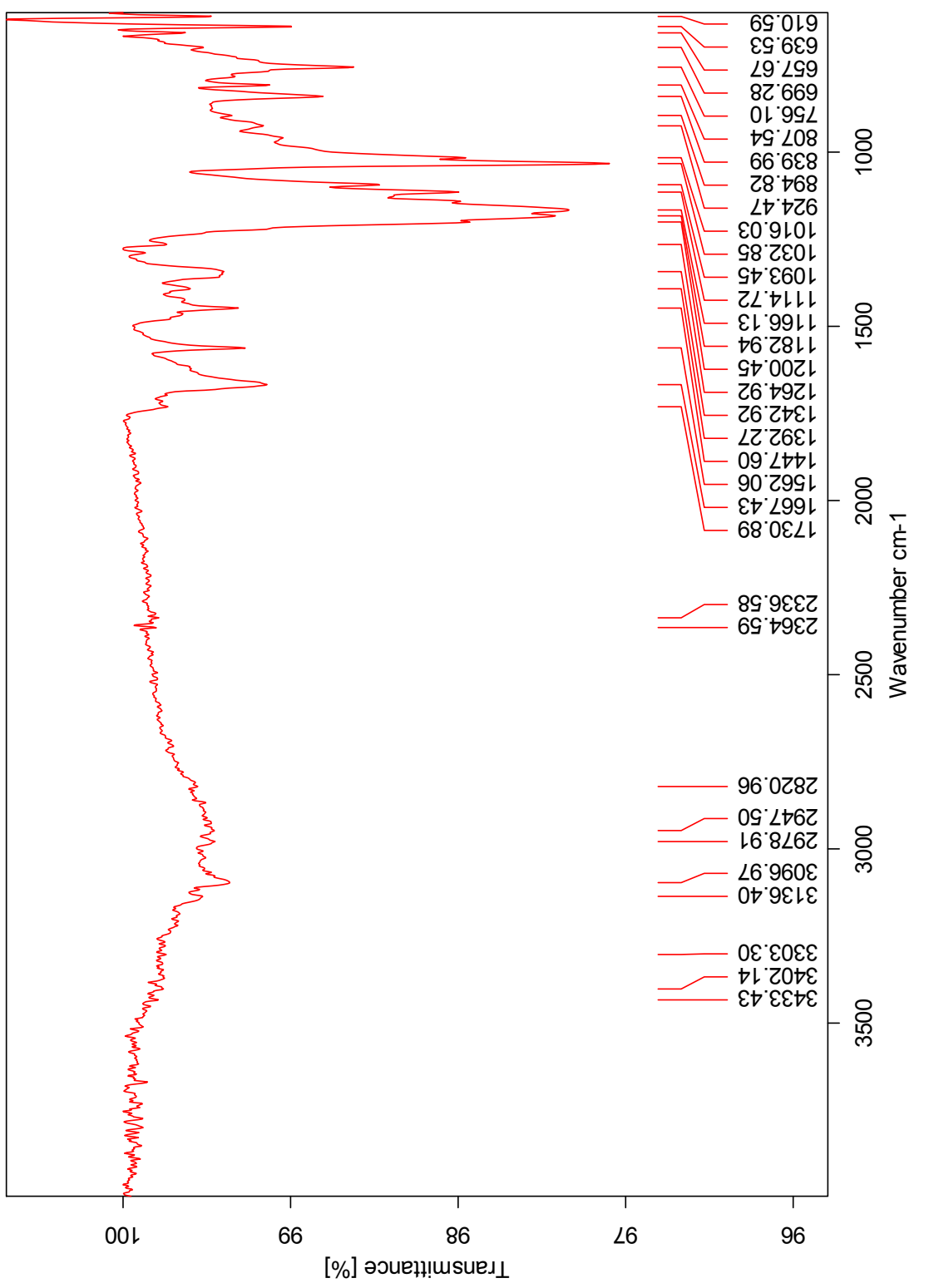
HSQC NMR Spectrum of 5b



HMBC NMR Spectrum of 5b



IR Spectrum of 5b



HRMS Spectrum of 5b

Elemental Composition Report

Page 1

Single Mass Analysis

Tolerance = 3.0 PPM / DBE: min = -1.5, max = 50.0

Element prediction: Off

Number of isotope peaks used for i-FIT = 3

Monoisotopic Mass, Even Electron Ions

954 formula(e)s evaluated with 2 results within limits (all results (up to 1000) for each mass)

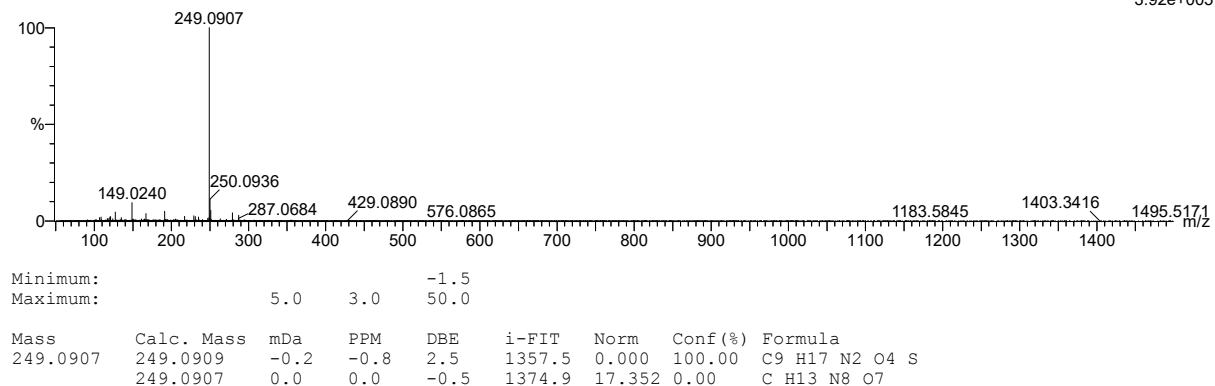
Elements Used:

C: 0-500 H: 0-1000 N: 0-100 O: 0-100 S: 0-3

2018-36 301 (5.859) AM2 (Ar,35000.0,0.00,0.00); Cm (297:308)

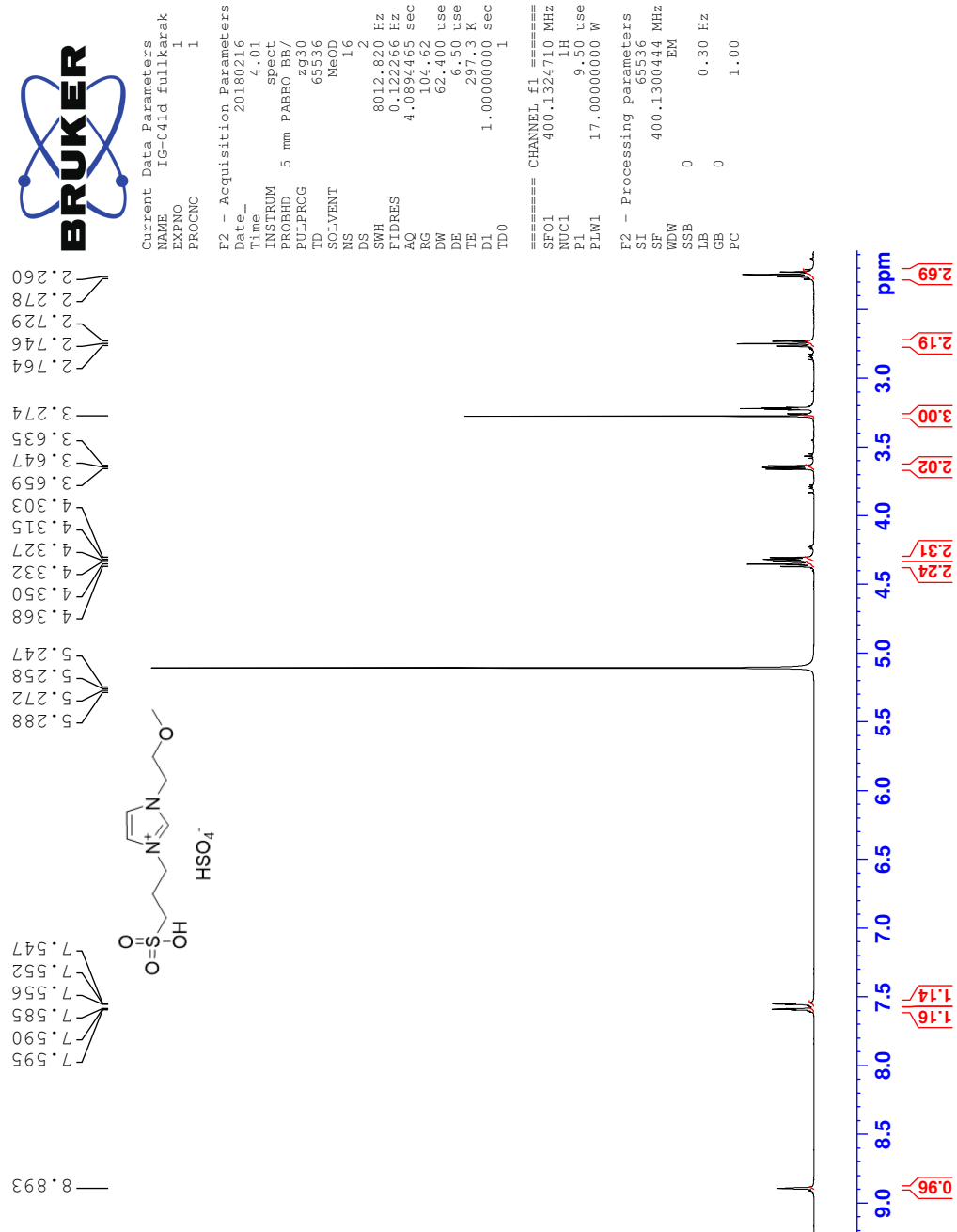
1: TOF MS ASAP+

3.92e+005

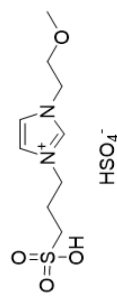
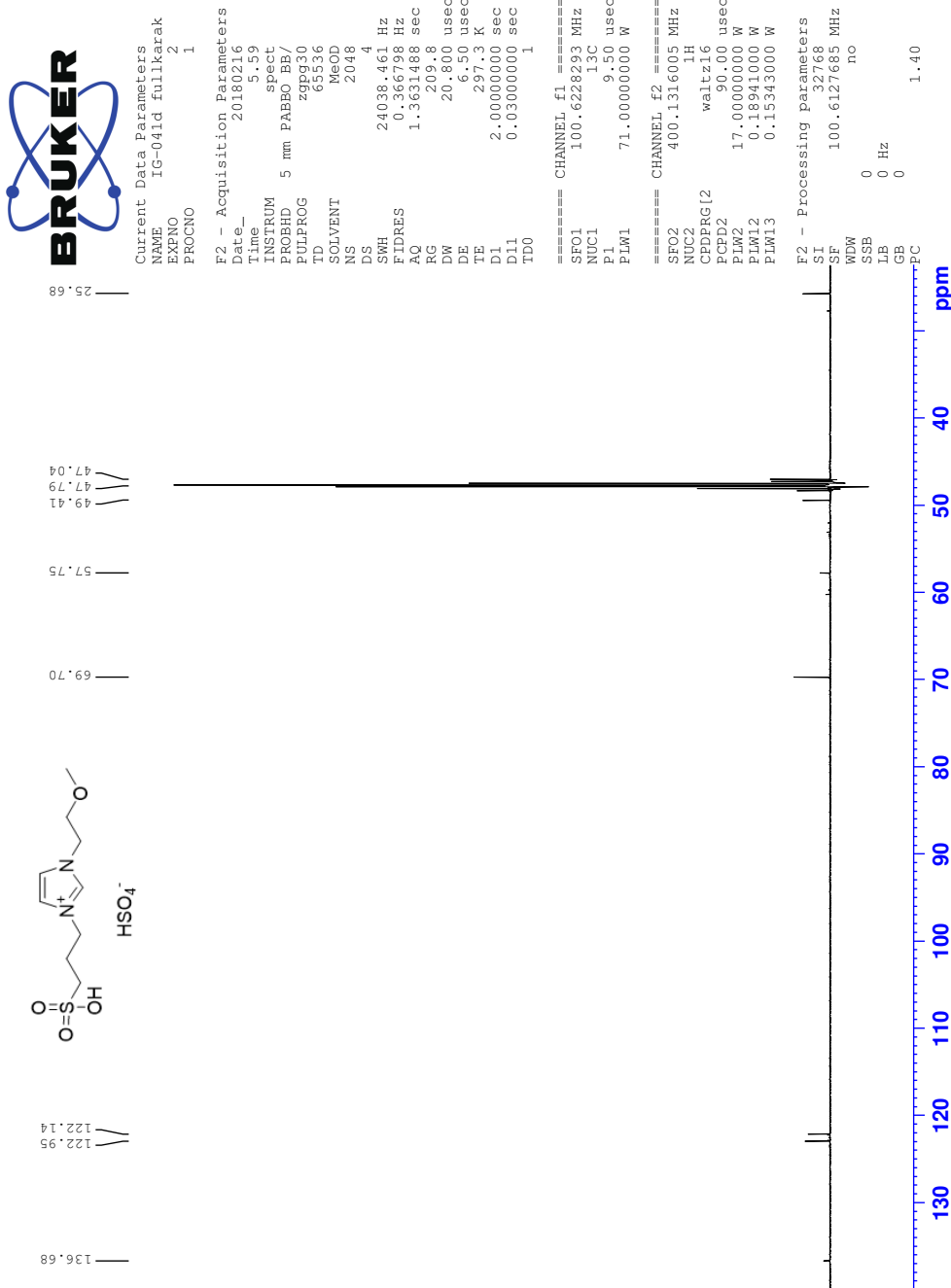


I Spectra of 1-(2-methoxyethyl)-3-(3-sulfopropyl)-1H-imidazol-3-ium hydrogen sulfate (5c)

¹H NMR Spectrum of 5c

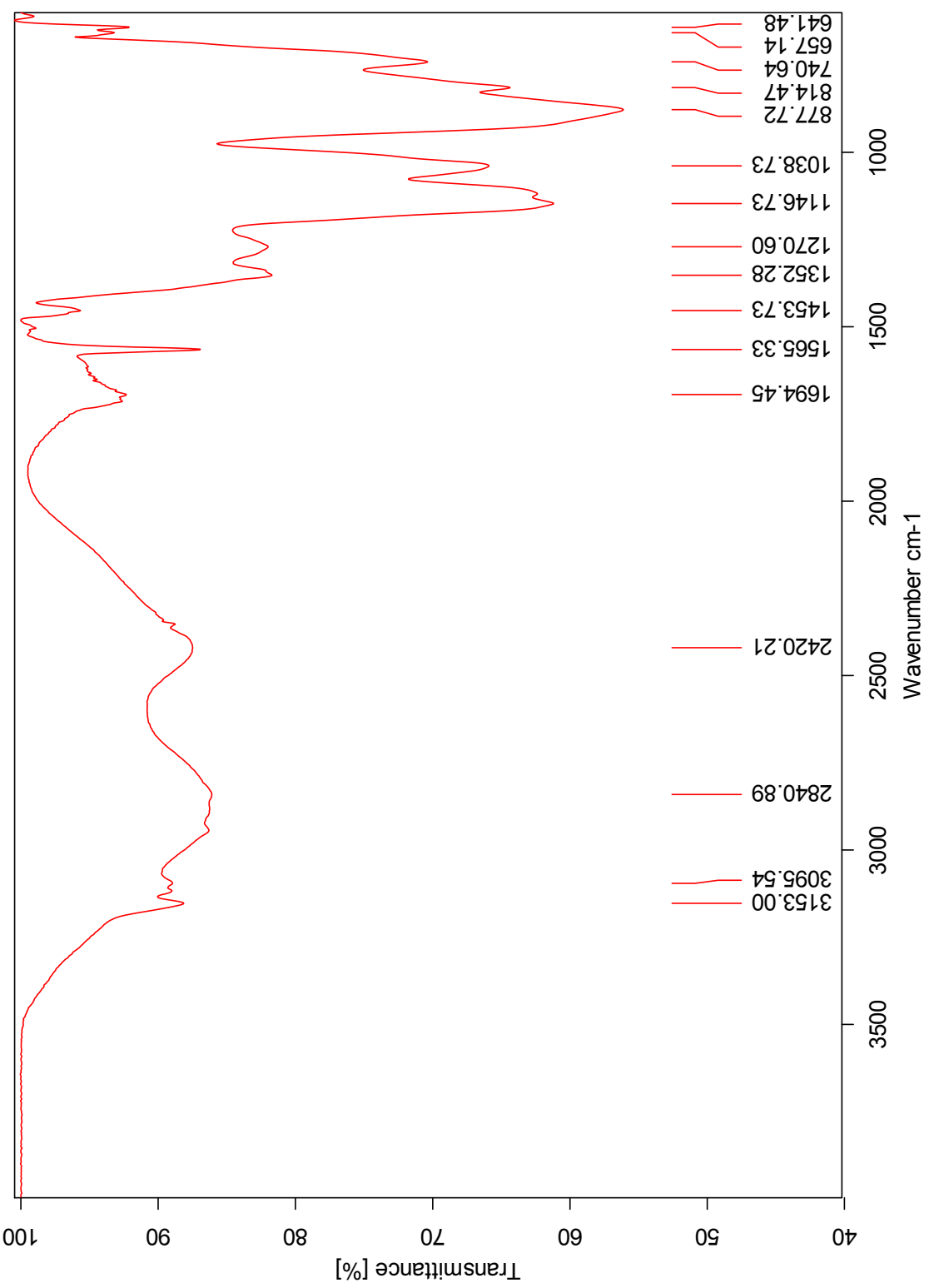


¹³C NMR Spectrum of 5c



IR Spectrum of 5c

C:\Users\ALPHA\Documents\bruker\opus_7.5.18\data\meas\IG-041d).0



HRMS Positive mode spectrum of 5c

Elemental Composition Report

Page 1

Single Mass Analysis

Tolerance = 2.0 PPM / DBE: min = -1.5, max = 50.0

Element prediction: Off

Number of isotope peaks used for i-FIT = 3

Monoisotopic Mass, Even Electron Ions

738 formula(e) evaluated with 3 results within limits (all results (up to 1000) for each mass)

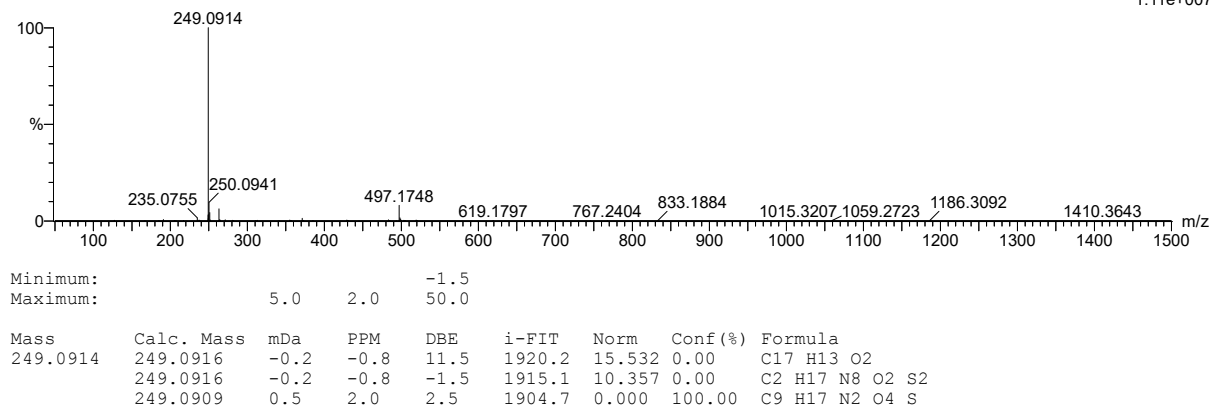
Elements Used:

C: 0-500 H: 0-1000 N: 0-10 O: 0-50 S: 0-2

2018-87pos 243 (2.260) AM2 (Ar,35000.0,0.00,0.00); Cm (241:245)

1: TOF MS ES+

1.11e+007



HRMS Negative mode spectrum of 5c

Elemental Composition Report

Page 1

Single Mass Analysis

Tolerance = 2.0 PPM / DBE: min = -1.5, max = 50.0

Element prediction: Off

Number of isotope peaks used for i-FIT = 3

Monoisotopic Mass, Even Electron Ions

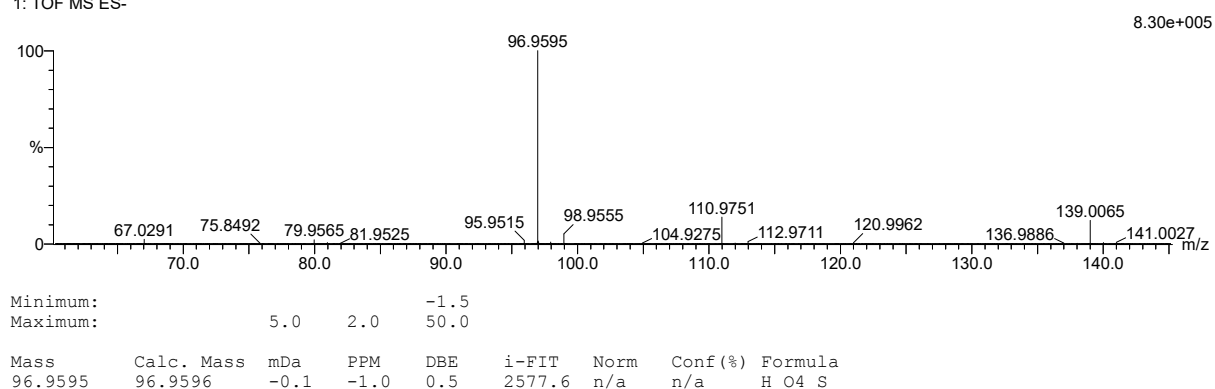
75 formula(e) evaluated with 1 results within limits (all results (up to 1000) for each mass)

Elements Used:

C: 0-500 H: 0-1000 N: 0-10 O: 0-50 S: 0-2

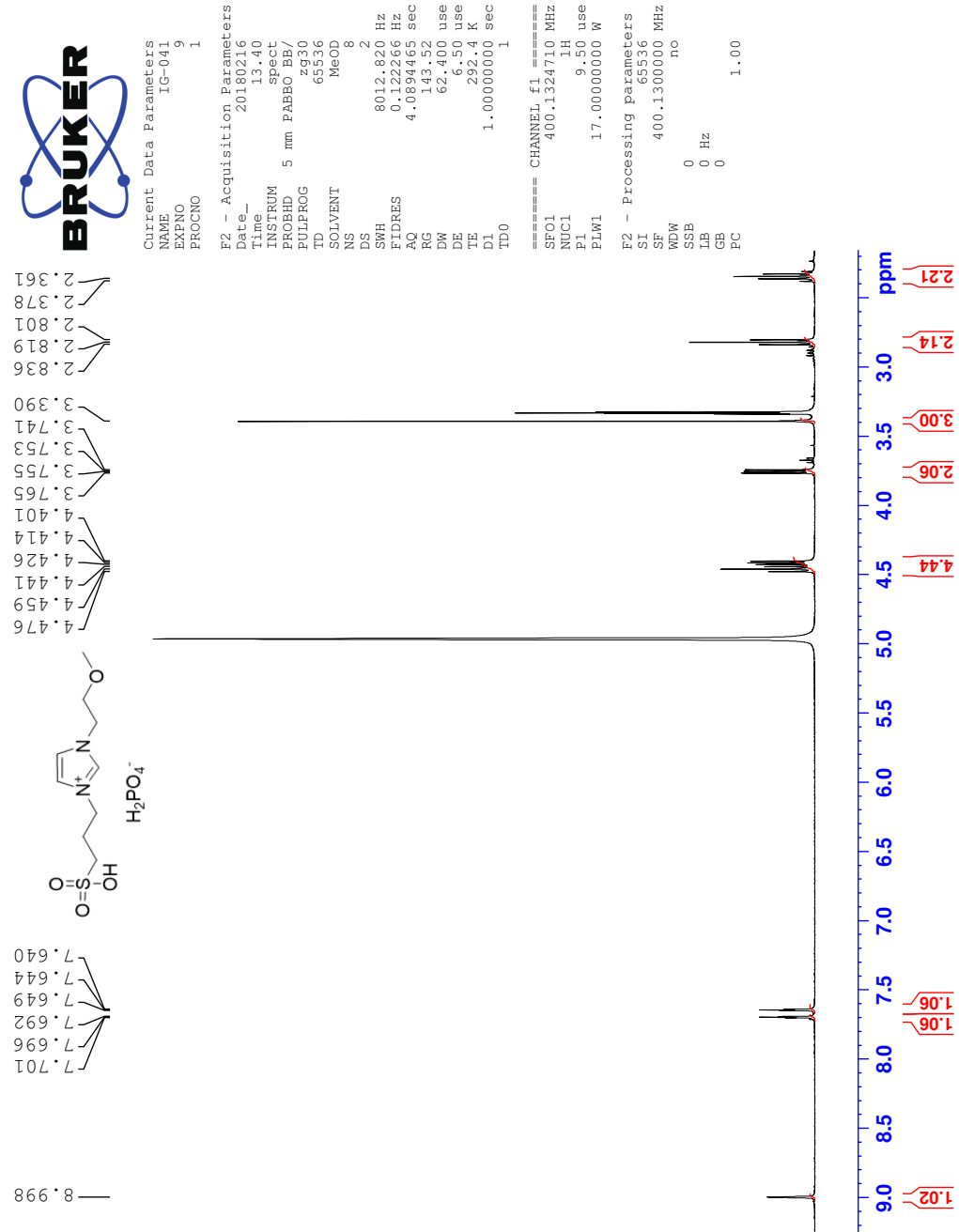
2018-87neg 87 (1.705) AM2 (Ar,35000.0,0.00,0.00); Cm (87:91)

1: TOF MS ES-



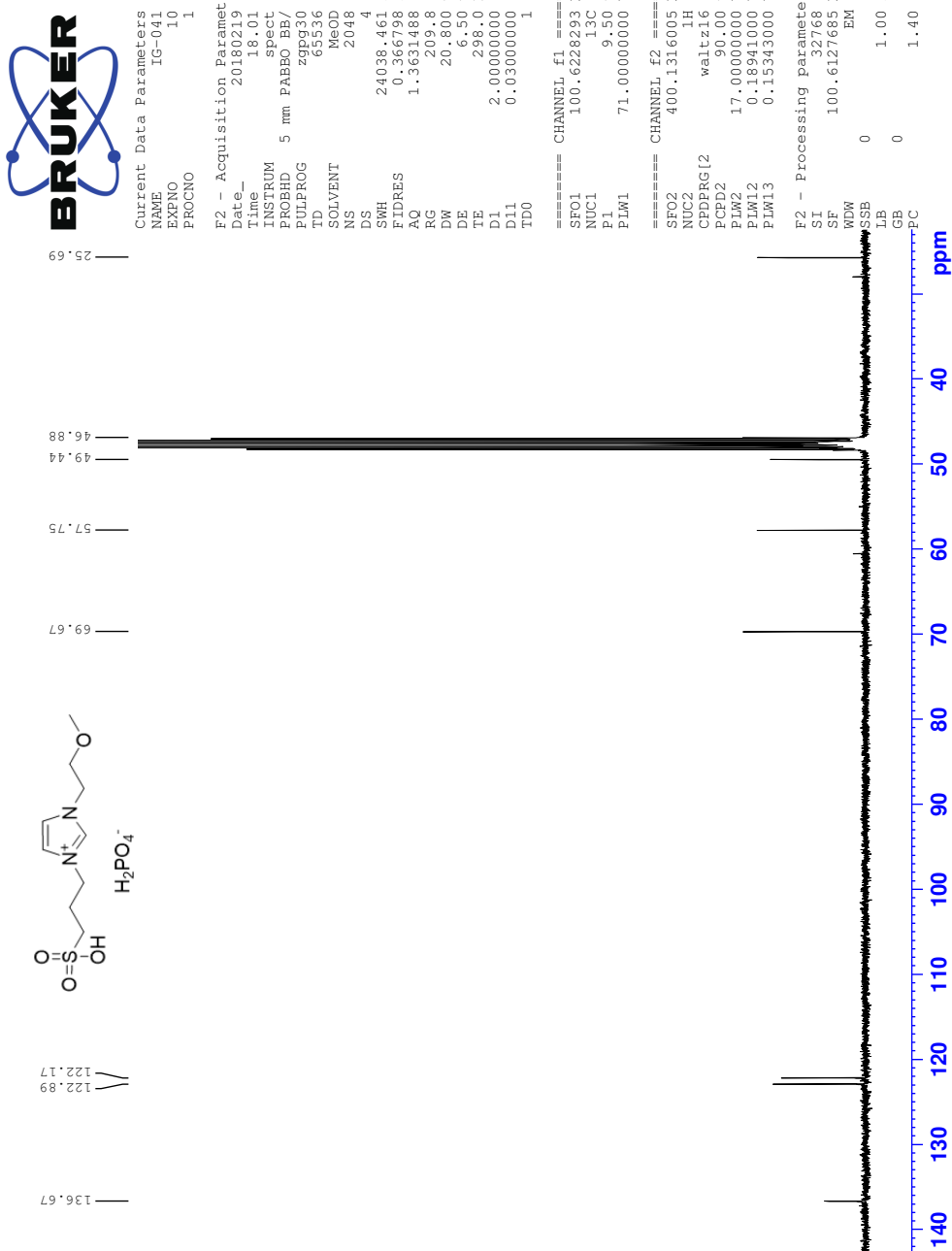
J Spectra of 1-(2-methoxyethyl)-3-(3-sulfopropyl)-1H-imidazol-3-i um dihydrogen phosphate (5d)

¹H NMR Spectrum of 5d



XL

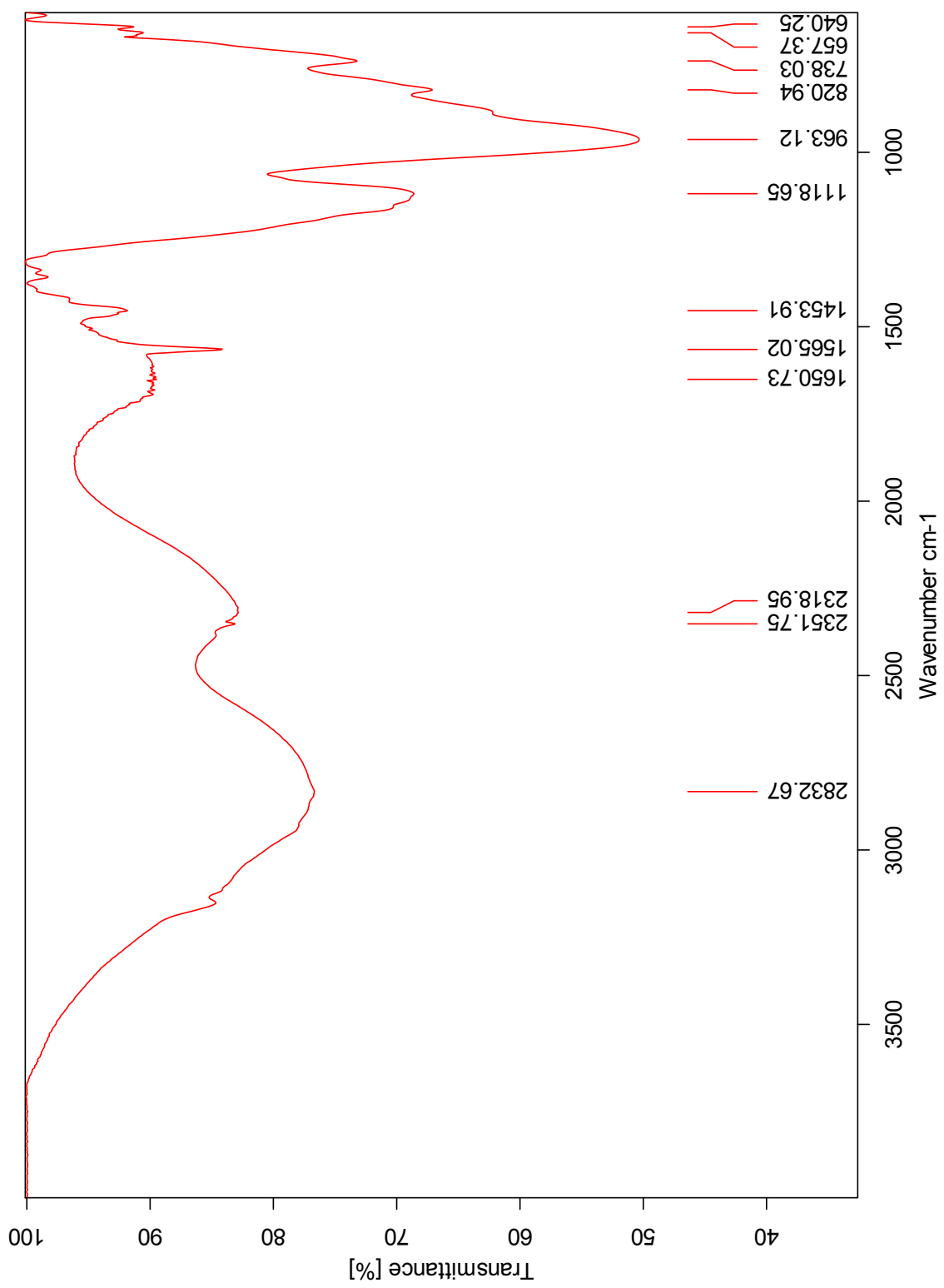
¹³C NMR Spectrum of 5d



XLI

IR Spectrum of 5d

C:\Users\ALPHA\Documents\Bruker\OPUS_7.5.18\DATA\MEAS\IG-041g.j0



HRMS Positive mode spectrum of 5d

Elemental Composition Report

Page 1

Single Mass Analysis

Tolerance = 3.0 PPM / DBE: min = -1.5, max = 50.0

Element prediction: Off

Number of isotope peaks used for i-FIT = 3

Monoisotopic Mass, Even Electron Ions

2728 formula(e) evaluated with 6 results within limits (all results (up to 1000) for each mass)

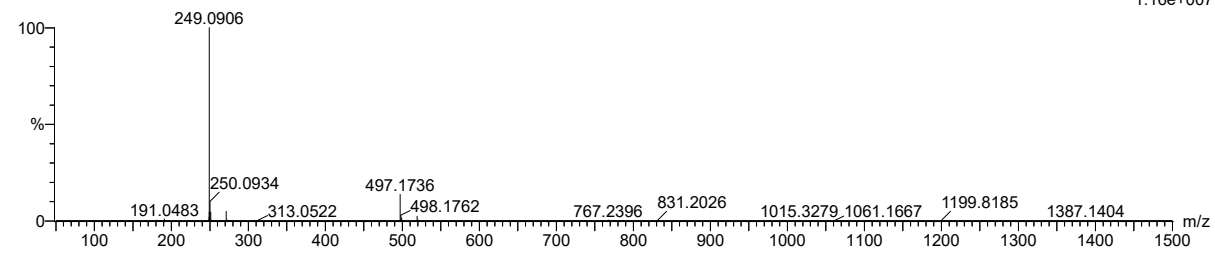
Elements Used:

C: 0-500 H: 0-1000 N: 0-200 O: 0-100 P: 0-5 S: 0-6

2018-73esipos 37 (0.368) AM2 (Ar,35000.0,0.00,0.00); Cm (35:38)

1: TOF MS ES+

1.16e+007



Minimum: -1.5
Maximum: 5.0 3.0 50.0

Mass	Calc. Mass	mDa	PPM	DBE	i-FIT	Norm	Conf (%)	Formula
249.0906	249.0909	-0.3	-1.2	2.5	1953.1	0.006	99.39	C9 H17 N2 O4 S
	249.0901	0.5	2.0	1.5	1958.9	5.785	0.31	C11 H22 P S2
	249.0899	0.7	2.8	-1.5	1958.9	5.801	0.30	C3 H18 N6 O3 P S
	249.0905	0.1	0.4	7.5	1966.3	13.215	0.00	C11 H14 N4 O P
	249.0911	-0.5	-2.0	-1.5	1966.5	13.397	0.00	C3 H20 N6 O P3
	249.0907	-0.1	-0.4	-0.5	1967.1	14.020	0.00	C H13 N8 O7

HRMS Negative mode spectrum of 5d

Elemental Composition Report

Page 1

Single Mass Analysis

Tolerance = 3.0 PPM / DBE: min = -1.5, max = 50.0

Element prediction: Off

Number of isotope peaks used for i-FIT = 3

Monoisotopic Mass, Even Electron Ions

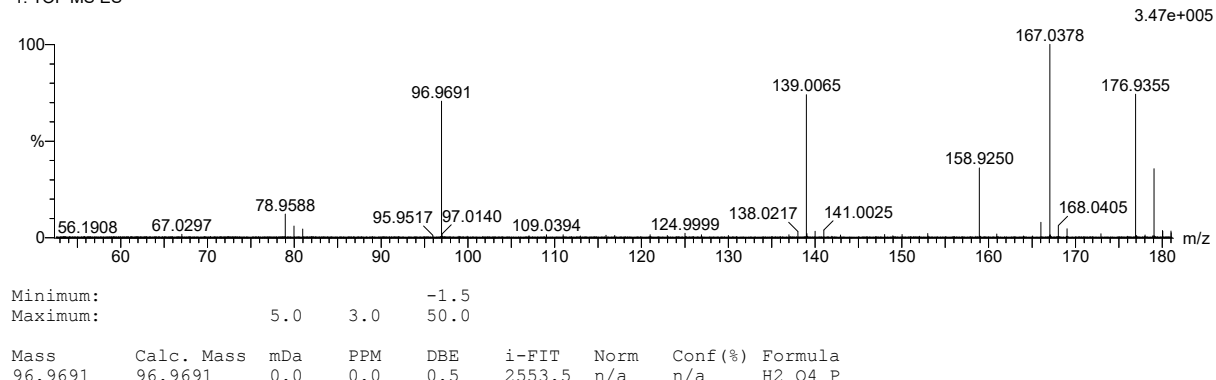
113 formula(e) evaluated with 1 results within limits (all results (up to 1000) for each mass)

Elements Used:

C: 0-500 H: 0-1000 N: 0-200 O: 0-100 S: 0-6 P: 0-5

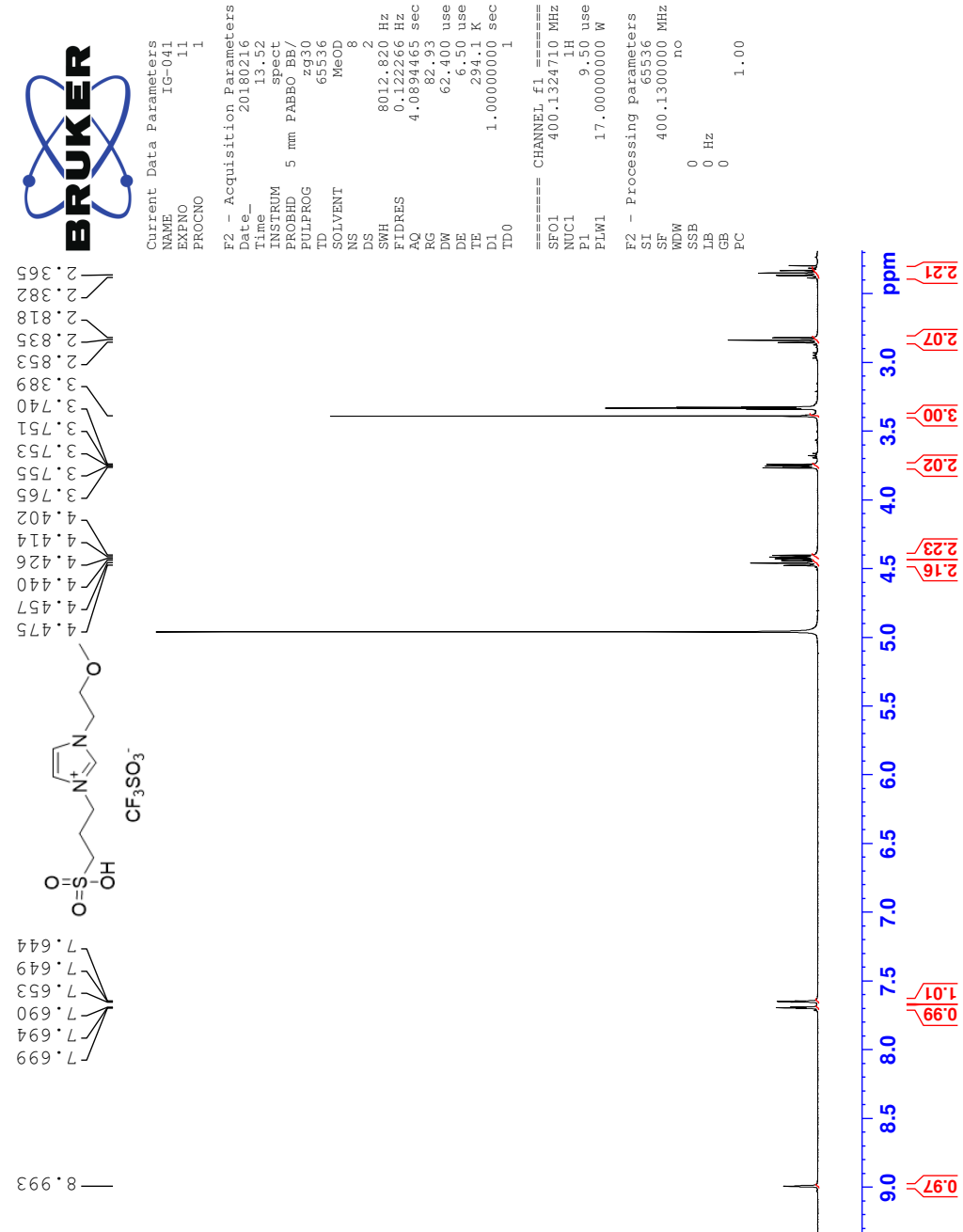
2018-73esiNEG 20 (0.414) AM2 (Ar,35000.0,0.00,0.00); Cm (20:22)

1: TOF MS ES-

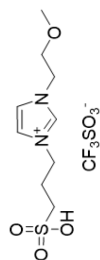
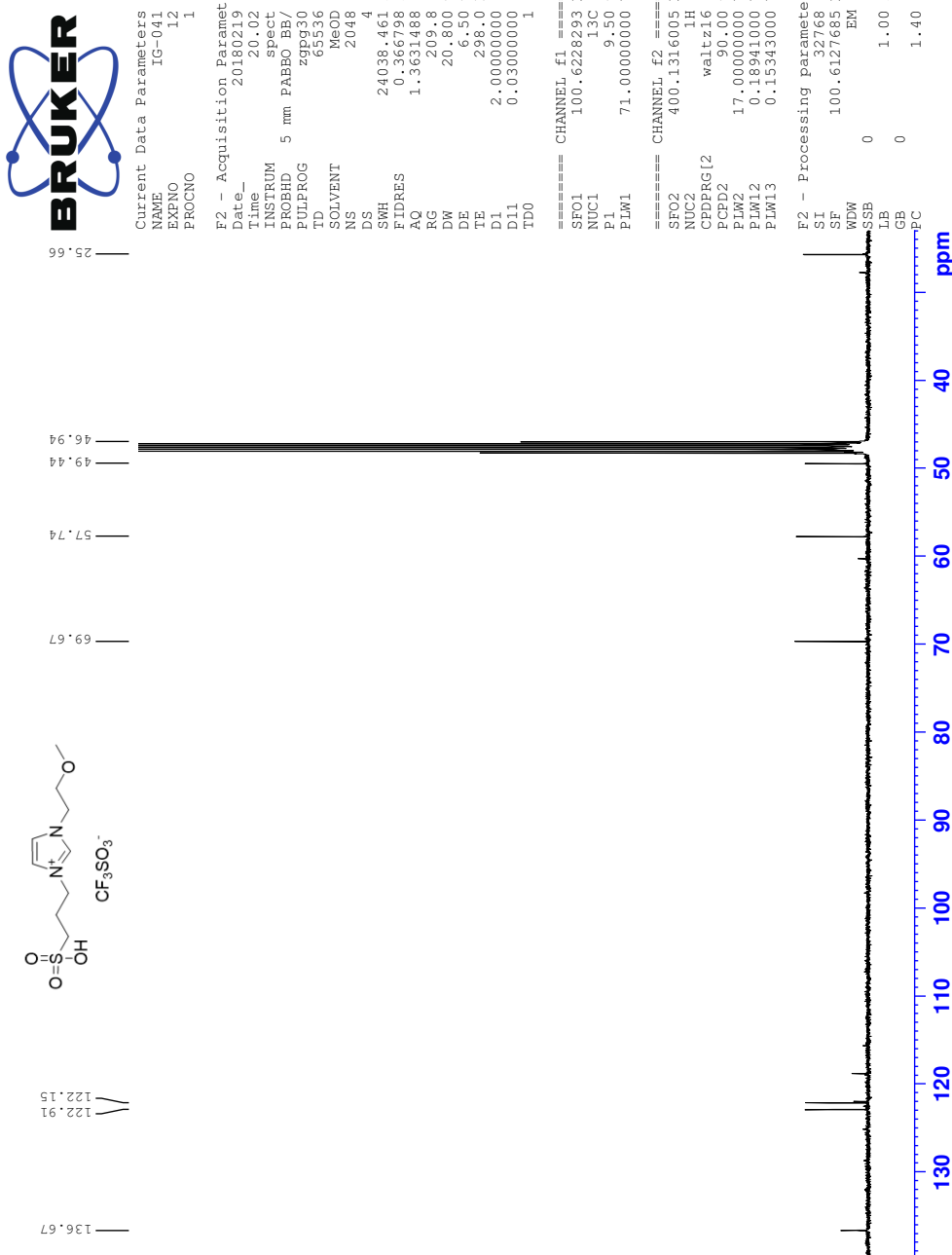


K Spectra of 1-(2-methoxyethyl)-3-(3-sulfopropyl)-1H-imidazol-3-ium trifluoromethanesulfonate (5e)

¹H NMR Spectrum of 5e



¹³C NMR Spectrum of 5e



¹⁹F NMR Spectrum of 5e



Current Data Parameters

NAME IG-041
EXPNO 15
PROCNO 1

F2 - Acquisition Parameters

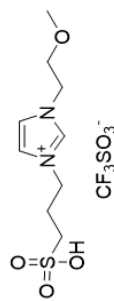
Date 20180227
Time 14.29
INSTRUM spect
PROBHD 5 mm PABBO BB/
PULPROG zg1qpn
TD 131072
SOLVENT MeOD
NS 16
DS 4
SWH 89285.711 Hz
FIDRES 0.681196 Hz
AQ 0.7340032 sec
RG 209.8
DW 5.600 usc
DE 6.50 usc
TE 292.2 K
D1 1.0000000 sec
TDO 1

===== CHANNEL f1 =====

SFG1 376.4607164 MHz
NUC1 19F
P1 17.50 usc
PLW1 19.0000000 W

F2 - Processing parameters

ST 65536
SF 376.4983662 MHz
WDW no
SSB 0
LB 0 Hz
GB 0
PC 1.00

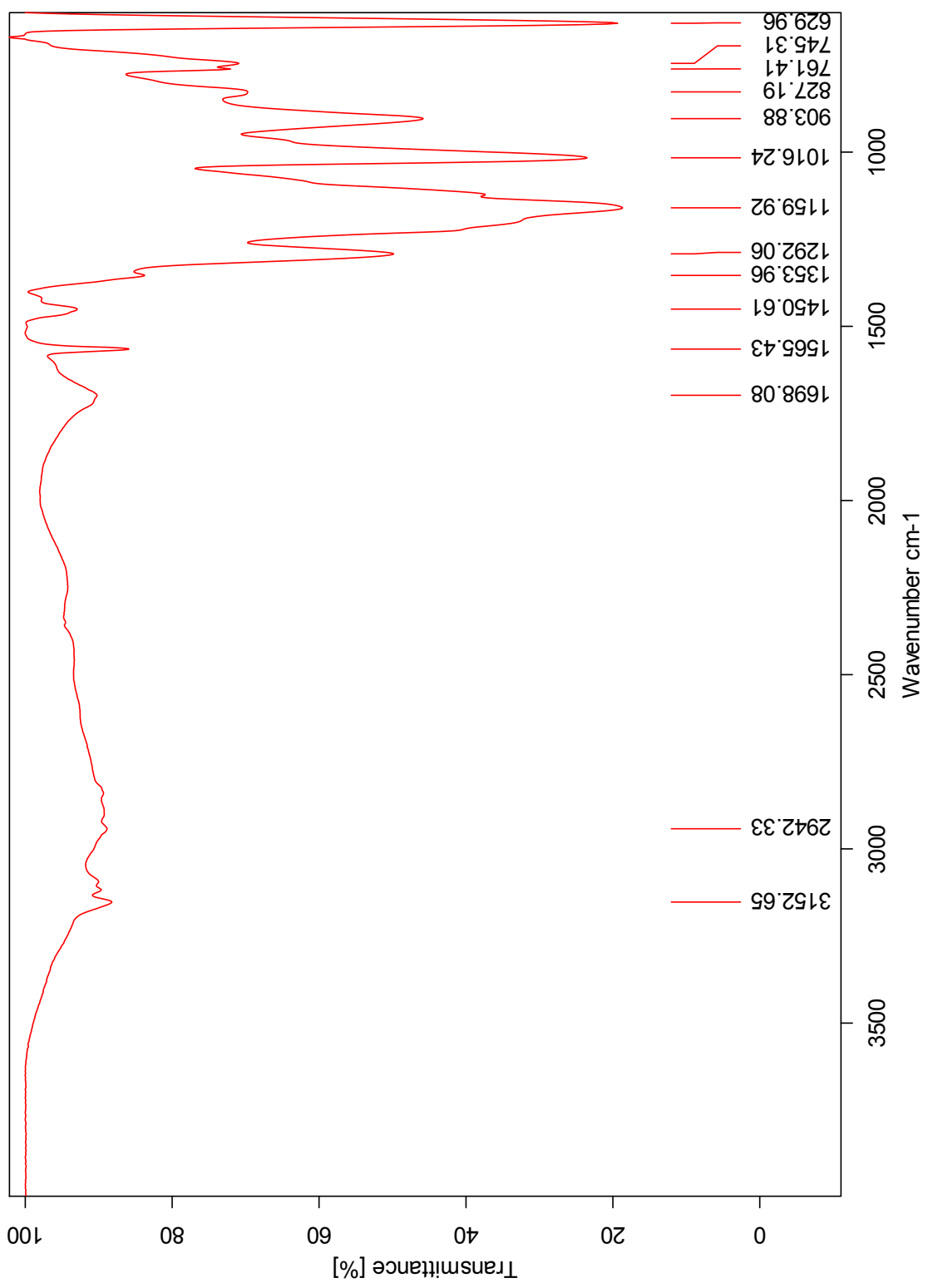


-80.1 —

-165.38 —



IR Spectrum of 5e



HRMS Positive mode spectrum of 5e

Elemental Composition Report

Page 1

Single Mass Analysis

Tolerance = 2.0 PPM / DBE: min = -1.5, max = 50.0

Element prediction: Off

Number of isotope peaks used for i-FIT = 3

Monoisotopic Mass, Even Electron Ions

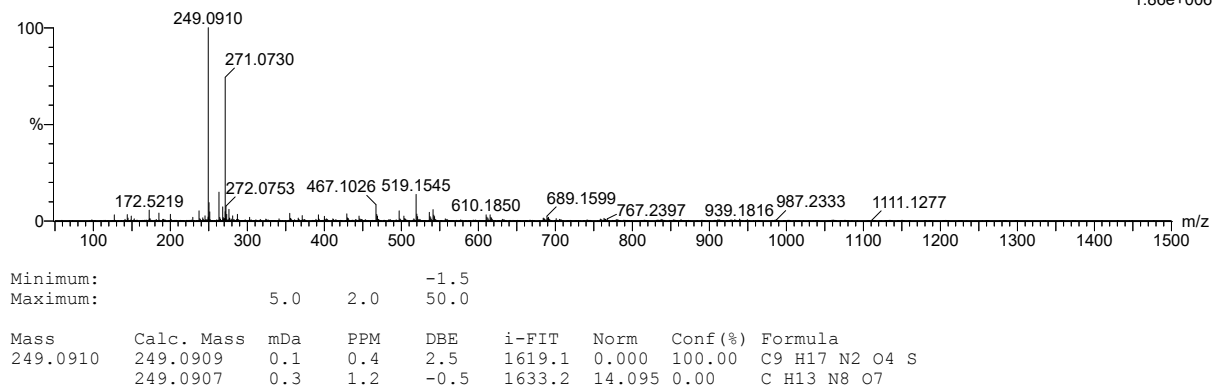
954 formula(e) evaluated with 2 results within limits (all results (up to 1000) for each mass)

Elements Used:

C: 0-500 H: 0-1000 N: 0-50 O: 0-100 S: 0-3
2018-49esi 104 (0.977) AM2 (Ar,35000.0,0.00,0.00); Cm (103:106)

1: TOF MS ES+

1.86e+006



HRMS Negative mode spectrum of 5e

Elemental Composition Report

Page 1

Single Mass Analysis

Tolerance = 2.0 PPM / DBE: min = -1.5, max = 50.0

Element prediction: Off

Number of isotope peaks used for i-FIT = 3

Monoisotopic Mass, Even Electron Ions

575 formula(e) evaluated with 2 results within limits (all results (up to 1000) for each mass)

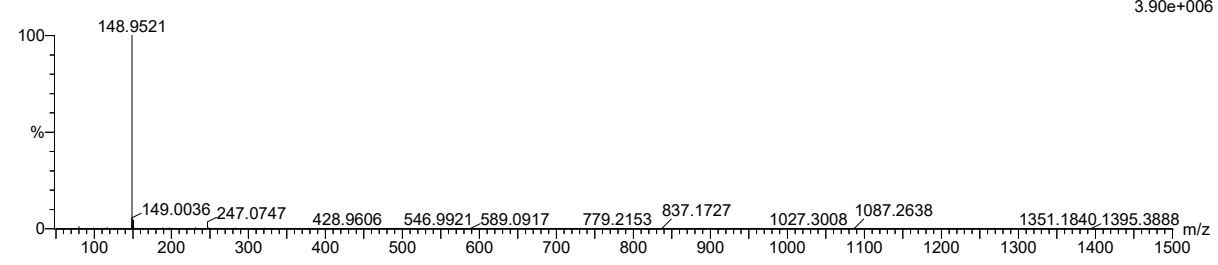
Elements Used:

C: 0-500 H: 0-1000 N: 0-50 O: 0-100 S: 0-3 F: 0-6

2018-49esineg 61 (1.207) AM2 (Ar,35000.0,0.00,0.00); Cm (61:63)

1: TOF MS ES-

3.90e+006



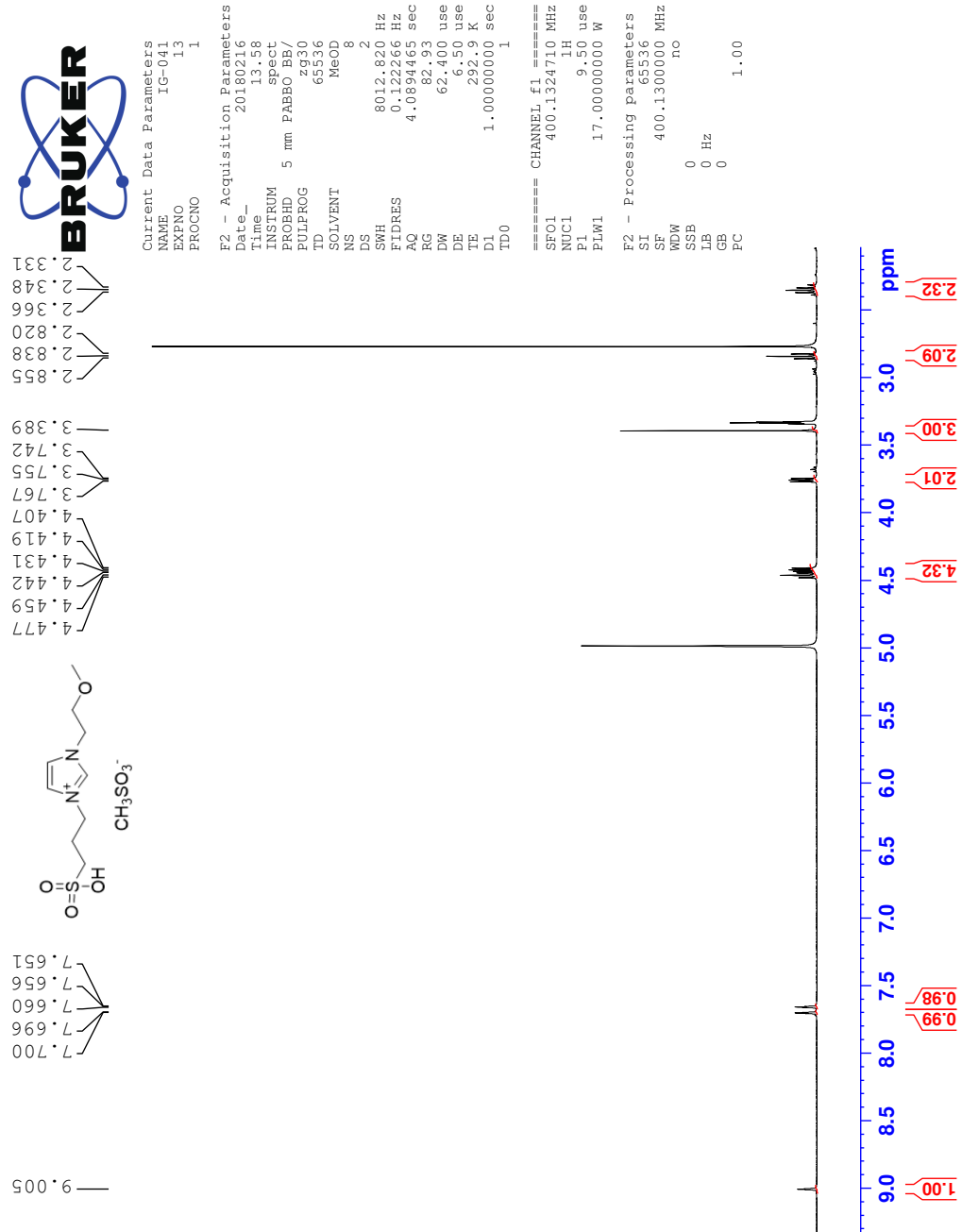
Minimum: -1.5
Maximum: 5.0 2.0 50.0

Mass	Calc. Mass	mDa	PPM	DBE	i-FIT	Norm	Conf (%)	Formula
148.9521	148.9520	0.1	0.7	0.5	2138.8	0.000	100.00	C ₇ O ₃ S F ₃
	148.9520	0.1	0.7	7.5	2149.1	10.280	0.00	C ₇ H S ₂

L

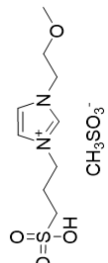
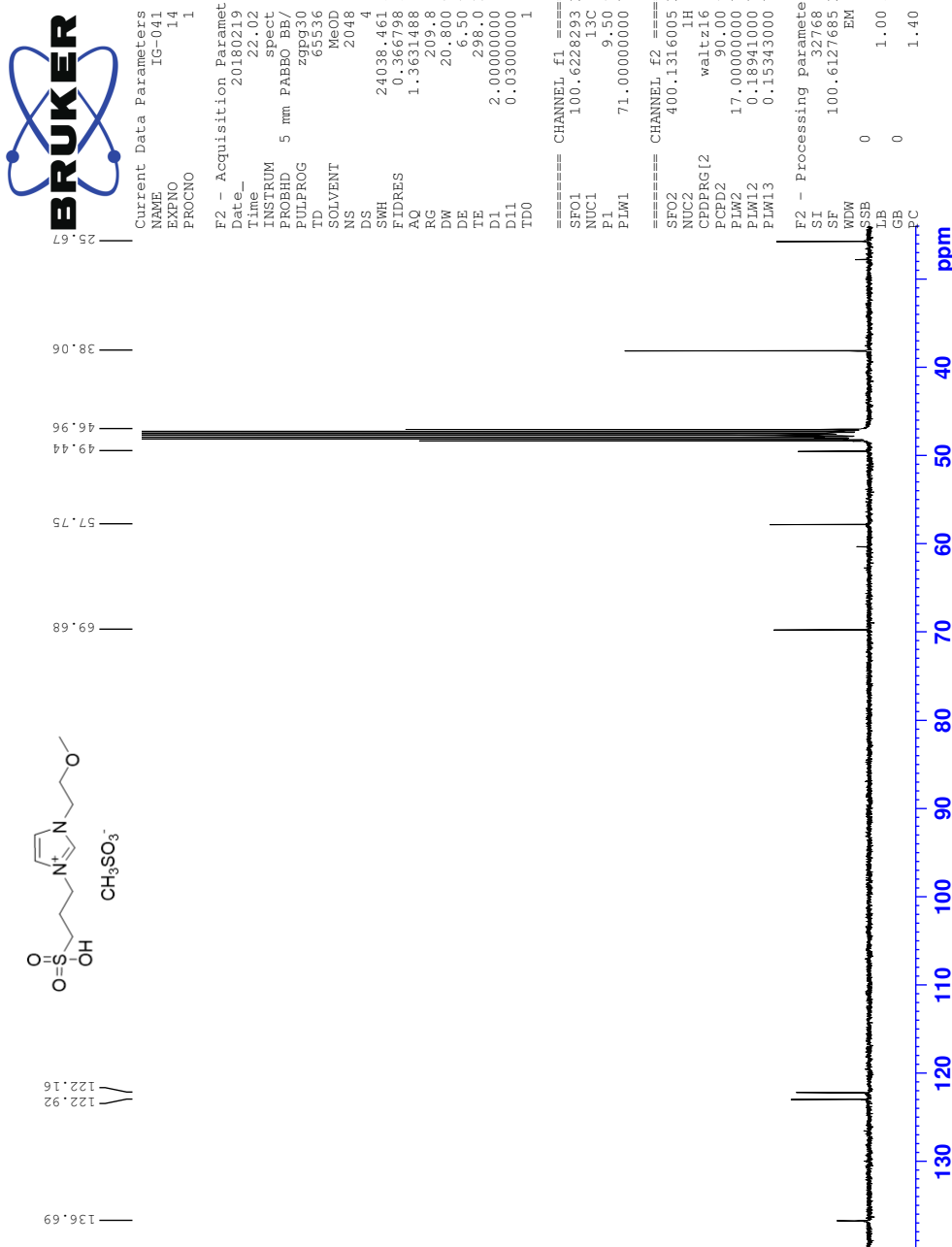
L Spectra of 1-(2-methoxyethyl)-3-(3-sulfopropyl)-1H-imidazol-3-ium methanesulfonate (5f)

^1H NMR Spectrum of 5f



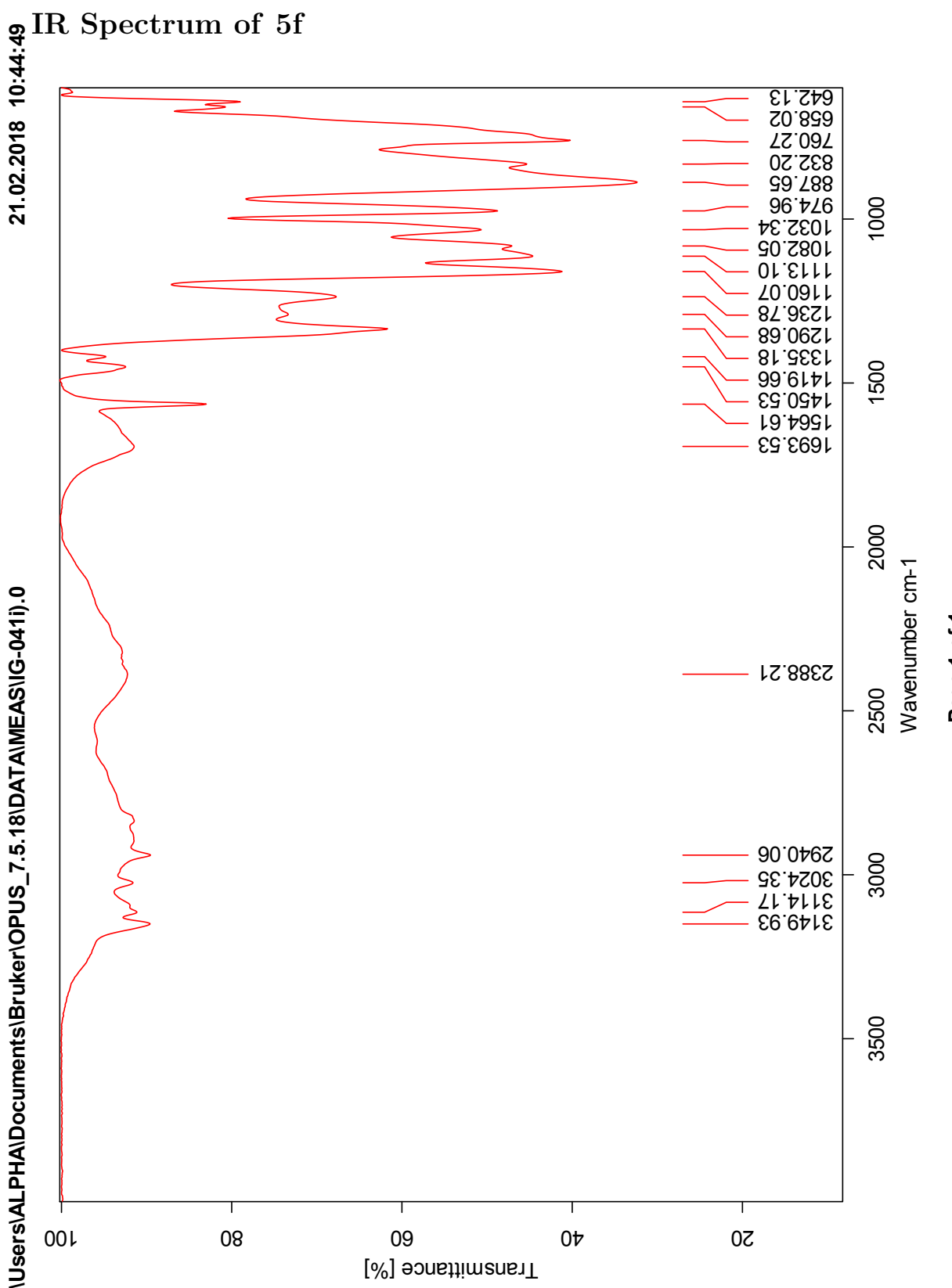
LI

¹³C NMR Spectrum of 5f



IR Spectrum of 5f

C:\Users\ALPHA\Documents\bruker\opus_7.5.18\data\meas\IG-041).0



III

Page 1 of 1

HRMS Positive mode spectrum of 5f

Elemental Composition Report

Page 1

Single Mass Analysis

Tolerance = 2.0 PPM / DBE: min = -1.5, max = 50.0

Element prediction: Off

Number of isotope peaks used for i-FIT = 3

Monoisotopic Mass, Even Electron Ions

954 formula(e) evaluated with 2 results within limits (all results (up to 1000) for each mass)

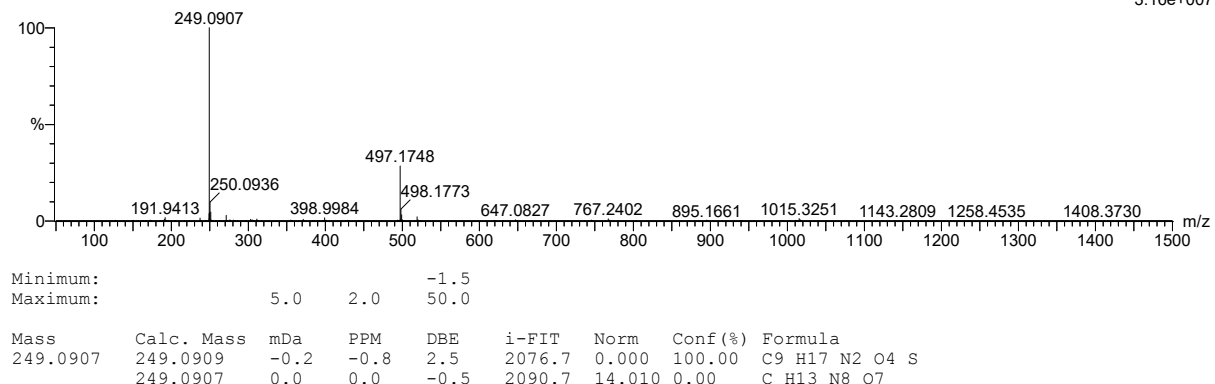
Elements Used:

C: 0-500 H: 0-1000 N: 0-50 O: 0-100 S: 0-3

2018-50esi 361 (3.351) AM2 (Ar,35000.0,0.00,0.00); Cm (361:371)

1: TOF MS ES+

3.16e+007



Minimum: -1.5
Maximum: 5.0 2.0 50.0

Mass	Calc. Mass	mDa	PPM	DBE	i-FIT	Norm	Conf (%)	Formula
249.0907	249.0909	-0.2	-0.8	2.5	2076.7	0.000	100.00	C ₉ H ₁₇ N ₂ O ₄ S
249.0907	0.0	0.0	-0.5	2090.7	14.010	0.00	0.00	C ₁₃ H ₁₃ N ₈ O ₇

HRMS Negative mode spectrum of 5f

Elemental Composition Report

Page 1

Single Mass Analysis

Tolerance = 2.0 PPM / DBE: min = -1.5, max = 50.0

Element prediction: Off

Number of isotope peaks used for i-FIT = 3

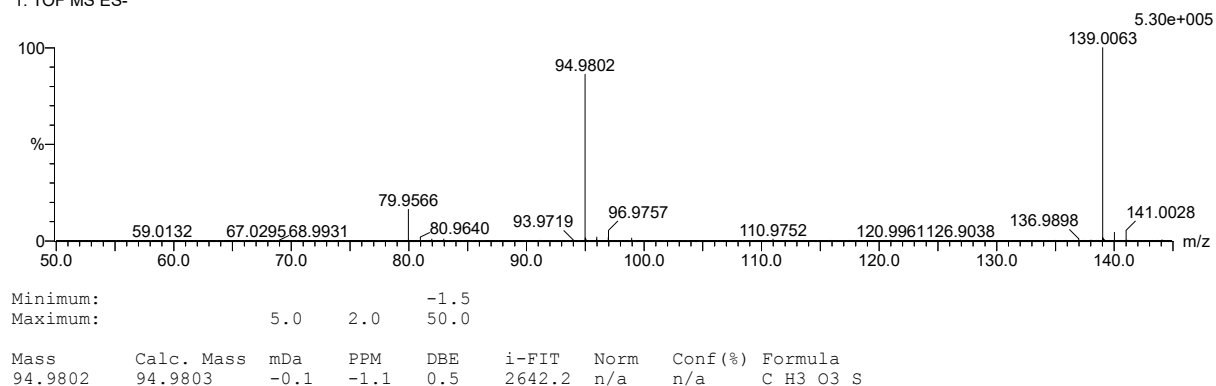
Monoisotopic Mass, Even Electron Ions

67 formula(e) evaluated with 1 results within limits (all results (up to 1000) for each mass)

Elements Used:

C: 0-500 H: 0-1000 N: 0-50 O: 0-100 S: 0-3
2018-50esineg 41 (0.829) AM2 (Ar,35000.0,0.00,0.00); Cm (38:43)

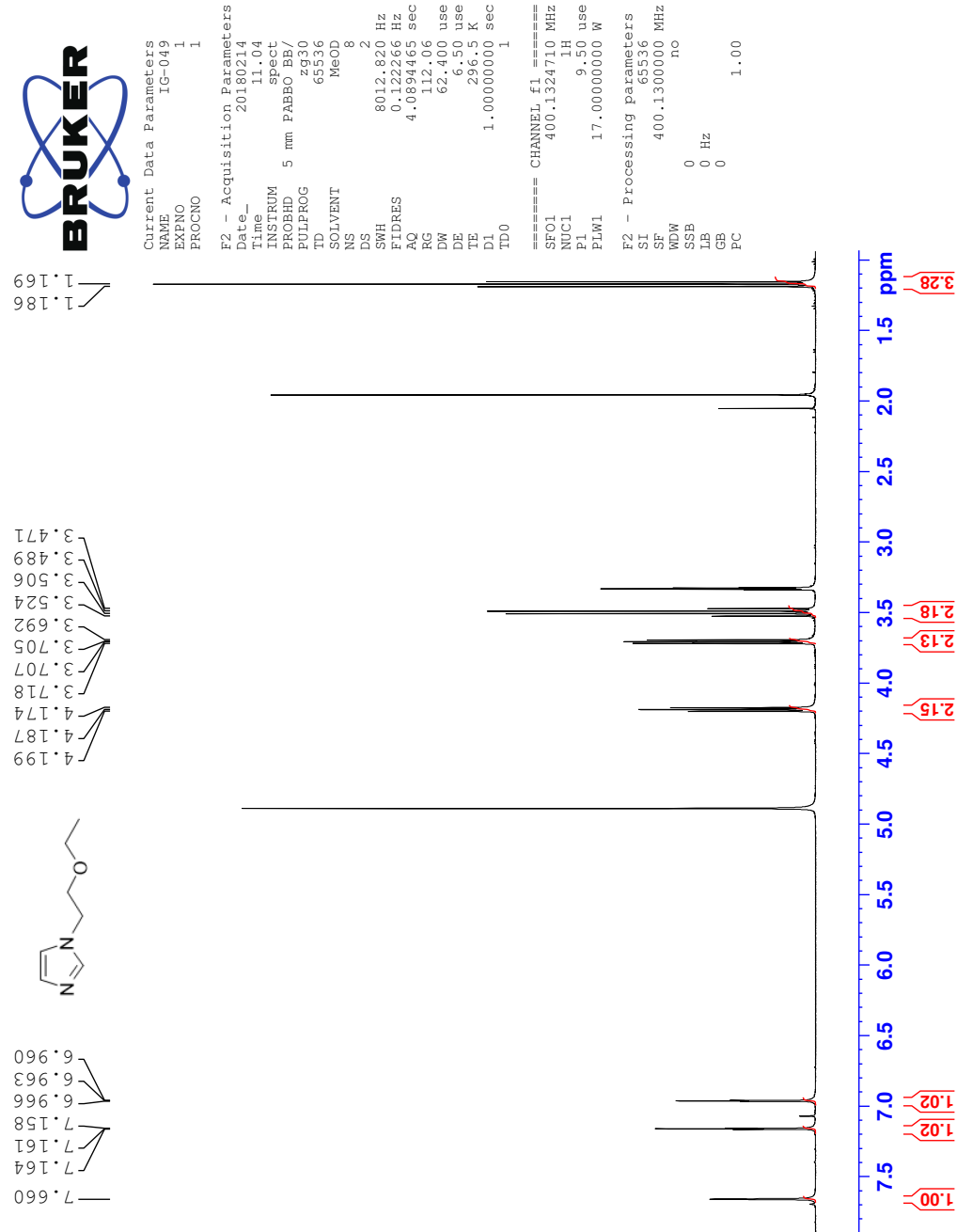
1: TOF MS ES-



LV

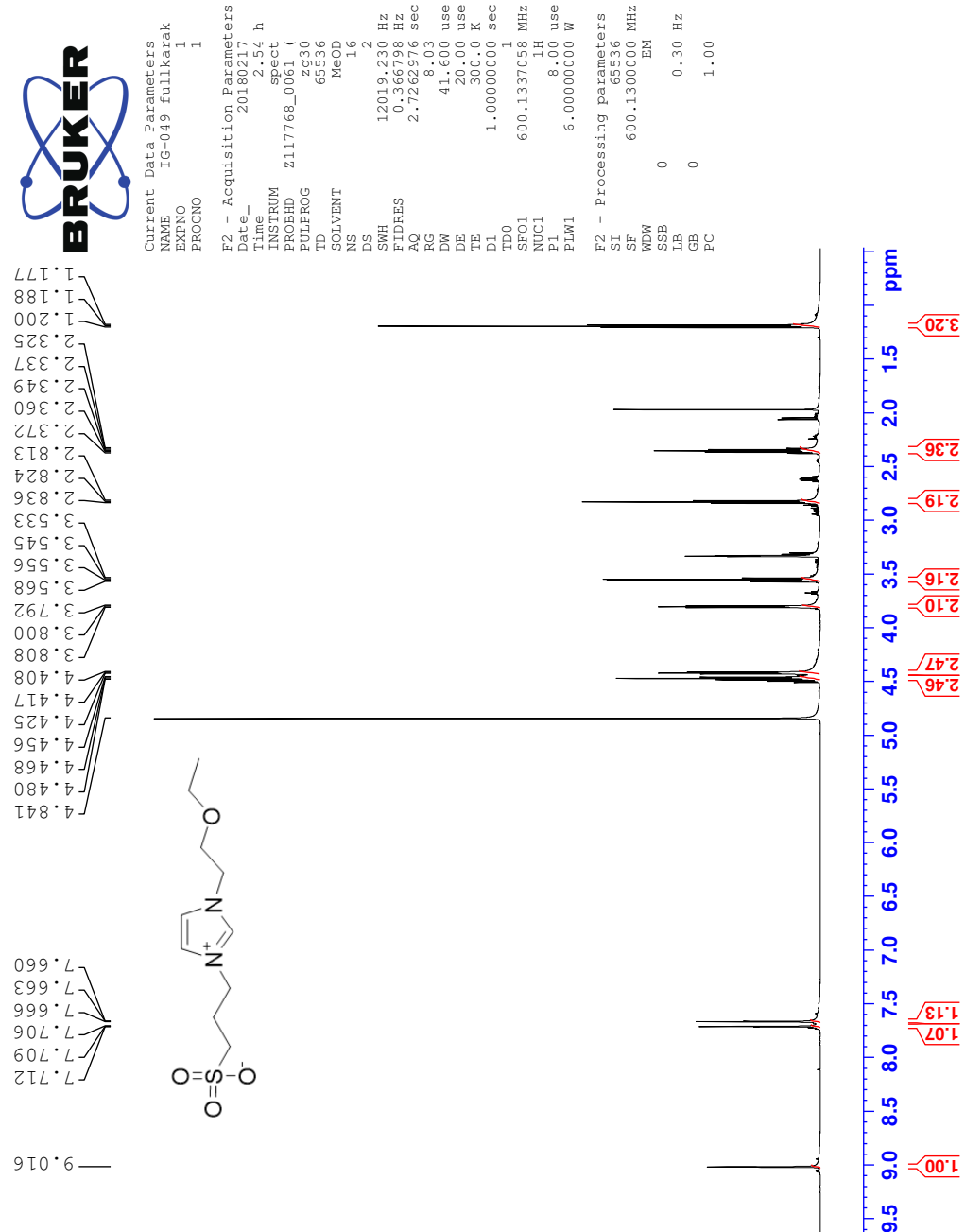
M Spectrum of 1-(2-ethoxyethyl)-imidazole (6a)

¹H NMR Spectrum of 6a

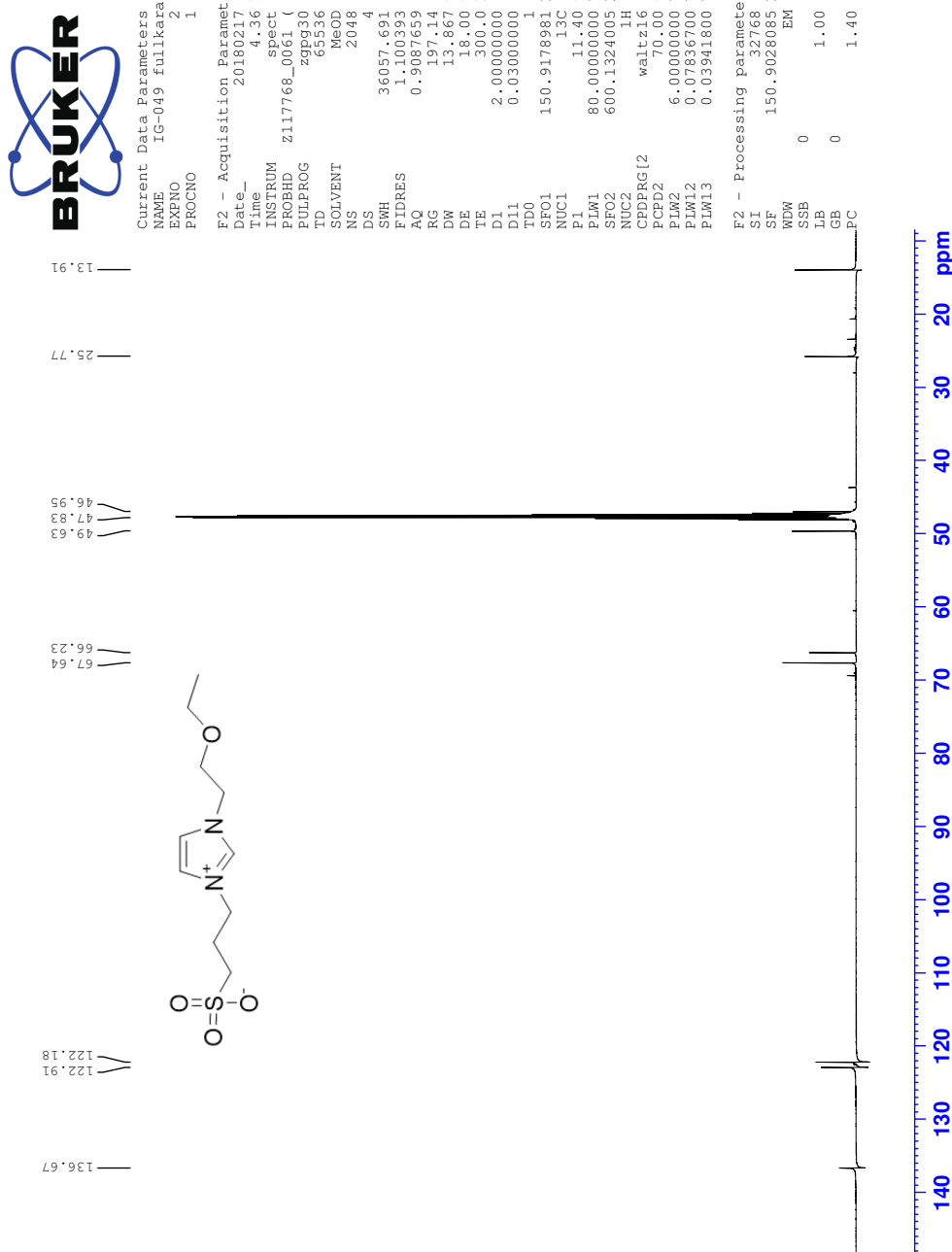


N Spectra of 3-(1-(2-ethoxyethyl)-imidazol-3-ium-3-yl)-propane-1-sulfonate (6b)

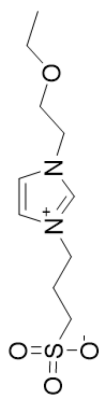
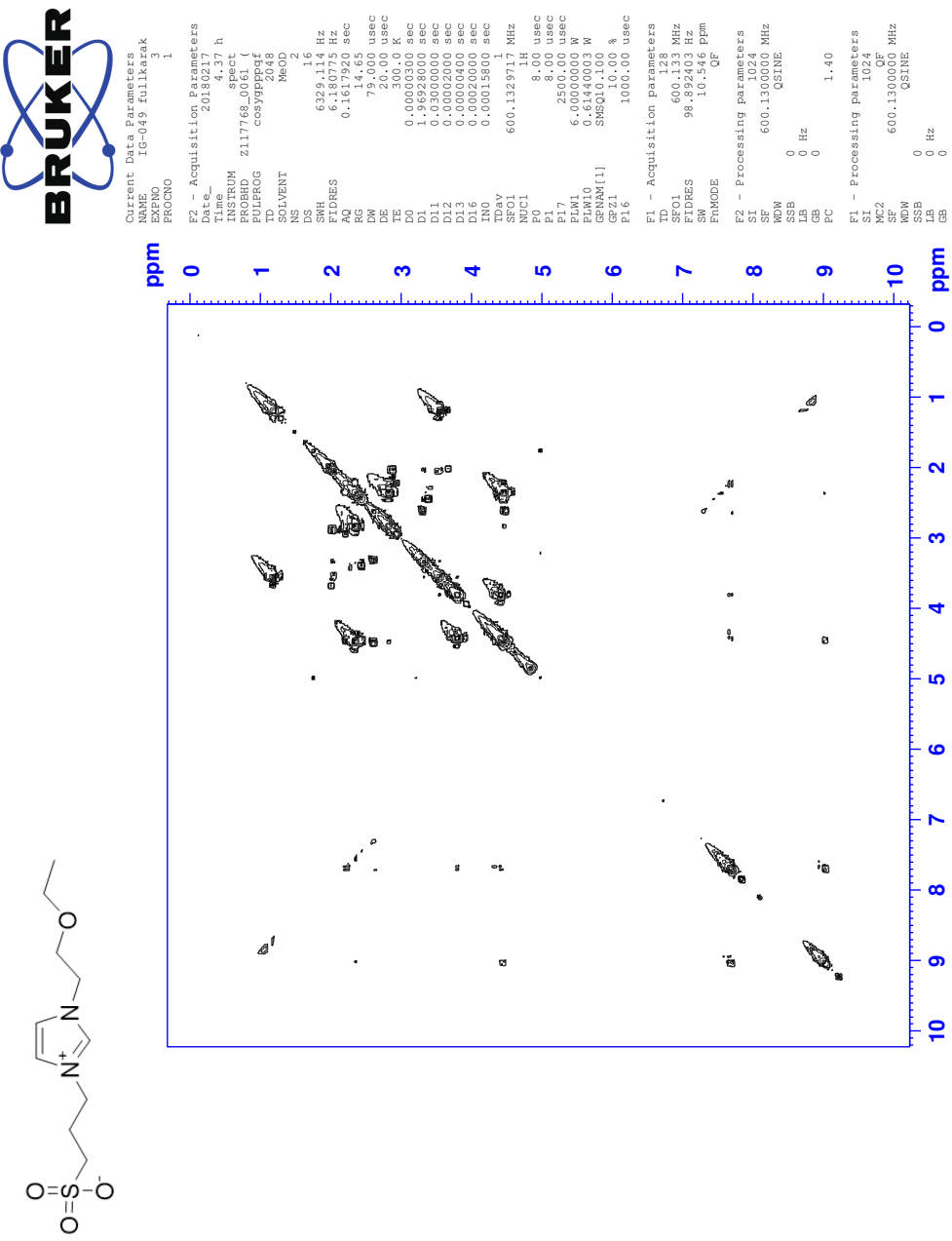
¹H NMR Spectrum of 6b



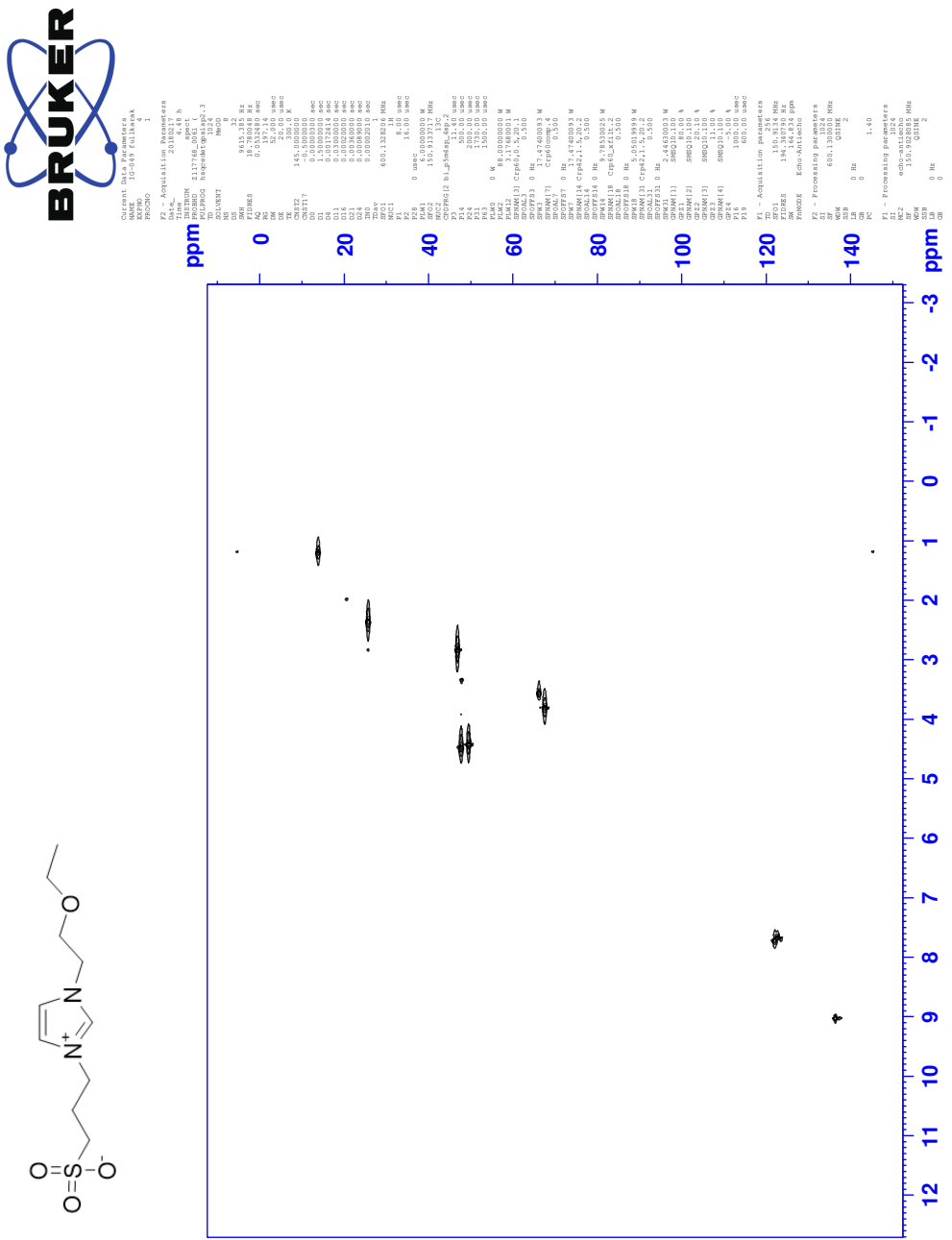
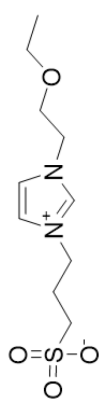
¹³C NMR Spectrum of 6b



COSY NMR Spectrum of 6b

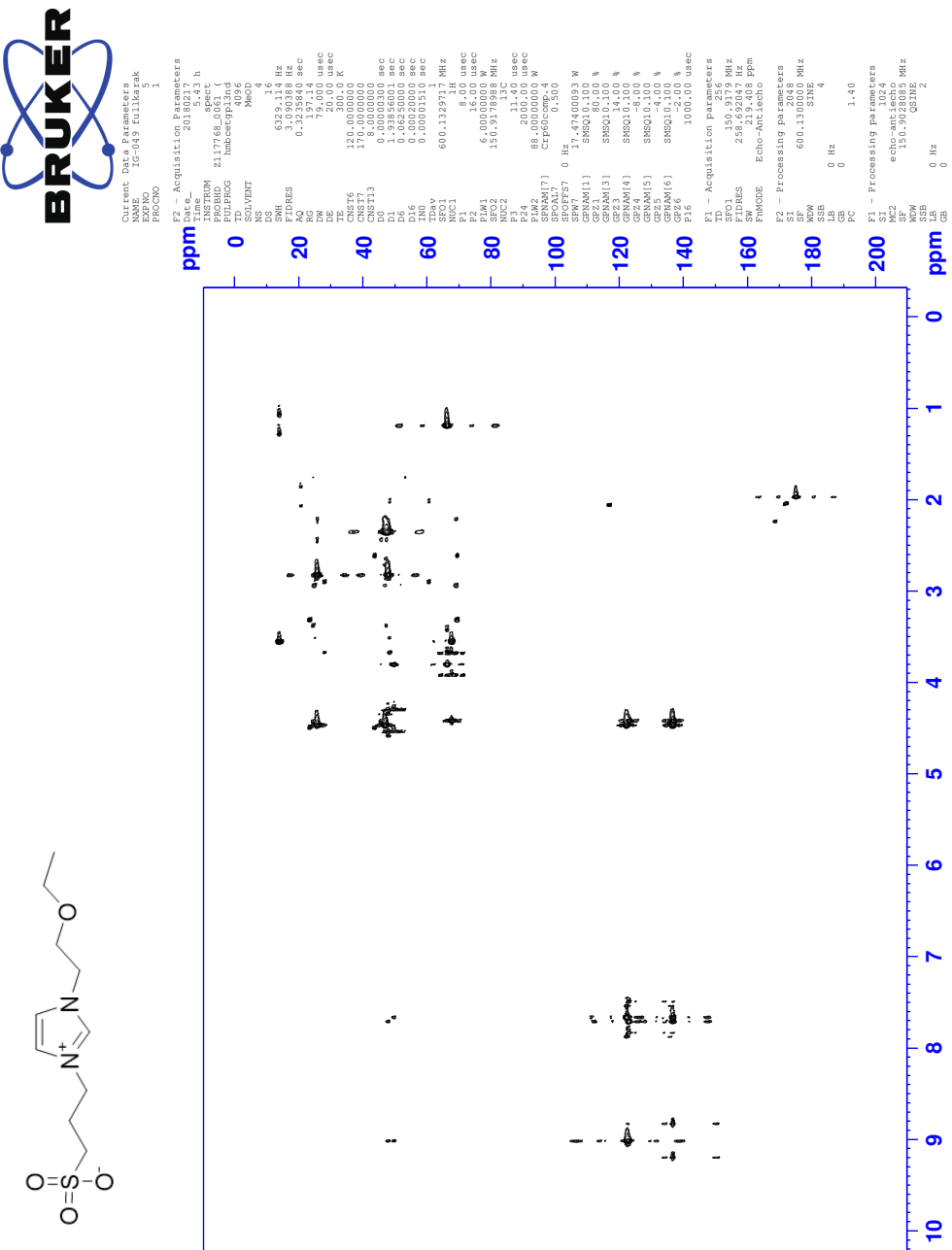


HSQC NMR Spectrum of 6b

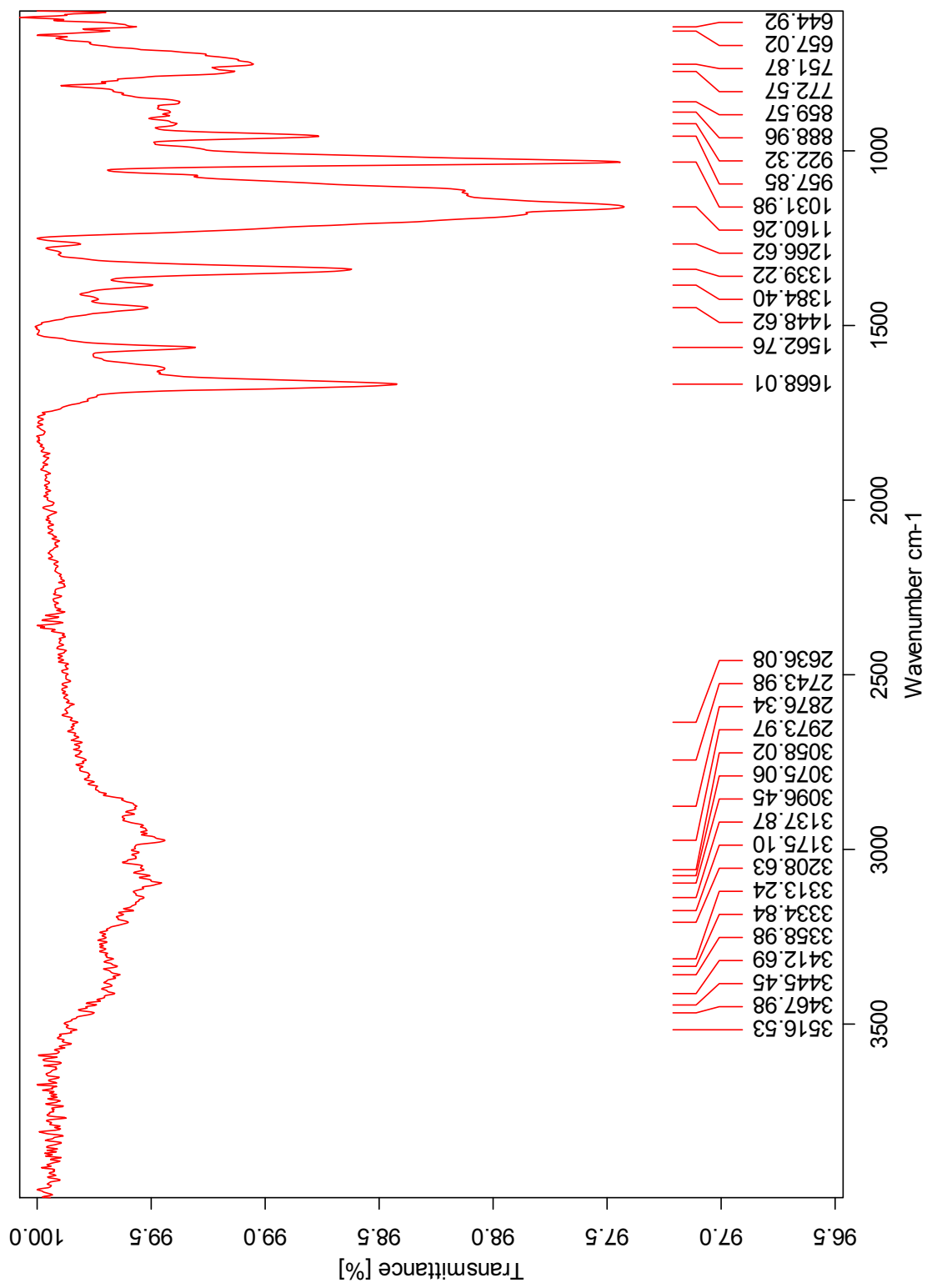


LX

HMBC NMR Spectrum of 6b



IR Spectrum of 6b



HRMS Spectrum of 6b

Elemental Composition Report

Page 1

Single Mass Analysis

Tolerance = 4.0 PPM / DBE: min = -1.5, max = 50.0

Element prediction: Off

Number of isotope peaks used for i-FIT = 3

Monoisotopic Mass, Even Electron Ions

1034 formula(e) evaluated with 2 results within limits (all results (up to 1000) for each mass)

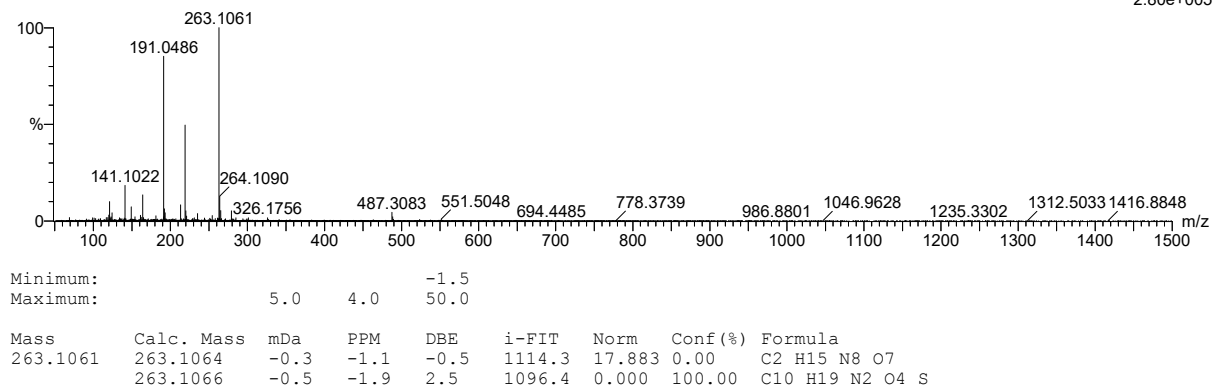
Elements Used:

C: 2-500 H: 0-1000 N: 0-100 O: 0-100 S: 0-3

2018-43 422 (8.202) AM2 (Ar,35000.0,0.00,0.00); Cm (412:432)

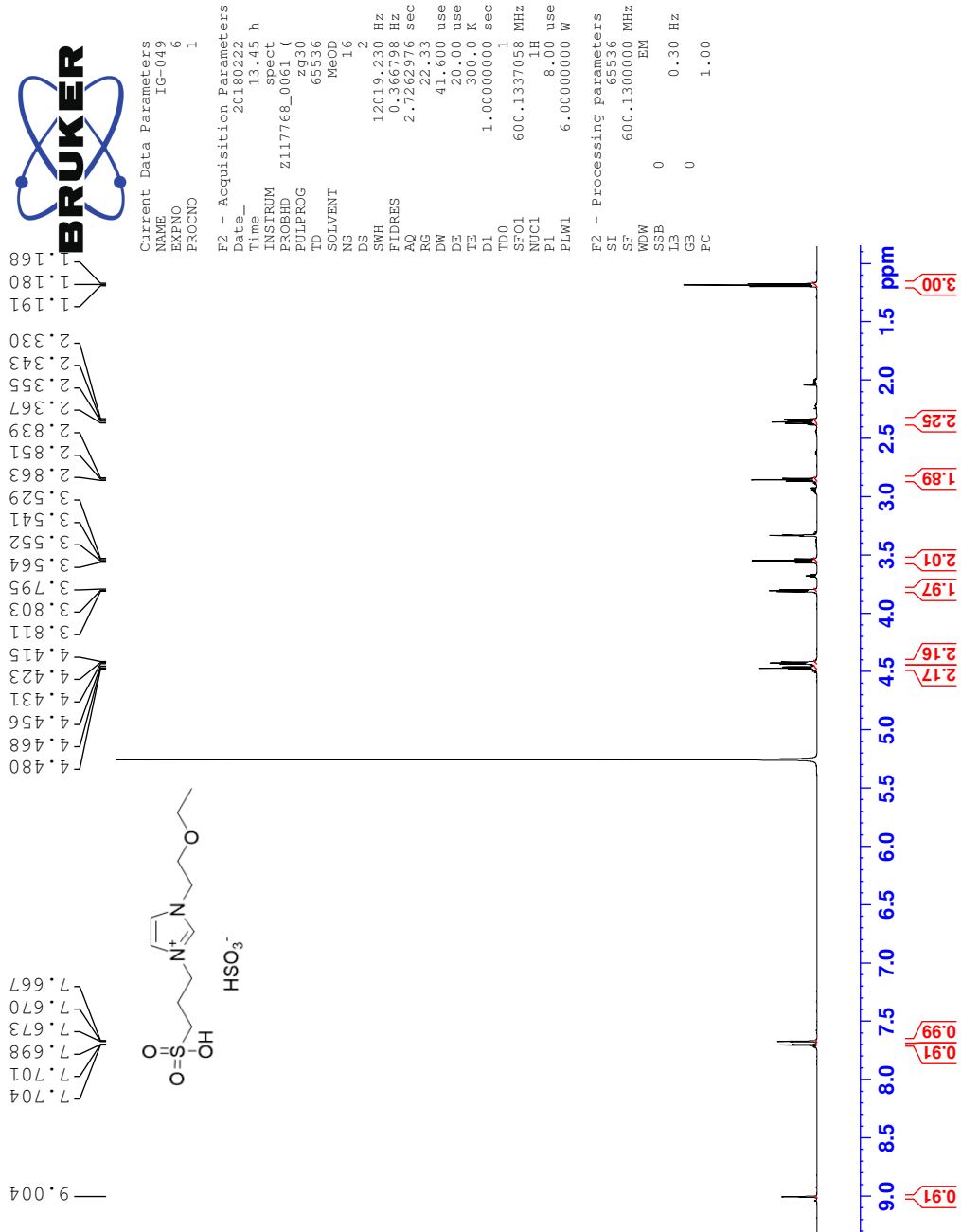
1: TOF MS ASAP+

2.80e+005

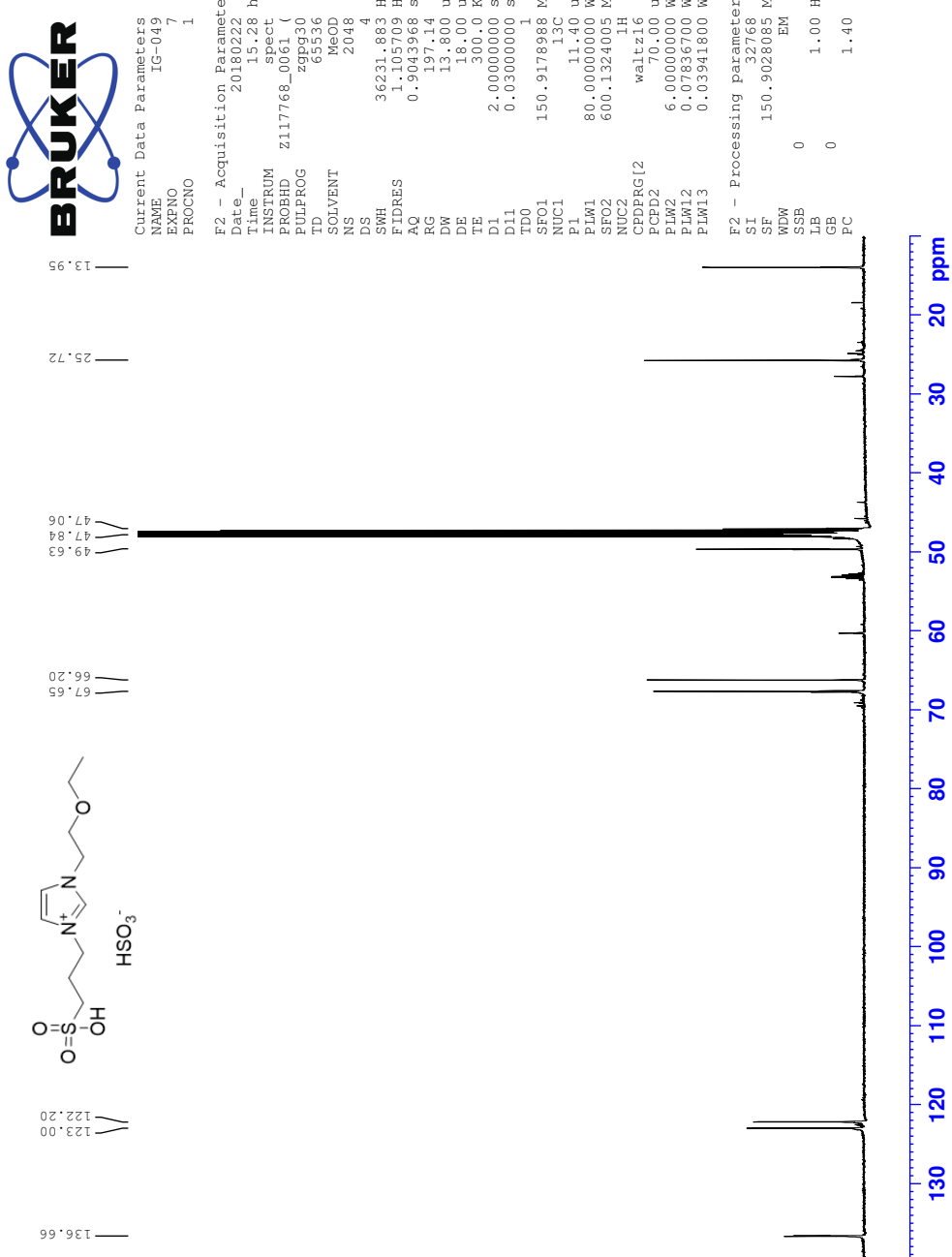


O Spectra of 1-(2-ethoxyethyl)-3-(3-sulfopropyl)-1H-imidazol-3-ium hydrogen sulfate (6c)

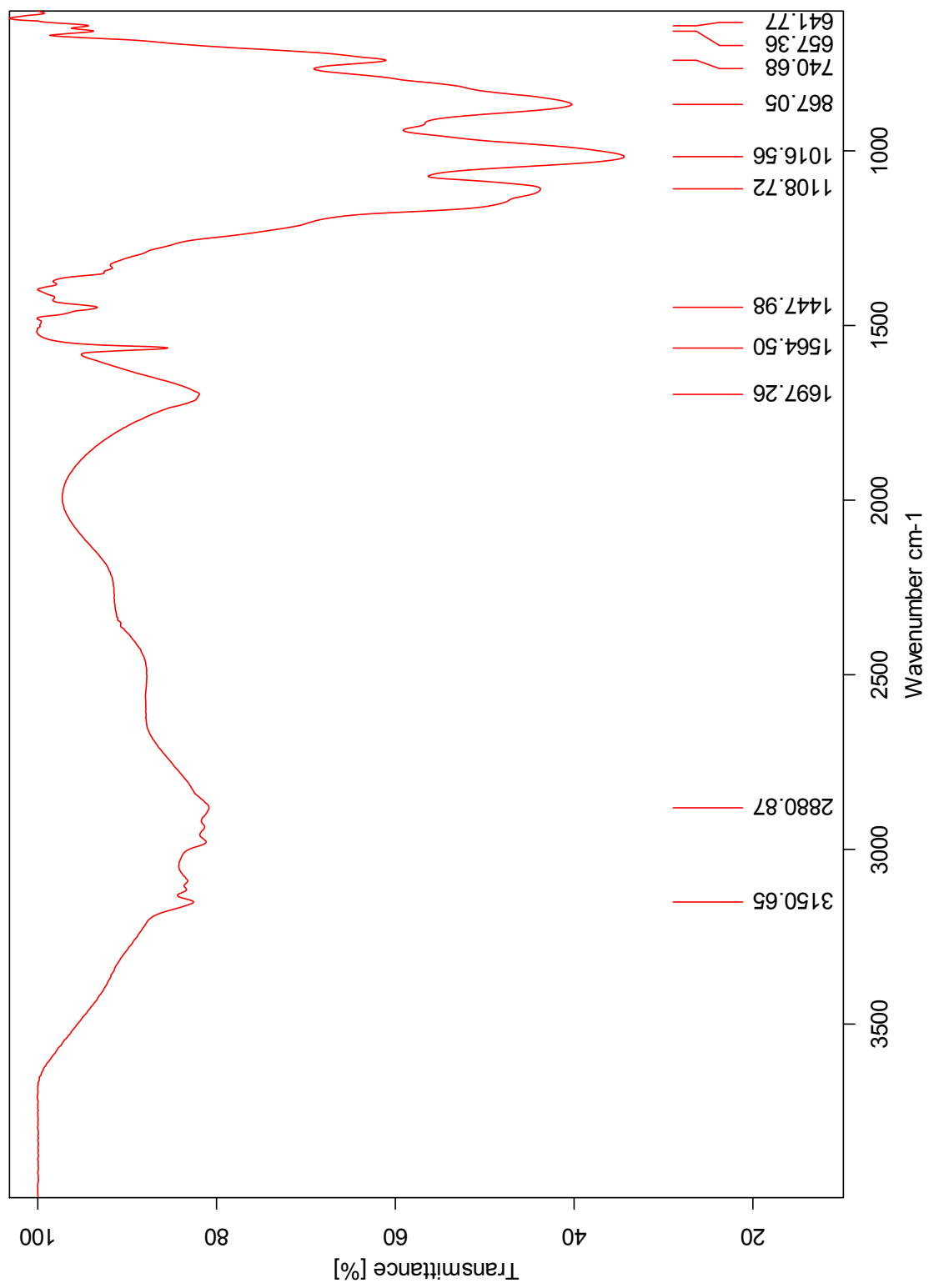
^1H NMR Spectrum of 6c



¹³C NMR Spectrum of 6c



IR Spectrum of 6c



HRMS Positive mode spectrum of 6c

Elemental Composition Report

Page 1

Single Mass Analysis

Tolerance = 3.0 PPM / DBE: min = -1.5, max = 50.0

Element prediction: Off

Number of isotope peaks used for i-FIT = 3

Monoisotopic Mass, Even Electron Ions

1138 formula(e) evaluated with 2 results within limits (all results (up to 1000) for each mass)

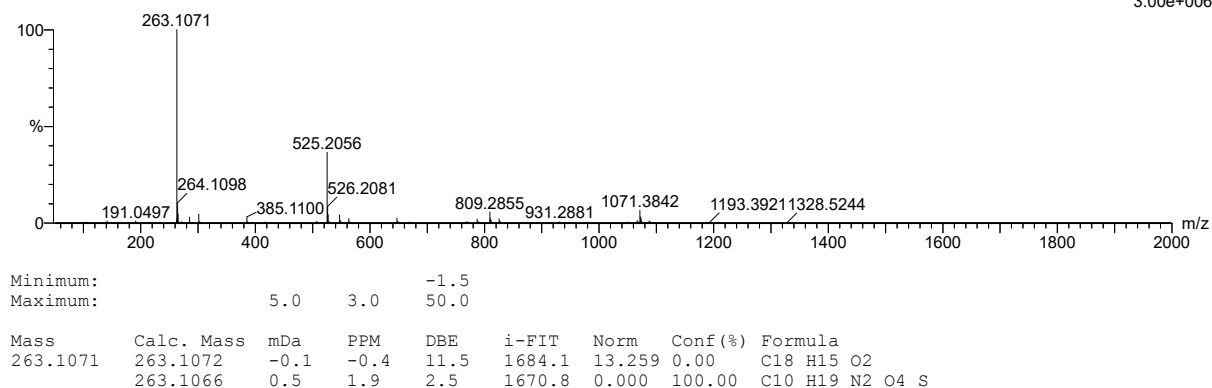
Elements Used:

C: 2-500 H: 0-1000 N: 0-5 O: 0-100 Na: 0-1 S: 0-3

SVG_20180226_ESI_POS_MSE_FIA_2018_53 82 (1.528) AM2 (Ar,35000.0,0.00,0.00); Cm (80:82)

1: TOF MS ES+

3.00e+006



HRMS Negative mode spectrum of 6c

Elemental Composition Report

Page 1

Single Mass Analysis

Tolerance = 100.0 PPM / DBE: min = -1.5, max = 50.0

Element prediction: Off

Number of isotope peaks used for i-FIT = 3

Monoisotopic Mass, Even Electron Ions

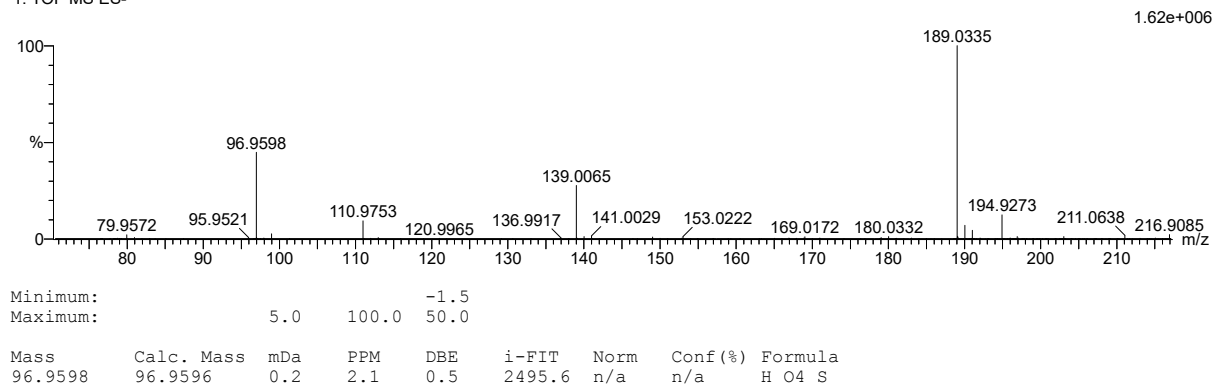
22 formula(e) evaluated with 1 results within limits (all results (up to 1000) for each mass)

Elements Used:

C: 0-500 H: 0-1000 O: 0-200 S: 0-6

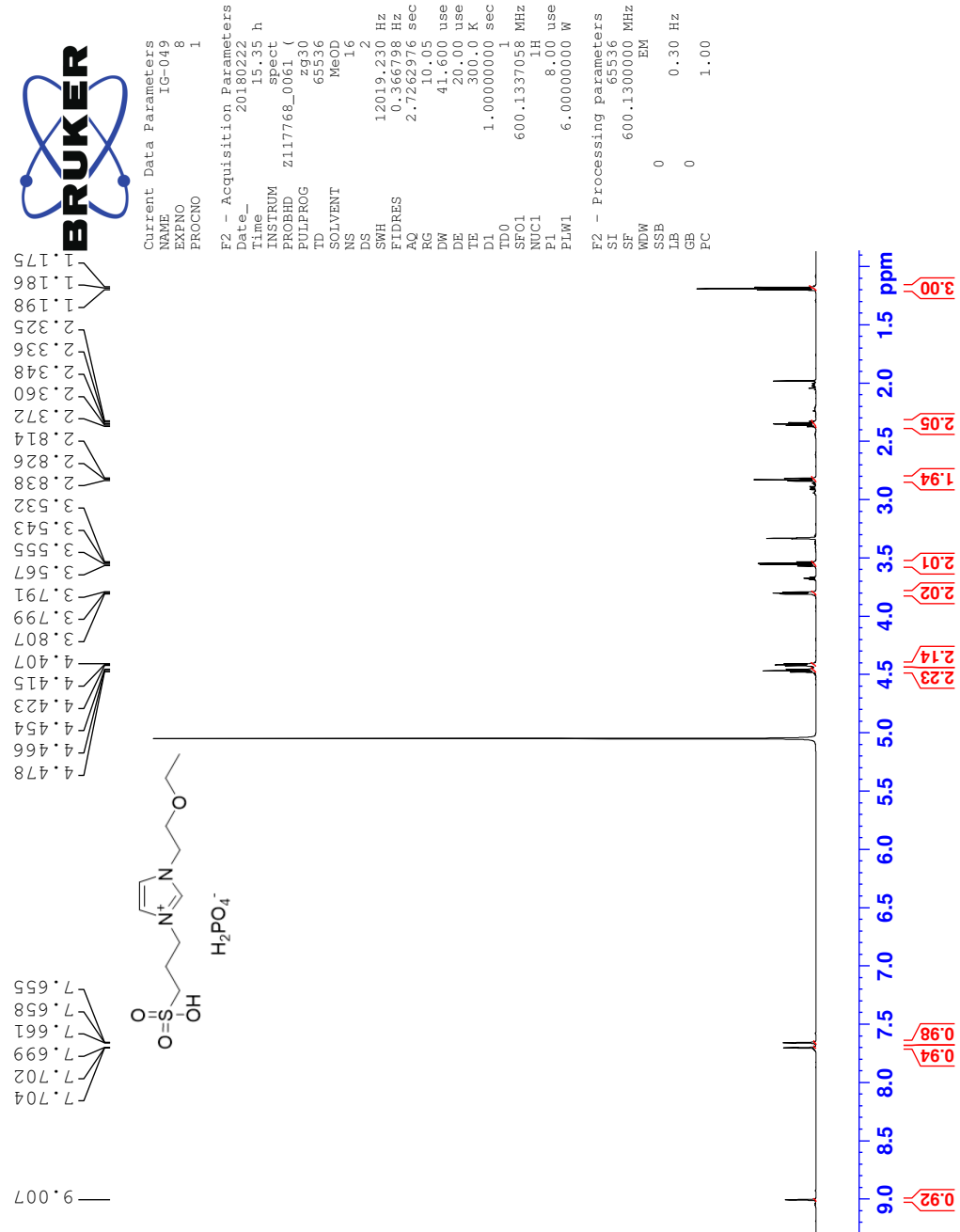
2018-53negb 41 (0.829) AM2 (Ar,35000.0,0.00,0.00); Cm (38:41)

1: TOF MS ES-

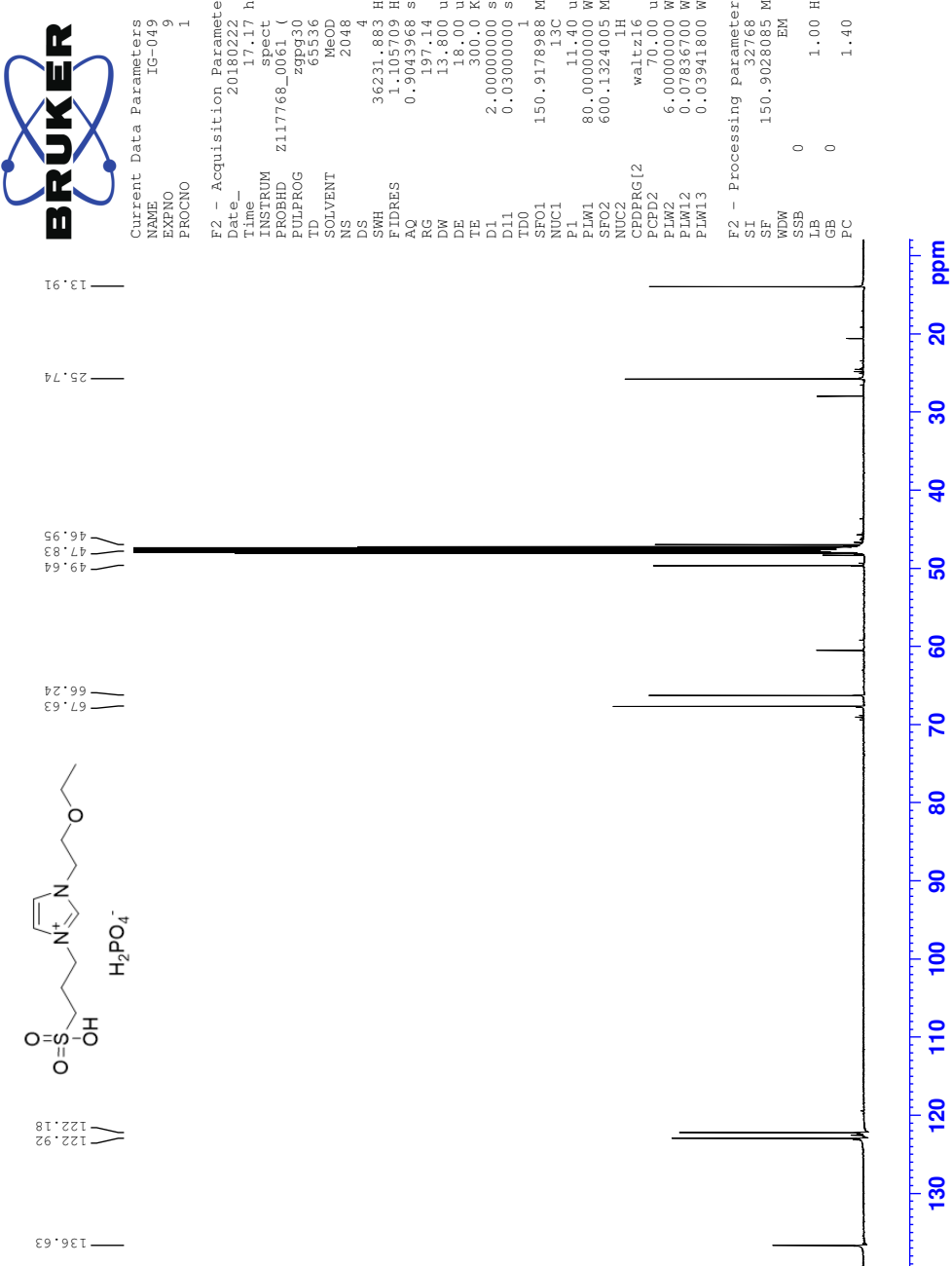


P Spectra of 1-(2-ethoxyethyl)-3-(3-sulfopropyl)-1H-imidazol-3-ium dihydrogen phosphate (6d)

¹H NMR Spectrum of 6d

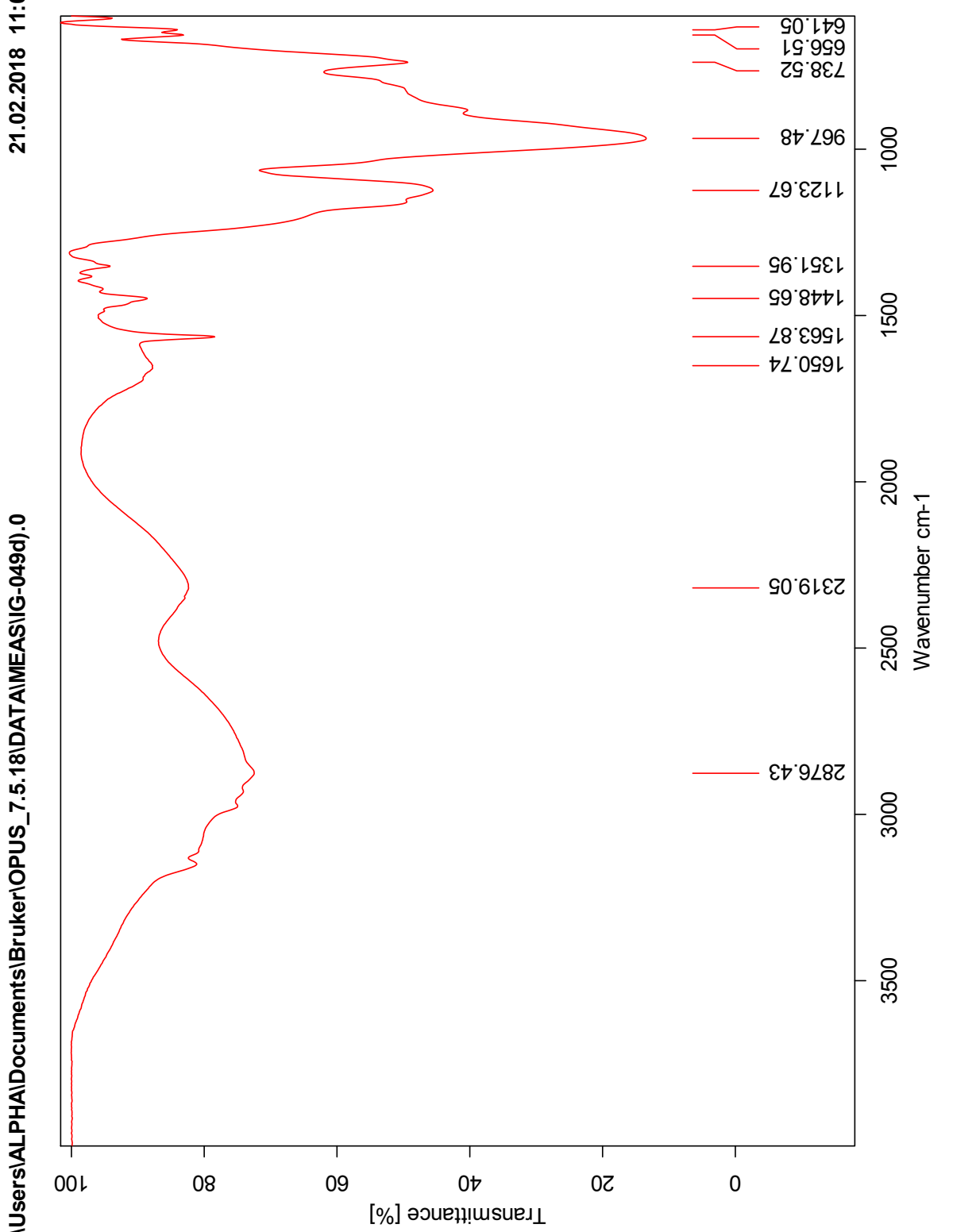


¹³C NMR Spectrum of 6d



IR Spectrum of 6d

C:\Users\ALPHA\Documents\Bruker\OPUS_7.5.18\DATA\MEAS\IG-049d).0



HRMS Positive mode spectrum of 6d

Elemental Composition Report

Page 1

Single Mass Analysis

Tolerance = 3.0 PPM / DBE: min = -1.5, max = 50.0

Element prediction: Off

Number of isotope peaks used for i-FIT = 3

Monoisotopic Mass, Even Electron Ions

1138 formula(e) evaluated with 2 results within limits (all results (up to 1000) for each mass)

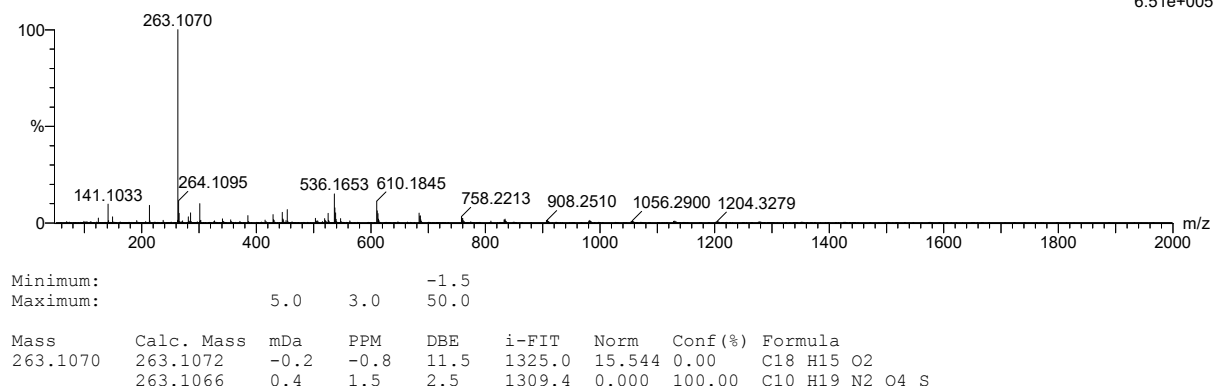
Elements Used:

C: 2-500 H: 0-1000 N: 0-5 O: 0-100 Na: 0-1 S: 0-3

SVG_20180226_ESI_POS_MSE_FIA_2018_54 51 (0.951) AM2 (Ar,35000.0,0.00,0.00); Cm (51:54)

1: TOF MS ES+

6.51e+005



Minimum: -1.5
Maximum: 5.0 3.0 50.0

Mass	Calc. Mass	mDa	PPM	DBE	i-FIT	Norm	Conf (%)	Formula
263.1070	263.1072	-0.2	-0.8	11.5	1325.0	15.544	0.00	C18 H15 O2
	263.1066	0.4	1.5	2.5	1309.4	0.000	100.00	C10 H19 N2 O4 S

HRMS Negative mode spectrum of 6d

Elemental Composition Report

Page 1

Single Mass Analysis

Tolerance = 10.0 PPM / DBE: min = -1.5, max = 50.0

Element prediction: Off

Number of isotope peaks used for i-FIT = 3

Monoisotopic Mass, Even Electron Ions

141 formula(e) evaluated with 1 results within limits (all results (up to 1000) for each mass)

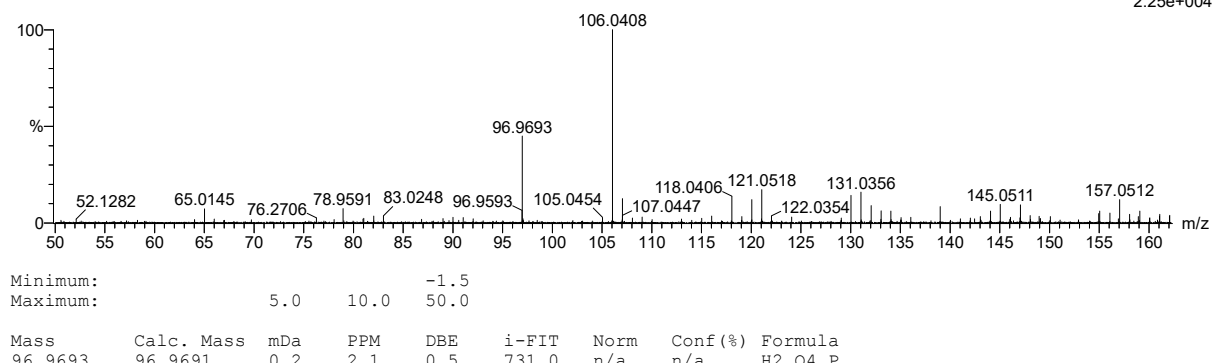
Elements Used:

C: 0-500 H: 0-1000 N: 0-5 O: 0-100 Na: 0-1 P: 0-1 S: 0-3

SVG_20180226_ESI_neg_MSE_FIA_2018_54 33 (0.620) AM2 (Ar,35000.0,0.00,0.00); Cm (32:33)

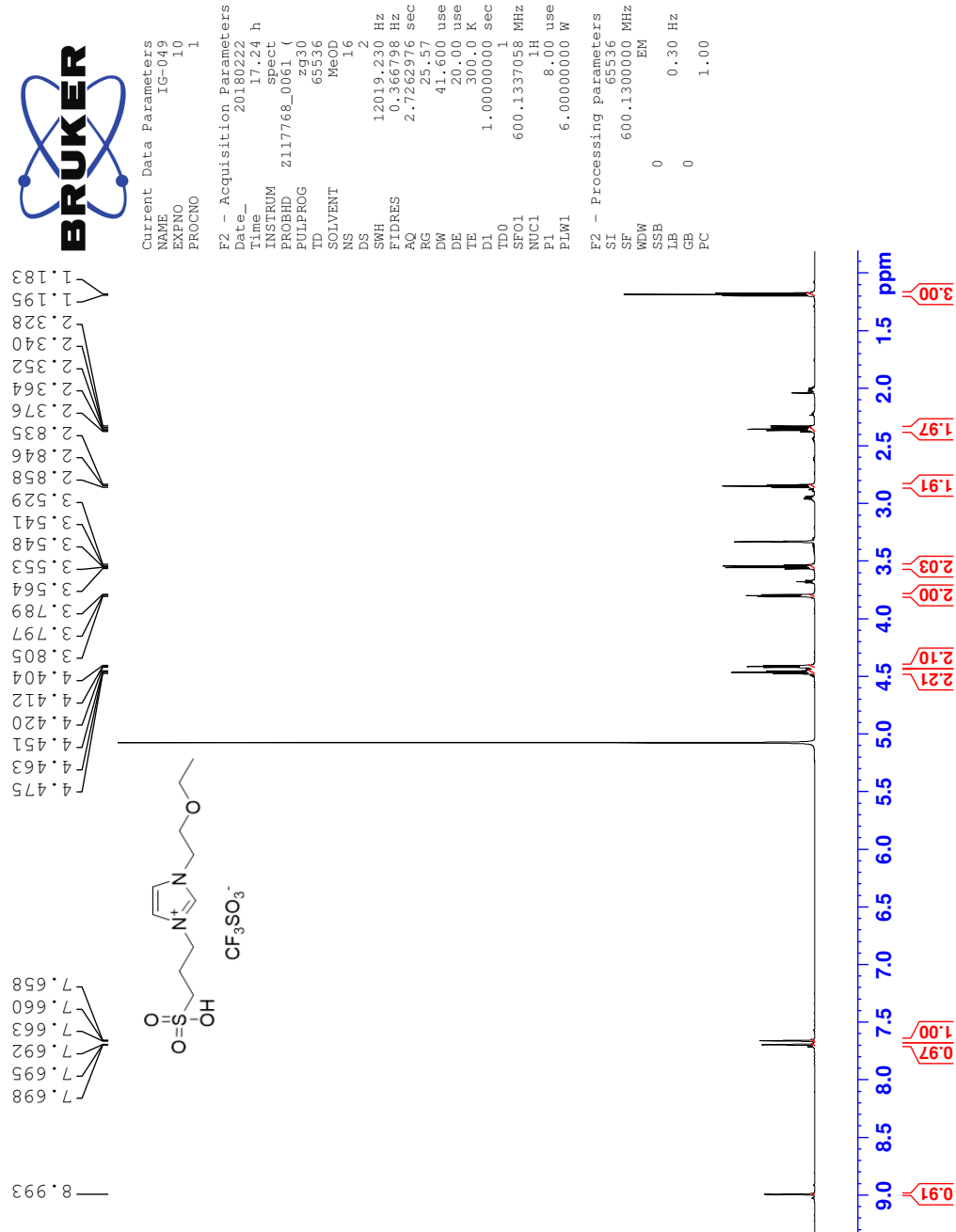
1: TOF MS ES-

2.25e+004



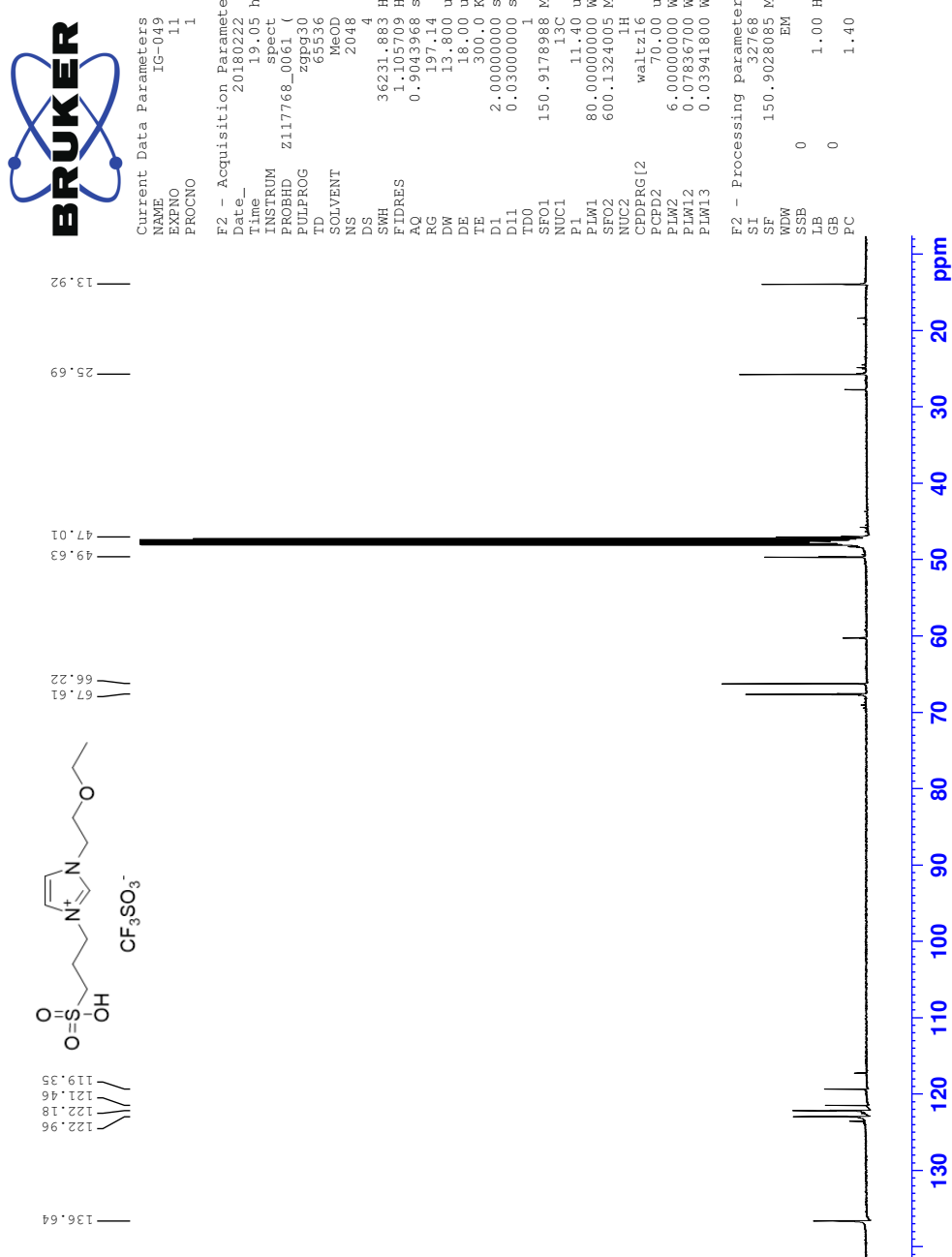
Q Spectra of 1-(2-ethoxyethyl)-3-(3-sulfopropyl)-1H-imidazol-3-ium trifluoromethanesulfonate (6e)

¹H NMR Spectrum of 6e

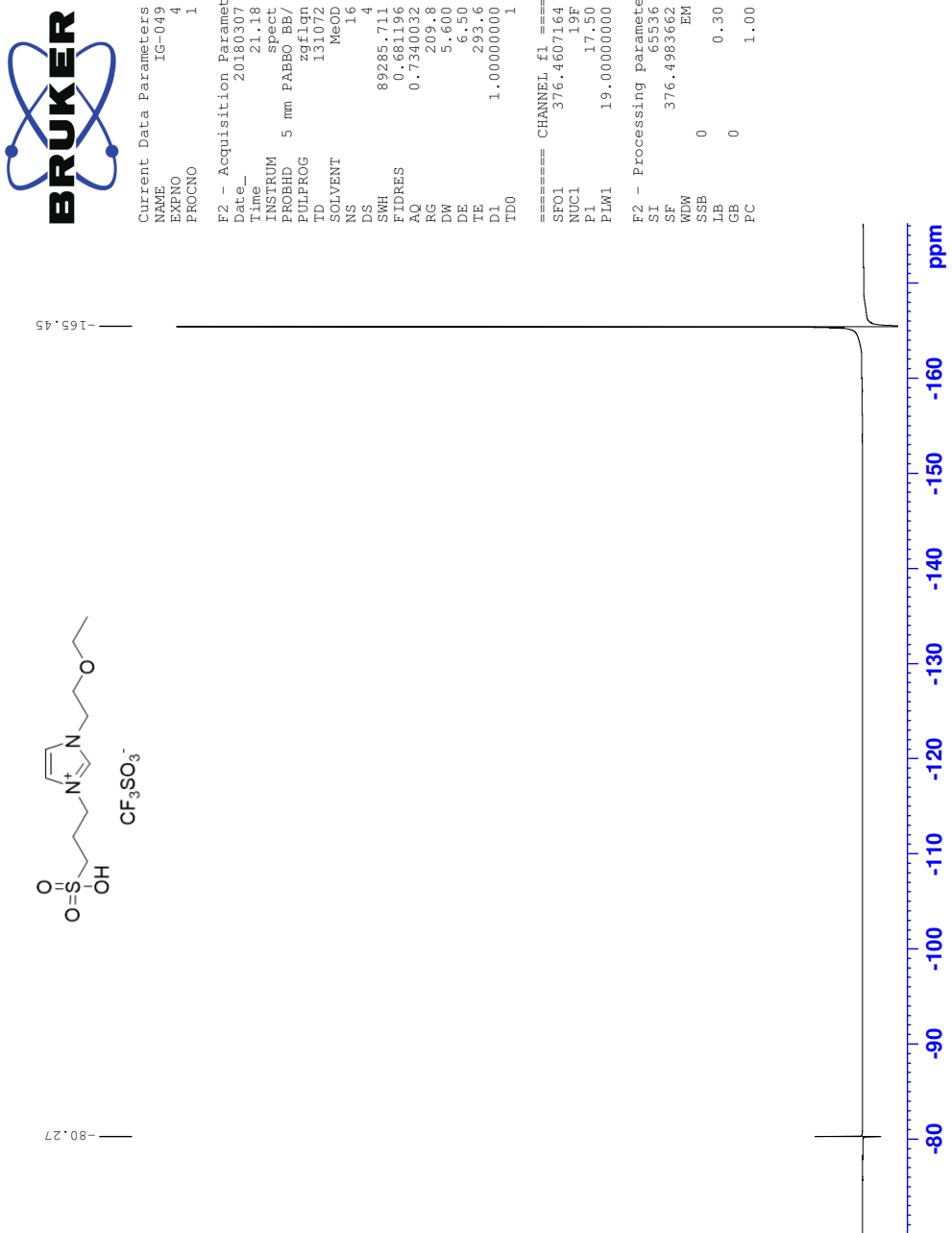


— 8.993 —

¹³C NMR Spectrum of 6e

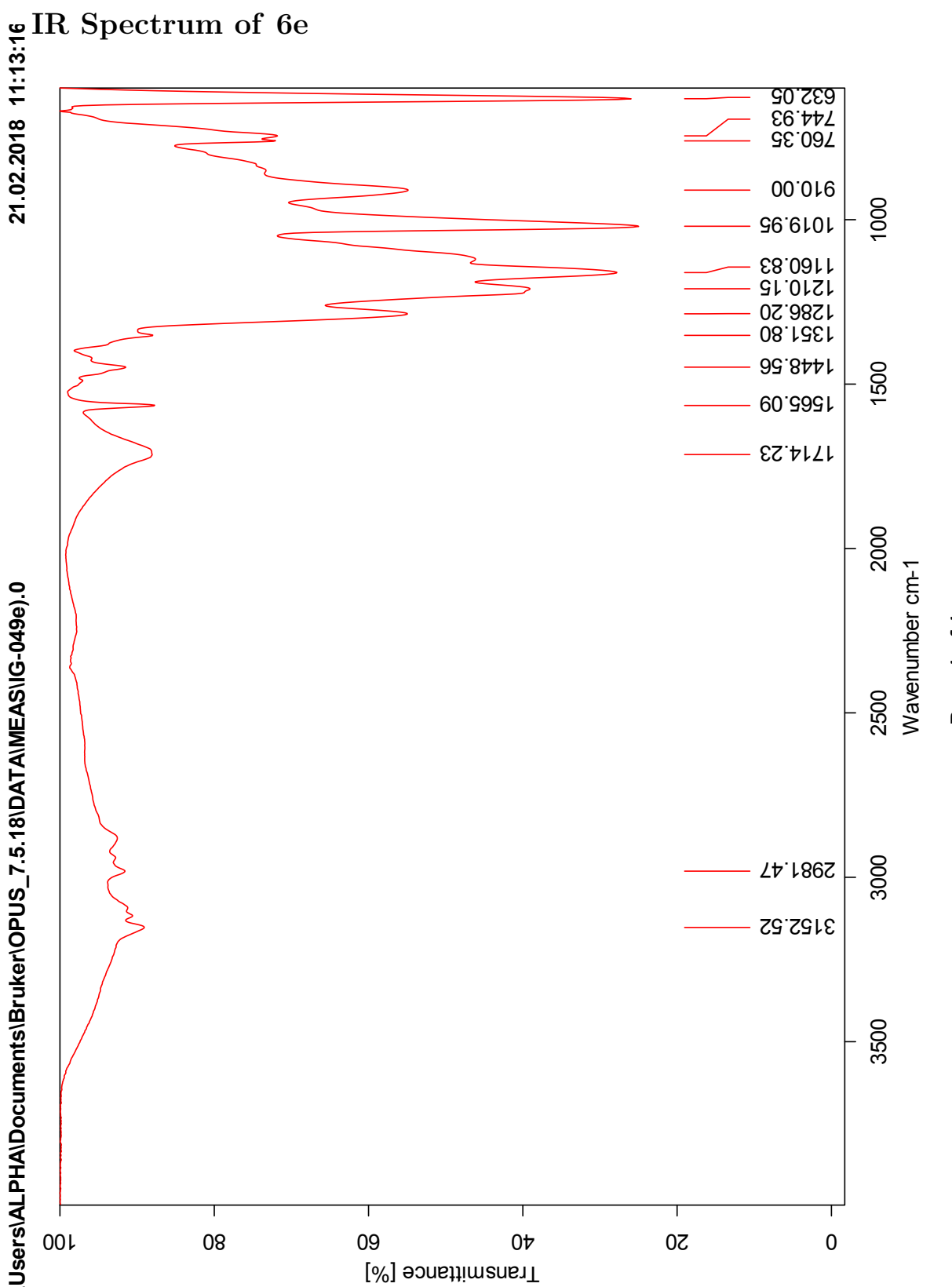


¹⁹F NMR Spectrum of 6e



IR Spectrum of 6e

C:\Users\ALPHA\Documents\Bruker\OPUS_7.5.18\DATA\MEAS\IG-049e.0



HRMS Positive mode spectrum of 6e

Elemental Composition Report

Page 1

Single Mass Analysis

Tolerance = 3.0 PPM / DBE: min = -1.5, max = 50.0

Element prediction: Off

Number of isotope peaks used for i-FIT = 3

Monoisotopic Mass, Even Electron Ions

1138 formula(e) evaluated with 2 results within limits (all results (up to 1000) for each mass)

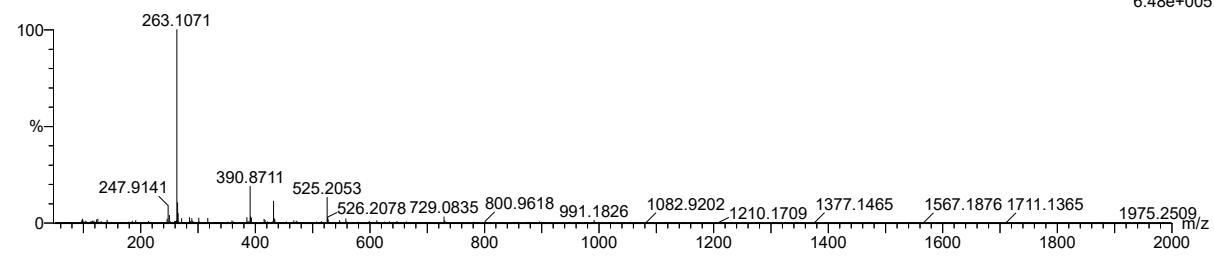
Elements Used:

C: 2-500 H: 0-1000 N: 0-5 O: 0-100 Na: 0-1 S: 0-3

SVG_20180226_ESI_POS_MSE_FIA_2018_55 83 (1.545) AM2 (Ar,35000.0,0.00,0.00); Cm (83:84)

1: TOF MS ES+

6.48e+005



Minimum: -1.5
Maximum: 5.0 3.0 50.0

Mass	Calc. Mass	mDa	PPM	DBE	i-FIT	Norm	Conf (%)	Formula
263.1071	263.1072	-0.1	-0.4	11.5	1345.6	13.792	0.00	C18 H15 O2
	263.1066	0.5	1.9	2.5	1331.8	0.000	100.00	C10 H19 N2 O4 S

HRMS Negative mode spectrum of 6e

Elemental Composition Report

Page 1

Single Mass Analysis

Tolerance = 3.0 PPM / DBE: min = -1.5, max = 50.0

Element prediction: Off

Number of isotope peaks used for i-FIT = 3

Monoisotopic Mass, Even Electron Ions

1192 formula(e) evaluated with 3 results within limits (all results (up to 1000) for each mass)

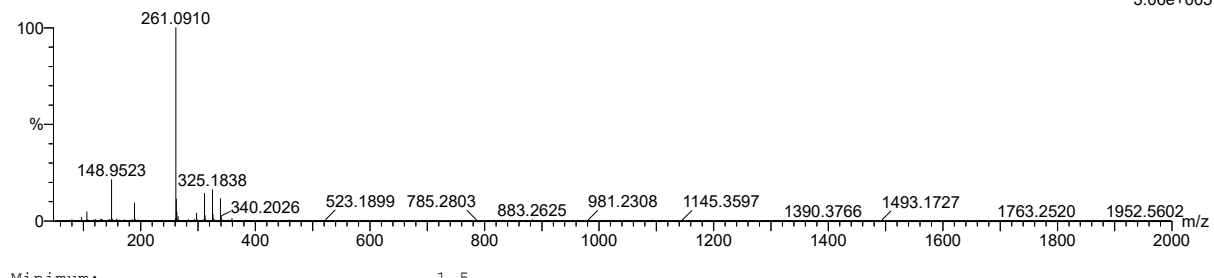
Elements Used:

C: 0-500 H: 0-1000 N: 0-5 O: 0-100 F: 0-6 Na: 0-1 P: 0-1 S: 0-3

SVG_20180226_ESI_neg_MSE_FIA_2018_55 27 (0.505) AM2 (Ar,35000.0,0.00,0.00); Cm (25:27)

1: TOF MS ES-

3.06e+005

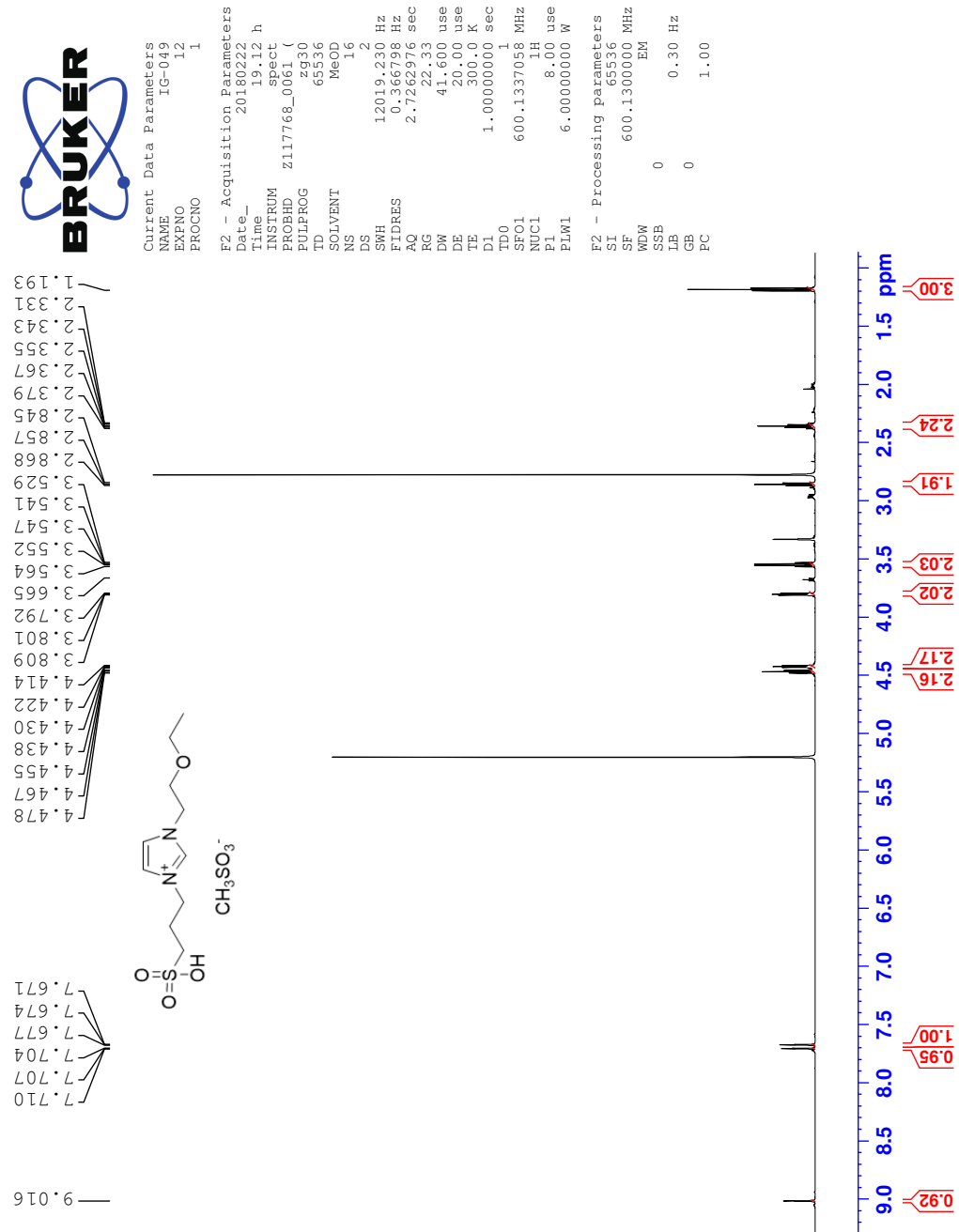


Minimum: -1.5
Maximum: 5.0 3.0 50.0

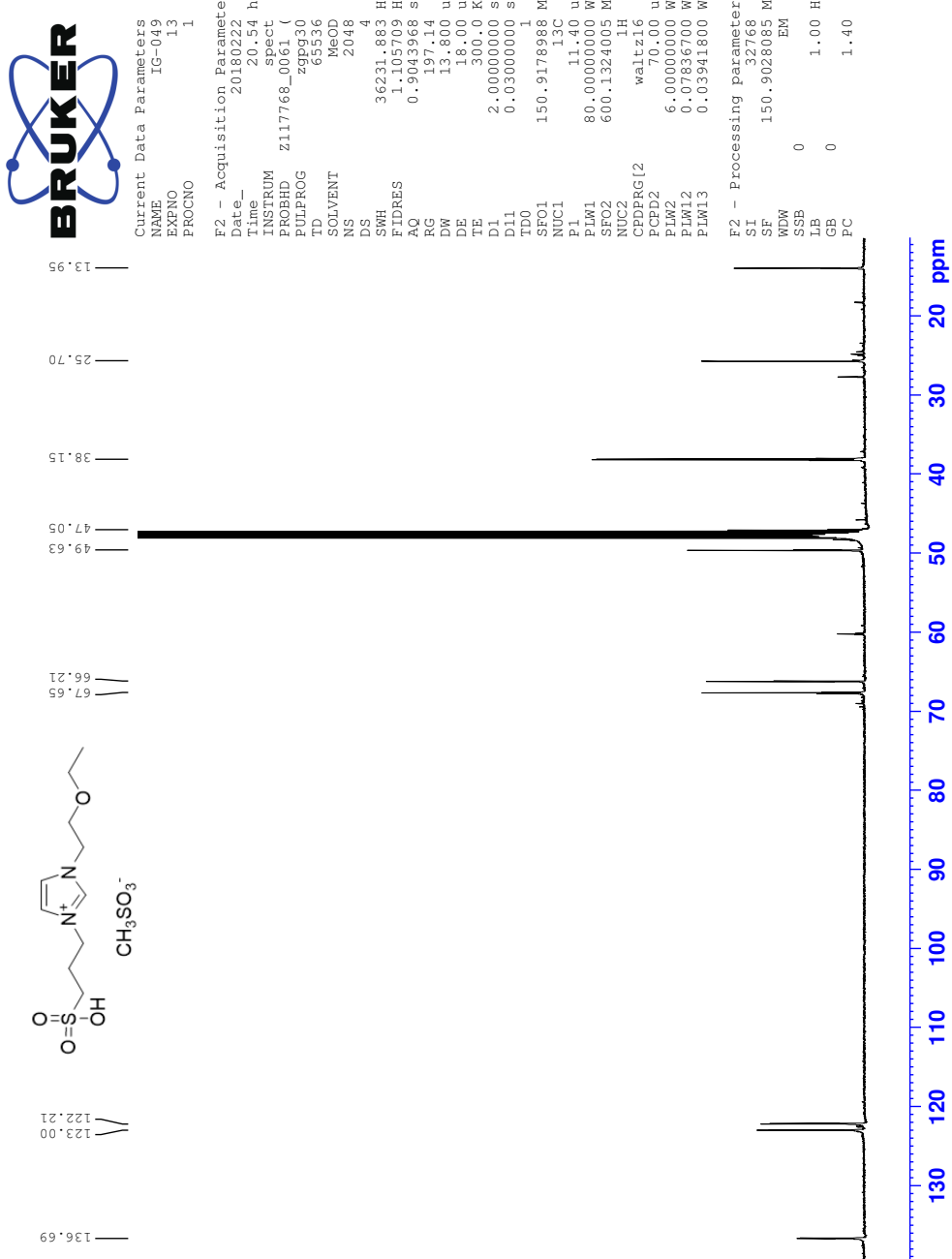
Mass	Calc. Mass	mDa	PPM	DBE	i-FIT	Norm	Conf (%)	Formula
148.9523	148.9521	0.2	1.3	0.5	860.7	2.803	6.06	C H2 O5 Na S
148.9520	148.9520	0.3	2.0	7.5	864.2	6.249	0.19	C7 H S2
148.9520	148.9520	0.3	2.0	0.5	858.0	0.065	93.75	C O3 F3 S

R Spectra of IL1-(2-ethoxyethyl)-3-(3-sulfopropyl)-1H-imidazol-3-ium methanesulfonate (6f)

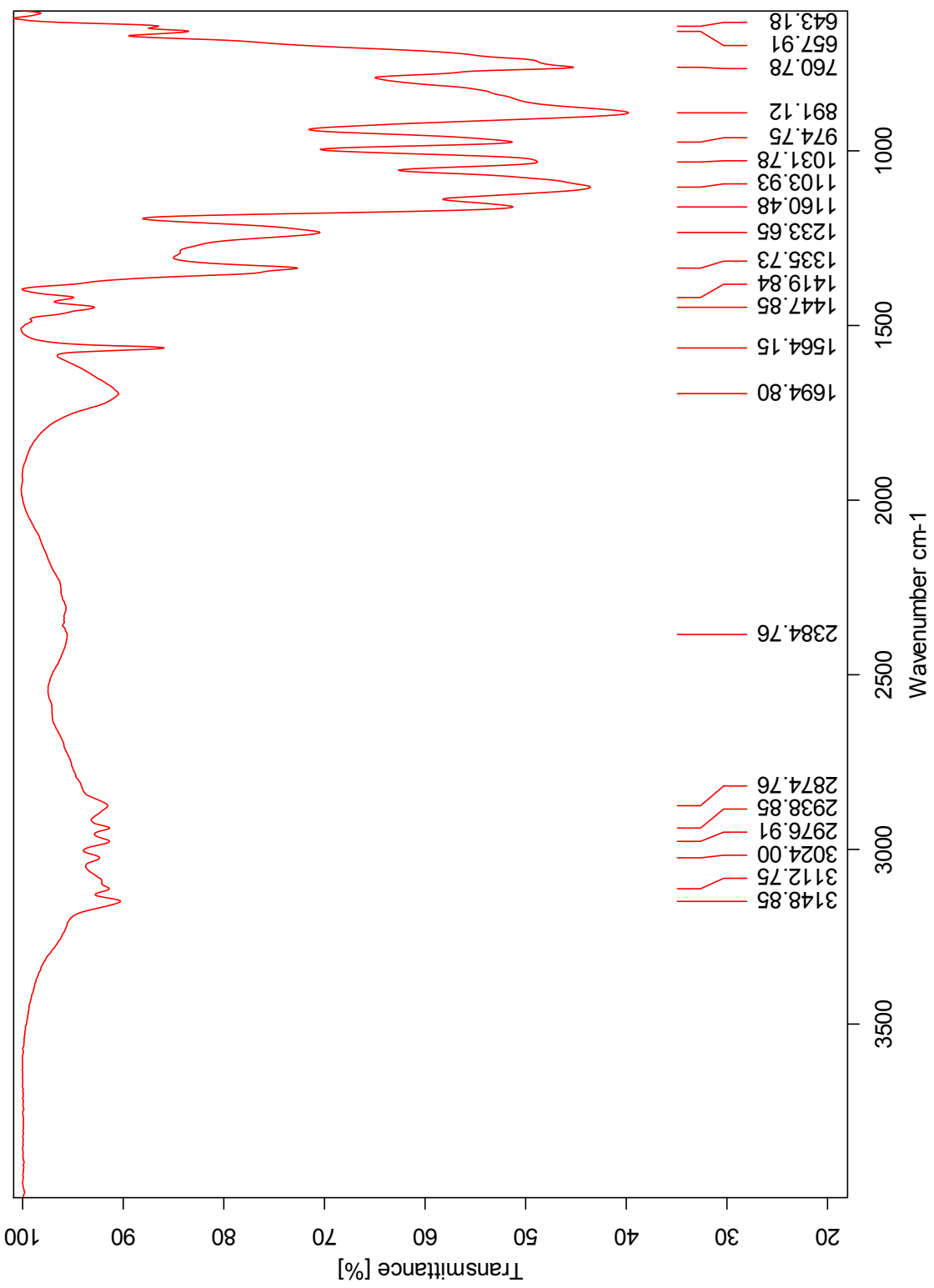
¹H NMR Spectrum of 6f



¹³C NMR Spectrum of 6f



IR Spectrum of 6f



HRMS Positive mode spectrum of 6f

Elemental Composition Report

Page 1

Single Mass Analysis

Tolerance = 3.0 PPM / DBE: min = -1.5, max = 50.0

Element prediction: Off

Number of isotope peaks used for i-FIT = 3

Monoisotopic Mass, Even Electron Ions

1138 formula(e) evaluated with 2 results within limits (all results (up to 1000) for each mass)

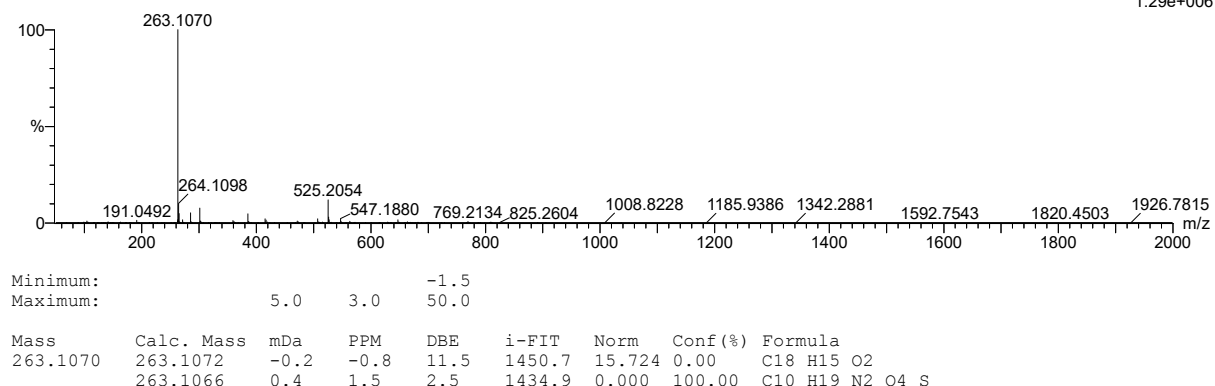
Elements Used:

C: 2-500 H: 0-1000 N: 0-5 O: 0-100 Na: 0-1 S: 0-3

SVG_20180226_ESI_POS_MSE_FIA_2018_56 86 (1.597) AM2 (Ar,35000.0,0.00,0.00); Cm (86:88)

1: TOF MS ES+

1.29e+006



Minimum: -1.5
Maximum: 5.0 3.0 50.0

Mass	Calc. Mass	mDa	PPM	DBE	i-FIT	Norm	Conf (%)	Formula
263.1070	263.1072	-0.2	-0.8	11.5	1450.7	15.724	0.00	C18 H15 O2
	263.1066	0.4	1.5	2.5	1434.9	0.000	100.00	C10 H19 N2 O4 S

HRMS Negative mode spectrum of 6f

Elemental Composition Report

Page 1

Single Mass Analysis

Tolerance = 3.0 PPM / DBE: min = -1.5, max = 50.0

Element prediction: Off

Number of isotope peaks used for i-FIT = 3

Monoisotopic Mass, Even Electron Ions

236 formula(e) evaluated with 1 results within limits (all results (up to 1000) for each mass)

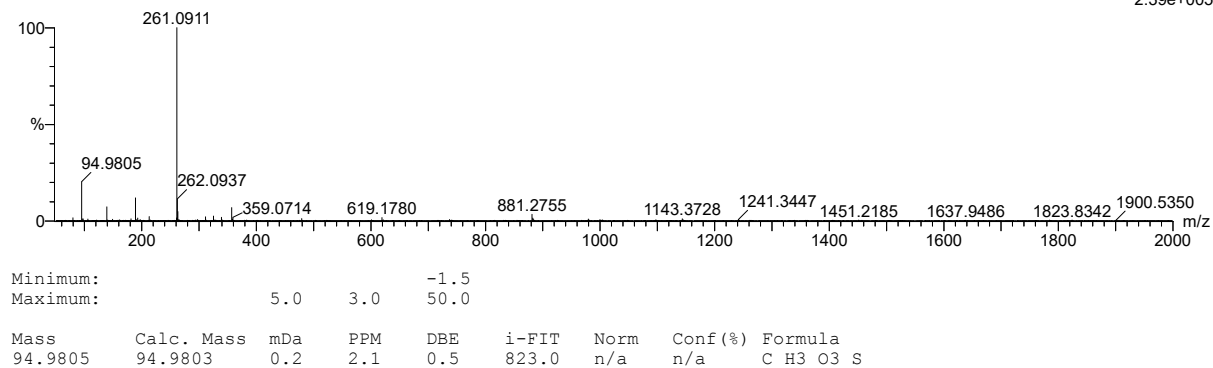
Elements Used:

C: 0-500 H: 0-1000 N: 0-5 O: 0-100 F: 0-6 Na: 0-1 P: 0-1 S: 0-3

SVG_20180226_ESI_neg_MSE_FIA_2018_56 52 (0.968) AM2 (Ar,35000.0,0.00,0.00); Cm (52)

1: TOF MS ES-

2.39e+005

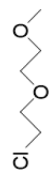
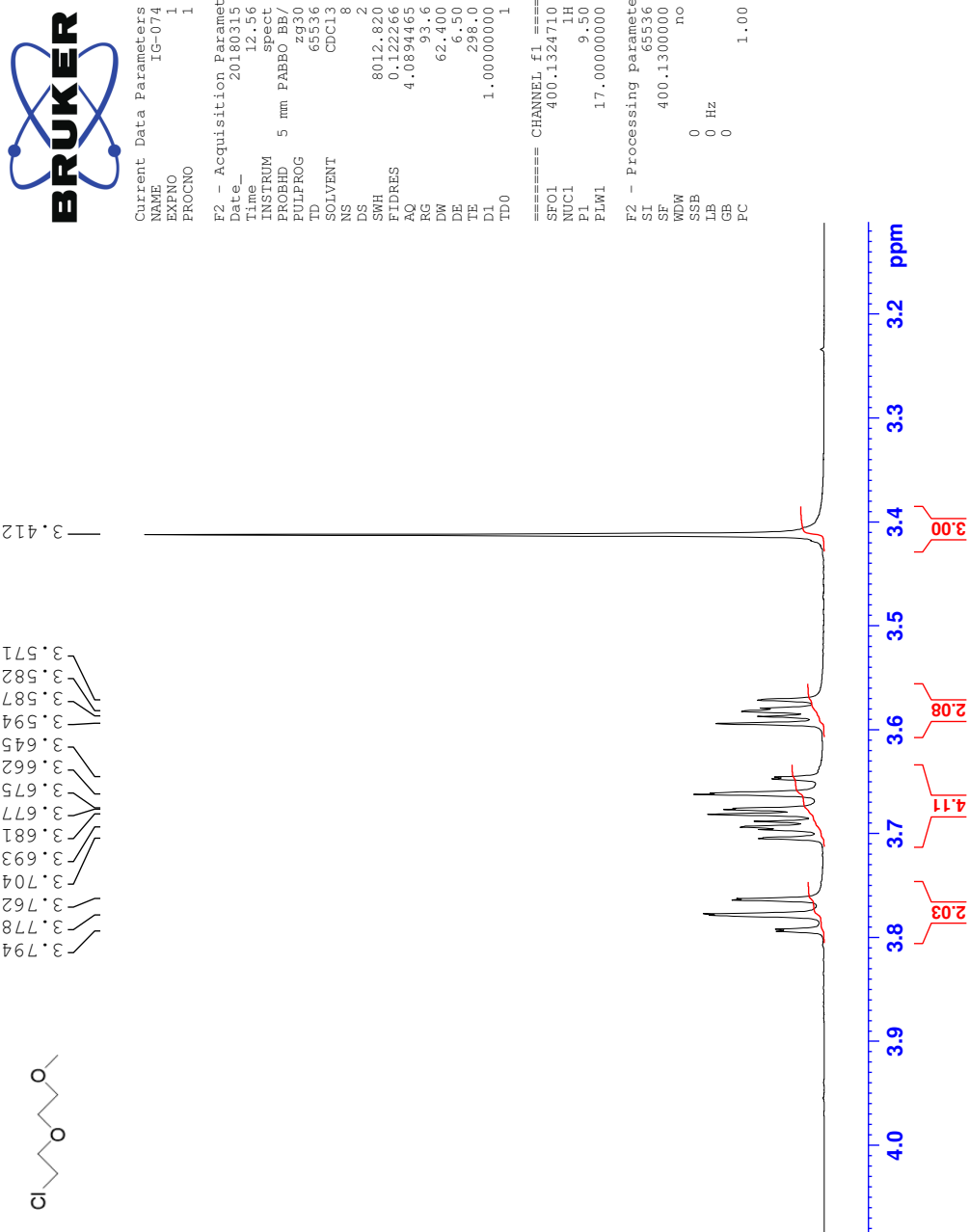


Minimum: -1.5
Maximum: 5.0 3.0 50.0

Mass	Calc. Mass	mDa	PPM	DBE	i-FIT	Norm	Conf (%)	Formula
94.9805	94.9803	0.2	2.1	0.5	823.0	n/a	n/a	C H3 O3 S

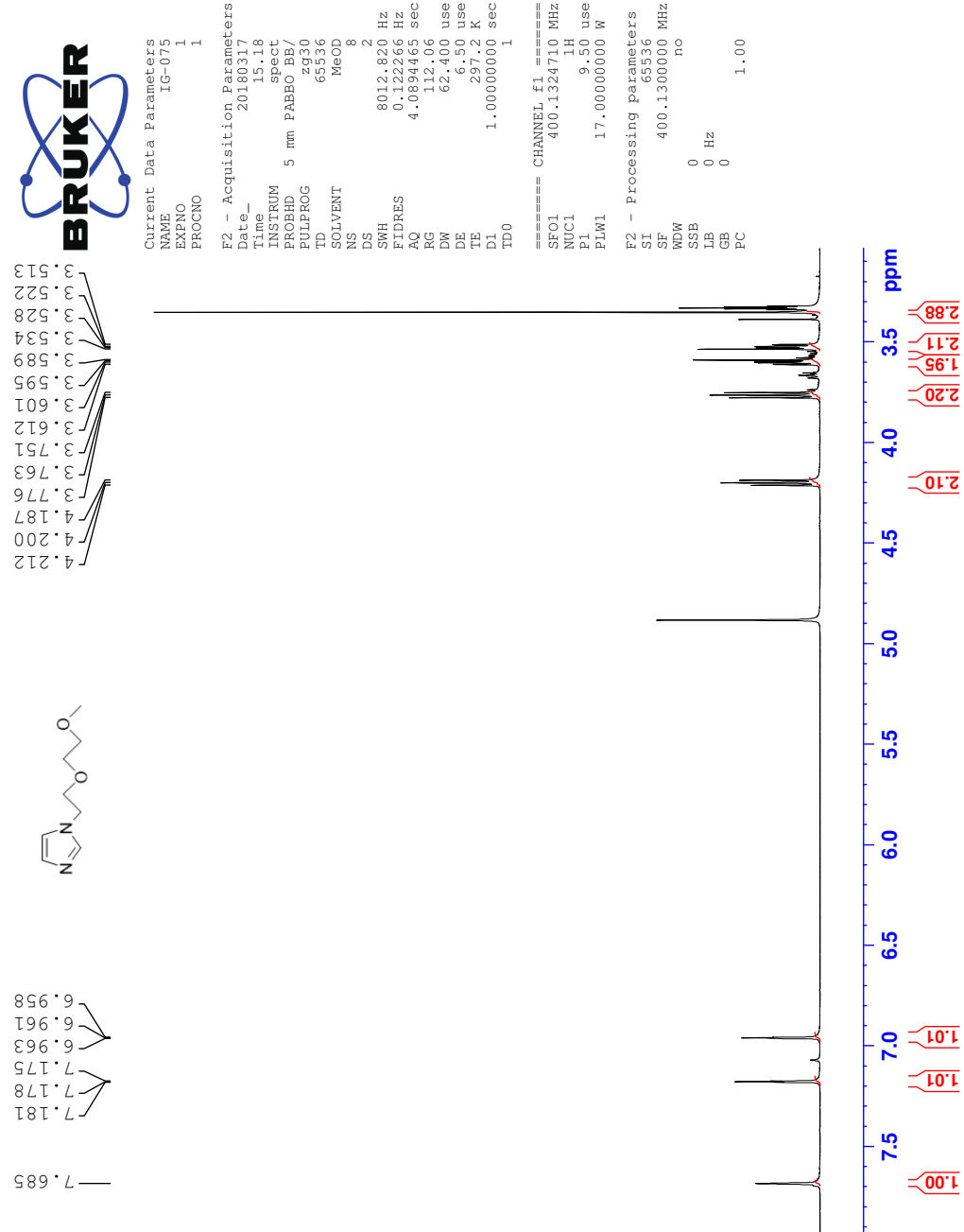
S Spectrum of 1-chloro-2-(2-methoxyethoxy)ethane (7)

¹H NMR Spectrum of 7



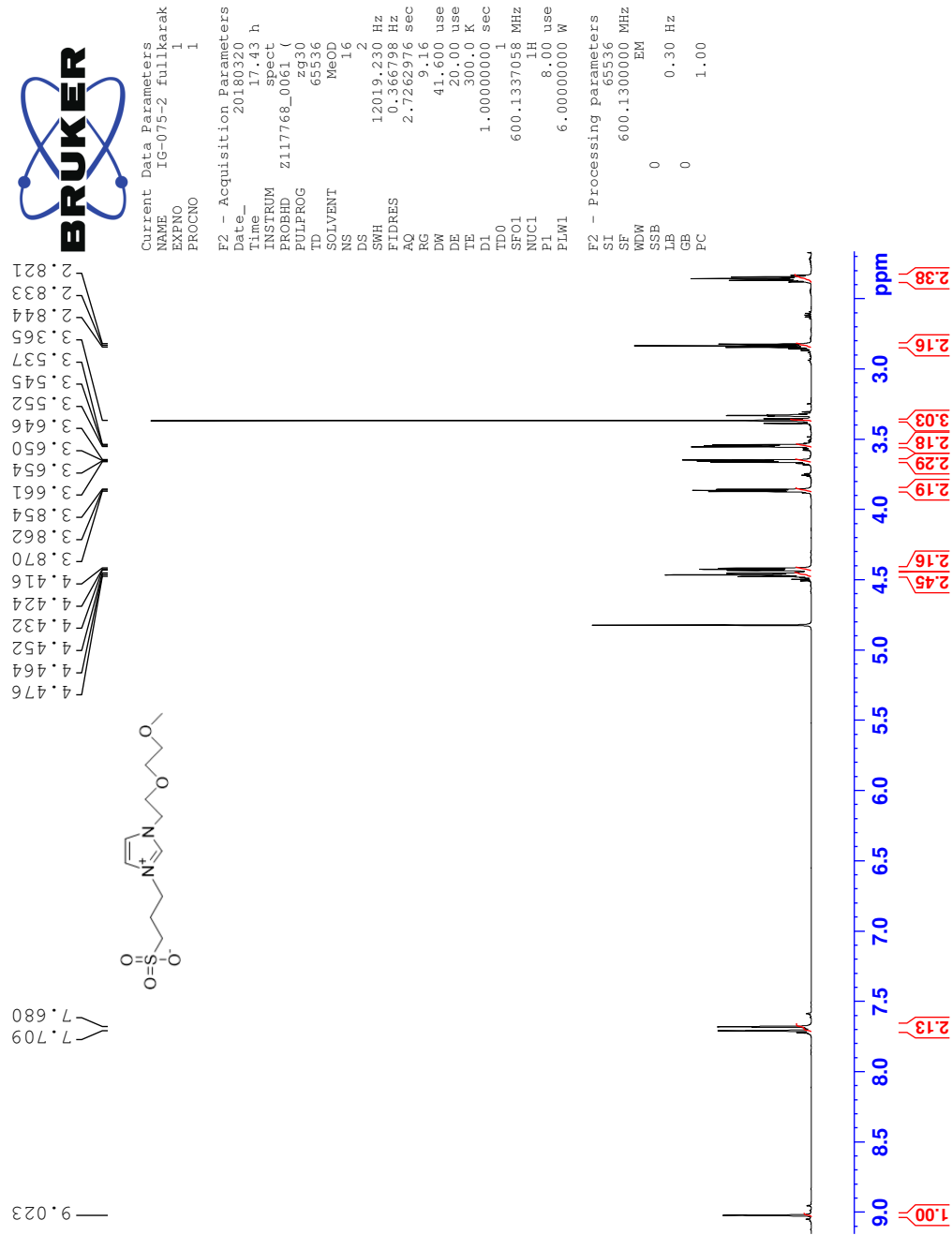
T Spectrum of 1-(2-(2-methoxyethoxy)ethyl)-imidazole (8a)

¹H NMR Spectrum of 8a

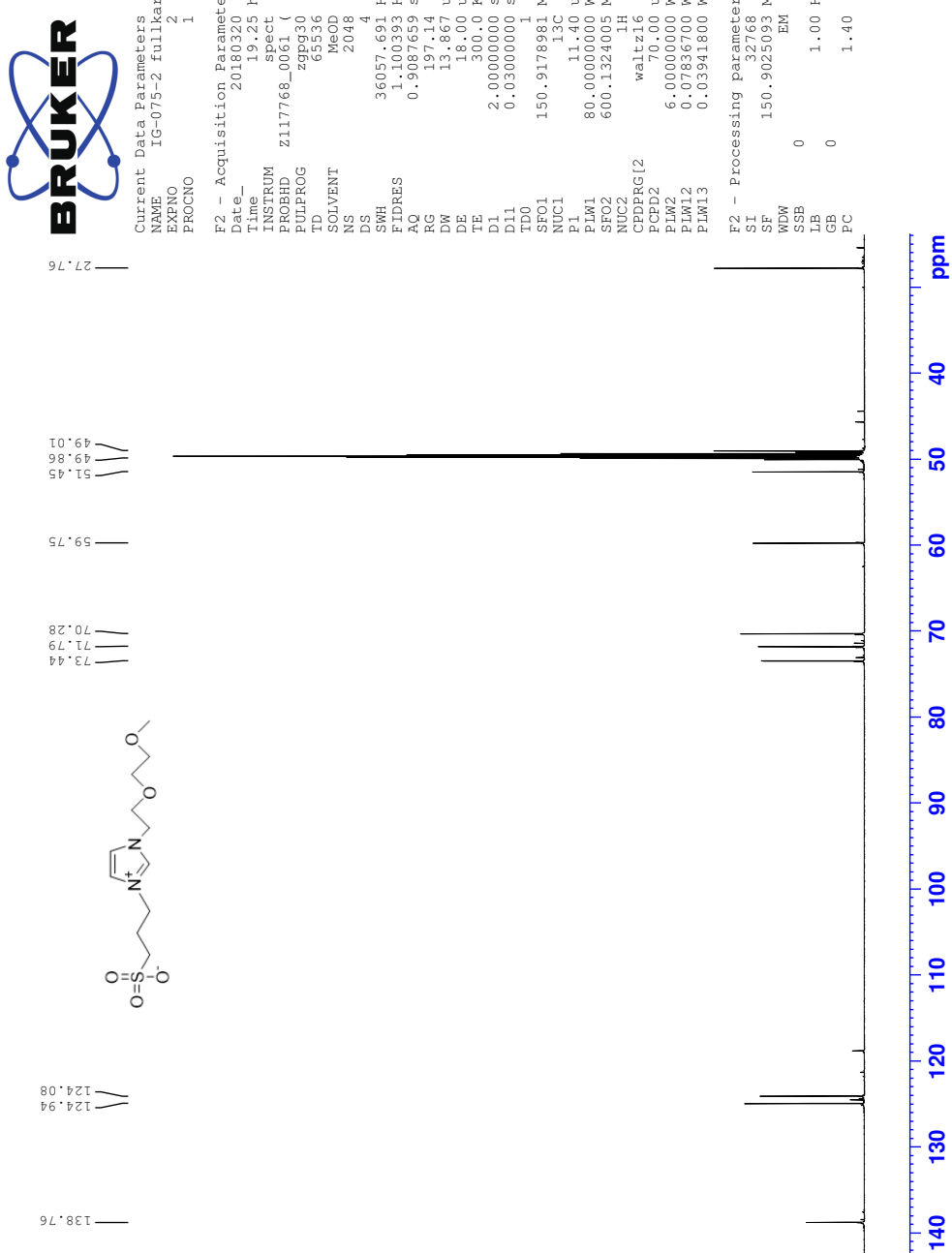


U Spectra of 3-(1-(2-(2-methoxyethoxy)ethyl)-imidazol-3-ium-3-yl)propane-1-sulfonate (8b)

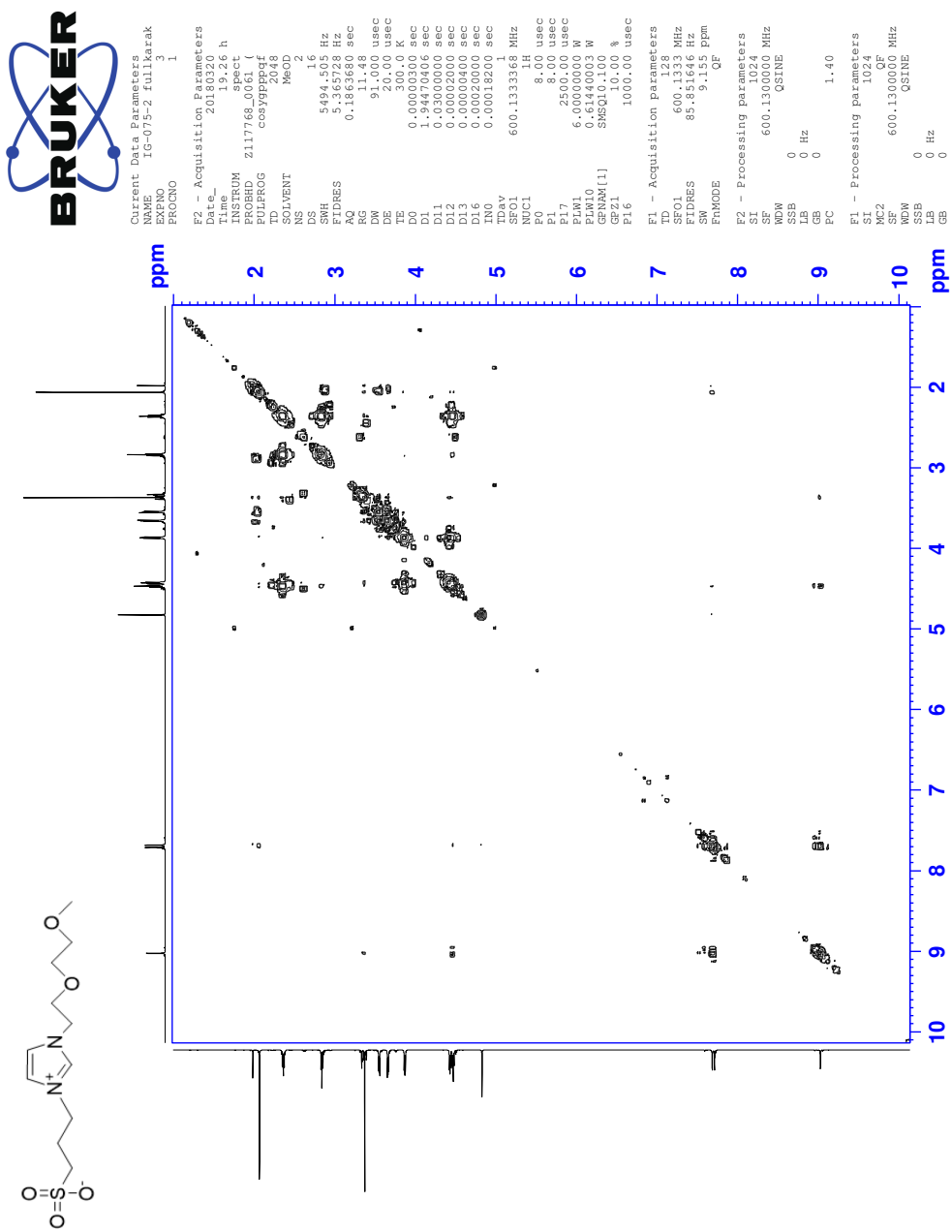
¹H NMR Spectrum of 8b



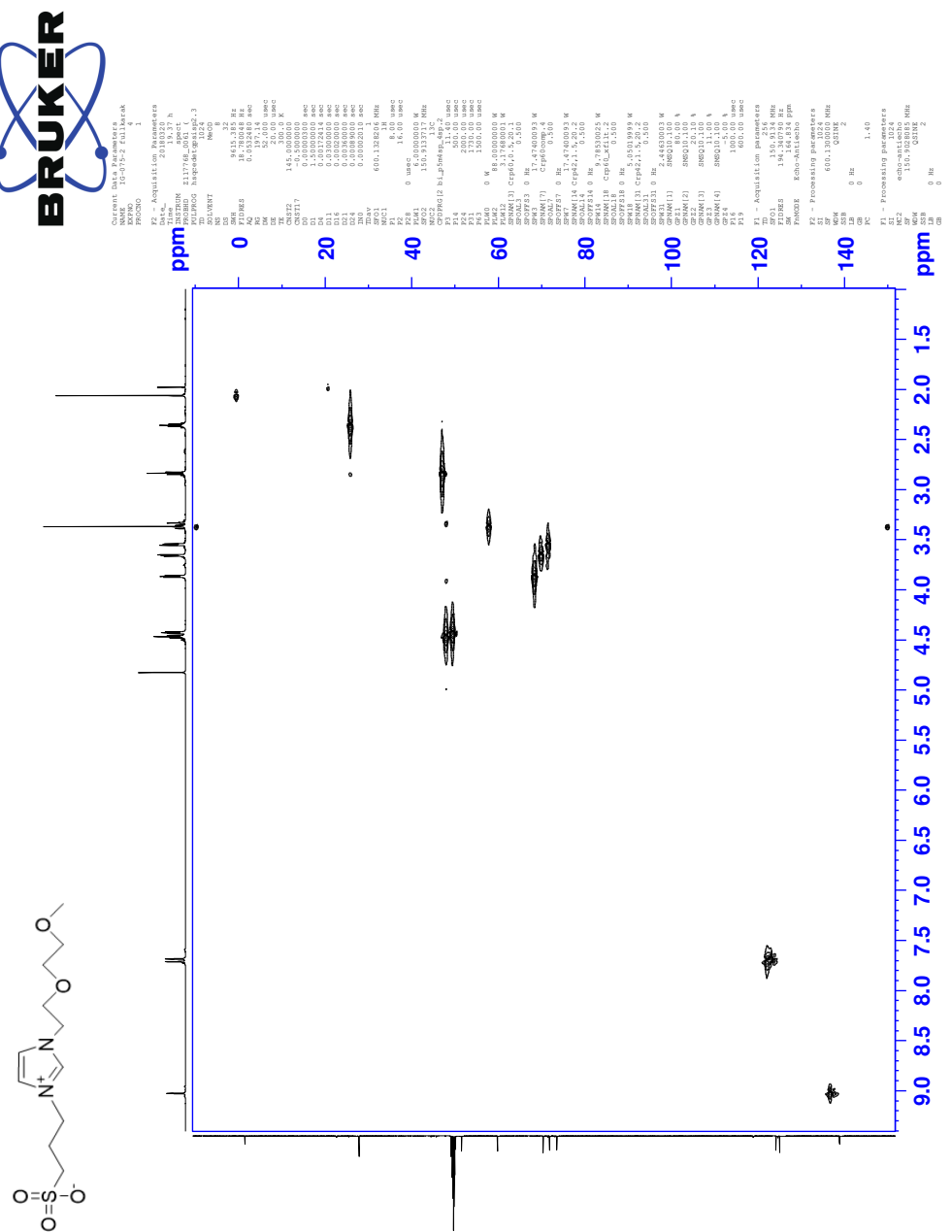
¹³C NMR Spectrum of 8b



COSY NMR Spectrum of 8b

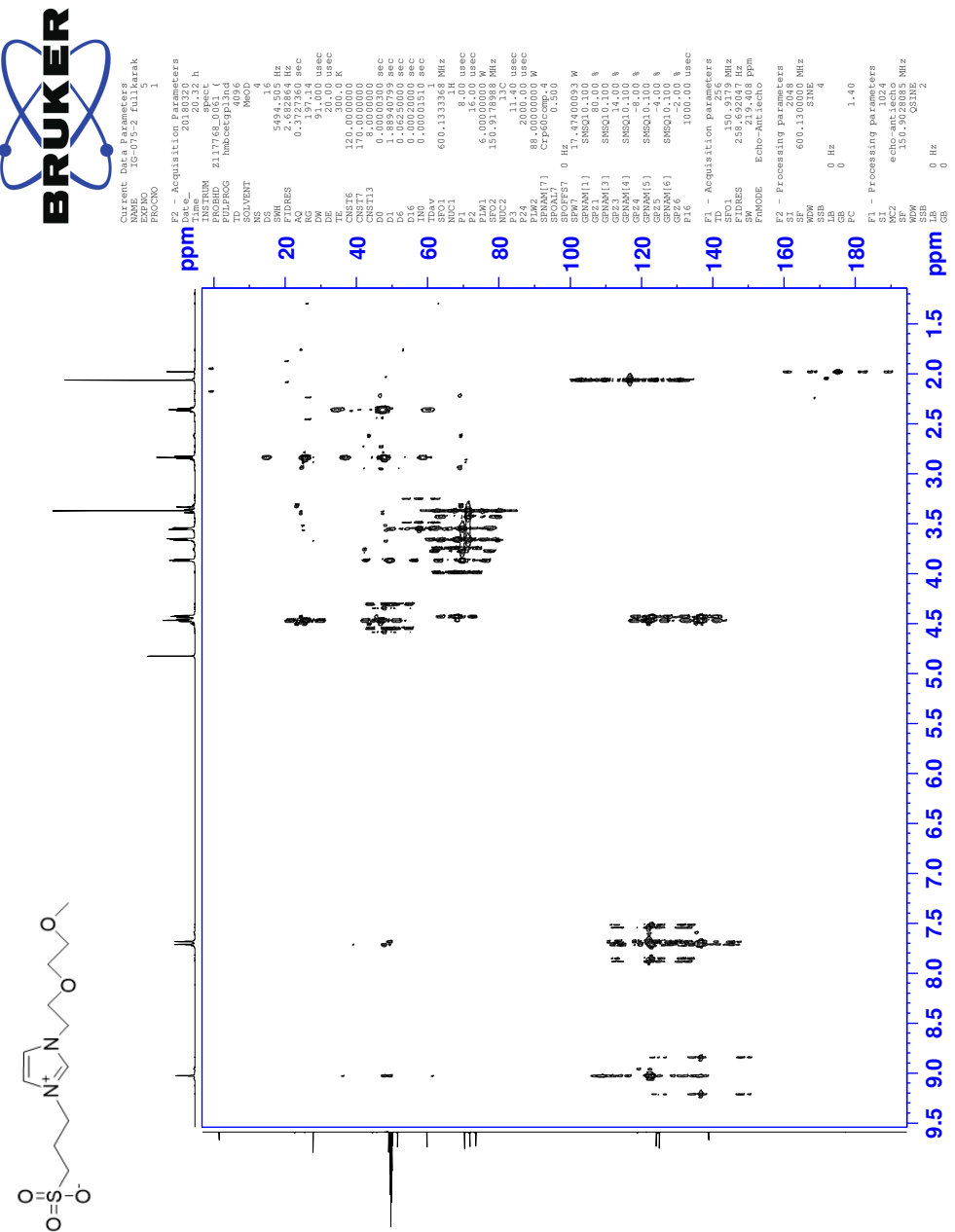


HSQC NMR Spectrum of 8b



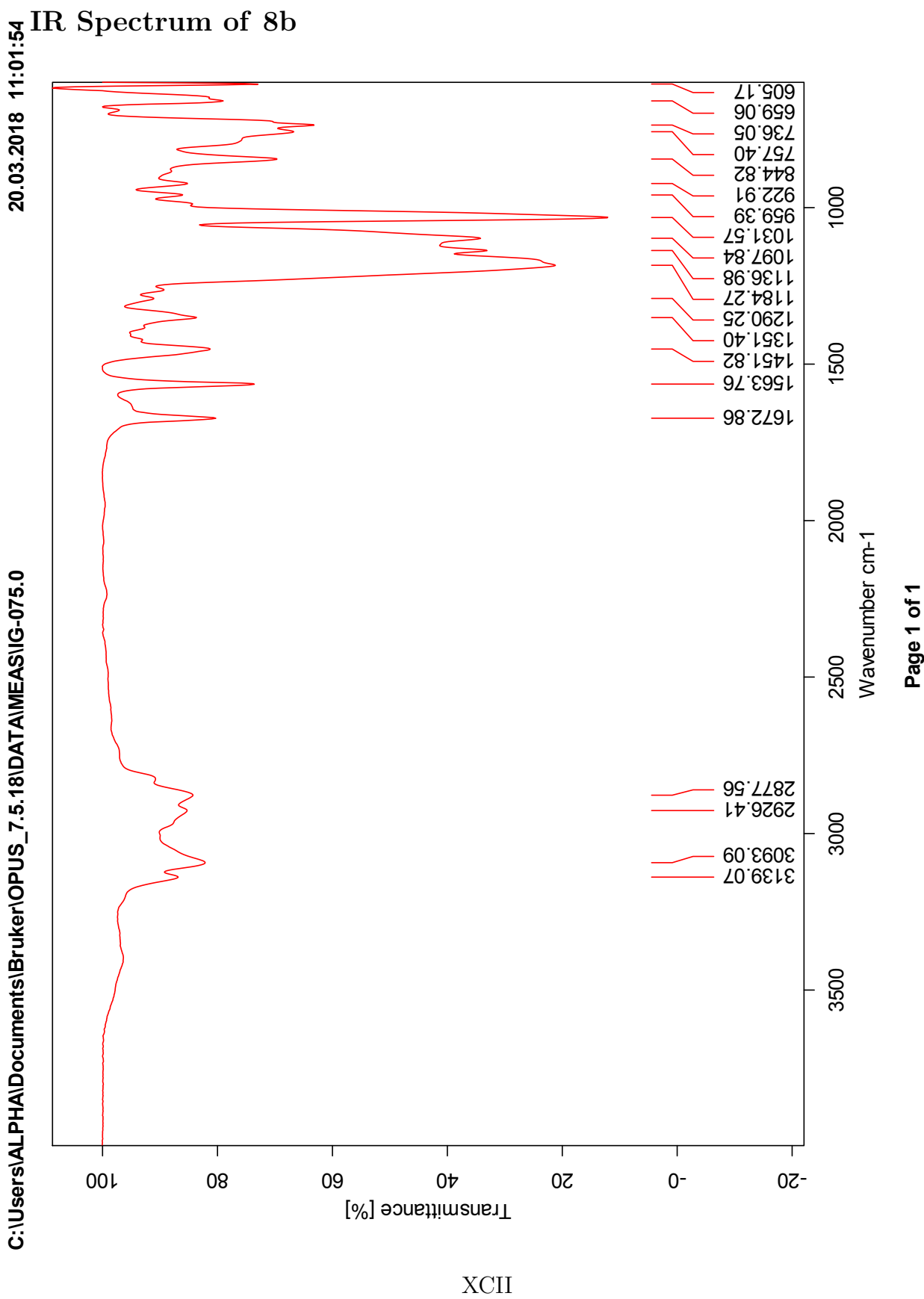
XC

HMBC NMR Spectrum of 8b



XCI

IR Spectrum of 8b



HRMS Spectrum of 8b

Elemental Composition Report

Page 1

Single Mass Analysis

Tolerance = 2.0 PPM / DBE: min = -1.5, max = 50.0

Element prediction: Off

Number of isotope peaks used for i-FIT = 3

Monoisotopic Mass, Even Electron Ions

2426 formula(e) evaluated with 4 results within limits (all results (up to 1000) for each mass)

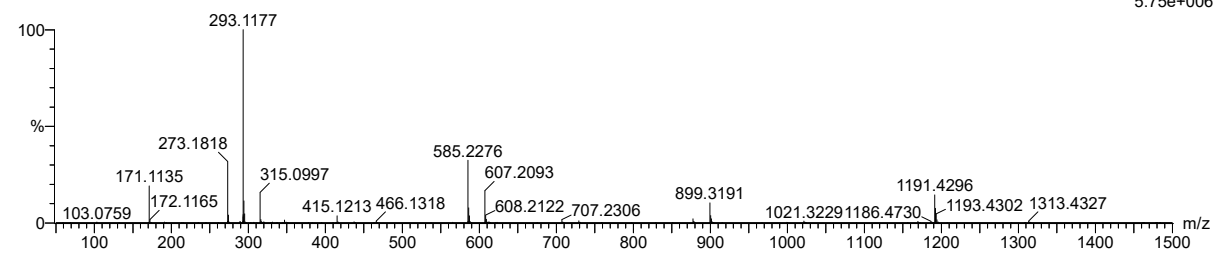
Elements Used:

C: 0-500 H: 0-1000 N: 0-10 O: 0-10 Na: 0-1 S: 0-5

2018-118pos 15 (0.157) AM2 (Ar,35000.0,0.00,0.00); Cm (15:18)

1: TOF MS ES+

5.75e+006

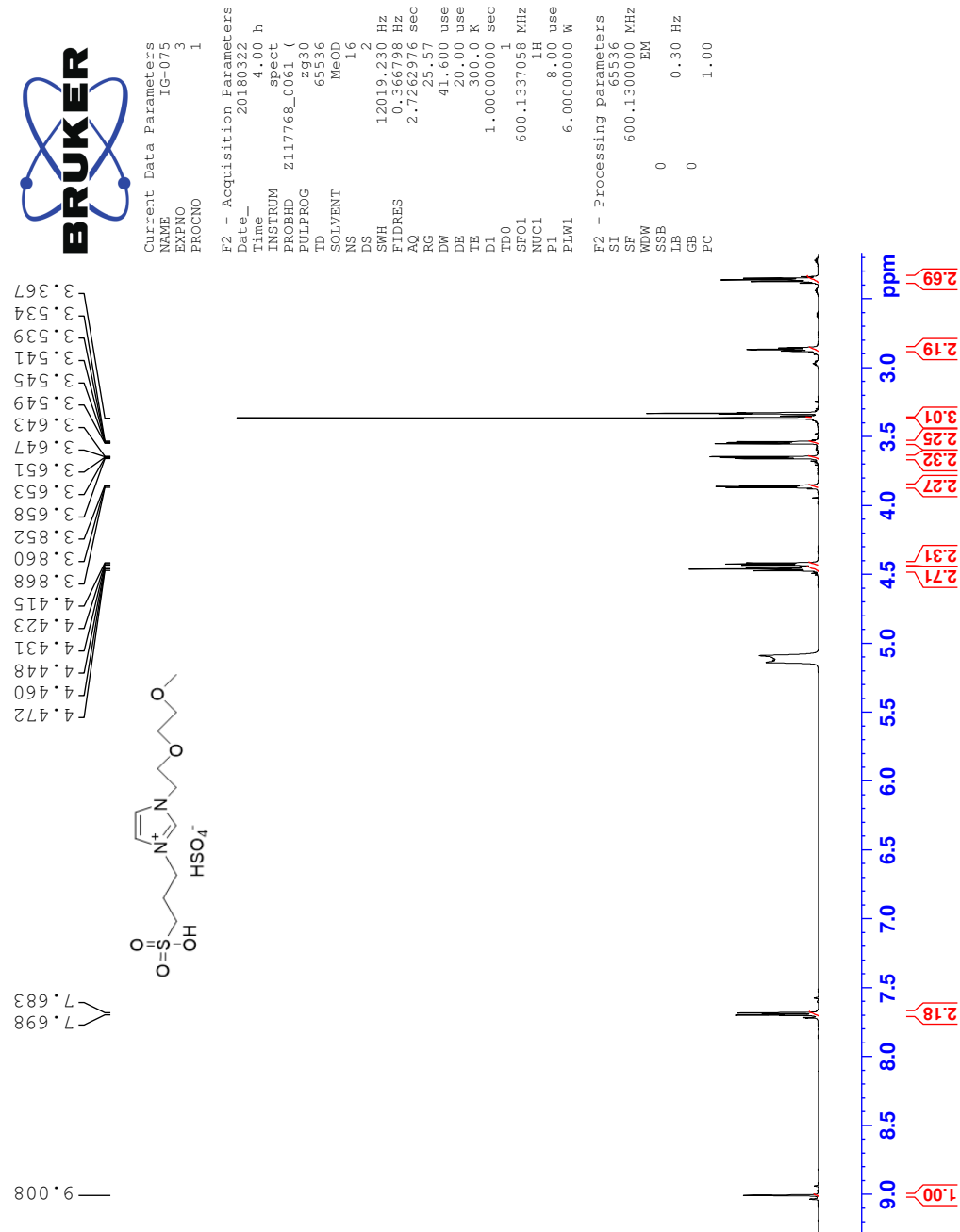


Minimum: -1.5
Maximum: 5000.0 2.0

Mass	Calc. Mass	mDa	PPM	DBE	i-FIT	Norm	Conf (%)	Formula
293.1177	293.1178	-0.1	-0.3	11.5	1530.9	13.104	0.00	C19 H17 O3
	293.1178	-0.1	-0.3	-1.5	1524.7	6.935	0.10	C4 H21 N8 O3 S2
	293.1180	-0.3	-1.0	1.5	1523.9	6.065	0.23	C12 H25 N2 S3
	293.1171	0.6	2.0	2.5	1517.8	0.003	99.67	C11 H21 N2 O5 S

V Spectra of 1-(2-(2-methoxyethoxy)ethyl)-3-(3-sulfopropyl)-1H-imidazol-3-ium hydrogen sulfonate (8c)

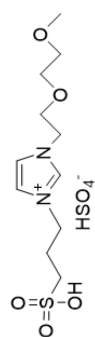
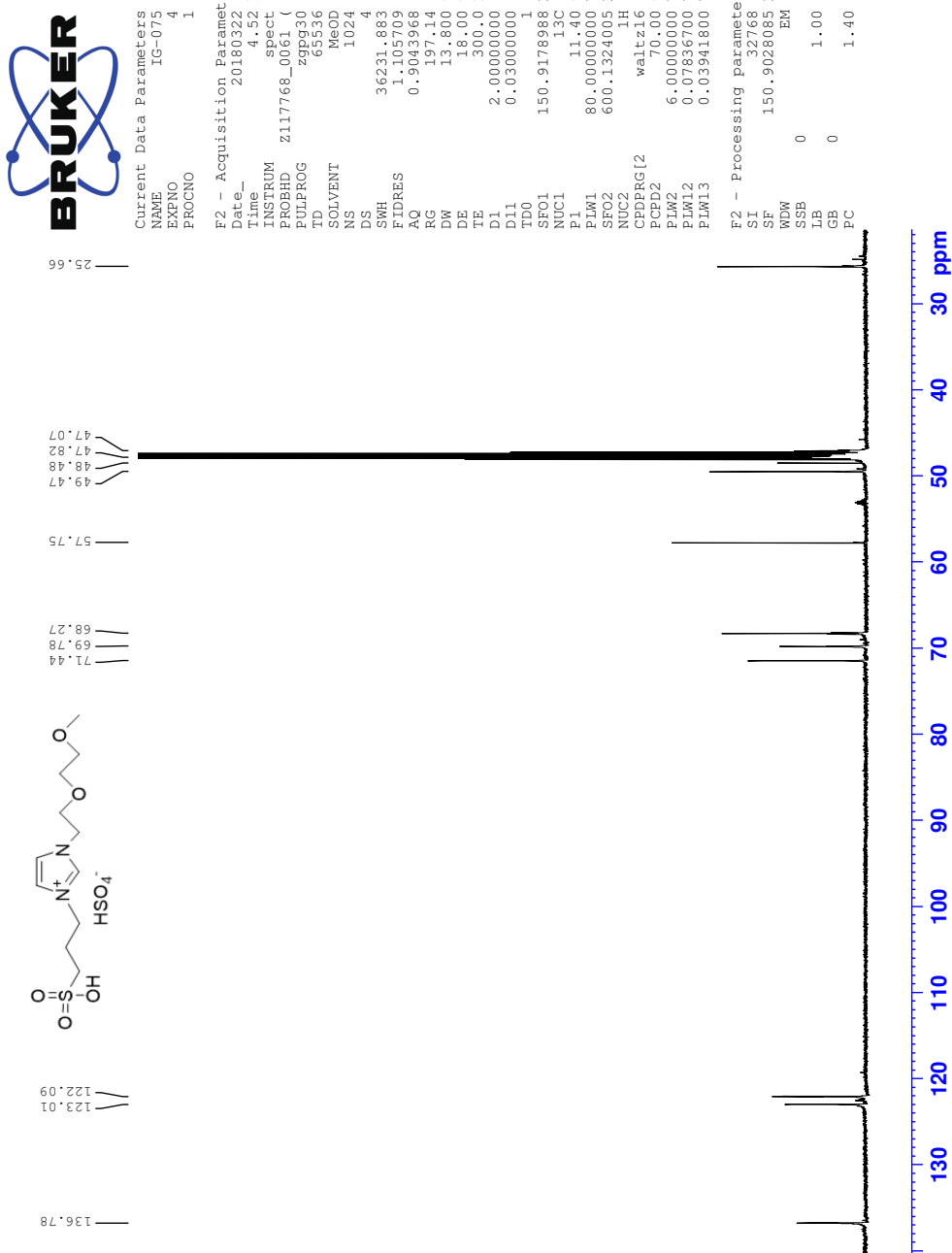
¹H NMR Spectrum of 8c



9.000 —

XClV

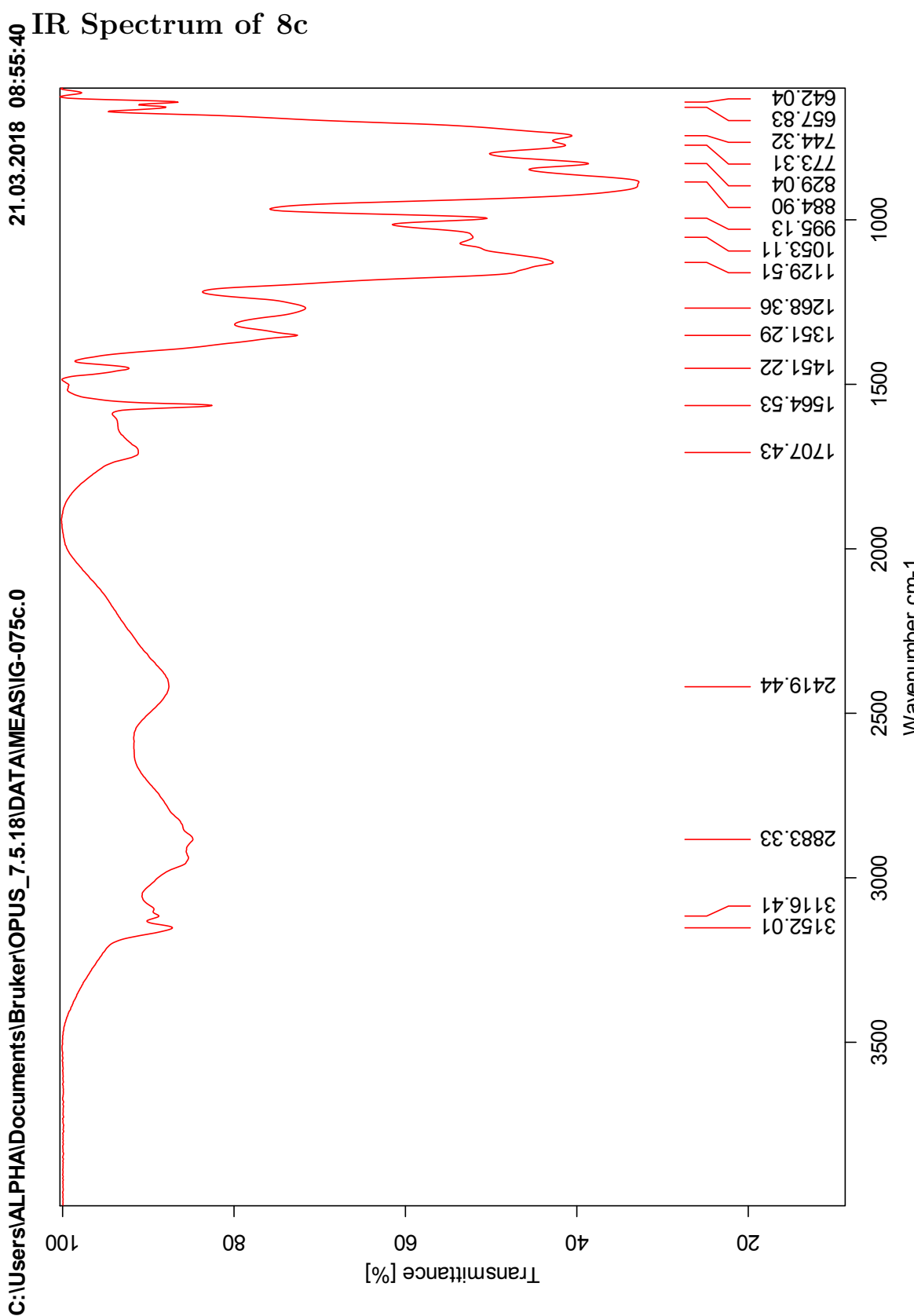
¹³C NMR Spectrum of 8c



XCV

IR Spectrum of 8c

C:\Users\ALPHA\Documents\Bruker\OPUS_7.5.18\DATA\MEAS\IG-075c.0



XCVI

HRMS Positive mode spectrum of 8c

Elemental Composition Report

Page 1

Single Mass Analysis

Tolerance = 2.0 PPM / DBE: min = -1.5, max = 50.0

Element prediction: Off

Number of isotope peaks used for i-FIT = 3

Monoisotopic Mass, Even Electron Ions

2426 formula(e) evaluated with 5 results within limits (all results (up to 1000) for each mass)

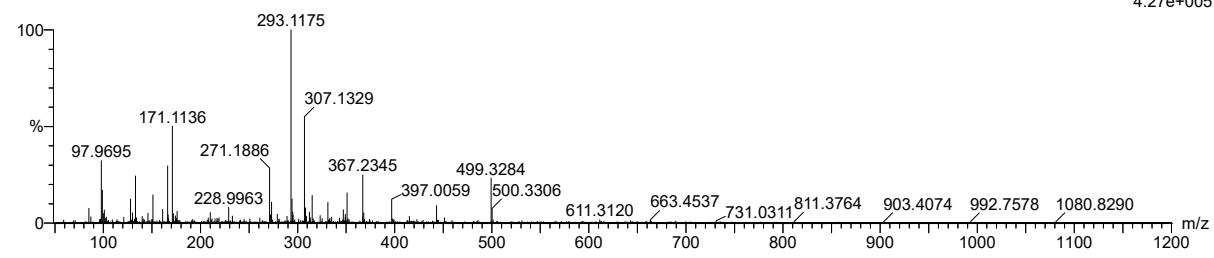
Elements Used:

C: 0-500 H: 0-1000 N: 0-10 O: 0-10 Na: 0-1 S: 0-5

2018-167 80 (1.483) AM2 (Ar,35000.0,0.00,0.00); Cm (80:84)

1: TOF MS ES+

4.27e+005



Minimum: -1.5
Maximum: 5000.0 2.0 50.0

Mass	Calc. Mass	mDa	PPM	DBE	i-FIT	Norm	Conf (%)	Formula
293.1175	293.1171	0.4	1.4	2.5	1192.3	0.000	100.00	C11 H21 N2 O5 S
	293.1178	-0.3	-1.0	-1.5	1203.9	11.556	0.00	C4 H21 N8 O3 S2
	293.1180	-0.5	-1.7	1.5	1204.5	12.226	0.00	C12 H25 N2 S3
	293.1169	0.6	2.0	-0.5	1208.8	16.463	0.00	C3 H17 N8 O8
	293.1178	-0.3	-1.0	11.5	1209.9	17.588	0.00	C19 H17 O3

HRMS Negative mode spectrum of 8c

Elemental Composition Report

Page 1

Single Mass Analysis

Tolerance = 50.0 PPM / DBE: min = -1.5, max = 100.0

Element prediction: Off

Number of isotope peaks used for i-FIT = 3

Monoisotopic Mass, Even Electron Ions

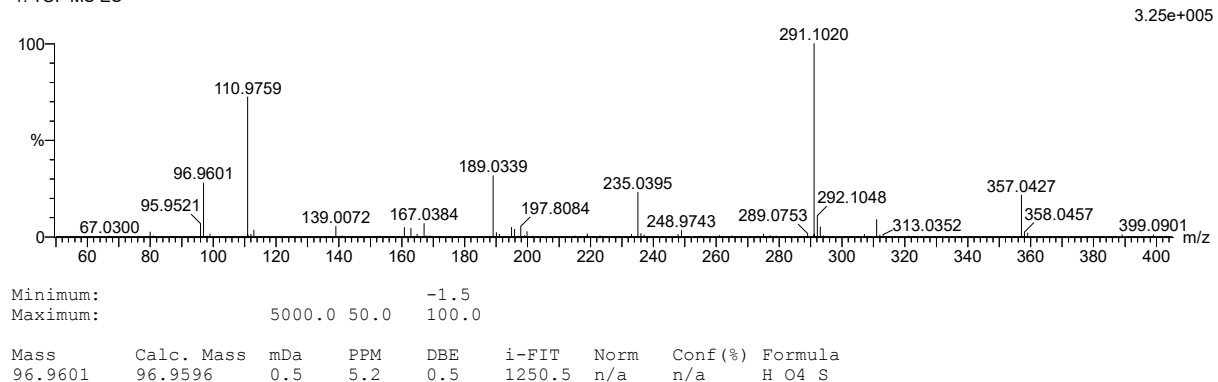
104 formula(e)s evaluated with 1 results within limits (all results (up to 1000) for each mass)

Elements Used:

C: 0-500 H: 0-1000 N: 0-10 O: 0-20 Na: 0-1 S: 0-4

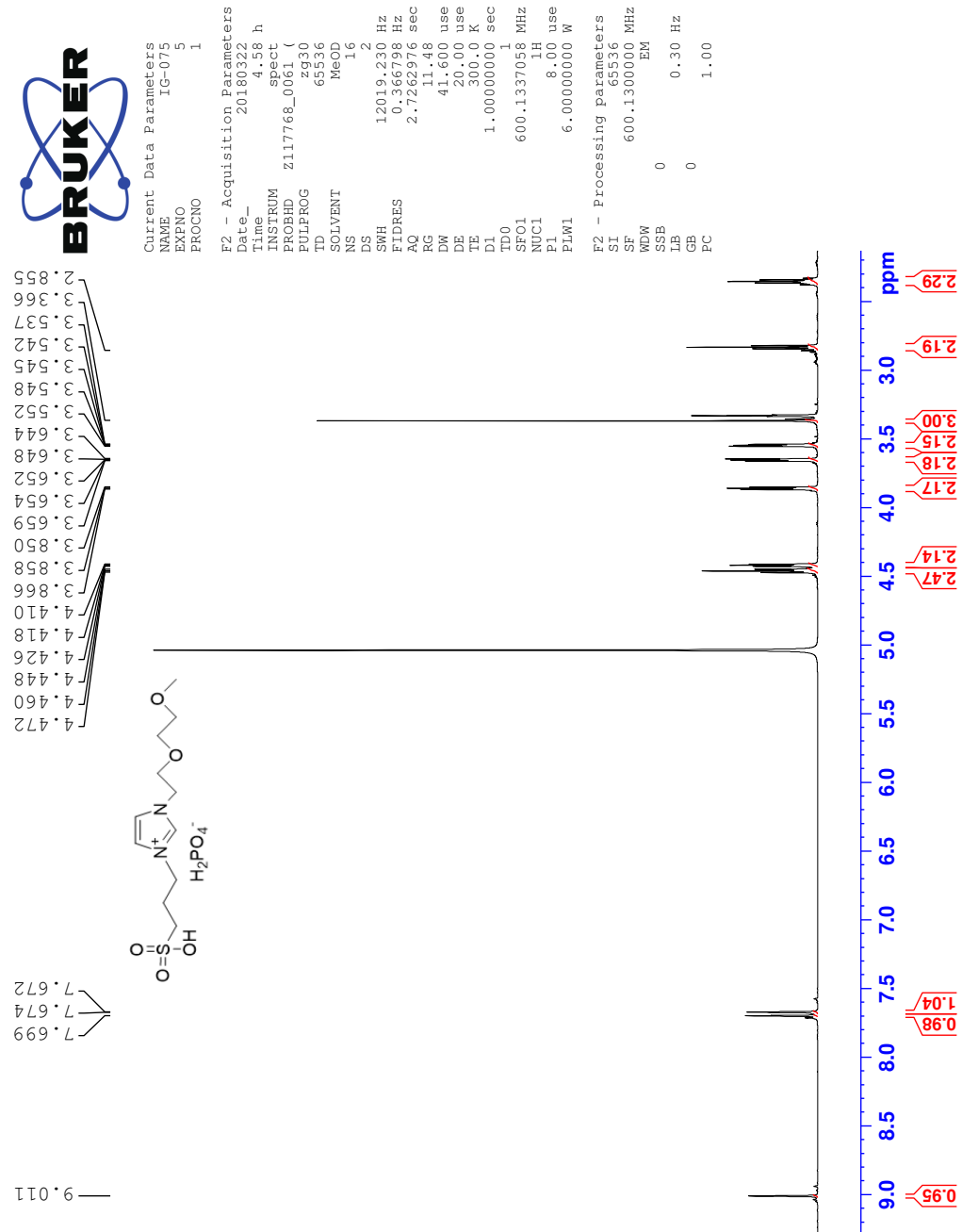
2018-167negZ 77 (1.516) AM2 (Ar,35000.0,0.00,0.00); Cm (77:78)

1: TOF MS ES-

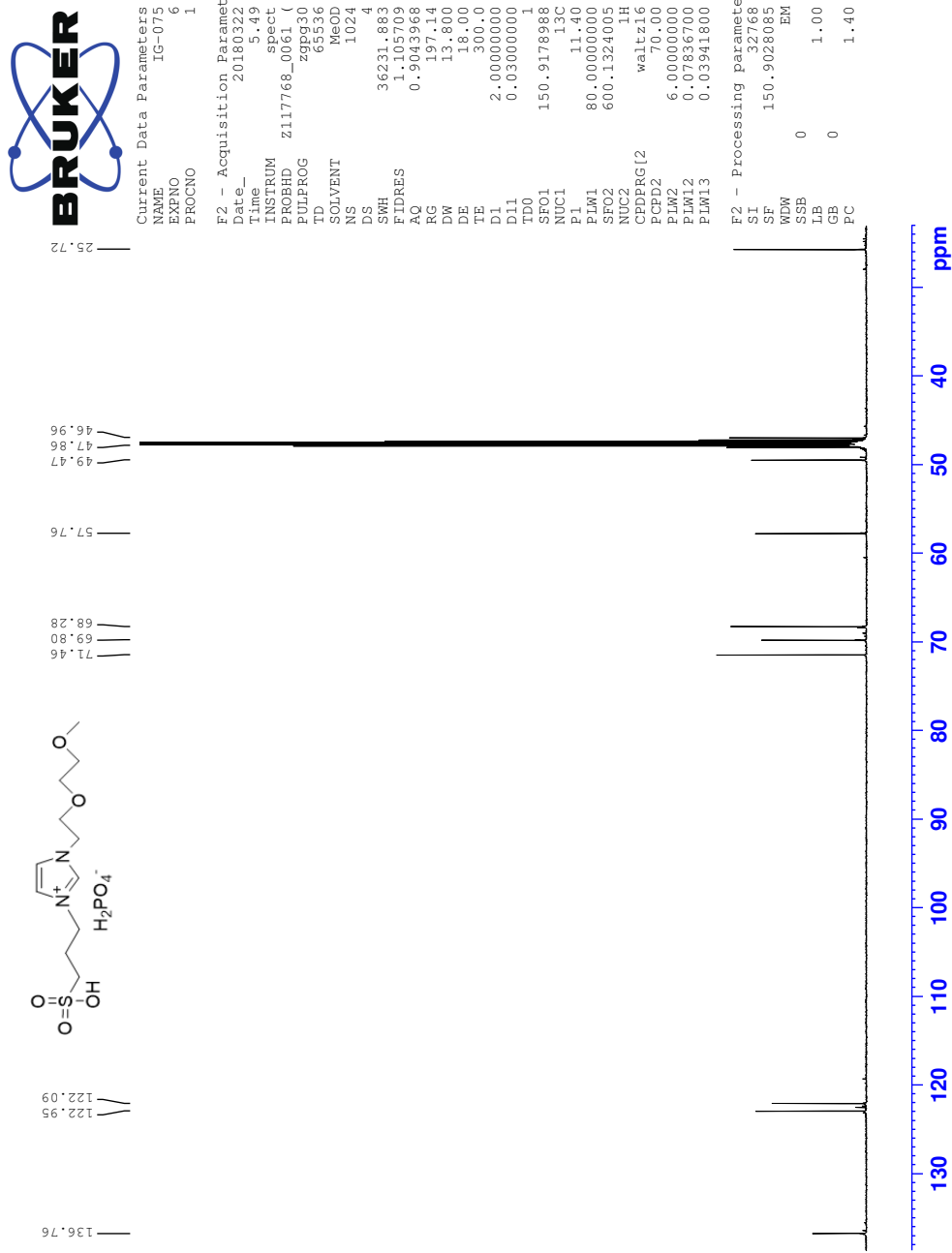


W Spectra of 1-(2-(2-methoxyethoxy)ethyl)-3-(3-sulfopropyl)-1H-imidazol-3-ium dihydrogen phosphate (8d)

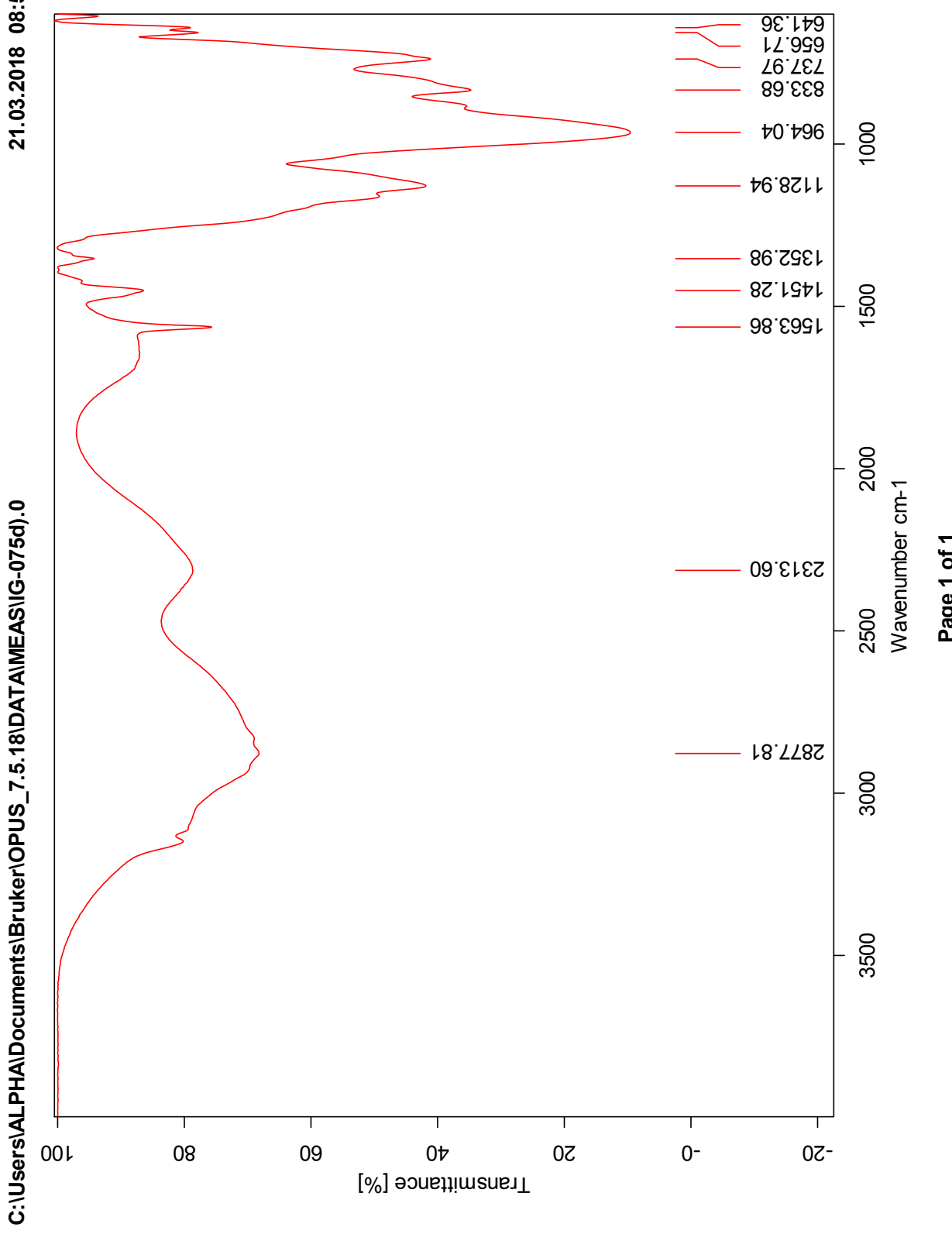
¹H NMR Spectrum of 8d



¹³C NMR Spectrum of 8d



IR Spectrum of 8d



HRMS Positive mode spectrum of 8d

Elemental Composition Report

Page 1

Single Mass Analysis

Tolerance = 2.0 PPM / DBE: min = -1.5, max = 50.0

Element prediction: Off

Number of isotope peaks used for i-FIT = 3

Monoisotopic Mass, Even Electron Ions

2897 formula(e) evaluated with 2 results within limits (all results (up to 1000) for each mass)

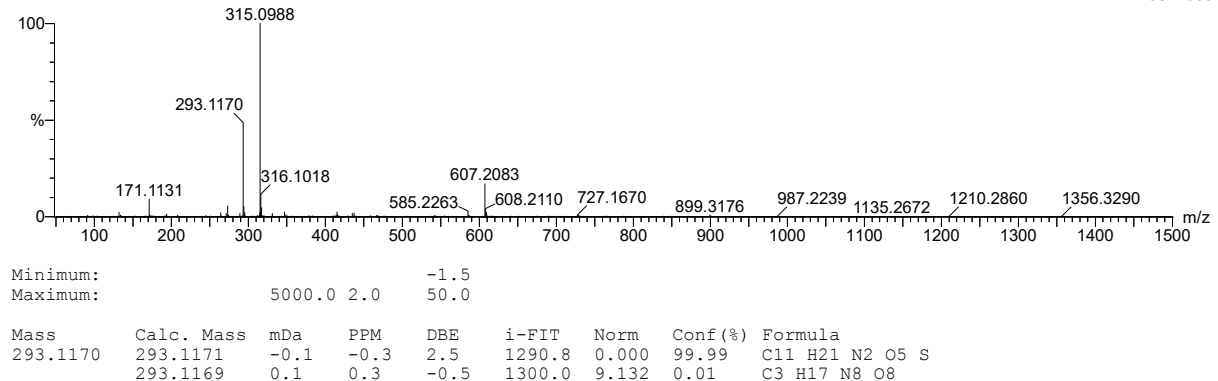
Elements Used:

C: 0-500 H: 0-1000 N: 0-10 O: 0-10 Na: 0-1 S: 0-5 I: 0-1

2018-129pos 5 (0.071) AM2 (Ar,35000.0,0.00,0.00); Cm (5:7)

1: TOF MS ES+

2.98e+006



Minimum: 5000.0 Maximum: 2.0 -1.5

Mass	Calc. Mass	mDa	PPM	DBE	i-FIT	Norm	Conf (%)	Formula
293.1170	293.1171	-0.1	-0.3	2.5	1290.8	0.000	99.99	C ₁₁ H ₂₁ N ₂ O ₅ S
	293.1169	0.1	0.3	-0.5	1300.0	9.132	0.01	C ₃ H ₁₇ N ₈ O ₈

CII

HRMS Negative mode spectrum of 8d

Elemental Composition Report

Page 1

Single Mass Analysis

Tolerance = 2.0 PPM / DBE: min = -1.5, max = 50.0

Element prediction: Off

Number of isotope peaks used for i-FIT = 3

Monoisotopic Mass, Even Electron Ions

153 formula(e) evaluated with 1 results within limits (all results (up to 1000) for each mass)

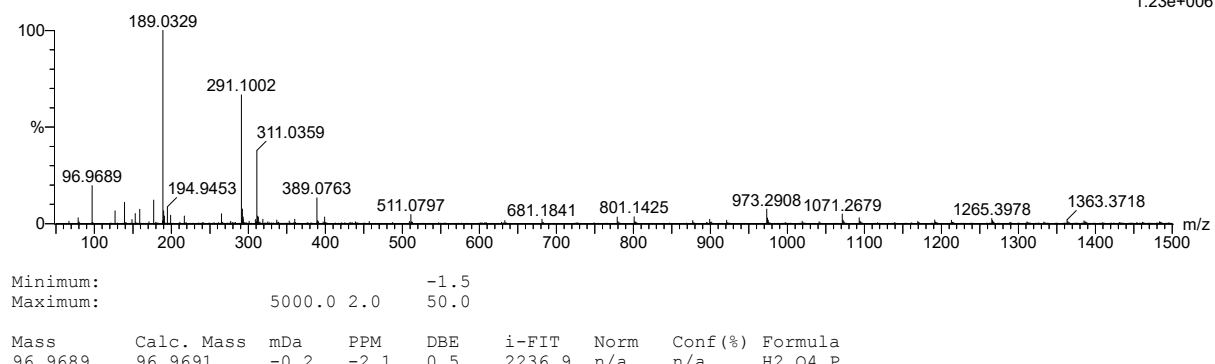
Elements Used:

C: 0-500 H: 0-1000 N: 0-10 O: 0-10 Na: 0-1 S: 0-5 I: 0-1 P: 0-2

2018-129negb 53 (1.051) AM2 (Ar,35000.0,0.00,0.00); Cm (52:54)

1: TOF MS ES-

1.23e+006

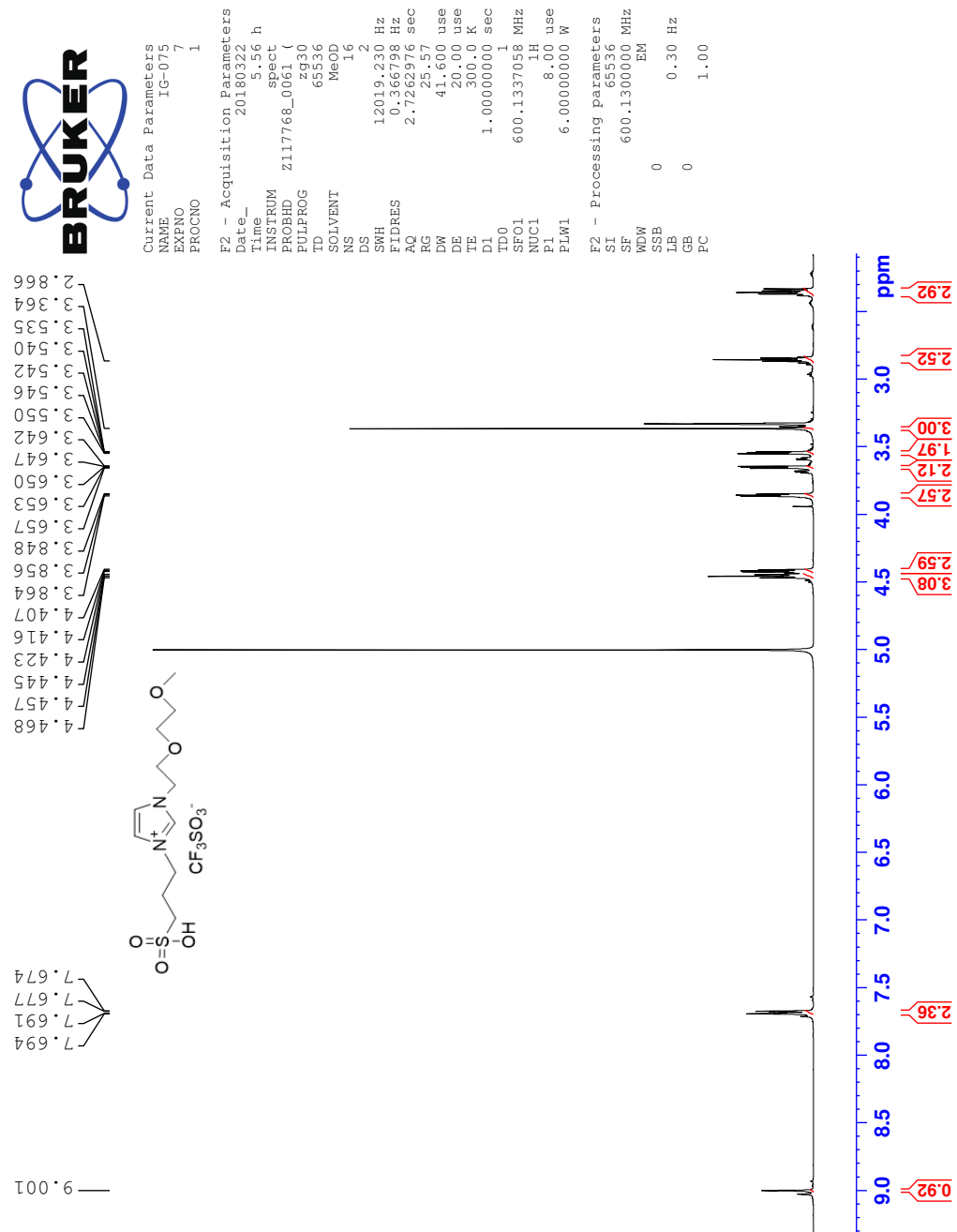


Minimum: -1.5
Maximum: 5000.0 2.0 50.0

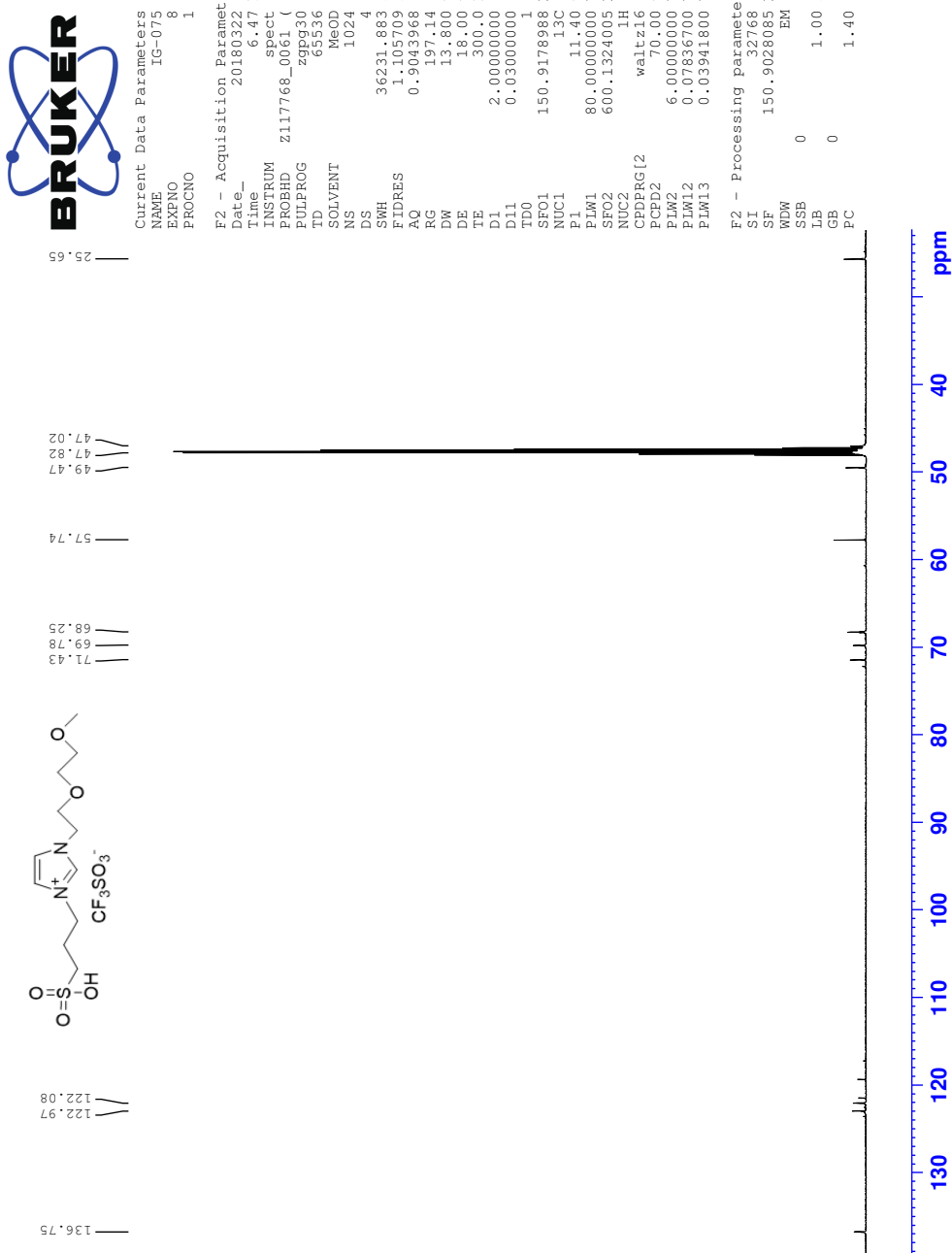
Mass	Calc. Mass	mDa	PPM	DBE	i-FIT	Norm	Conf (%)	Formula
96.9689	96.9691	-0.2	-2.1	0.5	2236.9	n/a	n/a	H ₂ O ₄ P

X Spectra of 1-(2-(2-methoxyethoxy)ethyl)-3-(3-sulfopropyl)-1H-imidazol-3-ium trifluoromethane-sulfonate (8e)

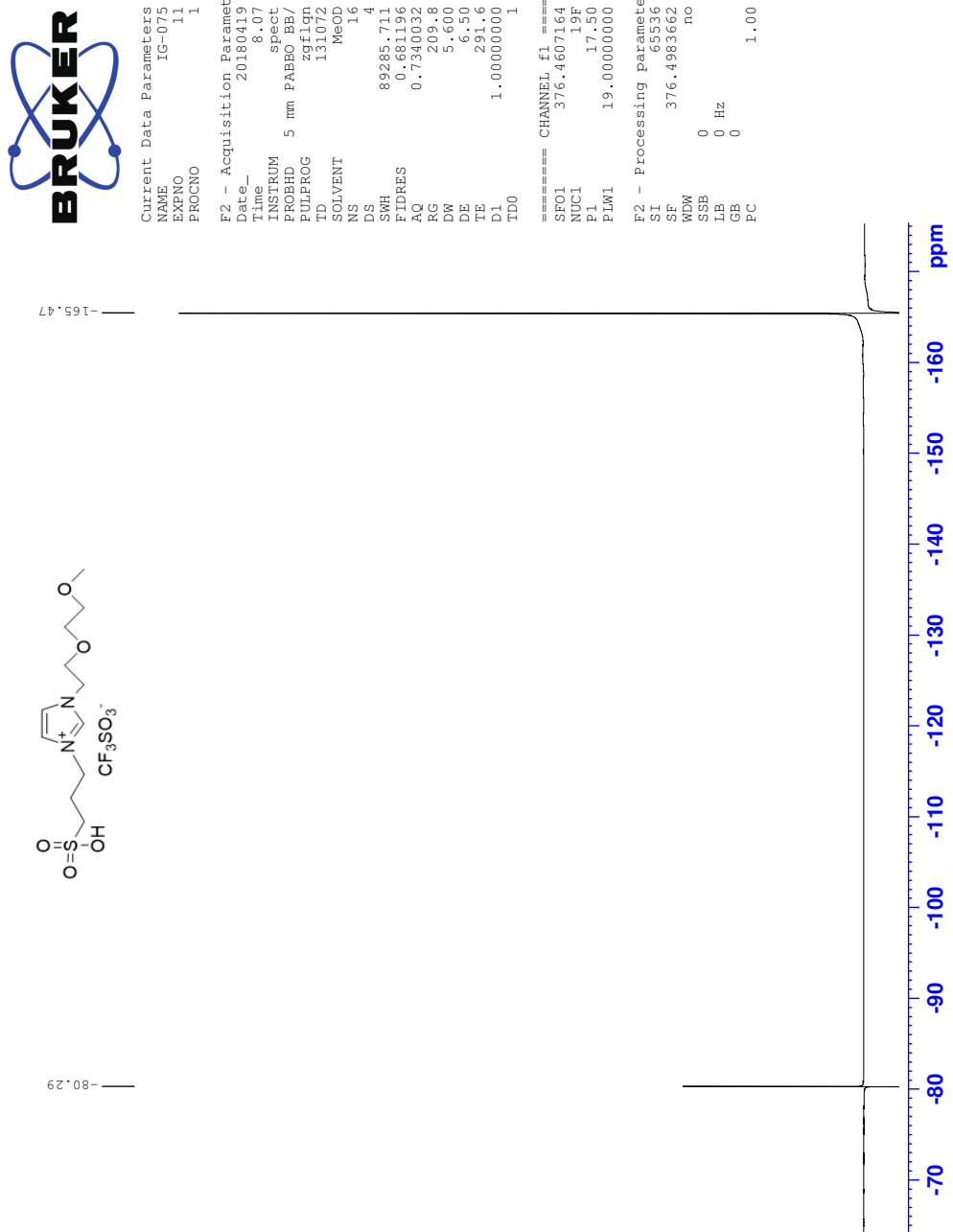
¹H NMR Spectrum of 8e



¹³C NMR Spectrum of 8e



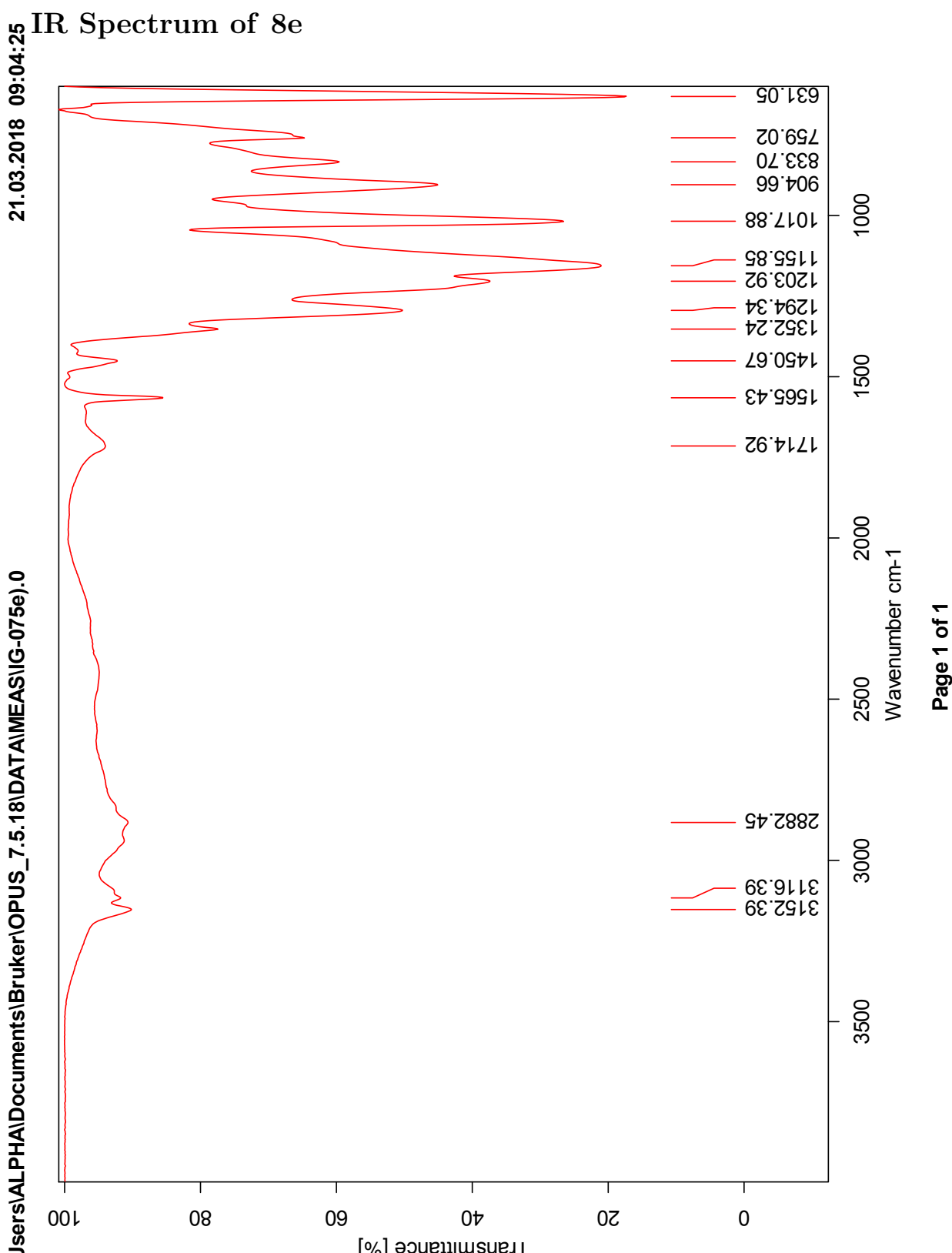
¹⁹F NMR Spectrum of 8e



CVI

IR Spectrum of 8e

C:\Users\ALPHA\Documents\Bruker\OPUS_7.5.18\DATA\MEAS\IG-075e.0



CVII

HRMS Positive mode spectrum of 8e

Elemental Composition Report

Page 1

Single Mass Analysis

Tolerance = 2.0 PPM / DBE: min = -1.5, max = 50.0

Element prediction: Off

Number of isotope peaks used for i-FIT = 3

Monoisotopic Mass, Even Electron Ions

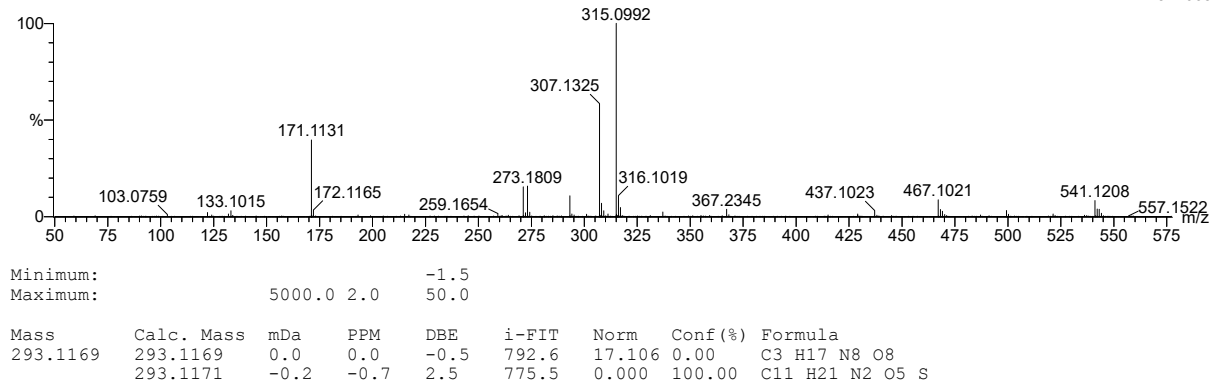
1632 formula(e) evaluated with 2 results within limits (all results (up to 1000) for each mass)

Elements Used:

C: 0-500 H: 0-1000 N: 0-10 O: 0-10 S: 0-5 I: 0-1

2018-130pos 69 (0.654) AM2 (Ar,35000.0,0.00,0.00); Cm (68:72)
1: TOF MS ES+

4.15e+005



HRMS Negative mode spectrum of 8e

Elemental Composition Report

Page 1

Single Mass Analysis

Tolerance = 2.0 PPM / DBE: min = -1.5, max = 50.0

Element prediction: Off

Number of isotope peaks used for i-FIT = 3

Monoisotopic Mass, Even Electron Ions

585 formula(e) evaluated with 2 results within limits (all results (up to 1000) for each mass)

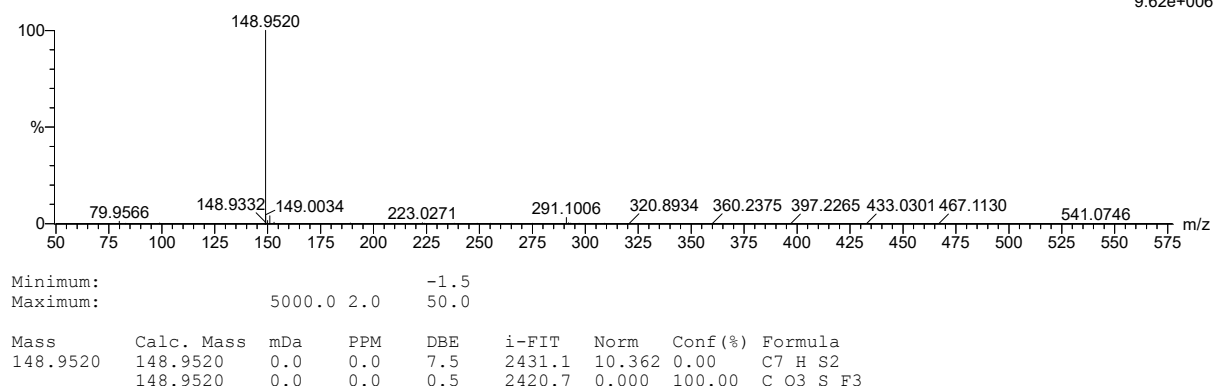
Elements Used:

C: 0-500 H: 0-1000 N: 0-10 O: 0-10 S: 0-5 I: 0-1 F: 0-10

2018-130neg_33 (0.674) AM2 (Ar,35000.0,0.00,0.00); Cm (33.38)

1: TOF MS ES-

9.62e+006

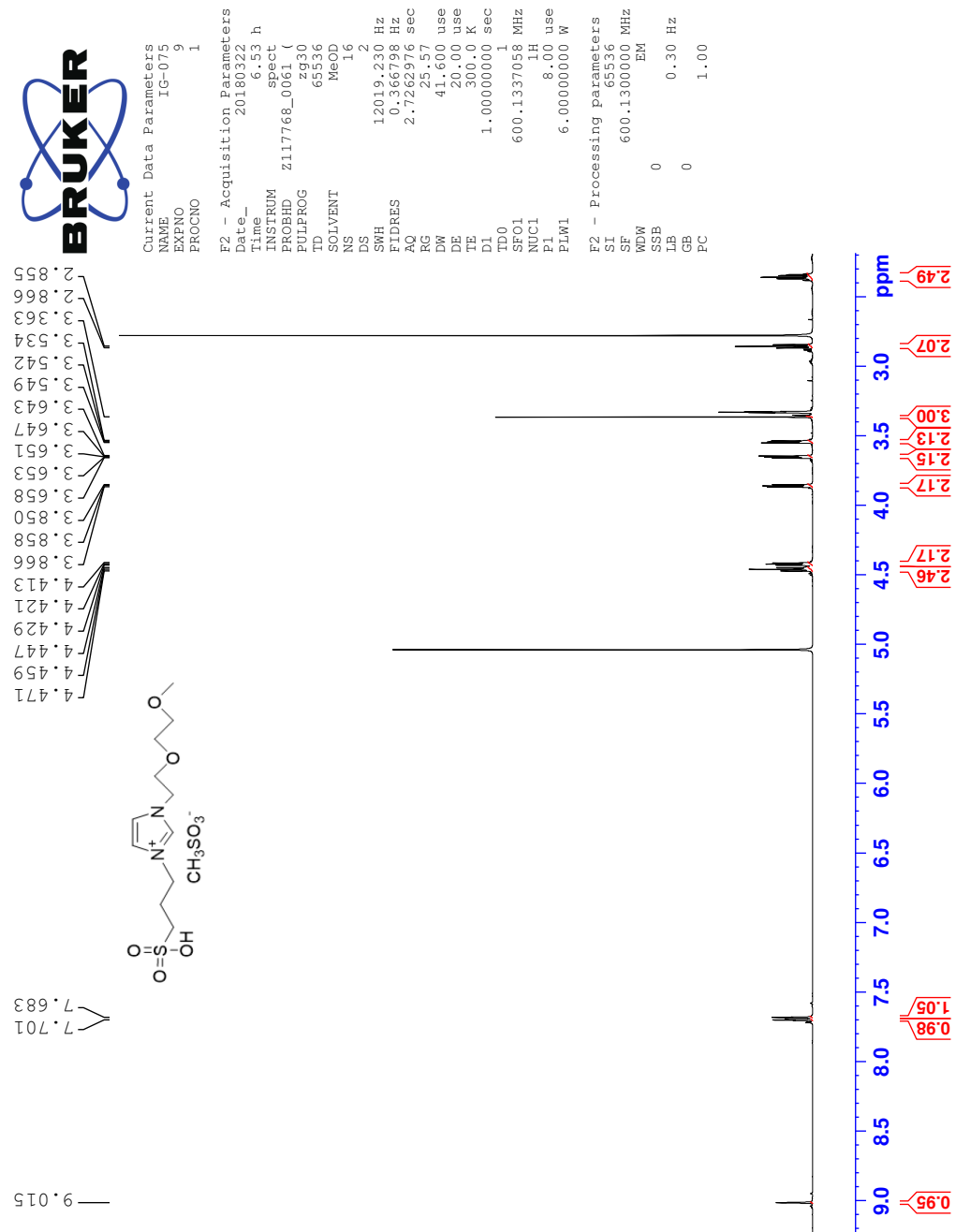


Minimum: -1.5
Maximum: 5000.0 2.0

Mass	Calc. Mass	mDa	PPM	DBE	i-FIT	Norm	Conf (%)	Formula
148.9520	148.9520	0.0	0.0	7.5	2431.1	10.362	0.00	C ₇ H ₈ S ₂
	148.9520	0.0	0.0	0.5	2420.7	0.000	100.00	C ₇ H ₈ S ₂

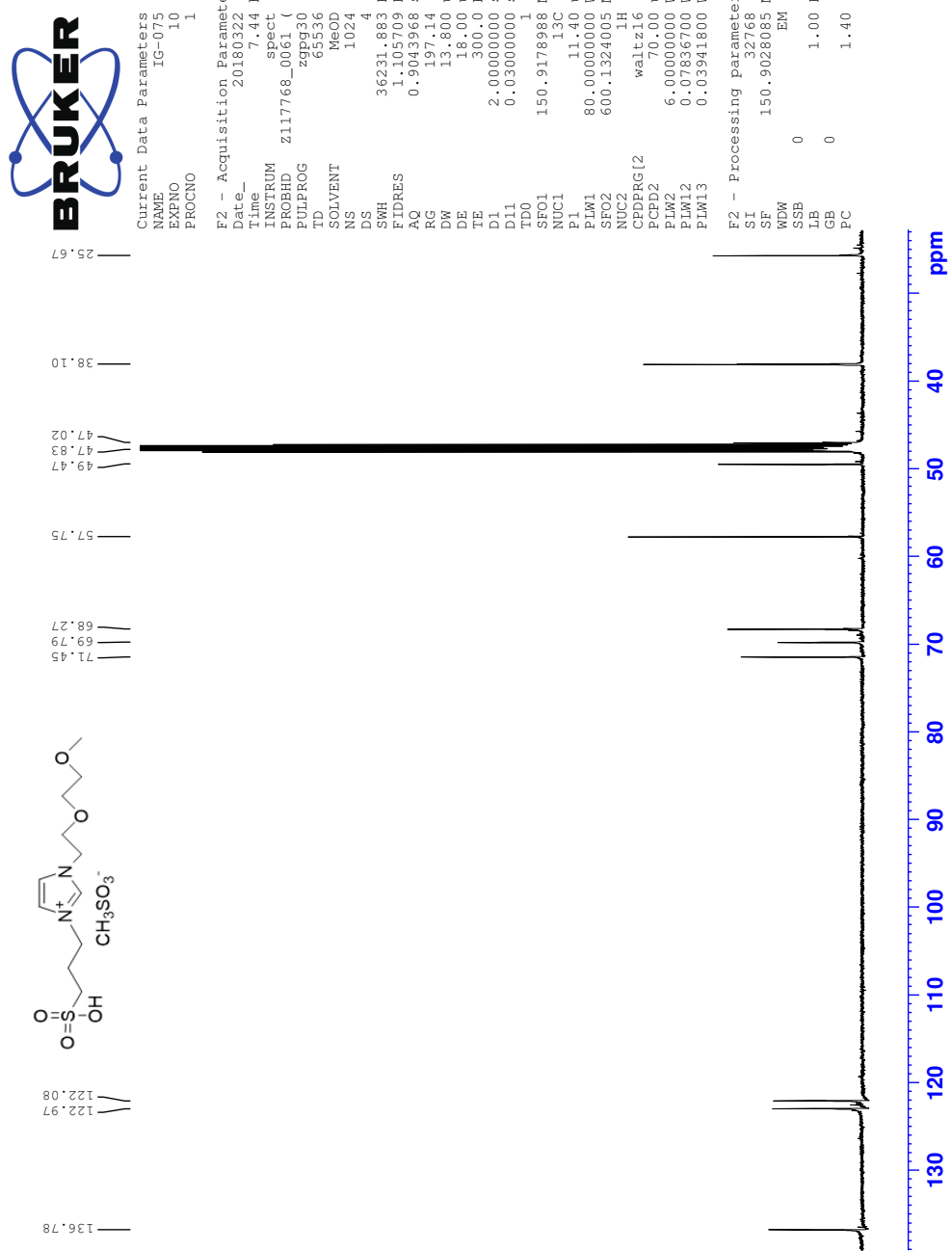
Y Spectra of 1-(2-(2-methoxyethoxy)ethyl)-3-(3-sulfopropyl)-1H-imidazol-3-ium methanesulfonate (8f)

¹H NMR Spectrum of 8f



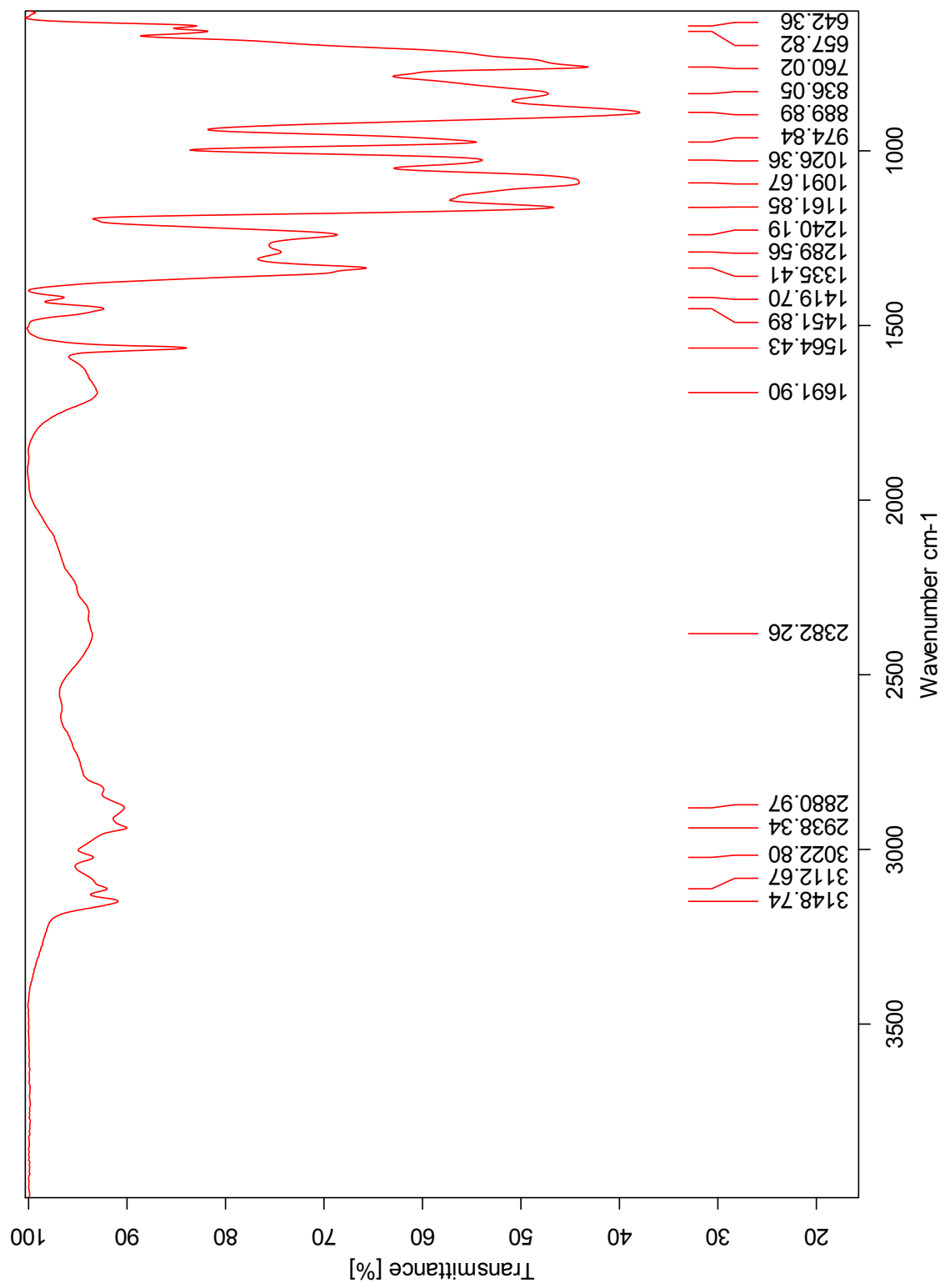
CX

^{13}C NMR Spectrum of 8f



CXI

IR Spectrum of 8f



HRMS Positive mode spectrum of 8f

Elemental Composition Report

Page 1

Single Mass Analysis

Tolerance = 2.0 PPM / DBE: min = -1.5, max = 50.0

Element prediction: Off

Number of isotope peaks used for i-FIT = 3

Monoisotopic Mass, Even Electron Ions

1632 formula(e) evaluated with 5 results within limits (all results (up to 1000) for each mass)

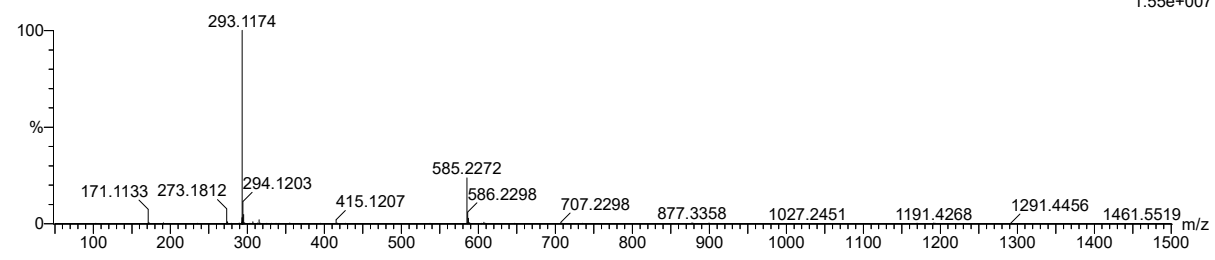
Elements Used:

C: 0-500 H: 0-1000 N: 0-10 O: 0-10 S: 0-5 I: 0-1

2018-131POS 56 (0.543) AM2 (Ar,35000.0,0.00,0.00); Crm (54:62)

1: TOF MS ES+

1.55e+007



Minimum: -1.5
Maximum: 5000.0 2.0 50.0

Mass	Calc. Mass	mDa	PPM	DBE	i-FIT	Norm	Conf (%)	Formula
293.1174	293.1171	0.3	1.0	2.5	1693.1	0.001	99.95	C11 H21 N2 O5 S
	293.1178	-0.4	-1.4	11.5	1707.5	14.407	0.00	C19 H17 O3
	293.1178	-0.4	-1.4	-1.5	1701.3	8.235	0.03	C4 H21 N8 O3 S2
	293.1169	0.5	1.7	-0.5	1705.3	12.206	0.00	C3 H17 N8 O8
	293.1180	-0.6	-2.0	1.5	1701.4	8.262	0.03	C12 H25 N2 S3

HRMS Negative mode spectrum of 8f

Elemental Composition Report

Page 1

Single Mass Analysis

Tolerance = 2.0 PPM / DBE: min = -1.5, max = 50.0

Element prediction: Off

Number of isotope peaks used for i-FIT = 3

Monoisotopic Mass, Even Electron Ions

125 formula(e) evaluated with 1 results within limits (all results (up to 1000) for each mass)

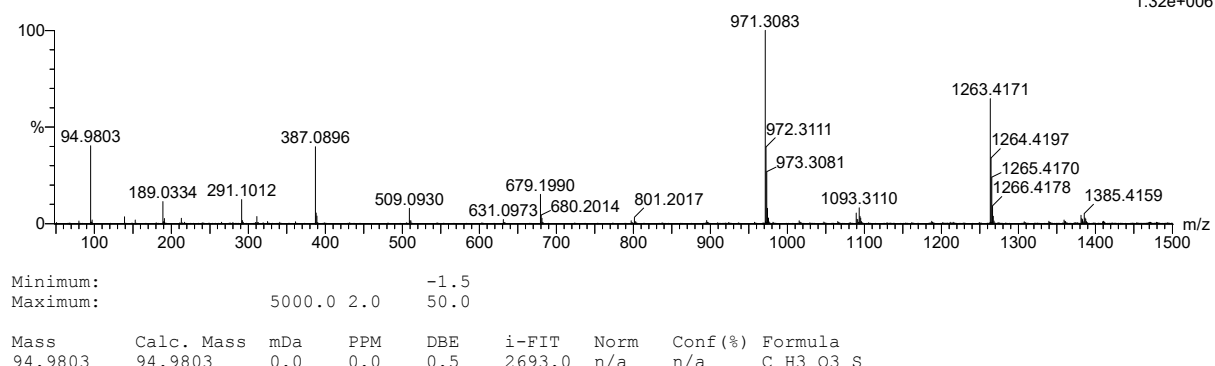
Elements Used:

C: 0-500 H: 0-1000 N: 0-10 O: 0-10 F: 0-10 S: 0-5 I: 0-1

2018-131NEG 26 (0.535) AM2 (Ar,35000.0,0.00,0.00); Crm (26:29)

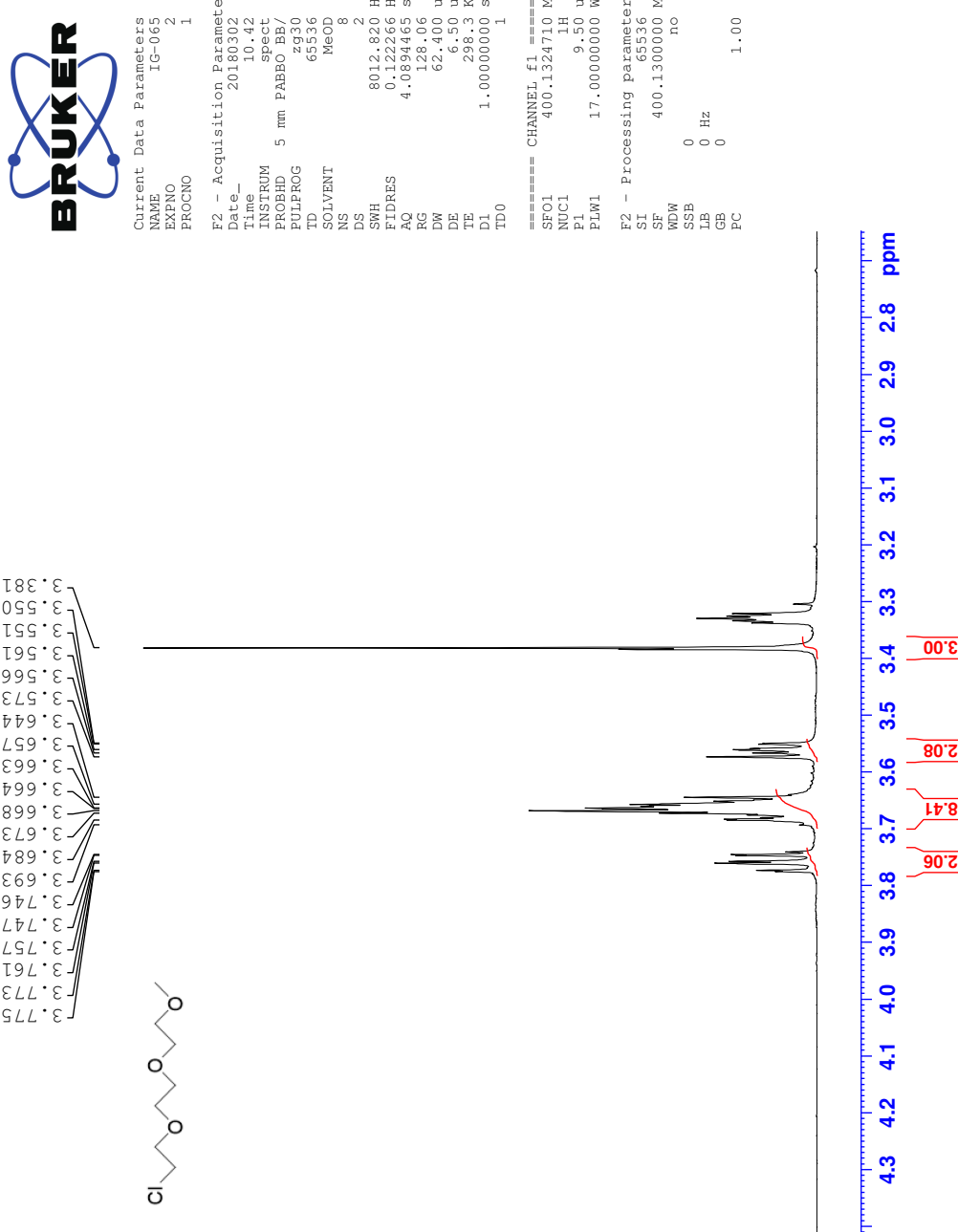
1: TOF MS ES-

1.32e+006



Z Spectrum of 1-chloro-2-(2-(2-methoxyethoxy)ethoxy)-ethane (9)

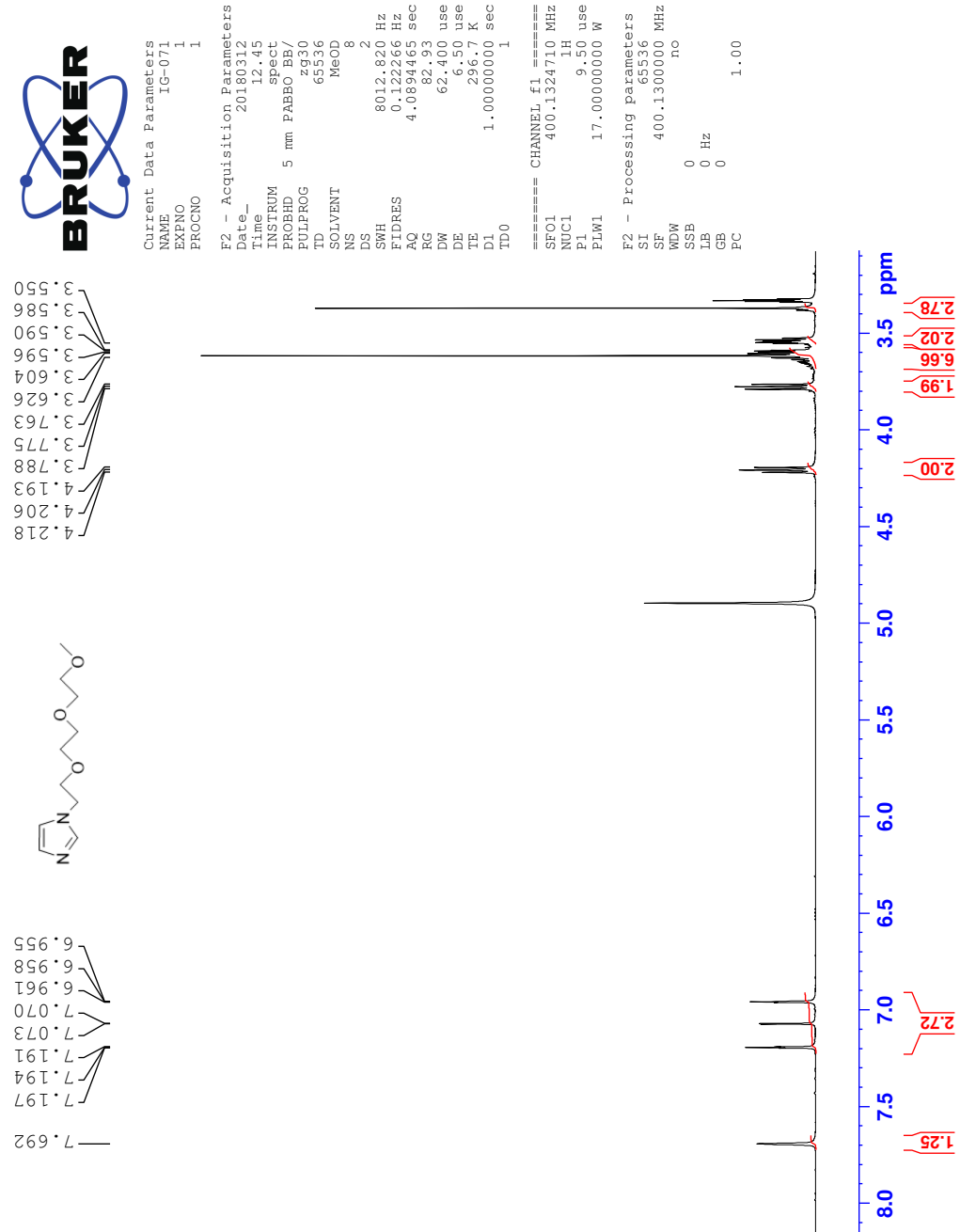
^1H NMR Spectrum of 9



CXV

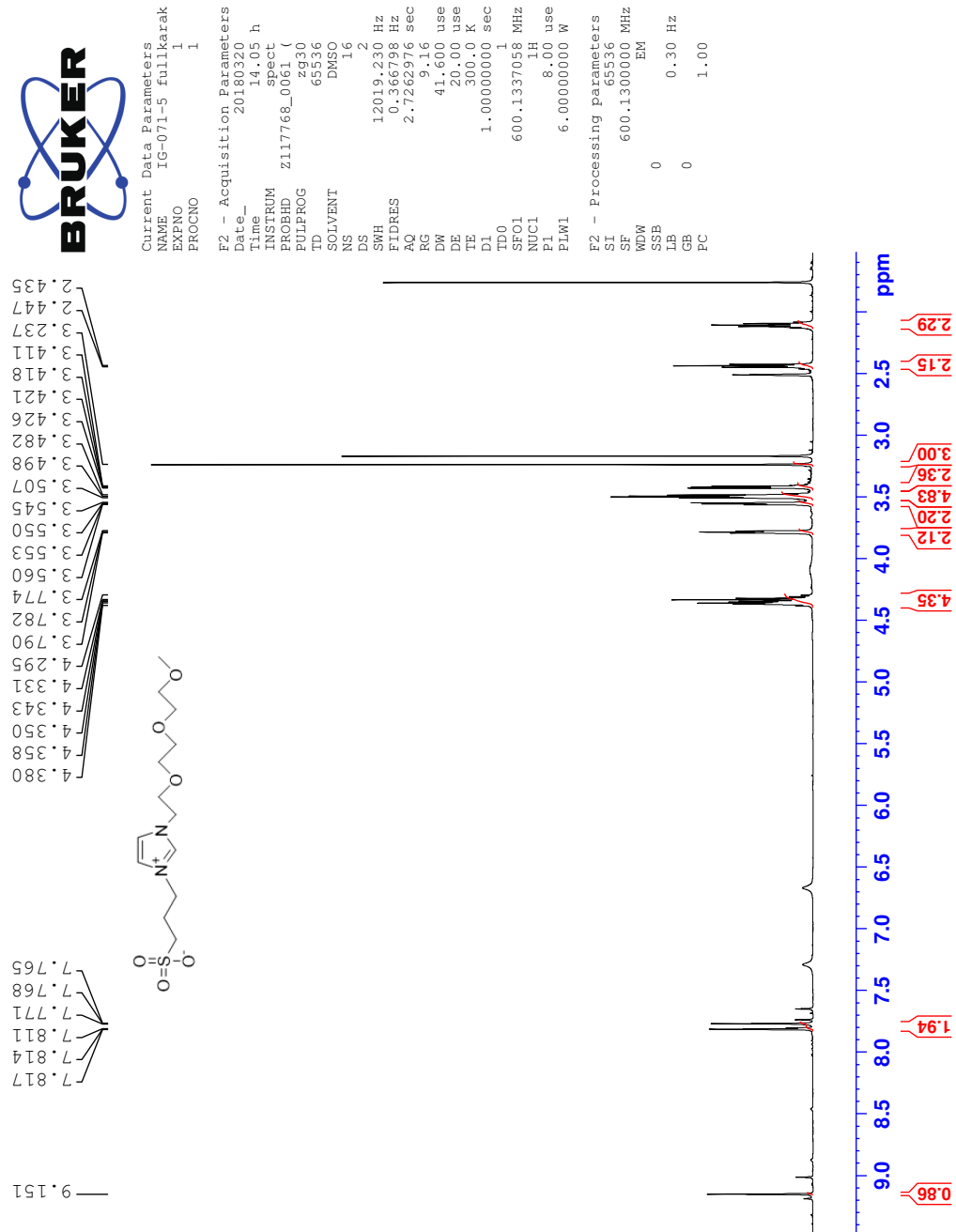
AA Spectrum of 1-(2-(2-methoxyethoxy)ethoxy)ethyl-imidazole (10a)

¹H NMR Spectrum of 10a

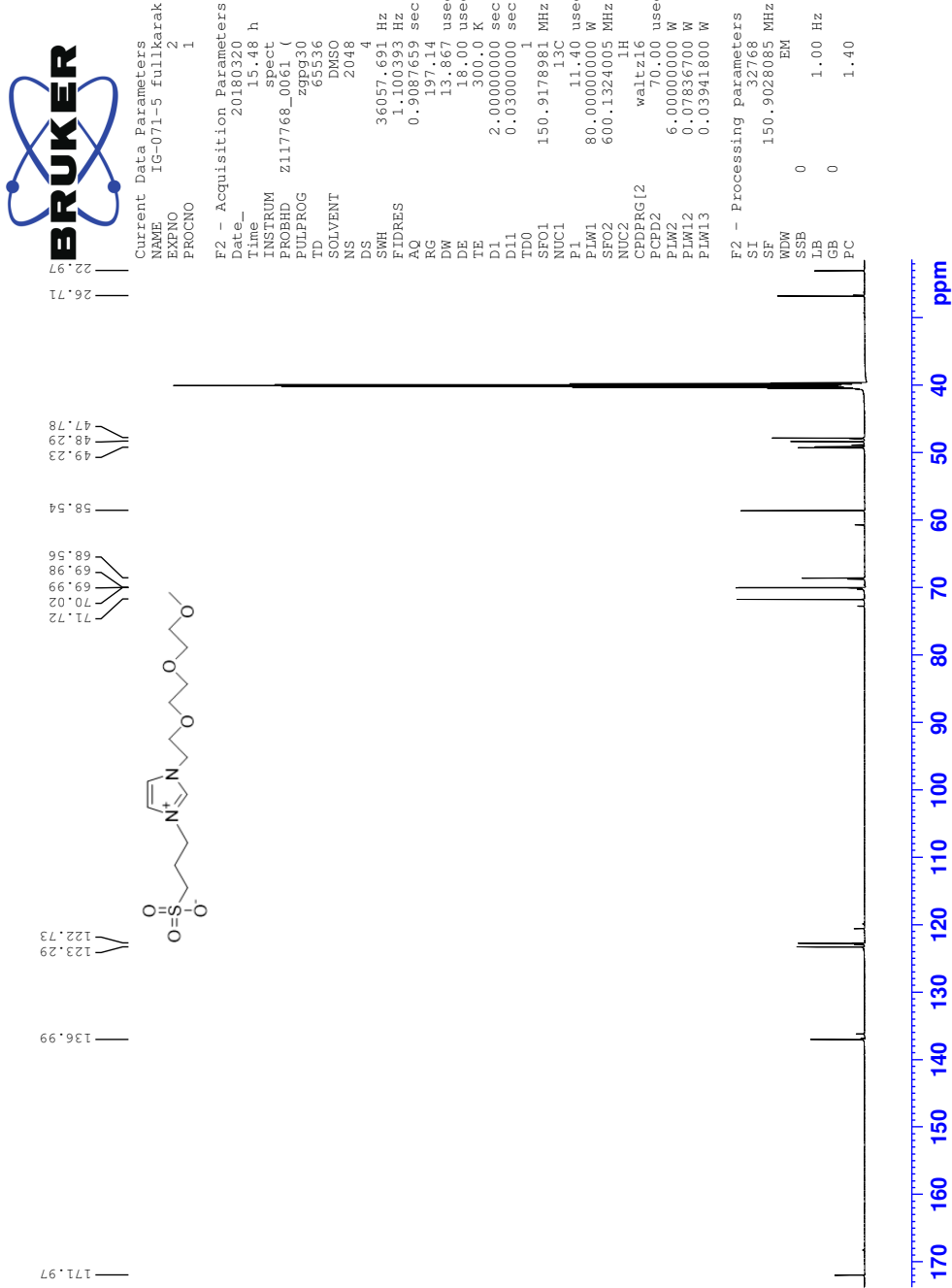


AB Spectra of 3-(1-(2-(2-methoxyethoxy)ethoxy)ethyl)-imidazol-3-ium-3-yl)propane-1-sulfonate (10b)

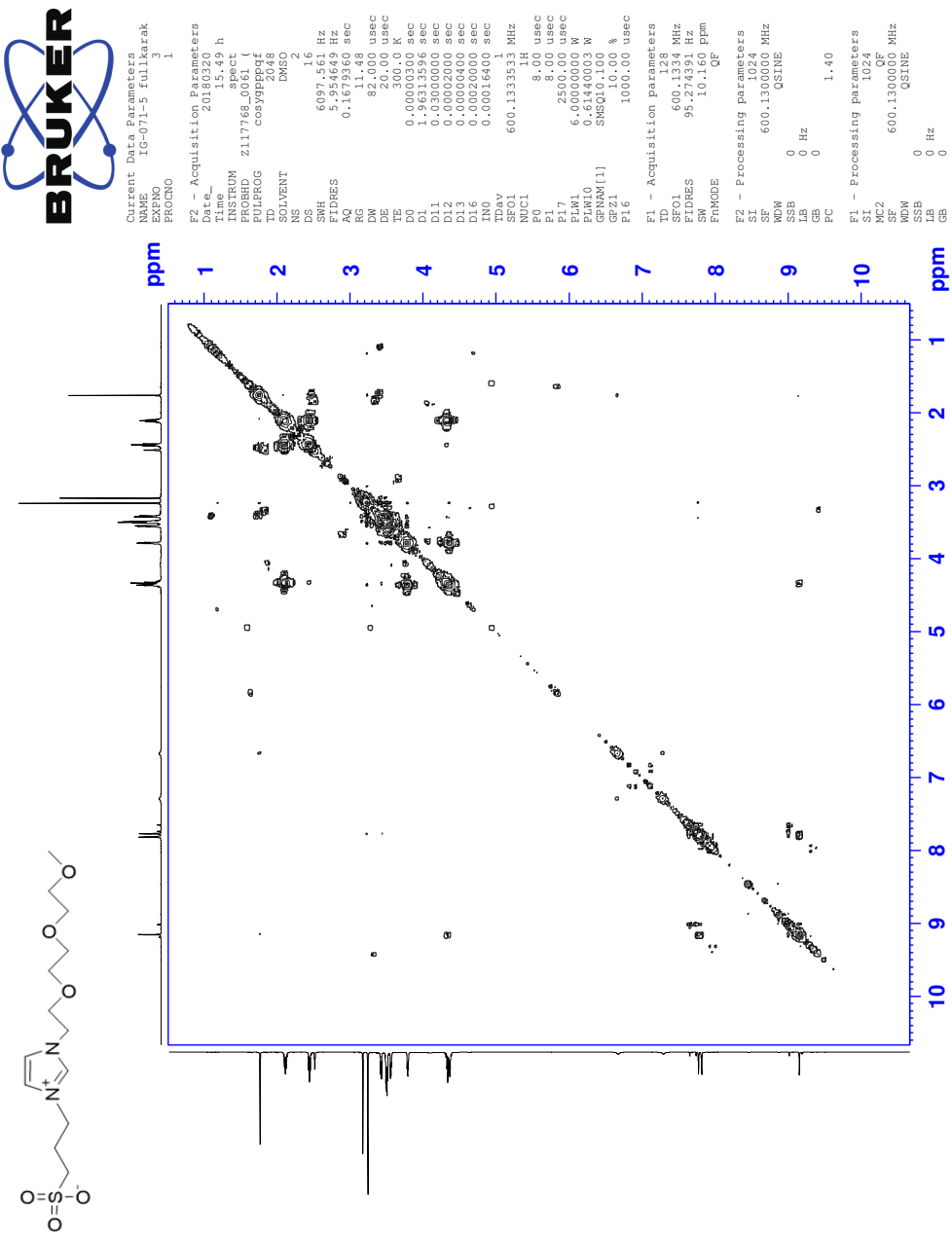
¹H NMR Spectrum of 10b



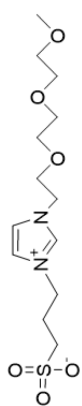
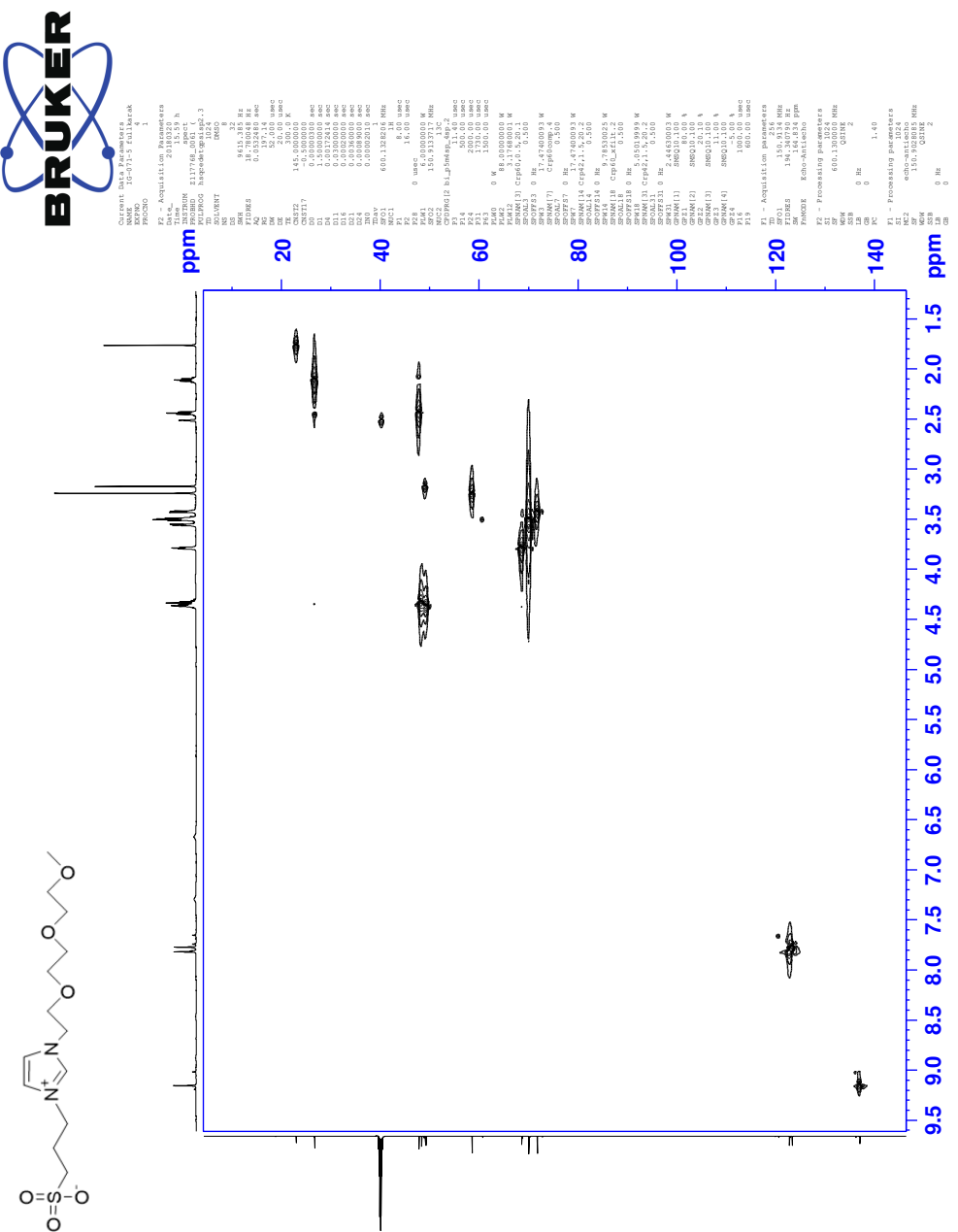
¹³C NMR Spectrum of 10b



COSY NMR Spectrum of 10b

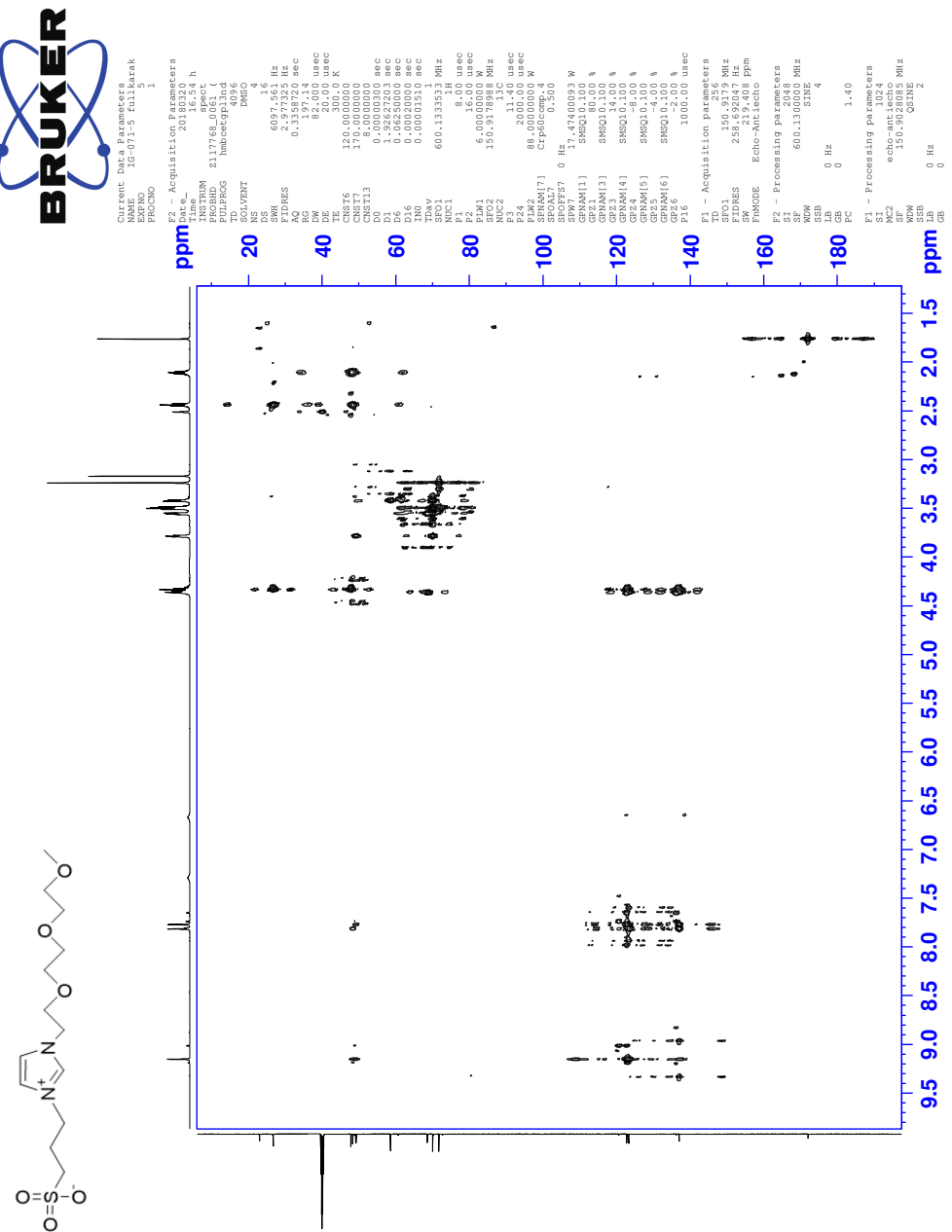


HSQC NMR Spectrum of 10b

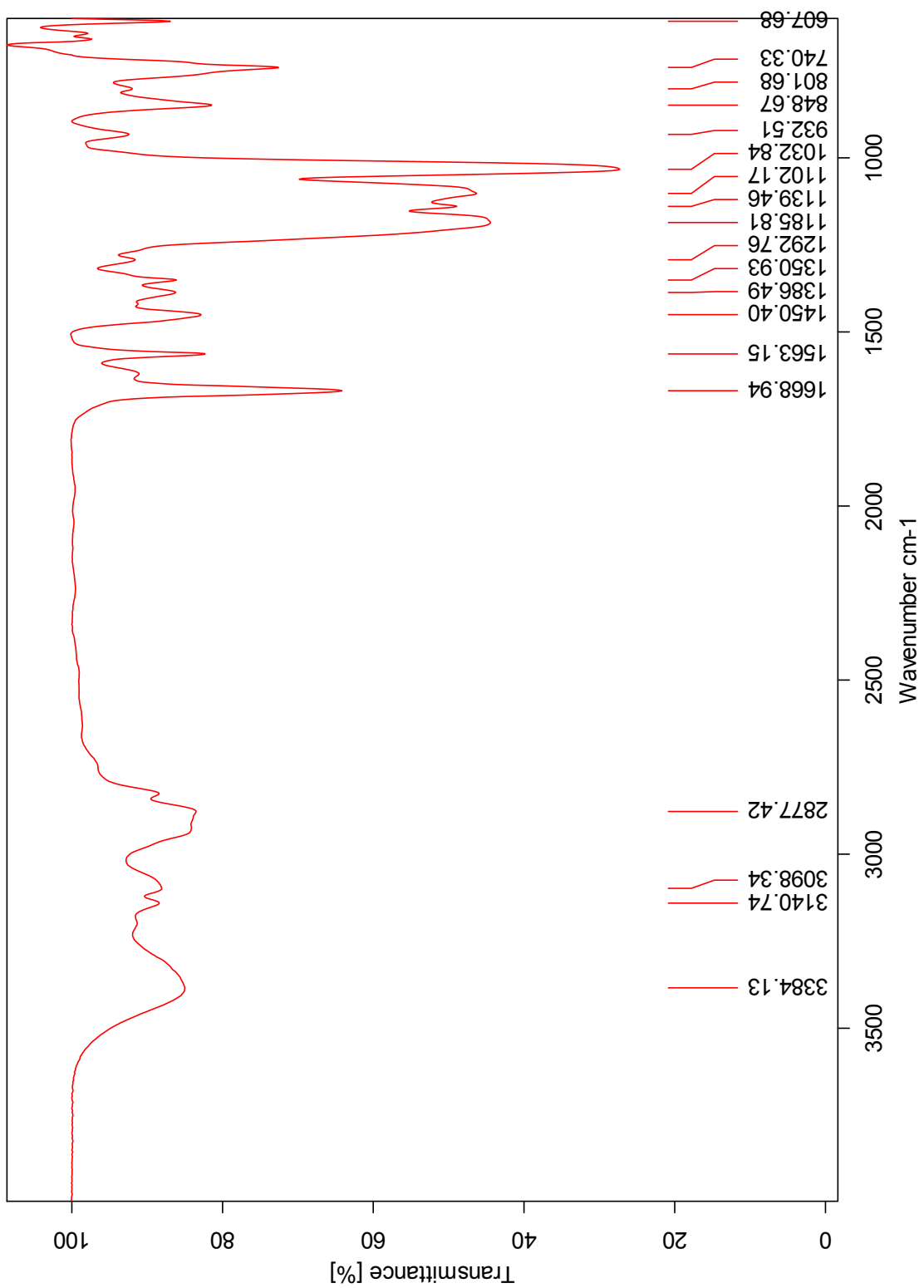


CXX

HMBC NMR Spectrum of 10b



IR Spectrum of 10b



HRMS Spectrum of 10b

Elemental Composition Report

Page 1

Single Mass Analysis

Tolerance = 2.0 PPM / DBE: min = -1.5, max = 50.0

Element prediction: Off

Number of isotope peaks used for i-FIT = 3

Monoisotopic Mass, Even Electron Ions

3314 formula(e) evaluated with 3 results within limits (all results (up to 1000) for each mass)

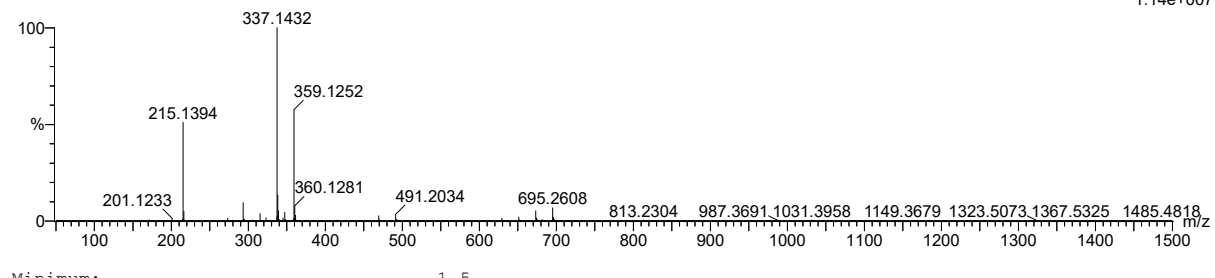
Elements Used:

C: 0-500 H: 0-1000 N: 0-10 O: 0-10 Na: 0-1 S: 0-5

2018-116POS 145 (1.363) AM2 (Ar,35000.0,0.00,0.00); Cm (143:150)

1: TOF MS ES+

1.14e+007

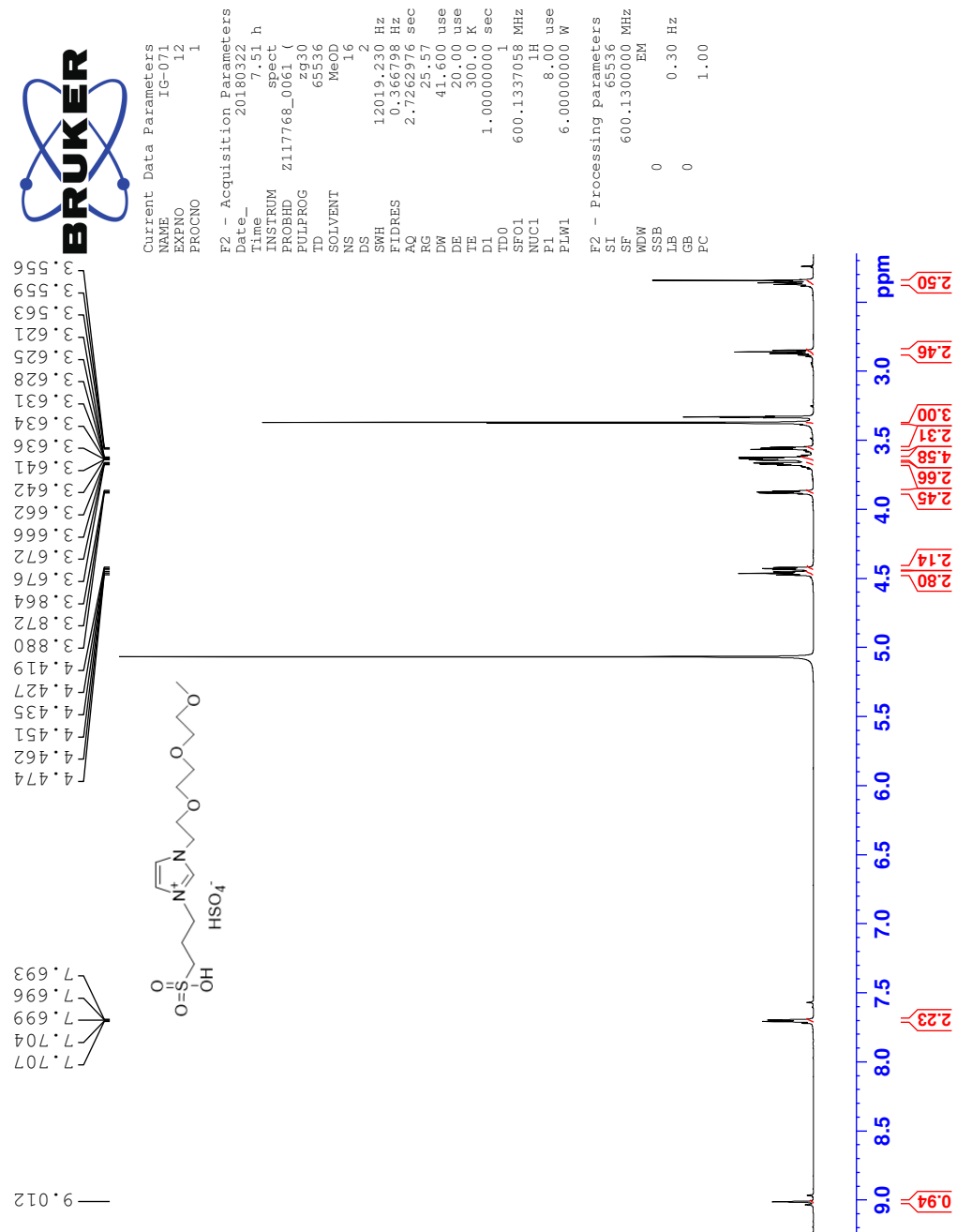


Minimum: -1.5
Maximum: 5000.0 2.0 50.0

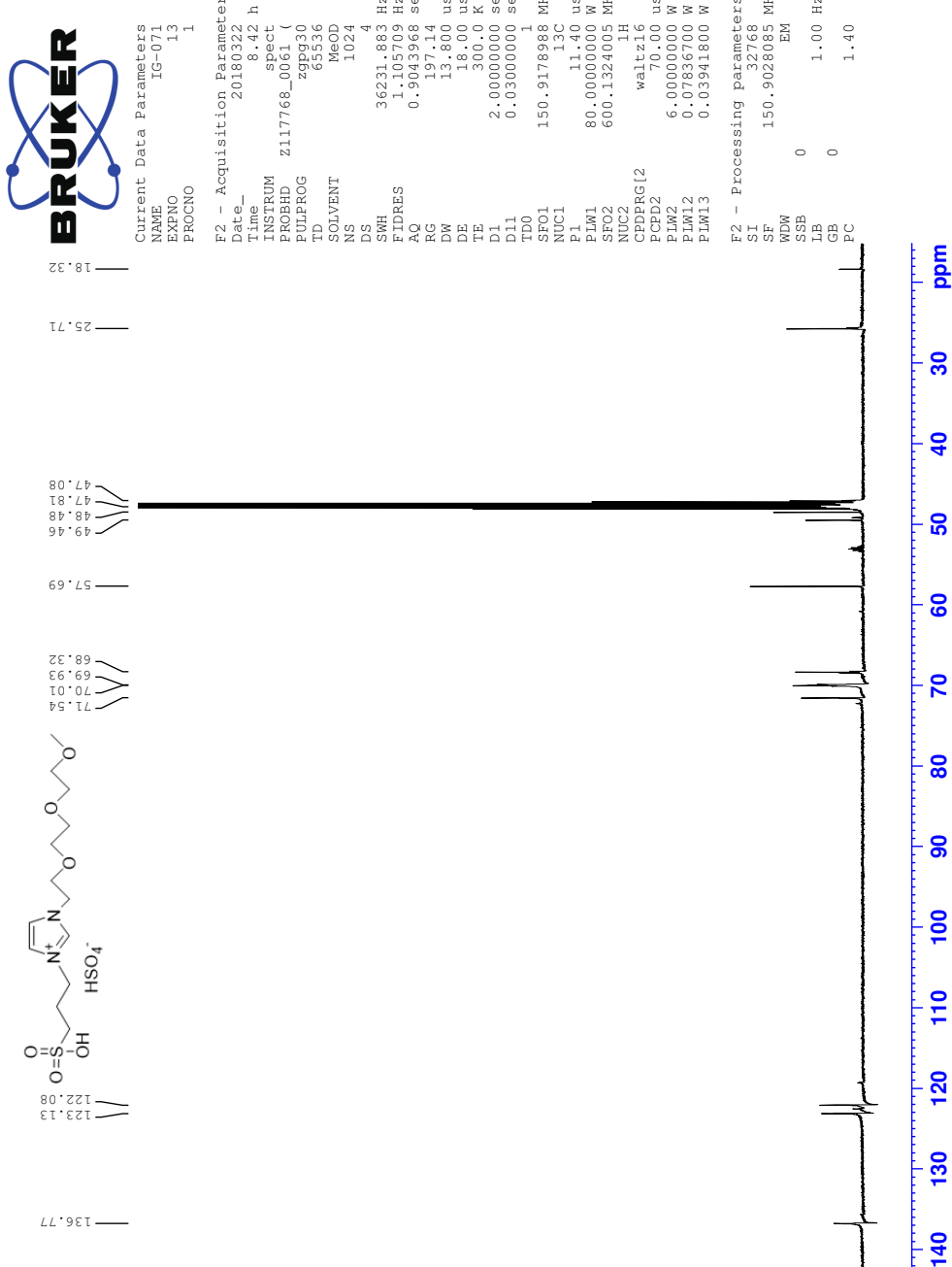
Mass	Calc. Mass	mDa	PPM	DBE	i-FIT	Norm	Conf (%)	Formula
337.1432	337.1433	-0.1	-0.3	2.5	1576.2	0.000	100.00	C13 H25 N2 O6 S
	337.1431	0.1	0.3	-0.5	1588.3	12.171	0.00	C5 H21 N8 O9
	337.1429	0.3	0.9	13.5	1590.7	14.532	0.00	C20 H18 N4 Na

AC Spectra of 1-(2-(2-methoxyethoxy)ethoxy)ethyl-3-(3-sulfopropyl)-1H-imidazol-3-ium hydrogen sulfonate(10c)

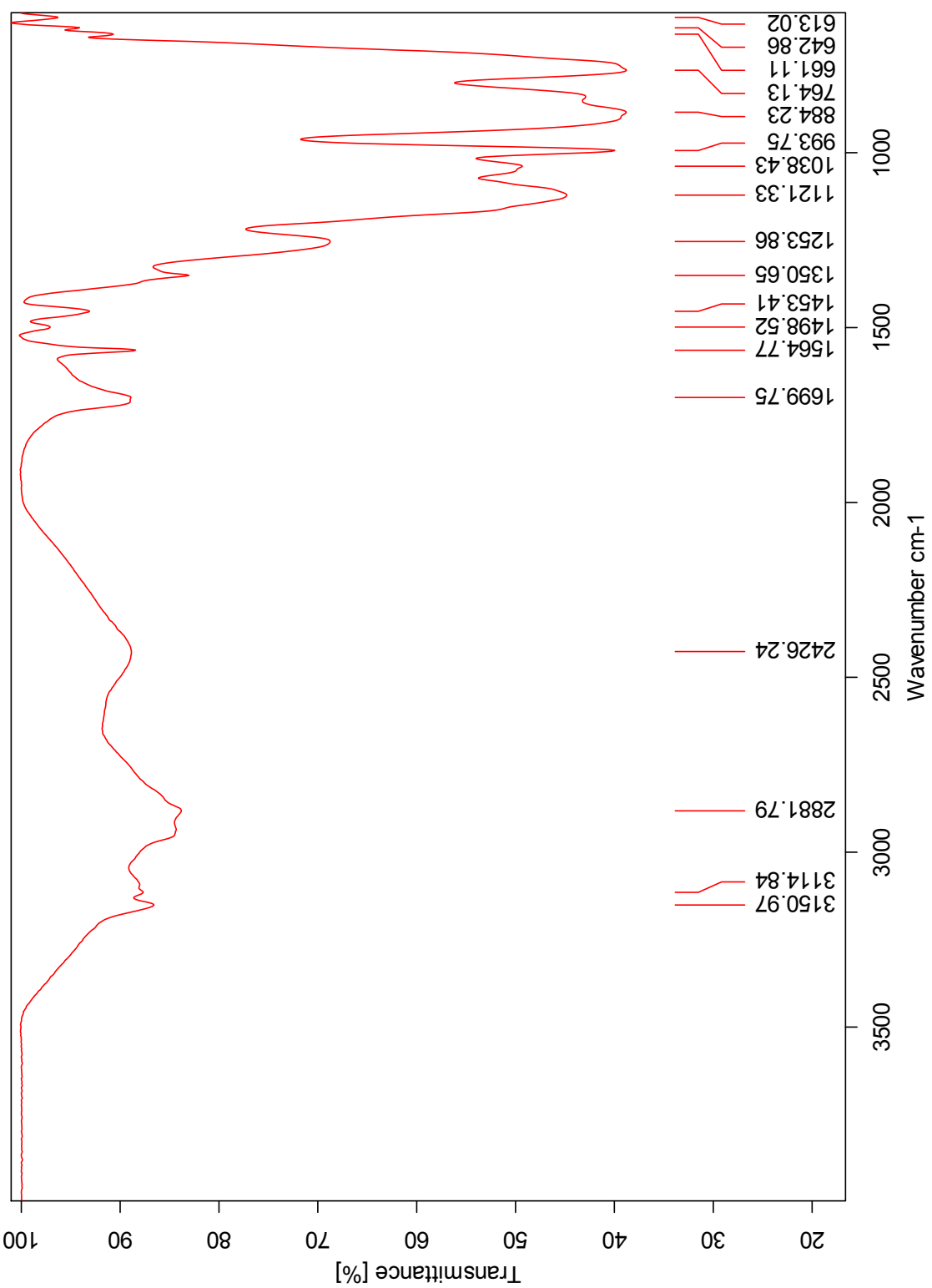
¹H NMR Spectrum of 10c



¹³C NMR Spectrum of 10c



IR Spectrum of 10c



HRMS Positive mode spectrum of 10c

Elemental Composition Report

Page 1

Single Mass Analysis

Tolerance = 3.0 PPM / DBE: min = -1.5, max = 50.0

Element prediction: Off

Number of isotope peaks used for i-FIT = 3

Monoisotopic Mass, Even Electron Ions

4269 formula(e) evaluated with 4 results within limits (all results (up to 1000) for each mass)

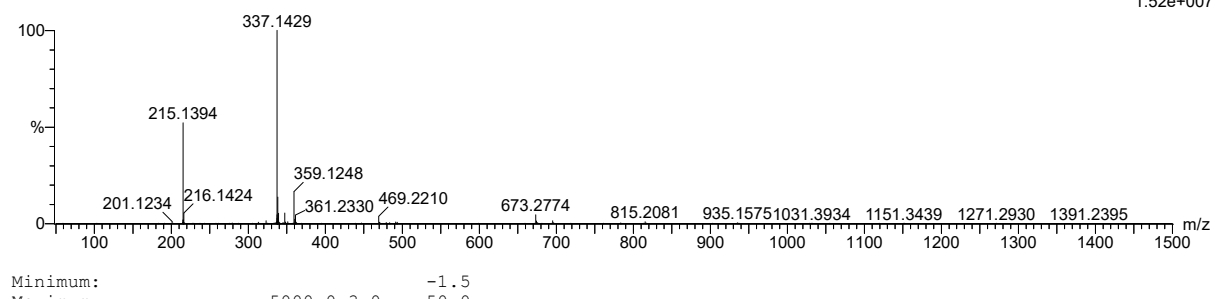
Elements Used:

C: 0-500 H: 0-1000 N: 0-10 O: 0-10 Na: 0-1 S: 0-5 I: 0-1

2018-138pos 9 (0.105) AM2 (Ar,35000.0,0.00,0.00); Cm (7:13)

1: TOF MS ES+

1.52e+007



Minimum: -1.5
Maximum: 5000.0 3.0 50.0

Mass	Calc. Mass	mDa	PPM	DBE	i-FIT	Norm	Conf (%)	Formula
337.1429	337.1433	-0.4	-1.2	2.5	1640.8	0.317	72.83	C13 H25 N2 O6 S
	337.1423	0.6	1.8	4.5	1641.8	1.303	27.17	C12 H22 N6 O2 Na S
	337.1431	-0.2	-0.6	-0.5	1652.4	11.919	0.00	C5 H21 N8 O9
	337.1429	0.0	0.0	13.5	1654.4	13.928	0.00	C20 H18 N4 Na

HRMS Negative mode spectrum of 10c

Elemental Composition Report

Page 1

Single Mass Analysis

Tolerance = 3.0 PPM / DBE: min = -1.5, max = 50.0

Element prediction: Off

Number of isotope peaks used for i-FIT = 3

Monoisotopic Mass, Even Electron Ions

104 formula(e) evaluated with 1 results within limits (all results (up to 1000) for each mass)

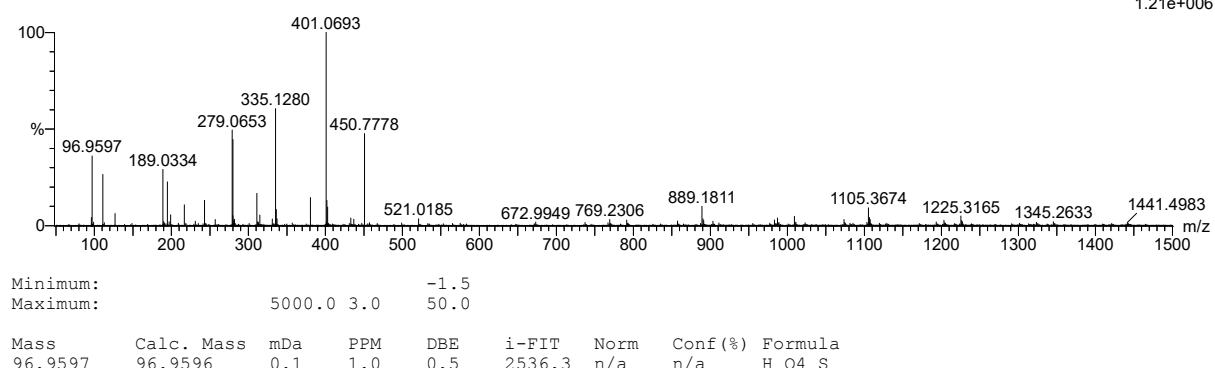
Elements Used:

C: 0-500 H: 0-1000 N: 0-10 O: 0-10 Na: 0-1 S: 0-5 I: 0-1

2018-138neg_7 (0.155) AM2 (Ar,35000.0,0.00,0.00); Cm (5:7)

1: TOF MS ES-

1.21e+006

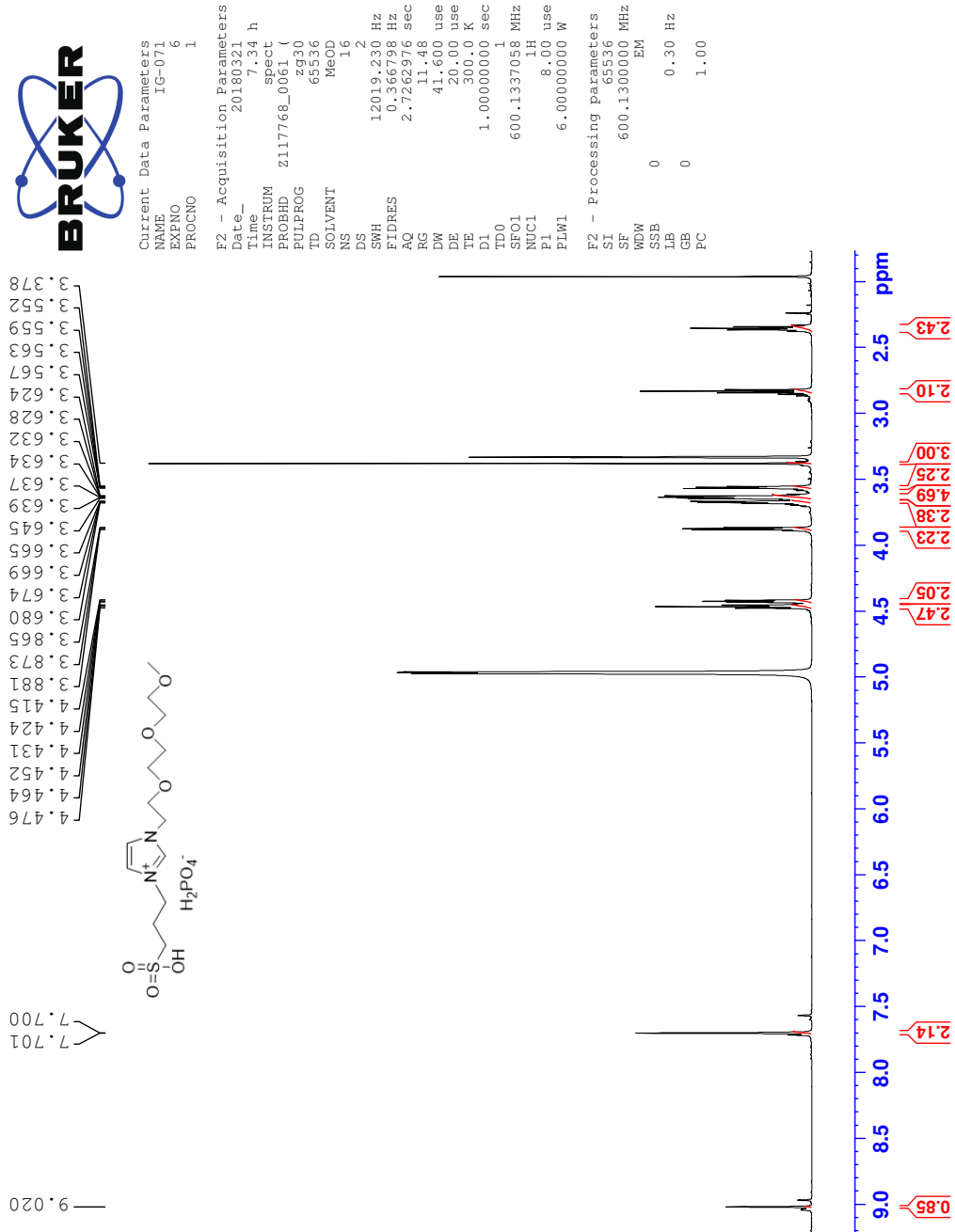


Minimum: -1.5
Maximum: 5000.0 3.0

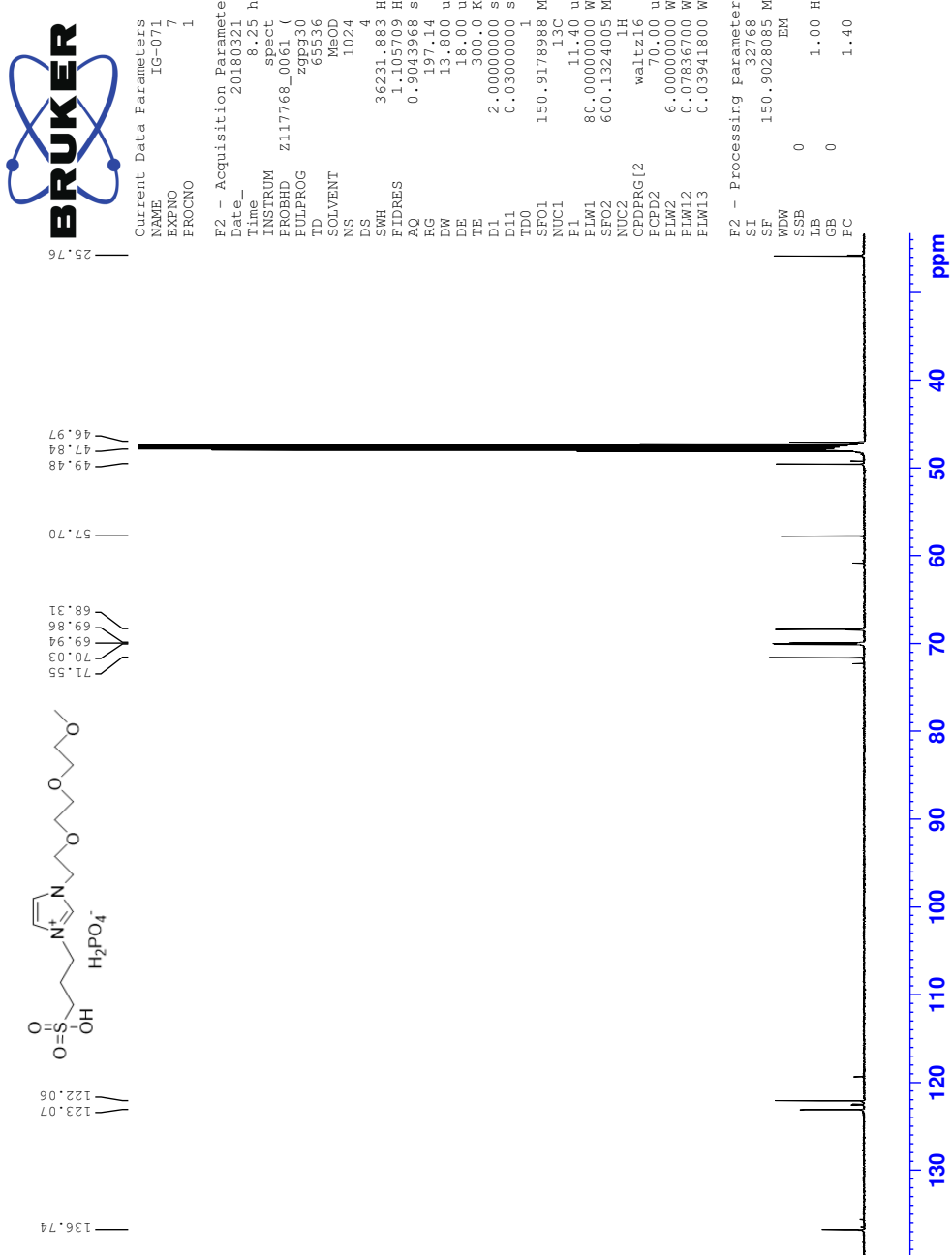
Mass	Calc. Mass	mDa	PPM	DBE	i-FIT	Norm	Conf (%)	Formula
96.9597	96.9596	0.1	1.0	0.5	2536.3	n/a	n/a	H O ₄ S

AD Spectra of 1-(2-(2-methoxyethoxy)ethoxy)ethyl-3-(3-sulfopropyl)-1H-imidazol-3-ium dihydrogen phosphate (10d)

¹H NMR Spectrum of 10d



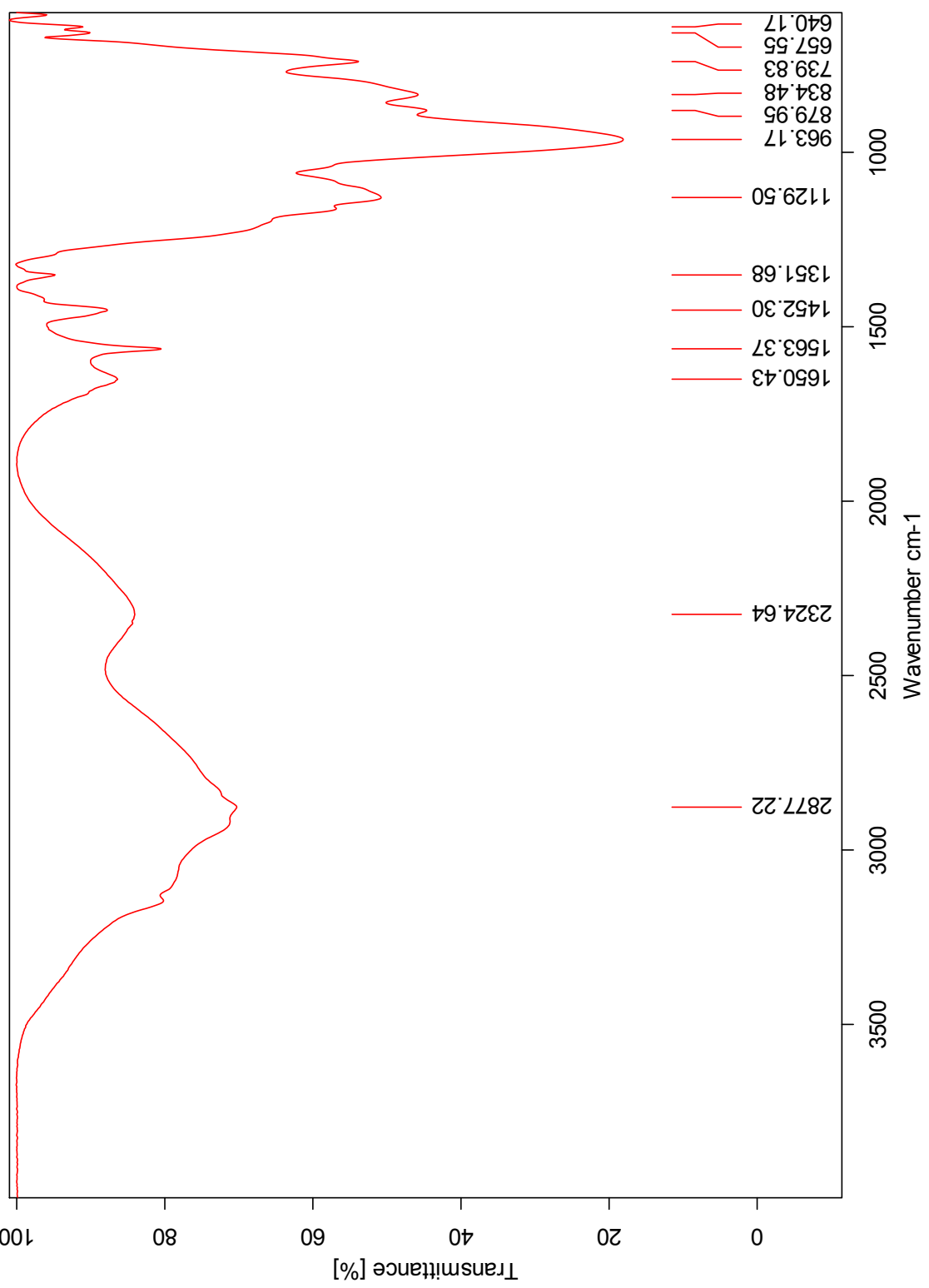
¹³C NMR Spectrum of 10d



CXXX

IR Spectrum of 10d

C:\Users\ALPHA\Documents\Bruker\OPUS_7.5.18\DATA\MEAS\IG-071d.0



HRMS Positive mode spectrum of 10d

Elemental Composition Report

Page 1

Single Mass Analysis

Tolerance = 2.0 PPM / DBE: min = -1.5, max = 50.0

Element prediction: Off

Number of isotope peaks used for i-FIT = 3

Monoisotopic Mass, Even Electron Ions

4572 formula(e) evaluated with 4 results within limits (all results (up to 1000) for each mass)

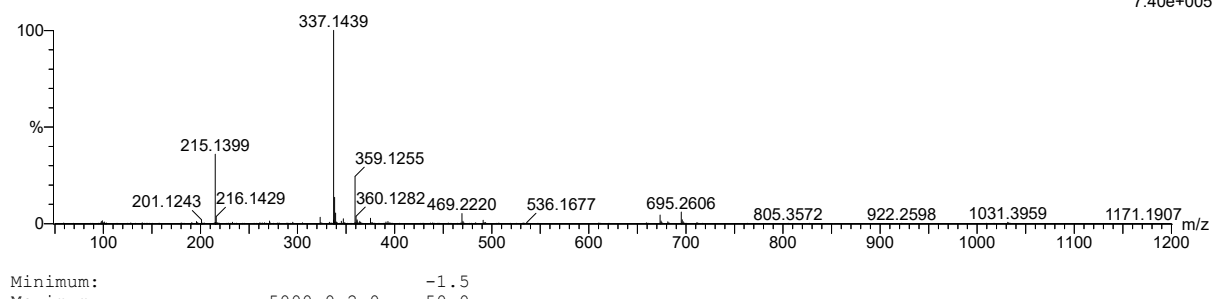
Elements Used:

C: 0-500 H: 0-1000 N: 0-10 O: 0-10 Na: 0-1 S: 0-5 I: 0-1 Au: 0-1

2018-144 27 (0.506) AM2 (Ar,35000.0,0.00,0.00); Cm (26:27)

1: TOF MS ES+

7.40e+005



Minimum: -1.5
Maximum: 5000.0 2.0 50.0

Mass	Calc. Mass	mDa	PPM	DBE	i-FIT	Norm	Conf (%)	Formula
337.1439	337.1440	-0.1	-0.3	11.5	1141.8	14.182	0.00	C21 H21 O4
	337.1440	-0.1	-0.3	-1.5	1135.8	8.107	0.03	C6 H25 N8 O4 S2
	337.1442	-0.3	-0.9	1.5	1137.0	9.312	0.01	C14 H29 N2 O S3
	337.1433	0.6	1.8	2.5	1127.7	0.000	99.96	C13 H25 N2 O6 S

HRMS Negative mode spectrum of 10d

Elemental Composition Report

Page 1

Single Mass Analysis

Tolerance = 50.0 PPM / DBE: min = -1.5, max = 50.0

Element prediction: Off

Number of isotope peaks used for i-FIT = 3

Monoisotopic Mass, Even Electron Ions

154 formula(e) evaluated with 2 results within limits (all results (up to 1000) for each mass)

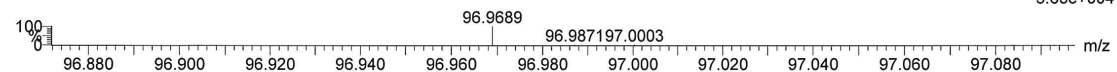
Elements Used:

C: 0-500 H: 0-1000 N: 0-10 O: 0-20 Na: 0-1 P: 0-2 S: 0-3

2018_144newneg 259 (2.409) AM2 (Ar,35000.0,0.00,0.00)

1: TOF MS ES-

5.63e+004

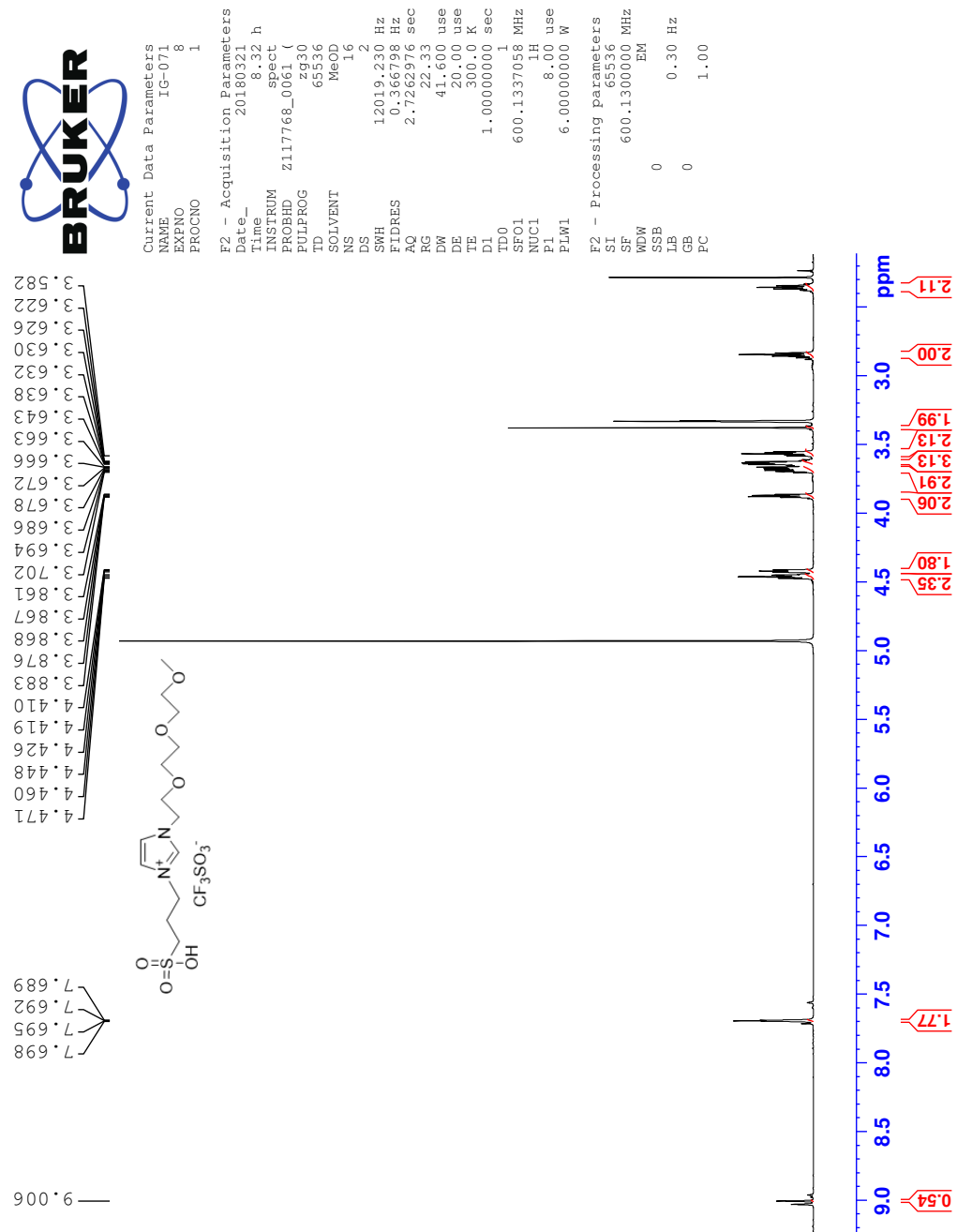


Minimum: -1.5
Maximum: 5.0 50.0

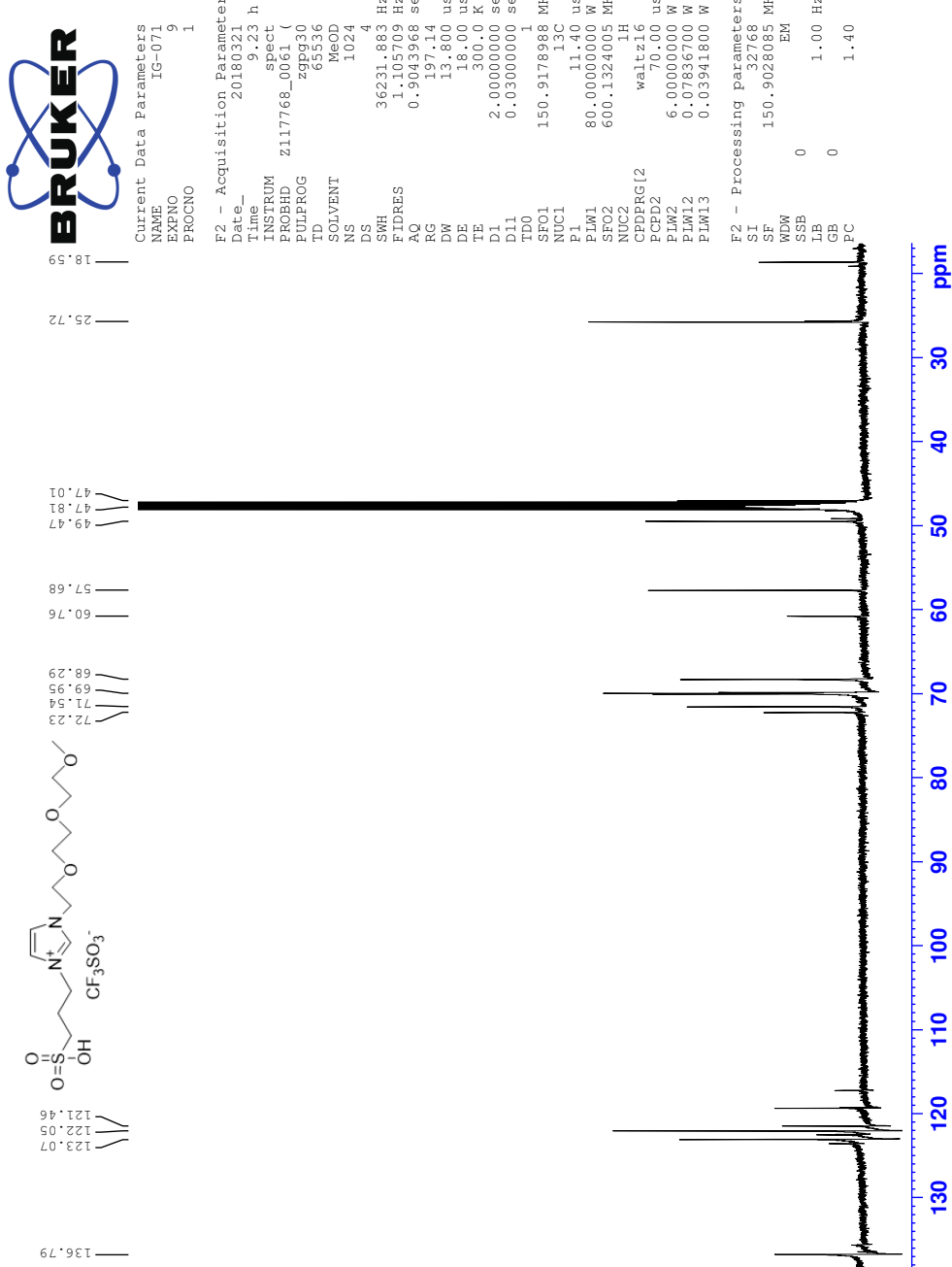
Mass	Calc. Mass	mDa	PPM	DBE	i-FIT	Norm	Conf (%)	Formula
96.9689	96.9691	-0.2	-2.1	0.5	51.7	0.002	99.84	H ₂ O ₄ P
	96.9724	-3.5	-36.1	1.5	58.1	6.427	0.16	C ₂ H ₂ O Na S

AE Spectra of 1-(2-(2-methoxyethoxy)ethoxy)ethyl-3-(3-sulfopropyl)-1H-imidazol-3-ium trifluoromethanesulfonate(10e)

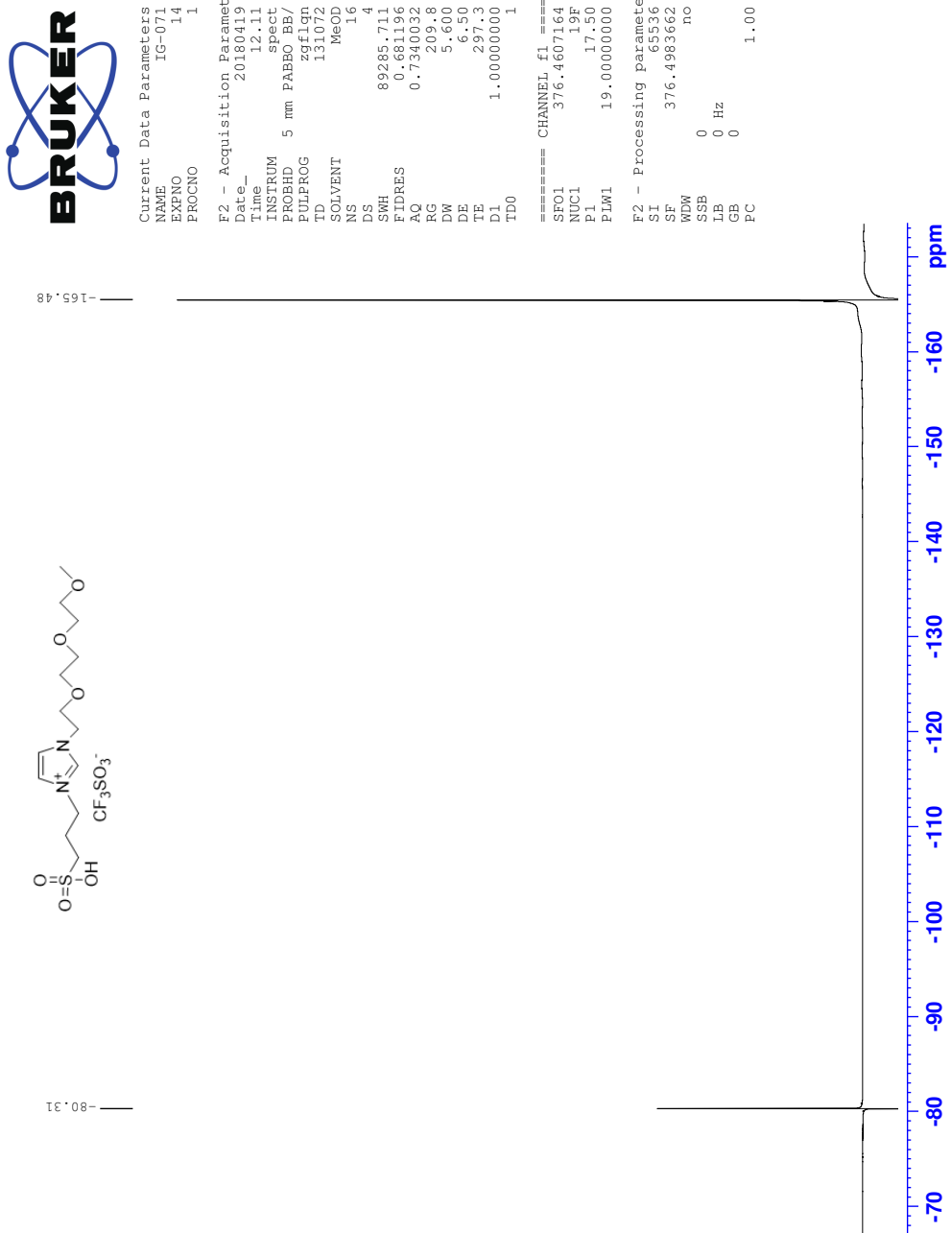
¹H NMR Spectrum of 10e



¹³C NMR Spectrum of 10e

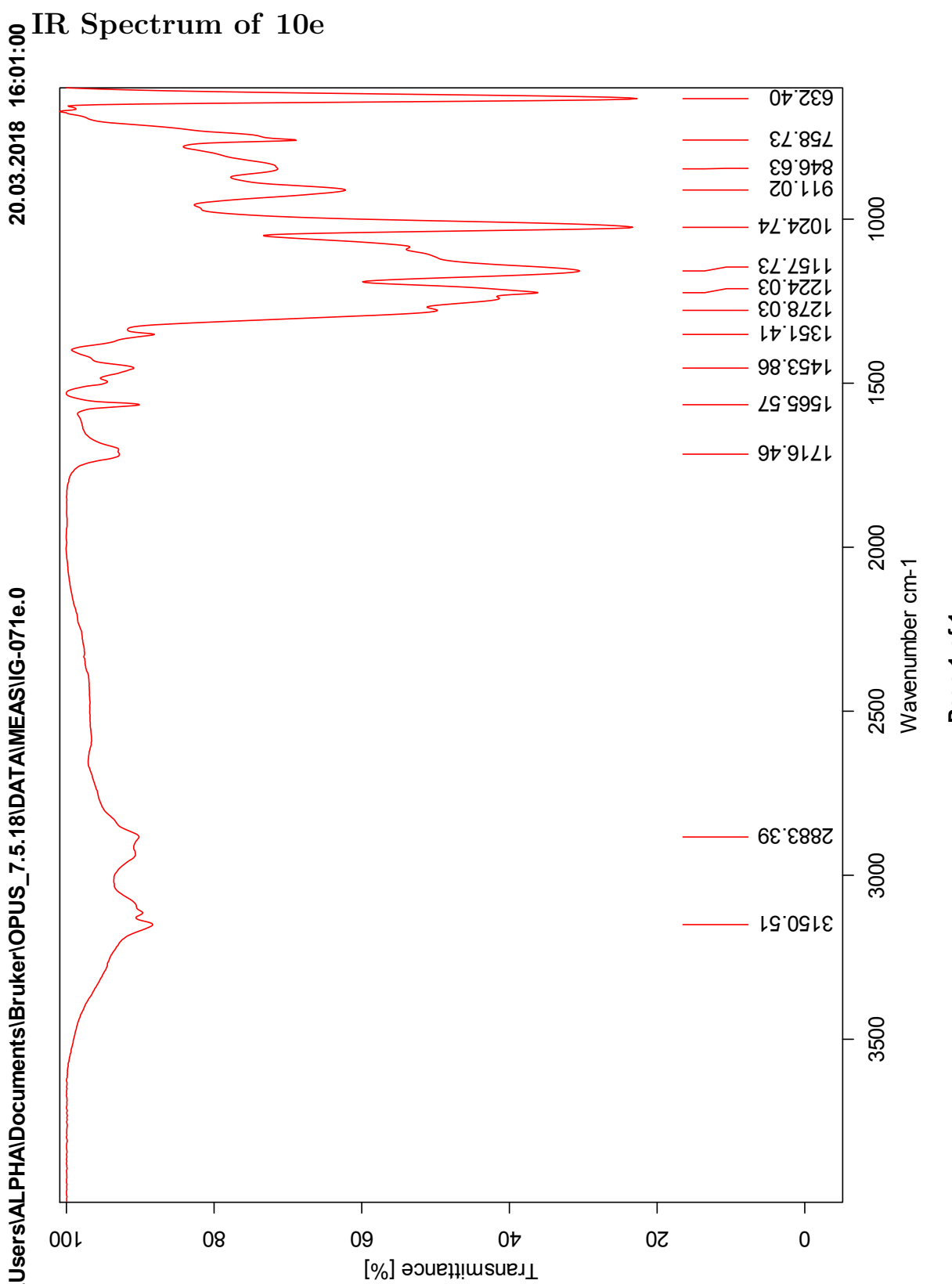


¹⁹F NMR Spectrum of 10e



IR Spectrum of 10e

C:\Users\ALPHA\Documents\Bruker\OPUS_7.5.18\DATA\MEAS\IG-071e.0



HRMS Positive mode spectrum of 10e

Elemental Composition Report

Page 1

Single Mass Analysis

Tolerance = 2.0 PPM / DBE: min = -1.5, max = 50.0

Element prediction: Off

Number of isotope peaks used for i-FIT = 3

Monoisotopic Mass, Even Electron Ions

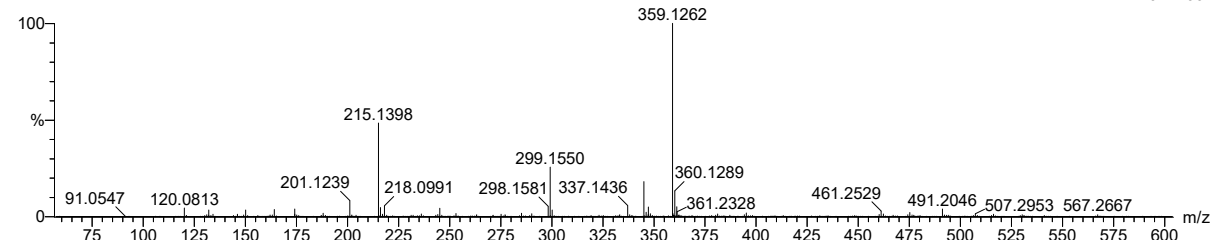
2379 formula(e) evaluated with 5 results within limits (all results (up to 1000) for each mass)

Elements Used:

C: 0-500 H: 0-1000 N: 0-10 O: 0-10 S: 0-5 I: 0-1

2018-125pos 125 (1.169) AM2 (Ar,35000.0,0.00,0.00); Crm (125:140)
1: TOF MS ES+

1.04e+007



Minimum: -1.5
Maximum: 5000.0 2.0 50.0

Mass	Calc. Mass	mDa	PPM	DBE	i-FIT	Norm	Conf (%)	Formula
337.1436	337.1433	0.3	0.9	2.5	1264.3	0.098	90.66	C13 H25 N2 O6 S
	337.1440	-0.4	-1.2	11.5	1272.6	8.349	0.02	C21 H21 O4
	337.1440	-0.4	-1.2	-1.5	1266.7	2.488	8.31	C6 H25 N8 O4 S2
	337.1431	0.5	1.5	-0.5	1271.7	7.448	0.06	C5 H21 N8 O9
	337.1442	-0.6	-1.8	1.5	1268.9	4.655	0.95	C14 H29 N2 O S3

HRMS Negative mode spectrum of 10e

Elemental Composition Report

Page 1

Single Mass Analysis

Tolerance = 2.0 PPM / DBE: min = -1.5, max = 50.0

Element prediction: Off

Number of isotope peaks used for i-FIT = 3

Monoisotopic Mass, Even Electron Ions

585 formula(e) evaluated with 1 results within limits (all results (up to 1000) for each mass)

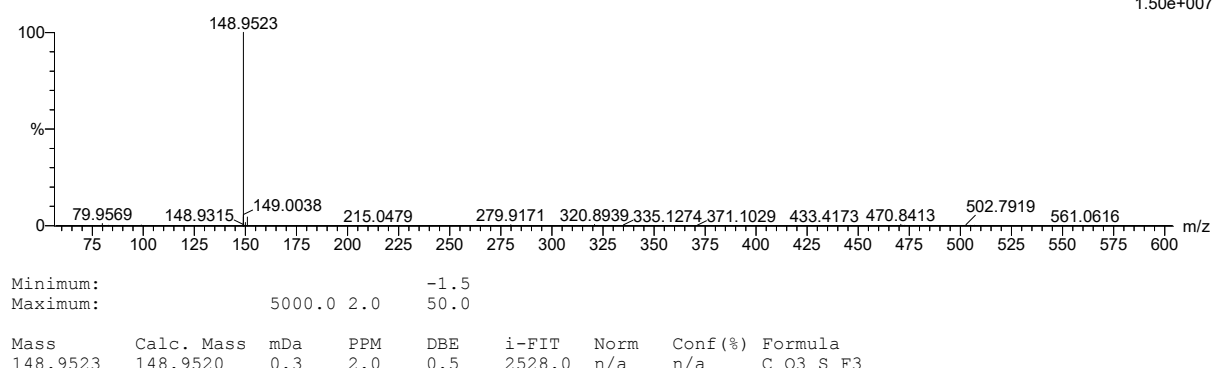
Elements Used:

C: 0-500 H: 0-1000 N: 0-10 O: 0-10 S: 0-5 I: 0-1 F: 0-10

2018-125neg 32 (0.637) AM2 (Ar,35000.0,0.00,0.00); Cm (30:32)

1: TOF MS ES-

1.50e+007

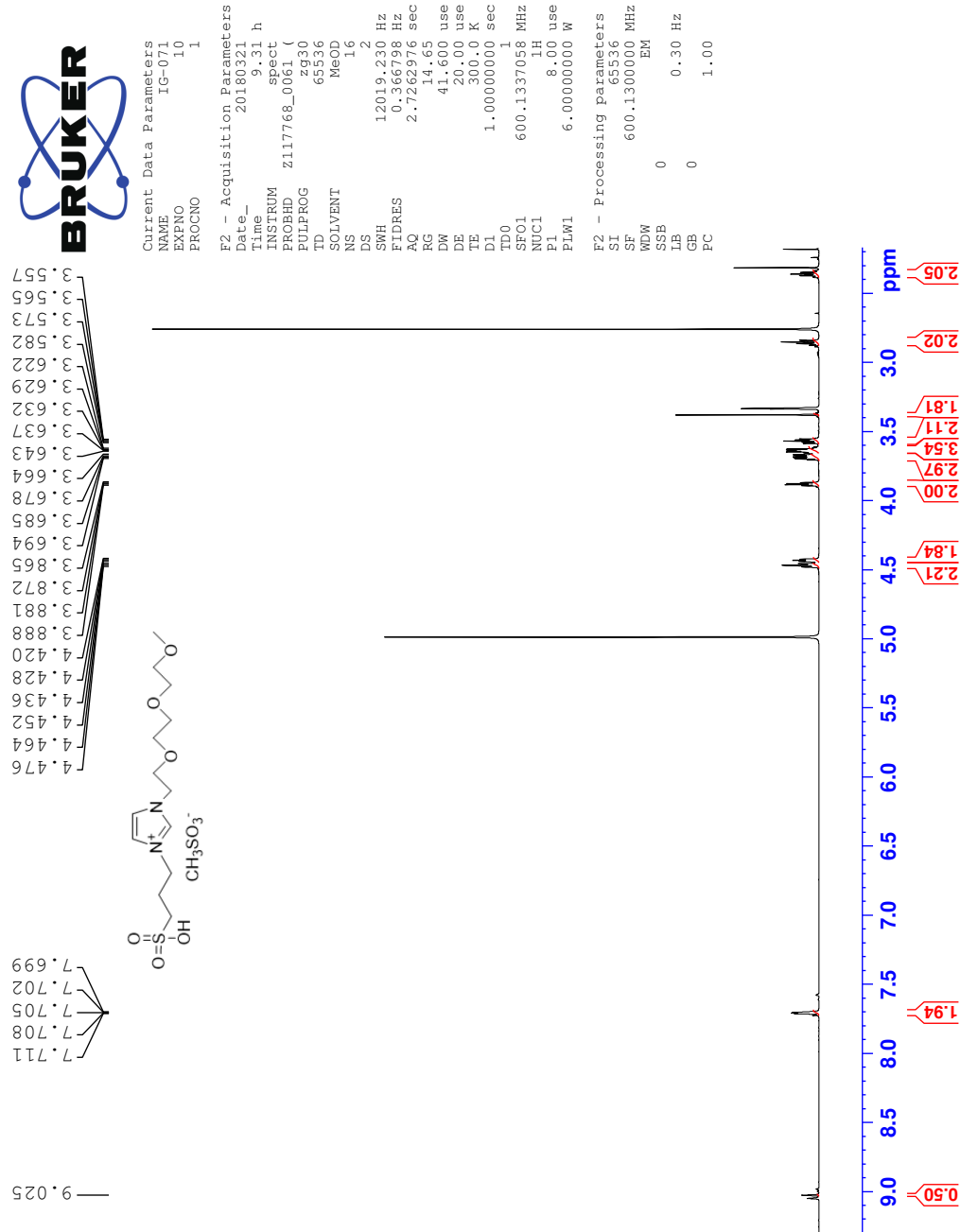


Minimum: -1.5
Maximum: 5000.0 2.0 50.0

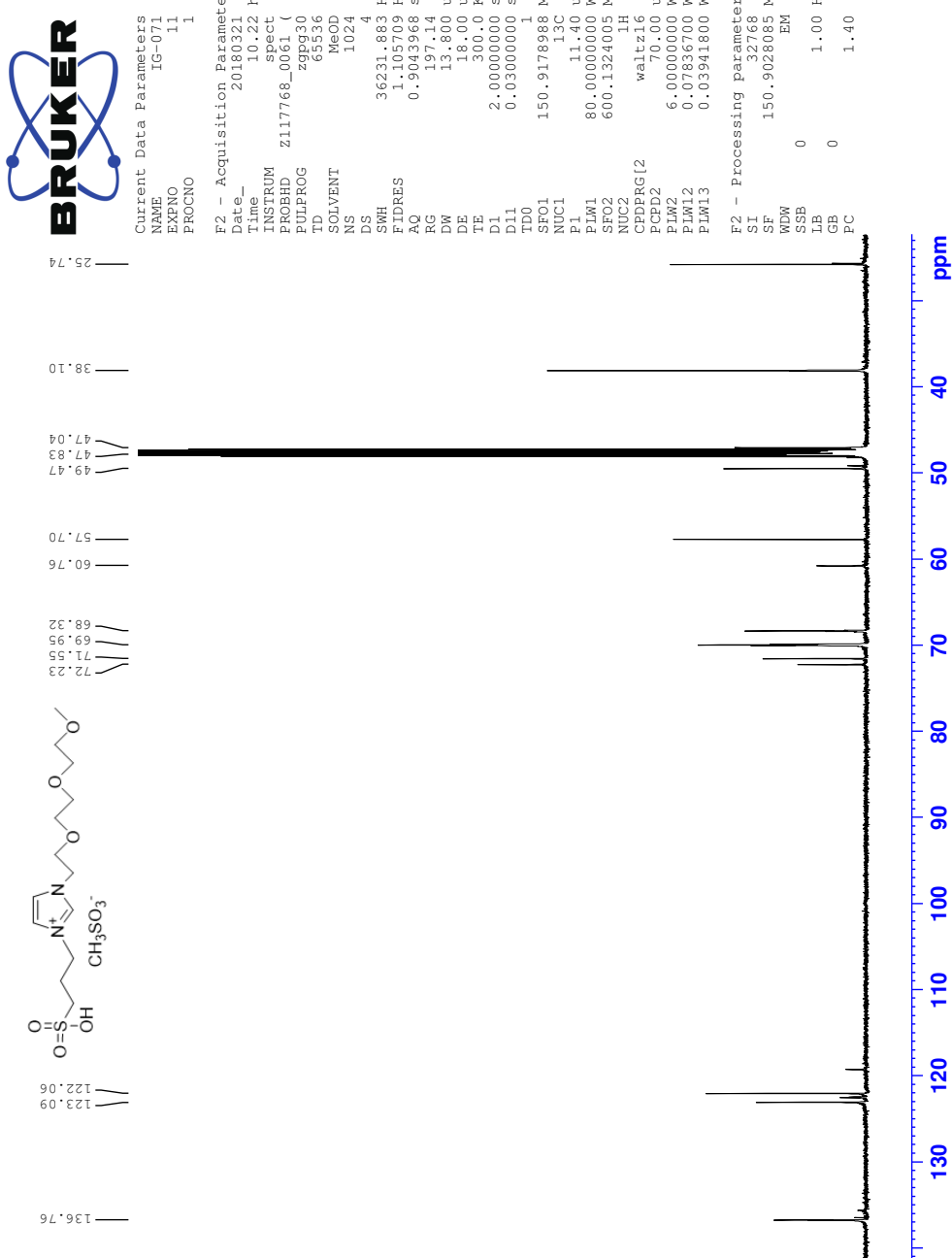
Mass	Calc. Mass	mDa	PPM	DBE	i-FIT	Norm	Conf (%)	Formula
148.9523	148.9520	0.3	2.0	0.5	2528.0	n/a	n/a	C O3 S F3

AF Spectra of 1-(2-(2-methoxyethoxy)ethoxyethyl)-3-(3-sulfopropyl)-1H-imidazol-3-ium methanesulfonate (10f)

¹H NMR Spectrum of 10f



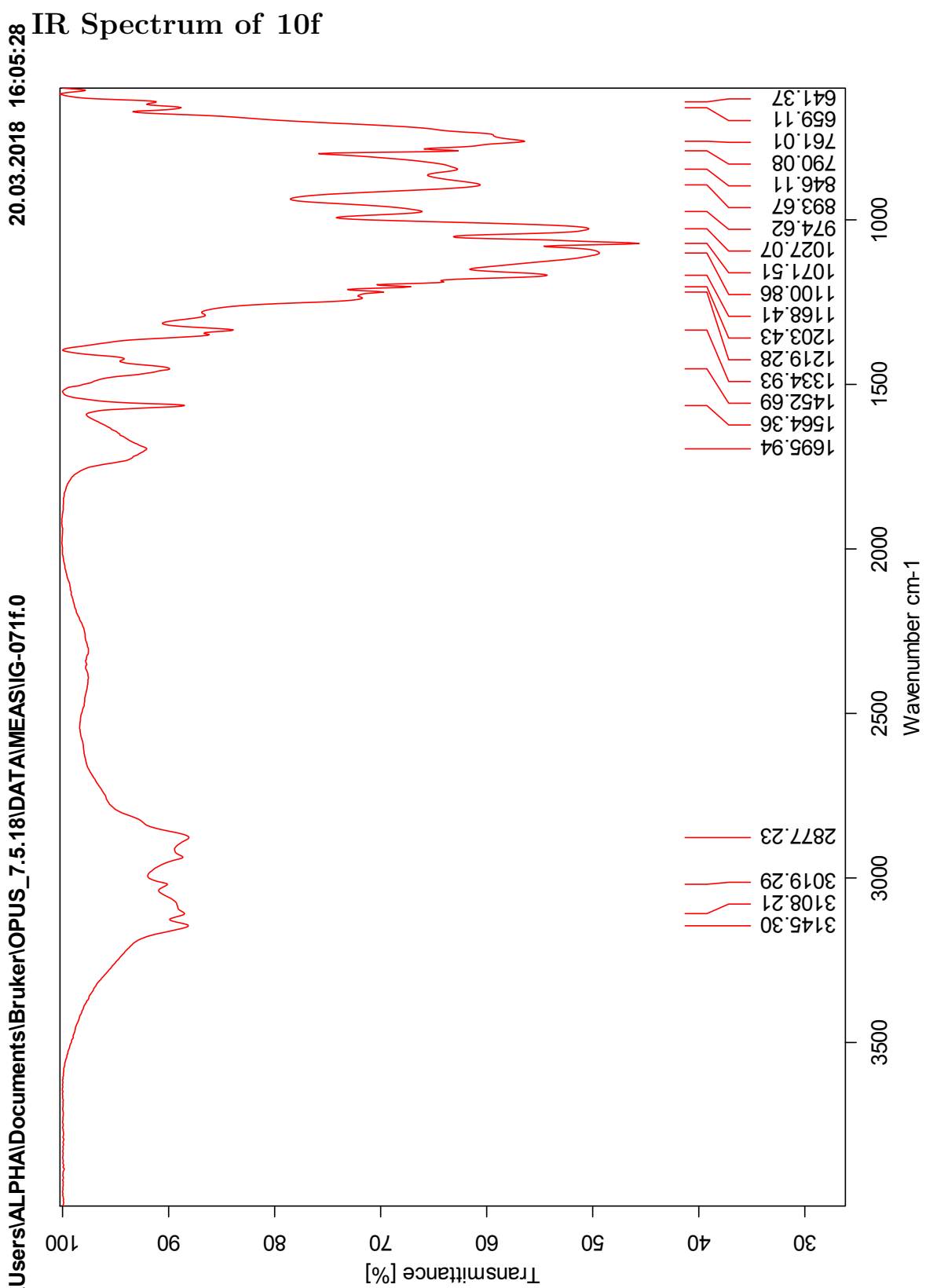
¹³C NMR Spectrum of 10f



CXLI

IR Spectrum of 10f

C:\Users\ALPHA\Documents\Bruker\OPUS_7.5.18\DATA\MEAS\IG-071f.0



HRMS Positive mode spectrum of 10f

Elemental Composition Report

Page 1

Single Mass Analysis

Tolerance = 2.0 PPM / DBE: min = -1.5, max = 50.0

Element prediction: Off

Number of isotope peaks used for i-FIT = 3

Monoisotopic Mass, Even Electron Ions

2379 formula(e) evaluated with 5 results within limits (all results (up to 1000) for each mass)

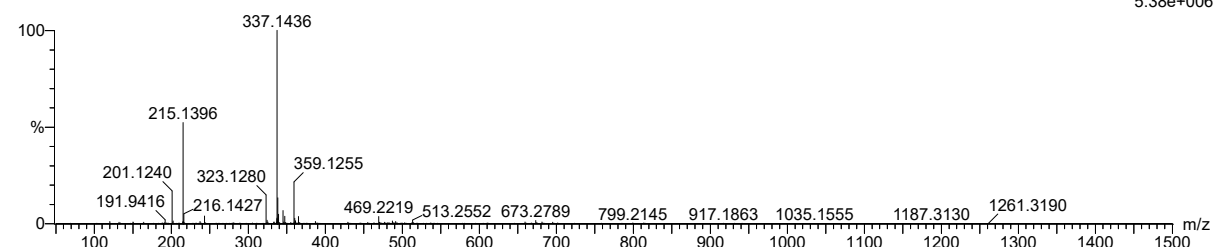
Elements Used:

C: 0-500 H: 0-1000 N: 0-10 O: 0-10 S: 0-5 I: 0-1

2018-126pos 45 (0.437) AM2 (Ar,35000.0,0.00,0.00); Cm (41:45)

1: TOF MS ES+

5.38e+006



Minimum: -1.5
Maximum: 5000.0 2.0

Mass	Calc. Mass	mDa	PPM	DBE	i-FIT	Norm	Conf (%)	Formula
337.1436	337.1433	0.3	0.9	2.5	1475.7	0.000	99.95	C13 H25 N2 O6 S
	337.1440	-0.4	-1.2	11.5	1489.4	13.664	0.00	C21 H21 O4
	337.1440	-0.4	-1.2	-1.5	1483.7	7.967	0.03	C6 H25 N8 O4 S2
	337.1431	0.5	1.5	-0.5	1487.0	11.220	0.00	C5 H21 N8 O9
	337.1442	-0.6	-1.8	1.5	1484.7	9.018	0.01	C14 H29 N2 O S3

HRMS Negative mode spectrum of 10f

Elemental Composition Report

Page 1

Single Mass Analysis

Tolerance = 2.0 PPM / DBE: min = -1.5, max = 50.0

Element prediction: Off

Number of isotope peaks used for i-FIT = 3

Monoisotopic Mass, Even Electron Ions

67 formula(e) evaluated with 1 results within limits (all results (up to 1000) for each mass)

Elements Used:

C: 0-500 H: 0-1000 N: 0-10 O: 0-10 S: 0-5 I: 0-1

2018-126neg 6 (0.138) AM2 (Ar,35000.0,0.00,0.00); Cm (6:7)
1: TOF MS ES-

4.36e+006

